# Mathematical Models of the Impact of Rabbit Calicivirus Disease (RCD) on the European rabbit, *Oryctolagus Cuniculus*, in Australia

FRANCESCA FIORENTINO

August, 2003


A Thesis Submitted to the University of London

for the Degree of

Doctor of Philosophy

Department of Mathematics

University College London





ProQuest LLC
789 East Eisenhower Parkway
P.O. Box 1346
Ann Arbor, MI 48106-1346

*Not chaos-like together crush'd and bruis'd,*
*But, as the world, harmoniously confused:*
*Where order in variety we see,*
*And where, tho'all things differ, all agree.*

—Alexander Pope

# DEDICATION

**To my parents Gabriella and Eugenio Fiorentino.**

# ACKNOWLEDGMENT

I would like to thank my supervisor Dr. R.M. Seymour for his generous and helpful criticism, valuable advice and enlightening discussions on all aspects of the research carried out in this thesis. I would like to thank my parents without whose encouragement I could not have completed this work. I am also indebted to the Department of Mathematics at UCL for hosting me during the years dedicated to this research and I would like to express my gratitude to my colleagues at the Mathematics department for many stimulating conversations as well as friendly support.

## Abstract

This thesis relates to the work of building a mathematical model of the impact of Rabbit Calicivirus Disease (RCD) on the European Rabbit, *Oryctolagus cuniculus*, in Australia. After introducing the general biology of rabbits and the immunology of RCD, we build a time-dependent single site model. We construct a single-site population dynamic model with age structure, seasonal birth rate, density dependent regulation of the population size and climatic variability for various regions of Australia. After investigating suitable parameter ranges, we incorporate the disease dynamics through an indirect transmission model based on two different hypotheses which we call the Strong Juvenile hypothesis and the Weak Juvenile hypothesis. These differ in their assumption about Juvenile immunity to the disease. The ecological impact of both hypotheses is tested for both the single site and multiple site (spatial) models. The disease impact is investigated by varying the disease virulence, i.e. a parameter measuring the "strength" of the virus.

Subsequently, a multiple site (spatial) model for the Riverina region is built by using the single-site model as building block. Data from Lake Urana is used to parameterize a seasonal emigration rate from each site. Density dependent immigration is added together with a hazard coefficient which rabbits face when leaving one site and trying to become established in another. Acceptance in a new site is regulated by the population density at the entry site. Several spatial configurations of sites are tested and the spatial dynamics of the disease is investigated.

Finally, we construct a model to investigate the long term evolution of the disease virus. We postulate the existence of several strains of the disease and trade-offs between disease characteristics. We allow for mutation of the virus and run the model for two contrasting geographical regions of Australia. We compare the results for the different regions and the different hypotheses regarding Juvenile immunity (the Strong Juvenile hypothesis and the Weak Juvenile hypothesis). It is shown, unexpectedly, that intermediate levels of disease virulence are not selected.

# Contents

# Chapter 1

# Introduction

The purpose of mathematical modelling is to use mathematics to test ideas and make predictions about the real world; even though, nowadays, any description is regarded as just a model, of greater and less accuracy and range, which mimics certain aspects of observed behaviour, thus enabling useful predictions to be made [40]. The research described in this thesis employs mathematical models to investigate the possible outcome of using *Rabbit Calicivirus Disease* (RCD) as a virological control for the European rabbit in Australia. This is achieved by constructing and simulating discrete-time stochastic, compartmentalised models with parameters derived from real data taken from field observations. Together with the complexity of the models, the choice of realistic parameters is designed to simulate realistic model outcomes. For this reason the accurate estimation of the parameters is essential to the validity of the models. The parameter values used will be derived from the biology of the rabbit, Australian climatic and ecological conditions, and the epidemiology of RCD.

What follows in this Introduction is a brief description of the origin of the rabbit pest problem in Australia, the main features of rabbit biology and RCD epidemiology, and a derivation of many of the parameters used in the subsequent models.

## 1.1 A bit of History

Members of the family Leporidae (rabbits and hares) first appeared in the late Eocene (40-70 million years ago) in Asia and North America and arrived in Europe during the Miocene (10-25

million years ago) [131]. The genus *Orictolagus*, was first recorded in Southern Spain and north Africa during the middle of the Pliocene period [131]. Now it has a widespread global distribution, primarily because of the influence of man in promoting its spread [114].

The European rabbit *Oryctolagus cuniculus* is one of the more successful mammals of the world, and appears to be equally at home in temperate and sub-tropical climatic conditions, to thrive in the inhospitable winds of Tierra del Fuego, and even to live in central Africa within two degrees of the Equator [116]. It was soon realized in the past that this success resulted in depressed agricultural production and forestry revealing what can be termed the 'rabbit pest potential' [37]. The threat that rabbits represent for the natural environment has not always existed. In fact, in Europe, especially in England, it was not until the nineteenth century that free-living rabbit populations started to increase, due to changes in farming practices, and the hunting by the nobility and trapping by tenant farmers of rabbit specific predators [116]. In Australia, as in Europe, as well as the favourable climatic conditions, human changes to the natural environment further improved the living conditions for rabbits resulting in the fastest rate of colonisation of any mammal anywhere in the world [131].

The research described in this thesis focuses particularly on the successful colonization of the European Rabbit in Australia, which is stated by E.C. Rolls [103] to be "unprecedented". The European Rabbit was most probably successfully introduced in Australia by Thomas Austin for sentimental reasons in the middle of the nineteenth century in Victoria and South Australia [94], and not long after this it was to be found in New South Wales, Queensland and Riverina, a disctrict in the south of New South Wales particularly favourable for rabbits. In fact the adaptability to various weather conditions allowed the rabbit to establish itself in hostile habitats such as the arid sand hills typical of central Australia, the snowy territory of the Southern Alps and the muddy sub-tropical Tweed River district.

## 1.2 Distribution and Abundance

Rabbits are capable of adapting to almost any kind of climate, soil and rainfall. Soil is a fundamental parameter for the abundance and distribution of rabbits, which tend to prefer deep well-drained soils with available water [131]. That is why in Australia rabbits are more abundant south of the tropic of Capricorn and tend to be more sporadic in very dense forests, which do not provide them

with appropriate food. In fact because of its small size, a rabbit can be very selective in what and how it eats [131]. Rabbits require a high-quality diet less than 40% fibre and $10 - 12\%$ protein for maintenance and 14% protein for reproduction [25]. Thus, tall tropical grasslands are nutritionally inadequate for rabbits, and pasture growth occurs at the wrong time for rabbit breeding [131]. In black soils, which crack and fill with water it becomes difficult for rabbits to breed in warrens which are prone to flooding. Rabbits also do not thrive at high altitudes, where the availability of food is strictly seasonal, or in very arid territories, where the breeding season is reduced due to the high temperatures outside and, especially, inside the warren, and the availability of water is reduced. Nevertheless, they do relatively well in dry habitats by selecting a diet with the highest available water content, by being mainly nocturnal and by burrowing [131]. Because of all these factors, rabbits are more likely to be found in deep sands, which protect them from temperature extremes and from predation and where the nutritional quality of the pastures is adequate, while their presence in other types of environment, like very arid territories, shallow soils (where predation is more successful) and black cracking soils (which become water logged), tends to be more strictly seasonal. After a run of good seasons, rabbits may be abundant over an entire region, while during severe droughts they may disappear completely from some land systems with their range contracting to refuge areas where there are large, deep warrens alongside drainage channels or dried-up swamps [131]. However Australia is on the whole an ideal environment for rabbits due to the favourable combination of climatic conditions, human changes and, most of all, the adaptability of the rabbit, so much so that its spread in this continent has been extraordinary.

In the early days this rabbit pestilence, which was slowly destroying some of the native flora and fauna in Australia, was not detected because its economic value was predominant in people's view: the export of rabbit skins and carcasses became a big business, and winter skins in particular were highly valued in the fur trade. The hope that it could be contained by natural agents like predators or, as in Britain, a naturally occurring epizootic (temporarily prevalent outbreak of a disease) like Myxomatosis, failed, and the numerous efforts by the authorities at the end of the nineteenth century to contain its damage by erecting barrier fences of wire-netting proved to be useless and very costly in time, money and human endurance [116]. The Australian government was pressured to bring in compulsory legislation. So in 1875 a Rabbit Bill was passed [103]. It set up District Councils to collect rates (local taxes) and employ rabbiters. This was only the first of several legal actions to control rabbit invasions; subsequently all sorts of methods were employed, like poisoning, trapping, fumigation, shooting and eventually the deliberate release of diseases like

myxomatosis in 1950 [116] (see section 1.5.1).

## 1.3 Biology of the Rabbit

### 1.3.1 Physiology

Rabbits and hares were originally classified with the rodents (or gnawing mammals) in the order Rodentia, but subsequently they have been classified in the order of Lagomorpha, a word coming from ancient Greek: lagos (= hare) and morphe (=shape). In particular, the rabbit species that is subject to the effects of Rabbit Calicivirus Disease RCD is of the family of Laporidae (*Lepus cuniculus*), and genus *Oryctolagus*, of which there is only one species (*Oryctolagus cuniculus*), originally settled in Europe and North Africa and that was later introduced to other parts of the world [116].

There can be many reasons why a given species may prove consistently succesful in the struggle for existence. Success may be due to such factors as the ability to thrive on varied types of diet, good food-conversion, disease-resistance, or high reproductive potential; and in the case of the rabbit some or all of these may be relevant [116].

The digestive system of the rabbit shows many adaptations to its mode of life, including the specialised nature of its teeth, its heavy production of bile, and its voluminous large intestines with a very large caecum ending in an appendix [116]. They eat a lot for their body size and their stomach is never empty but frequently contains only pellets. In fact it is of particular interest for this research that rabbits re-ingest their excreta (coprophagia) [70]. This was hypothesized in the seventeenth century, and after several experiments from 1882 [72] to 1939 [67], it was eventually proven that re-ingestion does occur. Morot [72] showed that there are two kinds of droppings: the first is the usual rounded hard type that is familiar to all who keep rabbits or walk over land where rabbits live, and the second is smaller, softer and mucus-coated and often found in rabbit stomachs. Morot therefore concluded that since the stomach pellets were so frequently present, they represented part of the normal digestive process of the species [116]. The result of this process is similar to rumination, and it was called "pseudo-rumination" by the naturalist Drane in 1865 [116]. Morot's experiments were eventually confirmed by Madsen and Copenhagen [67], who in their experiments prevented the rabbits from re-ingesting the soft pellets for over a month by using collars.

They found that soft pellets were passed at night in contrast to the hard ones, which were passed during the day. So, hard pellets are not simply the soft ones re-ingested but another type of droppings, since the rabbits in the experiments of Madsen and Copenhagen still passed hard pellets even though they were prevented from re-ingesting the soft ones. Soft and hard pellets have a common origin. There is some sorting in the intestine of large and small particles of food and the finer particles form into pellets that get a heavy mucus coating that stops further absorption of water and nutrients in the hind gut. These become soft pellets. The heavy particles are also aggregated into pellets but are not so well protected from further absorbion and modification in the hind gut. These are passed out as the dry, fibrous "hard pellets" [29].

Nevertheless the phenomenon of re-ingestion is observed even among animals that are not fully weaned. Watson observed it among rabbits less than 3 weeks old. Thompson and Worden [116] affirm that re-ingestion is a form of biological adaptation, since it ensures a better use of food, by allowing micro-organisms in the lower parts of the alimentary tract to act twice upon it. In ruminants, this happens in the rumen, before it goes to the "true stomach". To a degree re-ingestion replaces rumination [116]. This fecal-oral route might be one of the means of spread of RCD from infected rabbits to susceptible rabbits, since RCD might be present in the feces of an infected individual and infect a susceptible one when the infected droppings are examined by a susceptible. In fact a rabbit that investigated hard pellets, scratched them about, then washed its paws by licking them as cats do would probably become infected [29]. This, the normal hard pellets are deliberately placed on buck-heaps (latrines) as signals to other rabbits and are often investigated closely - though probably not eaten. Both hard pellets and soft pellets would almost certainly contain viral particles but this has not been experimentally demonstrated [29].

### 1.3.2 Reproduction

Reproductive characteristics are another feature of the capacity of rabbits to adapt to their environment. In fact, the strong seasonal trend of the reproductive cycle links reproduction with day length and the seasonal availability of suitable food [131]. Boyd and Bray [14] claim that specific chemicals in rapidly growing or drying-out plant tissues might be responsible for the start of the breeding season. In Australia, particularly in the South, summers are long and dry and vegetation is mostly available in autumn and spring, which is when reproduction takes place. The breeding season starts in autumn but does not reach the high peaks that it reaches in spring, with winter be-

ing an interval of lower breeding activity. Figure 1.1 shows the seasonal variation in the percentage of adult (older than nine months) females pregnant at five sites in Australasia [47].

Williams et al. [131] say that females as young as three months can breed, but adult pregnancy rates are not attained until seven months. Fenner and Ratcliffe [37] affirm that European rabbits may be sexually mature by the time that they are 3 or 4 months old. The period of gestation ranges from 28 to 33 days (Wood [132] and Gilbert [47]), and most litters consist of three to seven young with mean litter size between 3.75 and 5.25 [37] depending on the geographical location (lower in Subalpine and higher in Riverina) [131]. Wood [132] calculated that in an arid environment in New South Wales (Australia) the average litter size was 4.3 kittens and that the average annual productivity in terms of kittens born per female was 14.6.

Female rabbits can become pregnant a few hours after they have given birth, with the result that almost all the sexually mature does can be pregnant in successive months in the breeding season [131]. A female rabbit can in fact have a litter about every 31 days, due to the fact that rabbits do not have a menstrual cycle but ovulate when stimulated, for example, by exposure to other *in oestrum* or pregnant females. *Post – partum oestrum* (*oestrum* after giving birth) might be another factor leading to mating. An interesting characteristic of wild rabbit reproduction is the high incidence of prenatal mortality: the doe can re-absorb the litters totally *in utero*, i.e. before they are born. This phenomenon results in the death of all (*in toto*) the embryos of many litters on, or about, the 11th-12th days of pregnancy. Brambell [15] observed that these embryos are re-absorbed rapidly: the resorption of the embryonic membranes and maternal placental tissues follows that of the embryos. Commonwealth Scientific and Industrial Research (CSIRO) studies attempted to correlate this phenomenon with the social status of the does or with environmental stress, but results were on the whole inconclusive [37]. This resorption of the litter results in the immediate reappearance of oestrus so it can play an important role in maintaining breeding efficiency [37].

It must be noted that some animal populations may compensate for sterility of a portion of the population through increased fecundity of the remaining fertile individuals or through increased survival with the consequence that population numbers are maintained at relatively high levels [119]. This applies for the rabbit and *post – partum oestrum* and resorption might be part of this mechanism. Density-dependent "compensation" is a major topic of fundamental interest in ecology. It is usually inferred from observational data, and has rarely been demonstrated from manipulative

experiments [119].

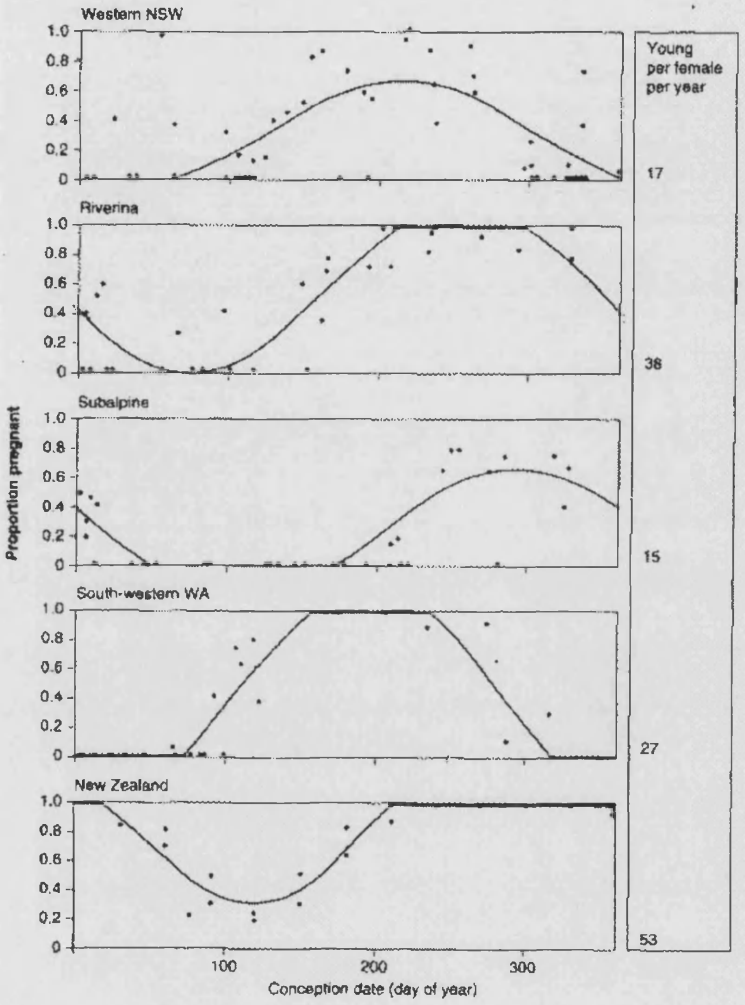


Figure 1.1: Adult pregnancy rates in relation to conception date [47].

### 1.3.3 Survival

A high rate of reproduction does not necessarily result in high population densities. For example rabbits hardly reach pest levels in New Zealand, because there is a high mortality of juveniles caused by predation and flooding of stops [131]. Moreover, food scarcity can cause mortality at weaning [86], [111]. Williams et al. [131] affirm that in Australia life expectation at emergence is about

three months and mean generation time is 1.5-2.0 years. The survival rate of juveniles is dependent on the time of the breeding season in which they were born. Williams et al. [131] affirm that juveniles born in the first or last part of the breeding season have low survival rates, since the early born face more predation pressure (increasing ground cover will afford greater protection against predators as the breeding season advances) while the late borns face scarcity of food [31] (late-born young have been found to show signs of protein deficiency or starvation as a result of lactation failure with the onset of dry summer conditions [132]) [See Figure 1.2]. Wheeler and King [127] observed that the increase in age-specific survival during the course of the breeding season is to be attributed to an increase in ground cover affording greater protection against avian predators. In contrast Cowan [31] reports how striking was the highly significant decline in survival probabilities amongst successive cohorts born during the course of the breeding season in his field observations: survival was significantly correlated with time of birth [47], [31]. Parer [87] considered that the decline in juvenile survival in the population he observed was due to an increase in the rate of predation, particularly by cats, operating in a density-dependent manner.

Moreover juvenile and subadult survival appear to vary even between different years: the difference in survivorship between years is highly significant, as shown in figure 1.3. Cowan [31] suggests that the marked variation between years in juvenile survival in the field is partly related to population density, with higher mortalities associated with higher population density. Coccidiosis and myxomatosis may also operate in a density-dependent manner, since it is probable that a minimum density of susceptible individuals is required before an epizootic occurs [105], [108].

Cowan [31] says that in his observations the mortality of rabbits from 4-8 weeks to more than 52 weeks of age was high: only 6.5% survived in this age interval [See Figure 1.4]. Survival to nine months of age may be as low as 0.25% or as high as 12% [131]. Wood [132] says that in his observations in an arid environment in New South Wales (stable sand dunes, sandy alluvial corridors and swamps), the mortality of rabbits under 9 months of age was never less than 88% and in one year reached 99.75%. Predation was the principle factor, particularly by foxes on nestlings, killing $26 - 75\%$ of a particular season's cohort, and it was more severe in dry years than in wet years. In fact, the rabbit is a major food item for foxes, though in good years it can share this 'privilege' with other animals such as small rodents, marsupial mice, eggs and ground nesting birds, lizards and large grasshoppers [132]. That is why predation on rabbits has a seasonal trend. Wood [132] reports that in New South Wales reproduction is more or less balanced by mortality,

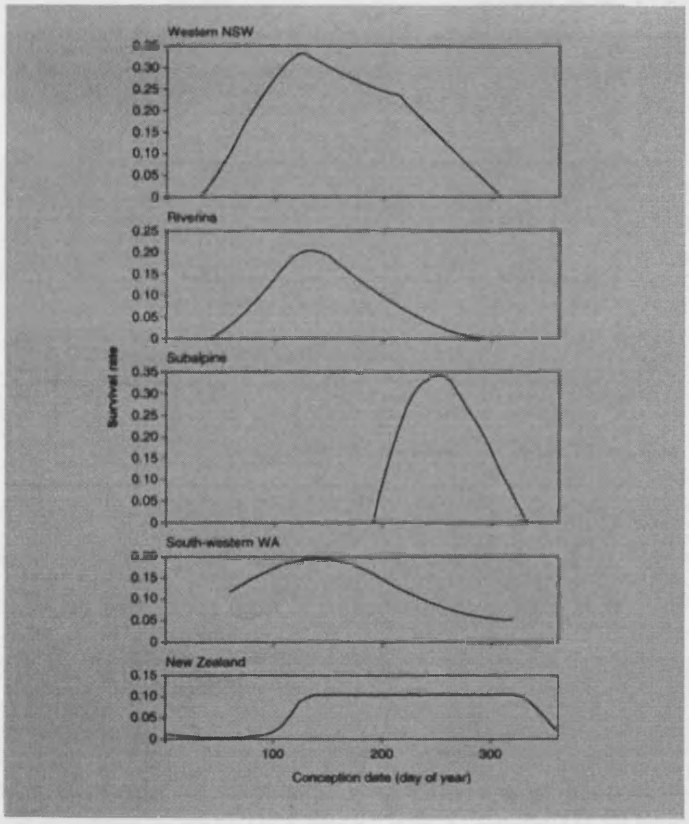


Figure 1.2: Computed survival rates from birth to 24 weeks of age plotted against conception date [47].

mostly due to predation. However in South Australia reproduction exceeds mortality until the population outstrips its food supply. So predation and starvation are two important population regulation factors in sandy environments and as a rule rabbit populations will maintain relatively stable numbers; violent fluctuations in numbers resulting from sequences of wet and dry years will not occur as they often do in Australia's arid zones [132].

Gilbert [47] says that survival to 4 weeks of age was generally of the order of 50%, but that this was probably an overestimate if unrecorded adult females are present in the population. Data from the observed sites show that all losses are almost all of complete litters, being due to lactation failure, social disturbance, fox, cat or goanna predation and drowning in burrows after rain, but the data does not distinguishes between causes [47]. Annual survival rates of adults is 40%-60% [31]. Cowan [31] observed that there was no difference in the annual survival probabilities of adult males and

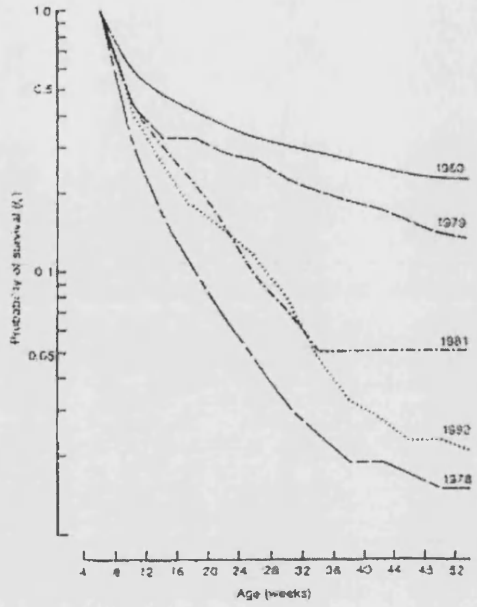


Figure 1.3: Variation in survival probabilities of juveniles, in 28-day periods from 4-8 week age interval to > 52 weeks of age, with the year in which they were born [31].

females, while there was a difference in mortality between male and female rabbits in the juvenile and subadult age interval. Rabbits rarely survive past six years of age in the wild [131].

### 1.3.4 Behaviour and Social Organization

The social system of the European rabbit probably evolved in response to a number of adaptive pressures, including predation and competition for patchily distributed resources such as good food and nesting sites; in fact it is the influence of environmental parameters that can determine the social behaviour (immigration, emigration and stability of social groups) which, in turn, influences the genetic structure [11]. In the U.K., the European wild rabbit exhibits a high degree of non-random mating (in classical models of population structure individuals mate randomly [115]) and social structuring, and a consequence of this is a high degree of genetic structuring within a population [114]. Thus, in favourable, stable conditions, as in the UK, strict, stable, social organization develops, leading to fine-scale genetic structuring. Under less stable conditions (ecological and demographic), as in Australia, social behaviour is more relaxed [113].

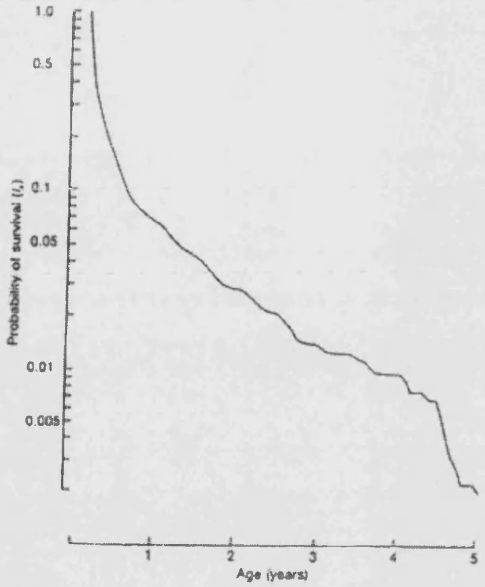


Figure 1.4: Survival probabilities of rabbits from 4-8 week-old age interval to 5 years old [31].

The daily life of a rabbit revolves around the warren. In fact the amount of time a rabbit spends in any one area is inversely proportional to the distance of the area from the warren [131]. The warren characteristics vary depending on the environment in which it is located. For example, in land with dense vegetation a warren will be smaller compared to one in open country such as clear land, grazed pasture or arid areas [131]. A larger warren in open land is the result of a greater need for protection from possible predators, as well as shade from heat and climatic extremes in general. There is a natural tendency not to excavate or build new warrens but to use those already existing [30]. If there is a lack of warrens, a rabbit will use a *squat*, which is a shelter in a soil depression or fallen timber [78]. Then the squat might eventually become a warren if inhabited for long enough, by pregnant females for example, who are the principal excavators and architects of the warren.

The warren is mainly inhabited during daylight and rabbits tend to come out and search for food at night. Typically, rabbits emerge 1-3 hours before sunset and move back into their warrens at about sunrise [131]. This limits their exposure to temperature fluctuations and other climatic extremes, and to possible predators.

The criteria for regional and local distribution of warrens is soil depth, soil hardness and permeability to water. Drowning and hypothermia are significant causes of mortality in badly drained

soils or in high rainfall areas [131]. That is why rabbits tend to prefer elevated, deep sandy soils that do not become water-logged and are not too hard to dig even in the drier months. Sandy soils become unfavourable only in very hot and dry years since the heat conductivity of sand can make the temperature inside the warren unbearable, especially for lactating females.

The European rabbit is what might be called a positively gregarious species. Every individual tries to be accepted in a social group if it is not a member of one already. Lockley [65] affirms that rabbits are essentially gregarious animals, siting their territories and activities as close to the warren they inhabit as they are physically able to do. On the approach of the breeding season, rabbits form themselves into social groups. The groups comprise any number of animals up to a maximum of about seven and each group establishes a territory, which is defended from trespassers from other groups. Each member of the group has a 'home range' to which it restricts its daily activities, but this can overlap with the home range of other members of the same group [37]. Within these groups, stable linear dominance hierarchies are observed in both males and females, with males competing for access to females and females competing for breeding sites [113]. When the breeding season is over the group structure weakens, even though there is a general tendency for group structure to persist from one breeding season to the next, although changes in group composition are continually taking place.

Young rabbits are normally more tolerated by resident adults and are allowed to move between group territories. The situation changes when they reach sexual maturity and they come into competition with the adults of the established groups and are often chased away from the group by the resident adults. If they fail to be accepted they disperse sometimes to untenanted territories [37].

Due to the importance of the warren in the life of the wild rabbit, extensive warren ripping has proved to be a successful means to control the density of rabbits. However, it cannot be totally successful since there is always a percentage of rabbits living above ground in dense vegetation or fallen timbers, although these are fewer than rabbits inhabiting warrens where, in most circumstances, the main breeding population lives. Since rabbits do not dig new warrens readily, destruction of warrens greatly inhibits resurgence and recolonization of treated areas, especially if coupled with other control techniques like fumigation, explosives (the aim is to destroy the warren or individual burrows), rabbit-proof fencing, shooting, trapping, poisoning [142] and immunocontraception [98]. Where rabbits use warrens, ripping is the most cost-effective and enduring of the available tech-

niques [131], especially when rabbit density is low, as there is a greater chance to eliminate all the rabbits.

### 1.3.5 Dispersion

Domestic rabbits arrived in Australia with the First Fleet in 1788. The first person to introduce wild rabbits to the Australian mainland was Thomas Austin. He brought 14 rabbits with him to Australia in 1859 for sport and game purposes [131]. Some were released or escaped soon after. Initially rabbits spread slowly, taking 15 years to reach New South Wales from Geelong, South of Victoria [103]. In another 15 years they reached Queensland and by 1900 they were in Western Australia and the Northern Territory [131]. The rate of advance reached 10-15 kilometers a year [131].

This incredible mass movement became less apparent at the beginning of the 20th century, and it now seems that the rabbit has become a more stable species and less prone to disperse and migrate when settled in a favourable environment. Evidence for this is found in the fact that the warren has a central role in the life of the rabbit. Rolls [103] presents the rabbit as a non-adventurer which adjusts its community life to fit the conditions within the area that its neighbours restrict it to. Once it has settled, only catastrophe - flood, famine or terror - will force it to migrate. Mykytowycz and Gambale [80] in their field observations report a tendency of the rabbit to congregate. During the early days of colonisation of Australia by the rabbit, the rate at which it spread indicates that an individual was more prone to detach itself freely from existing population concentrations [80]. However these authors say that on no occasion was any individual seen to establish itself in a new territory during the breeding season, but only during the non-breeding season or during the re-grouping period which precedes each breeding season. Very few individuals changed their native warrens and most of those that did were males and generally they were highly sexually active [80]. It was probably a strong sexual drive that put them into conflict with the dominants in their parental warrens [80]. Parer [88], though, claims that although the rabbit has a strong attachment to its warren, mass movements seem to have been common in Australia before the introduction of myxomatosis in 1950, i.e. rabbits in dense populations seemed to have a looser attachment to their warrens than they do now.

Biologists and ecologists have put forward different hypotheses to account for the phenomenon of dispersion, since no particular factor seems to strictly determine its occurrence. Fenner and Ratcliffe

[37] assert that it is impossible to determine the distances actually covered by mass movements, although it is popularly believed that, in extreme conditions, like a prolonged drought, they may approach or exceed 100 miles. Douglas [35] agrees that it is possible that once a rabbit leaves its original warren to search for a more favourable habitat, it might travel very far, even up to 85 miles in 2 years. However, this is probably an extreme case: movements for long distances, up to 25 kilometers, have been observed but mainly the trend is that a dispersing rabbit of any age seeks shelter and establishment in neighbouring social groups. This appears to be related to the fact that animals in inland or low rainfall areas tend to migrate mostly seasonally in search of water and better pastures, while individuals in more advantageous climatic and environmental conditions tend to be more sedentary. In general, according to Fenner and Ratcliffe, it is the imbalance between a high rabbit density and inappropriate climatic conditions that is the major factor that can push a rabbit to disperse from its original burrow in search of a more favourable habitat. This still does not explain why this migration often happens in mass movements, but it could be accounted for by the fact that rabbits are normally organized in a linear hierarchy, so it might be that when the 'leaders' (dominant adult in a group) are driven to migrate, the rest of the rabbits follow [37]. Finally, Fenner and Ratcliffe suggest that human interference can, in a minor way, impel rabbits that have been disturbed by trapping or dogging to disperse.

Besides large-scale movements, there are also minor individual dispersions which are prompted, according to Fenner and Ratcliffe, by two main circumstances: food shortage and social outcasting. Food shortage is mainly a seasonal occurrence, linked to the lack of green pastures and availability of water; social outcasting is seasonal as well, because it is linked to breeding activity, which is in turn seasonal (see section 1.3.2). Fenner and Ratcliffe [37] argue that the movement of that fraction of the population which finds itself surplus to the local 'establishment' will occur, in the main, at two times of the year: in the pre-breeding period, when the social groups are re-formed after the reproductive inactivity of the middle and late summer, and again in the late spring and early summer when the maturing survivors of the autumn litters are forced out of the breeding groups by their parent adults. These outcasts then roam in search of a new settlement together with other rabbits, since the rabbit tends to be a gregarious animal. Parer [88] affirms that dispersal movements by young rabbits are strongly seasonal. In his observations, most rabbits moved in October-December and the increase in the movement of males was probably related to social reorganization at the beginning of the breeding season; adult females rarely disperse. Moreover he observed that rabbits tend to move into depopulated areas and that young rabbits disperse further in drought years [88].

Parer [88] reports data on the time of dispersal, dispersal distance and age class of young male and female rabbits dispersing from a site. From this data it is possible to determine the probability that a young rabbit will disperse from its warren at a certain time of the year, how far it might disperse and to what age class it belongs to (see tables 1, 2 and 3 in Parer [88]). These tables are reported below and this data will be used later in this thesis to model emigration (see chapter 5 and 11). Daly [34] observed that most dispersal at Urana (NSW) was by pre-adult animals, and that adults were sedentary [46]. In fact dispersal was by subadults during the pre-breeding season in autumn. This is explained by Daly [34] as a response to the re-establishment of social groups at this time of the year. Daly [34] also reports a major dispersal of juveniles at the end of the breeding season, which appeared to be a response to the drying out of pastures.

In addition, there are other observations and hypotheses on rabbit dispersal. For example, Williams et al. [131] affirm that young rabbits disperse throughout the breeding season, especially at the beginning of the summer in Australia due to scarcity of food. In fact one or 2 month old rabbits are most likely to disperse, together with subadults (mostly males), when the breeding season starts, with its consequent social reorganization, in autumn and early winter [131]. Rolls [103], too, is of the opinion that immature rabbits are the most likely to leave the group in which they were born, presumably due to high population density in food shortage conditions. Gibb [46] asserts that rabbits older than 8 months rarely disperse, since they are probably already established in a warren hierarchy and that density is a likely factor in causing these migrations. Cowan [32] and Henderson [59] both observe that migration normally occurs from high to low density warrens and from areas of high production of young to areas of low production.

In general it is rare for an adult to leave and join another social group [113]. In England, Surridge et al. [113] observed that rabbits exhibit gender-biased natal dispersal with males leaving their social group prior to their first breeding season and females remaining within the group. The genetic structure of rabbit populations is expected to be affected by this gender-biased dispersal and the limited migration of adults between breeding groups. However, increasing competition within the group for resources such as nesting sites, is more detrimental to younger females within the group than to dominant adult females, prompting the younger ones to disperse. In fact direct cooperation between females is not an important aspect of social behaviour in the European wild rabbit in England [115]. In Australia, though, the social structuring in rabbit populations does not appear to have major genetic consequences at the intrapopulation level [34], leading to the conclusion that

even stable, socially organized populations can approximate a panmitic population. In view of this we have no reason to believe that in Australia the response to a disease, and disease transmission, will be different between individuals on different levels of the group hierarchy.

Table 1: Parer's [88] data on the time of dispersal of young male and female rabbits (number of adults in parentheses).

| Years | Sex | J | J | A | S | O | N | D | J | F | M | A | M |
|---|---|---|---|---|---|---|---|---|---|---|---|---|---|
| 1967-68 | M | 0 | 0 | 2 | 2 | 13 | 25 | 8(1) | 1 | 1(1) | 1(1) | 1 | 1 |
| | F | 0 | 0 | 3 | 2 | 7 | 24(1) | 5 | 12 | 0(1) | 0(2) | 1 | 0 |
| 1968-69 | M | 0(1) | 0 | 1(1) | 2(2) | 5(5) | 8(1) | 4 | 2 | 3 | 7 | 3 | 2 |
| | F | 0 | 2 | 0 | 0 | 4 | 8 | 1 | 2 | 2 | 0 | 2 | 0 |
| 1969-70 | M | 2 | 0(1) | 3(1) | 3 | 4 | 12(2) | 6 | 3 | 3 | 5 | 4 | 2 |
| | F | 1 | 1 | 5 | 0 | 4 | 7 | 5 | 1 | 0 | 0 | 0 | 0 |
| 1970-71 | M | 2(2) | 0(1) | 2(1) | 4 | 2 | 5 | 6 | 1 | - | - | - | - |
| | F | 1 | 0 | 0 | 0 | 0 | 4 | 3 | 1(1) | - | - | - | - |
| 1977-78 | M | 0 | 0 | 1 | 7 | 21 | 2 | 1 | 0 | 0 | 0 | - | - |
| | F | 0 | 0 | 0 | 1 | 17 | 6 | 0 | 0 | 0 | 0 | - | - |

Table 2: Parer's [88] data on the dispersal distances (in metres) of young male and female rabbits.

| Years | Sex | 0-200m | 201-400m | 401-800m | >800m | Total |
|---|---|---|---|---|---|---|
| 1967-68 | M | 4 | 11 | 13 | 27 | 55 |
| | F | 6 | 7 | 12 | 18 | 43 |
| 1968-69 | M | 20 | 4 | 4 | 5 | 33 |
| | F | 6 | 5 | 6 | 4 | 21 |
| 1969-70 | M | 19 | 11 | 5 | 9 | 44 |
| | F | 17 | 3 | 2 | 2 | 24 |
| 1970-71 | M | 12 | 3 | 2 | 5 | 22 |
| | F | 4 | 0 | 2 | 3 | 9 |
| 1977-78 | M | 7 | 8 | 10 | 7 | 32 |
| | F | 0 | 9 | 8 | 77 | 24 |

Table 3: Parer's [88] data on the number of young male and female rabbits of different age classes (in days) which dispersed.

| Years | Sex | 20-60days | 61-100days | 101-140days | 141-180days | >180days |
|---|---|---|---|---|---|---|
| 1967-68 | M | 18 | 19 | 9 | 5 | 4 |
| | F | 14 | 15 | 8 | 6 | 0 |
| 1968-69 | M | 3 | 4 | 12 | 4 | 10 |
| | F | 12 | 1 | 4 | 1 | 3 |
| 1969-70 | M | 18 | 5 | 4 | 4 | 13 |
| | F | 12 | 2 | 4 | 0 | 6 |
| 1970-71 | M | 12 | 5 | 3 | 2 | 0 |
| | F | 7 | 1 | 0 | 0 | 1 |
| 1977-78 | M | 23 | 6 | 3 | 0 | 0 |
| | F | 24 | 0 | 0 | 0 | 0 |
| All years | M | 74 | 39 | 31 | 15 | 27 |
| | F | 69 | 19 | 16 | 7 | 10 |

Dispersion is an important factor in rabbit ecology: Williams et al. [131] advance the hypothesis that dispersal can be an important factor in population regulation. In fact, the extinction of rabbits due to overgrazing and scarcity of food on small islands has been observed and described by Armstrong [8] and Watson [125]. Moreover, it must be noted that whenever an individual disperses, it is bound to face an increased degree of hazard before it finds harbour in a new burrow [131]. Parer [88] agrees with Williams et al. [131] on the importance of dispersal in relation to control strategies, even though there have been few significant studies of dispersal movements in rabbits.

### 1.3.6 Predators

The success of the rabbit as a colonizer and its ability to reach high population densities, even after being reduced to low numbers, might lead us to forget that there are actually other species that prey on rabbits. In fact rabbits are prey for a vast number of predator types, the most significant of which, in Australia, are: the feral cat, the fox, the dingo, the wedge tail eagle, the little eagle, the brown goshawk, the brown falcon, and the goanna, [81], [87]. But the two most significant predators

are the feral cat and the fox [143] whose population dynamics is so bound to that of rabbits that their densities subside after a time lag when there is a collapse in rabbit population density. During the time lag, however, predation is normally intensified since there are many predators seeking few rabbits. Ratcliffe [95] states that "the observed failure of the fox in South Australia to effect the clean-up of the few drought-surviving rabbits must be regarded as the last nail in the coffin of the popular idea that the pest can be exterminated, or even controlled, by an animal enemy. No more perfect conditions could be imagined than those which favour the fox in arid Australia. Yet the control that it exercises is hopelessly ineffective, and extermination is as far away as ever." Even though an ineffective means to control rabbit numbers, predators like foxes, dingoes and feral cats could be an effective control agent when acting together with other means like RCD, myxomatosis, warren ripping and shooting.

Catling [22] and Lugton [66] propose that rabbits are the main source of sustenance for foxes, which would not persist in the absence of rabbits in the rangelands; and with a low density population of rabbits they could be a significant regulating factor [92]. Williams et al. [131] point out that as rabbits are a substantial part of the diet of most birds of prey and mammalian carnivores, high numbers of rabbits keep the populations of these predators high. The effect of this strong dependence of some predators on rabbits could be higher predation on rare native mammals when rabbit density is low. This might be particularly intense before and just after a collapse in rabbit density. So keeping low the number of rabbits might help to maintain the delicate natural balance of the prey-predator world.

Nevertheless, one of the principal reasons for the success of the rabbit in Australia is probably the scarcity of mammalian predators, especially Mustelidae: small carnivorous mammals which dig rabbits out of the warren and kill them [131]. Martens, beech-martens and stone martens belong to this family. For a detailed examination of the effects of predators on wild rabbits, see Trout and Tittensor [117].

## 1.4 Bunny or pest?

It is hard to identify the rabbit characterised in many fairy tales- friend to children and furry stuffed puppet- with the description that many scientists report of the rabbit [135]. Ratcliffe [95] narrates the story of a young girl who wanted to see the rabbits during one of the plagues in Australia.

When she saw men killing the rabbits which had been caught in one of the dams, the little girl was very moved and shocked at the sight of all those bunnies being killed. After spending two weeks at one of the stations for the monitoring of the rabbit plague, the girl wanted to kill the bunnies herself after having heard grown-ups converse on the consequences of the rabbit invasion for the flora and fauna of the affected area [95]. For example in South Australia rabbit pests seem to have doomed the mulga, *Acacia ancura*, the most important drought fodder tree in Australia, by grazing on the seedlings: the existing trees will eventually die of old age with no new ones to replace them. Moreover even if the seedlings of certain trees are not palatable to rabbits, they might still not survive due to the lack of water in the root zone as a result of low infiltration into an eroded soil denuded of mulch by rabbits [55], the increase in ground heat, consequent on the lack of soil cover, and macro pores in the soil allowing for deep water penetration [131].

Many biologists and ecologists have turned their attention to the effect of rabbit grazing on the flora and fauna of habitats where rabbits live [143], [144]. In the early part of the 19th century, Wallis [124] and Farrow [36] studied how rabbit grazing modifies the environment in Britain. When rabbits exert a high grazing pressure due to high population density, they might leave no green pasture for any larger animal, while no woody plants can establish themselves because they have their bark gnawed [116], [143], [144]. Fenton [39] reports that even grass can succumb to rabbit grazing, being replaced by mosses and lichen. Rabbits alone are capable of preventing the regeneration of many plant species that are palatable to them. Lack of vegetation, or its extreme impoverishment, causes soil erosion, as discussed at length by Pick [94], who asserts that some good authorities are quite ready to believe that the rabbit has been the major cause of destruction of inland Australian habitats; and he defines it as "... the greatest biological scourge with which Australia has been visited...which released those forces of erosion which have made the inland a desert. Eventually they starve to death. But they never all starve. Enough survivors always manage to exist to provide the nucleus for a fresh plague when the good season returns."

Competition between rabbits and other native mammals should not be underestimated as a detrimental consequence of high rabbit density. Moreover domestic sheep are in direct grazing competition with rabbits, especially when there is a drought and green biomass is noticeably reduced: rabbits can push other stock to graze the perennial shrubs more heavily than they would in their absence [131]. Local extinction of both rabbits and native mammals can occur in drought regions, but then the capability of rabbits to rebuild to high density is noticeably higher than for other

mammals.

The distribution and abundance of many species of birds and other animals will be seriously affected by the long-term decline in the tree and shrub populations in the rangelands [131]. In their study of birds in Australia, Reid and Fleming [96] defined the rabbit interaction with native flora and fauna, especially birds, as a "biological time-bomb quietly ticking away." Thus, when rabbit density is high, the population of predators feeding on them increases, but in a drought period, when the rabbit population collapses, there will be a time delay before the predator populations decrease: in this time lag, predators will enhance predation pressure on other native species, as well as on the remaining rabbits, and might cause extinction of the former [143]. No known native mammal has become extinct north of the range of the rabbit since European settlement [131]. In the central deserts of Western Australia by contrast, extinction of some native species occurred after the rabbit arrived, but before the fox became established there [18].

## 1.5 Virological Control

Since traditional rabbit control techniques, such as trapping, fumigating, shooting, poisoning and warren ripping, have proved to be inefficient, scientists have suggested the possibility of using infectious diseases as control methods. Myxomatosis was deliberately released in various parts of the world like South America (where it was first detected), Europe and Australia, and Rabbit Calicivirus is currently being evaluated as a possible means of control for rabbits.

### 1.5.1 Myxomatosis

Myxomatosis was scientifically observed for the first time in 1896 by Professor Sanarelli of the University of Siena, who noticed that some domestic European rabbits, probably imported from South America, were killed by some highly infectious and lethal disease which had never been observed before and that produced numerous mucinous tumors in the skin of the infected animals [37]. It was more than a decade after Sanarelli's observations that cases of myxomatosis were reported, especially in South America (Argentina, Brazil, Chile and Panama), at the beginning of the 19th century. In Chile, it was subsequently intentionally released and used as a control agent in 1954. But the major impact of this infectious disease has been in Europe and Australia [37]. It was introduced in Australia in 1950 as a control agent after several laboratory experiments to

asses its impact. In Europe it was introduced privately in France in 1952. In both Australia and Europe the outcome was a fast spread and a coextension with the wild rabbit population; it is now endemic and still often a lethal infection of wild European rabbits in both Europe and Australia [37].

The decision to use myxomatosis as a control agent for rabbits in Australia took a long time to be taken, and even though scientists advanced the hypothesis of its regulating effect as early as 1919, it was only in 1950 that it was officially introduced; before that it was actively opposed due to the highly profitable trade in rabbit meat and skin. In this thirty years of hypotheses and experimentation on myxomatosis, it was discovered that it is highly lethal and is transmitted by vectors such as fleas and mosquitoes, which transmit it mechanically by biting an infected animal followed by a susceptible one; that it spreads more easily in wet climate environments, but that it does not seem to persist in the field constantly: epizootics appear to develop periodically in association with local and seasonal vector activity [37]. The strains of myxomatosis periodically occurring are of different virulence and have been classified into one of five 'grades' of virulence depending upon the mean survival time of inoculated rabbits [37]. In Australia current field strains kill about 40%-60% of the susceptible rabbits in field populations, and it is mainly the intermediate strains that are most successful since the most virulent ones kill their host too quickly for it to infect another individual, and the least virulent strains give the rabbit a chance to survive. Field observations have shown that there has been selection for increased genetic resistance of rabbits to myxomatosis, resulting in rabbit populations which have been exposed to high virulence strains of the disease over a long period showing a decreased mortality rate and proportion of severe cases. Thompson and Worden [116] claim that this is part of the process of host-parasite co-evolution, which can be due either to the attenuation of the virus, an increase in the innate resistance of the rabbits, or the 'passive-resistance' of young rabbits having maternal antibodies acquired during gestation or lactation. Williams et al. [131] claim that the increased resistance by rabbits to the disease and the increased virulence of the virus are compensatory so it may be that the capacity of the disease to kill has not been significantly affected.

Fenner and Ratcliffe [37] describe the myxoma virus as causing an infection which produces many infectious tumors, and which kills the host within 5 days of the onset of infectivity. In a large population of susceptible rabbits, and with an efficient vector, this incubation period is long enough for the virus to spread through the whole population. In winter, though, there is a lower number

of susceptible rabbits and of vectors: "... a virus which causes a disease which is infectious for only five days fails to survive; long persistence of infectious lesions is an essential condition for successful survival through the winter...", and this is the effect of lower virulence strains. However strains with very low virulence are ineffective since the rabbit recovers too rapidly for effective transmission to occur. "Selection on the basis of transmissibility is probably the correct explanation for the replacement of the highly virulent strain of myxoma virus" by intermediate ones [37].

The myxoma virus appears to be specific to only *Sylivilagus* and *Oryctolagus cuniculus* and two species of *Lepus* [17]. Rabbits that have been infected with myxomatosis are likely to die, but if they survive, they can acquire immunity and the antibody can be transferred from the doe to the fetus *in utero* [37]. Even though the immunity is not life-long, it enables a rabbit to challenge the disease and survive its weaker strains. The efficacy of the disease is altered by temperature mainly, but also by malnutrition and the effect of other infections. In fact, the virus appears to be less effective at very high temperatures, higher than $35^oC$ [90] and more effective at very low temperatures, lower than $4^oC$ [69], since at cold temperatures the immune response of the rabbit is weaker, as is the case for malnourished rabbits. Moreover Fenner and Ross [38] and Parer et al. [89] have found evidence that resistance to the disease is itself conditioned by the locality in which the rabbit resides: rabbits from temperate climates are less resistant than rabbits from hot climates. The outcome of an epizootic of myxomatosis is highly dependent on the environmental conditions and vector abundance in which it takes place, so it will vary from one area to the other, in particular in Australia, where a wide variety of climatic conditions occurs. The actual cause of death from myxomatosis is obscure. In fact from the primary lesion it spreads first to the lymph nodes and subsequently to the blood (the cells most involved appear to be the white blood cells, probably the lymphocytes), the spleen and the lungs [68], [41]. But even though high titres are found in the skin in many parts of the body with lumps which are hardly true tumors, vital organs are less affected, especially the brain and the nervous system [37]. Generally there is an accumulation of mucinous material more than a cellular proliferation, even though some cellular proliferation is observed.

Unfortunately, even though epizootics of myxomatosis have helped in controlling the rabbit population in some areas of Australia, it has not solved the rabbit problem. Myers [77] claims that in an area in Riverina (New South Wales), rabbit density recovered to about half pre-myxomatosis levels in just two years after the first outbreak. Williams et al. [131] assert that "... no reliance should be placed on the continuous effectiveness of myxomatosis, but it is still important in preventing

explosive increases in rabbit numbers. There is no way of predicting how much longer this will continue."

### 1.5.2 Rabbit Calicivirus Disease

Rabbit Calicivirus Disease (RCD), also known as Rabbit Haemorrhagic disease (RHD) or Viral Haemorrhagic Disease (VHD), is an acute fatal disease of rabbits (animals die 6-12 hours after the onset of the disease symptoms [126]) caused by a virus classified in the family Caliciviridae [83], [84], [91]. From this the name Rabbit Calicivirus Disease is derived; it is an RNA virus with a calix shape. Not much is known about RNA viruses, especially about how they attack, penetrate cells, and their replication process once they have infected the host cell [126]. The existence of RHD was noticed for the first time in China in 1984 [121], but Chinese scientists assert that it must have originated somewhere else and then spread to China when some rabbits were imported from Europe [122]. Rodak et al. [100] suggest that the disease was already present in Europe before it spread to China. Antibodies to the disease were found in rabbit blood serum samples collected up to 12 years before the first outbreaks of RHD were reported in China [100]. In Europe it was first detected in southern Italy in 1986 but after only two years it was observed in the whole of the European continent, and subsequently in Asia, Africa and central America.

It seems to be specific only to the *O. cuniculus* species of the *Leporidae* family: various tests and experiments have indicated that RCV (Rabbit Calicivirus) has a tightly restricted host range; i.e. just the European rabbit [138], [63]. The main reason why doubt has been expressed about the possibility of transmission of the virus to other species is the experience with the animal calicivirus San Miguel Sea-Lion (SMSLV) which has a very wide host range. Caliciviruses are RNA viruses, which, when replicating, produce antigenic variants that can cause host switching. Actually, in the case of SMSLV, the reason for the breadth of host range is due to the wide distribution among animals of the receptor used by the virus for cell attachment [138]. However, the majority of Caliciviruses such as the Feline calicivirus (FCV) and the foot and mouth disease virus have not yet "mutated" to switch host. A report conducted by the CSIRO Australian Animal Health Laboratory [138] concludes that if RCV had a divergent host range, this would have been demonstrable during the extensive testing undertaken with the virus, both in Australia and elsewhere. There is no evidence of virus multiplication in any of the animals so far tested other than rabbits, a result that has been verified by studies in other countries [138].

RCD has a distinct age profile [126]. It has been observed that rabbits younger than about two months do not develop clinical signs or pathological lesions from RCD, even though they are infected and excrete the virus. The reason for this is not understood and various hypotheses and observations have been made; some of which will be discussed below.

Young rabbits (less than 2 months old) develop an immune response to RCV that can persist for a considerable period [126]. Morisse et al. [71] say that young animals are resistant to the virus, and that experiments conducted in France on groups of 10 young rabbits aged 4-10 weeks and born of antibody-free dams have shown that their susceptibility, zero at 4 weeks, increases rapidly thereafter [See Figure 1.5]. Cancellotti and Renzi [19] observe that from 1986 to 1988 almost all RCD outbreaks in rabbits occurred among adult animals (> 50 days). Williams et al. [131] report that nestling rabbits, less than 18 days old, do not die, but they excrete virus and develop antibodies. Capucci et al. [20] say that newborn animals show a low but detectable anti-RCV titre due to transfer of maternal antibodies. In the majority of young animals, the anti-RCV titre sharply decreases after weaning at the age of 5 weeks, after which they were subject to a new infection detected by a new occurrence of positive titre in the animal. Motha and Clarke [73] claim that infection occurs in rabbits of all ages, but clinical disease is observed only in rabbits more than 40-50 days old. Studdert [112] observes that an "unusual" feature of RCD is that rabbits less than two months of age do not develop fatal illness. Mutze et al. [76] state that most of the antibody-positive survivors were 3-7 weeks old when challenged and that mortality is considerably lower among rabbits younger than 8 weeks compared to older rabbits. From his experiments and observations Villafuerte [120] concluded that only adult animals are affected by RHD, and that only adult animals were found dead. Cooke [141] states that young rabbits are temporarily protected from RHD antibodies acquired from their mothers (maternal immunity). However these antibodies last for only about 8 weeks and, after they are lost, the young rabbits loose their protection and most succumb to RHD. The consensus is therefore that young rabbits below four weeks of age do not develop clinical disease and those between five to eight weeks old are less likely to develop acute disease than susceptible adults. Those born to recovered mothers carry maternal antibodies to RCV acquired through the placenta and retain them till about 8 weeks of age, after which they can suffer a high mortality similar to infected adults [141].

RCD mainly affects the liver, spleen, lymphocytes, lungs, heart and kidney where frequently conspicuous haemorrhagies are observed [41], [63]. The actual cause of death seems to be acute lack

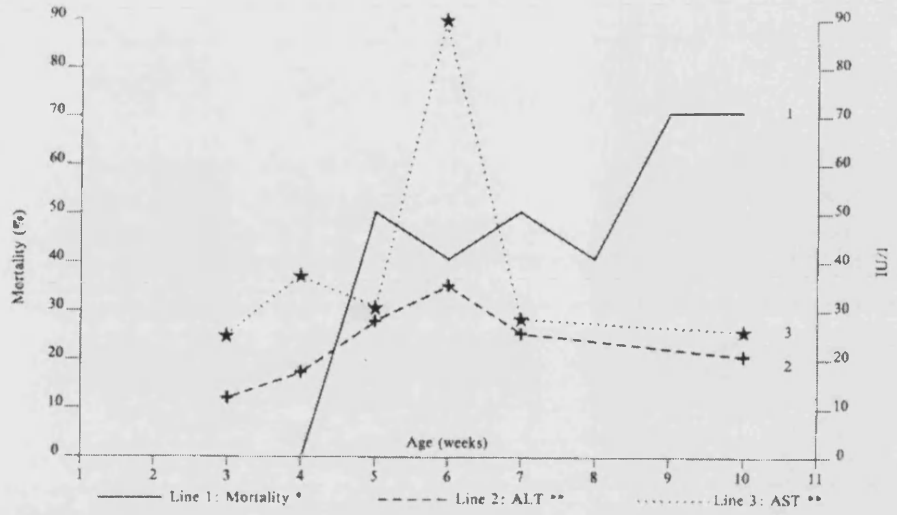


Figure 1.5: Mortality following experimental infection with VHD virus (*Line 1, 7 groups of 10 animals aged 4-10 weeks). Physiological evolution of hepatic transaminases (**Lines 2 and 3, 6 groups of 10 animals aged 3-10 weeks) [71].

of oxygen and heart failure, but a rabbit affected by this disease appears to die quietly with no overt indication of distress [131]. Infection with RHD usually leads to acute clinical disease in 1 to 3 days: such animals usually die 6-12 hours after the onset of the disease [126]. Studdert [112] says that clinically RCD is characterised, after an incubation period of 24 to 48 hours, by a quiet death quickly after the onset of overt symptoms and that more than 90% die within 5 days of infection. Williams et al. [131] affirm that there are no external signs of the disease until 24 hours after infection and rabbits die quietly at 30-40 hours after infection. The mortality rate is 50% for 4-5 week-old rabbits and 95% for rabbits nine weeks or older. Gobbet [49] in his model assumes a non-infectious "incubation" phase of 24 hours followed by a 24 hour infectious phase, then death (100% disease mortality). Barlow [10] suggests that the mean length of the infectious stage is 1.5 days for acute RCD. Motha and Clark [73] say that RHD is characterised by a mortality rate between 40% and 90%, while Mutze et al. [76] say that in their observations 95% of the infected population was considered to have died from RHD.

The mechanism through which the virus is transmitted is not yet clear. One hypothesis which has been suggested is the fecal-oral route, described in section 1.3.1, especially under field conditions [71], [109]. Gregg et al. [51] state that feces of surviving rabbits were infected for up to four weeks

after infection, and indirect transmission from contaminated feed and materials has been reported by Ohlinger et al. [85]. Also it has been observed that infectious virus survives in the carcasses of rabbits killed by RCD: they are therefore a persisting source of virus and so play a role in the maintanance of the virus in the field [139]. In contrast Collins et al. [24] claim that they failed to detect RCV antigens in the feces of infected rabbits.

Another hypothesis suggests the presence of a vector for the mechanical transmission of the disease in the wild; this is because it is highly unlikely that contact between rabbits could explain the high rates of spread of the disease across totally uninhabited areas of arid inland Australia [9]. Flying vectors, scavenging birds or people deliberately moving rabbits remain major possibilities for explaing long distance dispersal [139]. However, the virus is not known to replicate in insects [136]. Insects like bushflies, blowfly species and mosquitoes become contaminated with RCV under natural conditions, but not necessarily to a level compatible with the ability to transmit the disease. Under experimental conditions in the laboratory, iridescent flies (*Phormia* sp.) were able to transmit the disease from the carcass of an infected rabbit to a susceptible host rabbit, resulting in death [45]. In this study, it was shown that as few as ten RCV particles could induce RCD when applied artificially to the conjunctiva of rabbits [45]. In laboratory experiments, bushflies and mosquitoes have also been shown to transmit the disease to susceptible rabbits. In the field, insects can become mechanically contaminated with the virus as a result of feeding on infected rabbits (mosquitoes) or rabbit carcasses (blowflies). Blowflies exploit rabbit carcasses both as a protein source and as a site for oviposition, even when rabbits die underground. In contrast, bushflies have more contact with live rabbits and their feces, as well as exposed rabbit carcasses [136].

In March 1995, tests started within a quarantine compound on Wardang Island, South Australia, to determine the efficacy of RCD as a potential biological control for wild rabbits. Despite all precautions, RCD crossed the quarantine barriers and was found in rabbits elsewhere on Wardang Island in late September 1995. It was then subsequently found on the mainland, initially at Point Pearce, the closest point to Wardang Island. It shortly became apparent RCD had spread far beyond Point Pearce and all attempts to contain it were abandoned. Within three months the virus had spread to a large part of north eastern South Australia and adjoining areas of New South Wales and Queensland [137].

Wardaugh and Rochester [136] noted the slow rate of progression of RCD in summer and used this to argue against the idea that bushflies and other insects could be major vectors of RCD.

They argued that, if RCD arrived in north eastern South Australia and killed an estimated 20 million rabbits, why did the rate of spread of the disease slow noticeably, despite there being a source of virus far, far greater than that provided by the few rabbits on Wardang Island, and in the favourable season for mosquito activity. These observations cast doubt on the proposition that mosquitoes are the primary method of transmission of RCD [136]. It has been suggested that some other factor, possibly related to the survival of the virus, must also be important [137]. For example in eastern South Australia, during summer, air temperatures commonly reach $45^0C$ and soil surface temperatures could be $60^0C$ or more. Consequently, survival of RCD in carcasses, on the soil surface or on day flying insects, is likely to be extremely short [137]. Moreover temperature is the main factor determining bush fly activity [136]. Humidity can also affect virus survival and consequently the epidemiology of RCD. However, bushflies have been shown to transmit the virus in the laboratory and RCD was detected on samples of bushflies collected in the field [137]. The likely involvement of winged vectors also implies the virus will spread more readily in some seasons than in others. Nevertheless, Cooke [137] states that despite the findings that insects may be vectors of the disease, there is no clear evidence to suggest that particular species are of singular importance.

Asgari et al. [9] report that RCV-carrying flies were present during epizootics of RCD. For example flies collected from a South Australian site prior to a deliberate release of the virus were not carrying RCV, whereas virus was detected in flies collected at the site soon after its release [9]. The decline of RNA in contaminated flies over time suggests that the virus does not infect internal tissues of the flies, but rather stays in the alimentary canal and the cuticular lining which is sloughed off at moulting [9]. No virus was detected more than 11 days after contamination of the insect [9]. Also, the detection of the virus in flyspots (oral and/or anal excretions) days after flies fed on contaminated material, and the demonstration that the flyspots contain enough viable virus to cause RCD in susceptible rabbits, further supports the notion that virus-carrying flies can transmit the disease [9]. However, the lack of persistence of virus particles on the legs of flies minimises the likelihood of surface-mechanical transmission of the virus.

The mechanism by which the disease persists in the field is not known. It was detected in frozen rabbit meat and it can survive in certain environmental conditions for up to 6 months [131]. The virus appears to be sensitive to temperature and can survive up to 225 days at $4^0$C but only for 2 days at $60^0$C. It has been detected after 105 days at $20^0$C when dried on cloth [101] and for 20 days (after death) in rabbit cadavers held at room temperature [139].

Seasonality appears to be another characteristic of RCD [62], [13]. Xu and Chen [123] have reported that in China the disease is at its peak between November and March, while less active during the summer, possibly due to the high summer temperatures. In Europe, by contrast, it is more effective from June to December when most juveniles have reached the susceptible age, i.e. are older than two months. It can affect 100% of a susceptible population of rabbits older than two months that hasn't previously been exposed to RCD, otherwise some cases of immunity will be observed. In fact, some biologists have hypothesized the existence of an avirulent strain of the disease, or a strain cross reactive with RCV, [23], [82], [118], [128], on the grounds that 12 years before the existence of the virus was reported, Rodak et al. [100], [101] had related the presence of RCV antibodies in sera collected from rabbits in the Czech Republic.

In summary, various questions remain unanswered about RCD, arising mainly from the inability to grow the virus in tissue culture [110], which is, according to Gould et al. [54], "... a stumbling block to the molecular manipulation of the virus as well as assessing its genetic variability once released into the Australian ecosystem." Moreover, there are many unanswered questions concerning the ecology of rabbits that, if answered, would help in understanding the mechanisms of transmission and persistence of the disease in the natural environment.

# Chapter 2

# Mathematical Models in Ecology and Previous RCD Models

In this chapter we begin by giving a general theoretical overview of mathematical modelling of the dynamics of a single species population (section 2.1), followed by a brief review of some aspects of epidemiological models of micro-parasite infectious diseases (section 2.2). The remaining sections discuss previous mathematical models of RCD.

## 2.1 Population Models

Underlying any mathematical model of disease transmission in an animal population is an assumed model of the population dynamics in the absence of the disease. Such models come in two basic varieties: (1) continuous-time models, in which population variables are tracked, and are assumed to change continuously in time; (2) discrete-time models, in which population variables are tracked only at multiples of a discrete time interval, even though such variables in fact change continuously. The relation between these two types is simple to describe as follows. The general model forms are

$$Continuous : \frac{d\mathbf{N}}{dt} = \mathbf{F}(\mathbf{N}),$$

$$Discrete : \mathbf{N_{t+1}} = \mathbf{N_t} + \mathbf{F}(\mathbf{N_t}),$$

where $\mathbf{N}= (N_1, N_2, ...)$ is a vector of (population) variables, and $\mathbf{F}$ is a vector valued function. Continuous models are determined by *rate* parameters (though they may also contain other, non-

rate parameters, such as carrying capacity), and discrete models are determined by corresponding *transition probabilities*. Thus, to derive a discrete form from a continuous form, we write $d\mathbf{N} = \mathbf{F}(\mathbf{N})dt$. Now replace $d\mathbf{N}$ by $\mathbf{N_{t+1}} - \mathbf{N_t}$, and replace any parameter on the right hand side of the form $\alpha dt$, where $\alpha$ is a rate, by a probability $a$. Thus, if $\alpha$ measures that rate of transition from state $A$ to state $B$, then $a$ measures the probability that this transition will occur in the given unit time interval $t$ to $t+1$. Of course, this scheme can be reversed to obtain continuous models from discrete models.

For ease of exposition we shall develop the following discussion only for continuous models. Parallel discrete formulations can be easily derived using the above scheme.

The simplest continuous-time population model which has any claim to realism has the form

$$\frac{dN}{dt} = \{\lambda(N) - \rho(N)\}N, \tag{2.1}$$

where $N = N(t)$ is the population density at time $t$, $\lambda(N) \geq 0$ is the (possibly density-dependent) average (per-capita) birth rate, and $\rho(N) > 0$ is the (possibly density-dependent) average (per-capita) death rate. It is usual to assume that birth rate can only decline (possibly due to a decline in physiological condition) and that death rate can only increase (due to starvation, increased susceptibility to predation or disease, or to injuries incurred while fighting) as the population density increases. These 'density-dependent' effects, if they exist, essentially result from increased intra-specific competition for scarce resources. For example, assuming no density-dependence in the birth rate, so that $\lambda(N) = \lambda_0$ is a positive constant, and a linear density-dependence in the death rate, $\rho(N) = \rho_0 + \rho_1 N$, we obtain from (2.1) the familiar logistic growth equation:

$$\frac{dN}{dt} = rN(1 - \frac{N}{K}), \tag{2.2}$$

where $r = \lambda_0 - \rho_0$ is the *intrinsic net reproductive rate* (assumed positive), and $K = \frac{r}{\rho_1}$ is the so-called *carrying capacity* of the environment [48]. This equation has an asymptotically stable population density at $N = K$. The other equilibrium $N = 0$, is unstable, so that an arbitrarily small, but positive population will grow and eventually reach equilibrium at $N = K$.

More generally, equation (2.1) has an equilibrium at $N = 0$, which is locally asymptotically stable if $\lambda(0) < \rho(0)$, and unstable if $\lambda(0) > \rho(0)$. In the latter case, small populations will grow, but in the former they will not. Non-zero equilibria are solutions of $\lambda(N) = \rho(N)$. If $\rho(N)$ is strictly

increasing and $\lambda(N)$ is decreasing (or constant), there can be at most one such equilibrium, say at $N = K$. This necessarily implies that $\lambda(0) > \rho(0)$ so that $N = 0$ is unstable. In this case, $N = K$ is necessarily locally asymptotically stable. In the context of disease epidemic models, $N = K$ is referred to as the *disease−free equilibrium.*

This simple model can be extended in various ways. We discuss some of these below, including the incorporation of age-structure and of spatial dynamics.

**Seasonality**. If the animals live in a strongly seasonal environment, then birth and death rates may depend explicitly on time: $\lambda = \lambda(t)$ and $\rho = \rho(t)$. In particular, in a deterministic environment they will be periodic with period one year. For example, a commonly used form to represent seasonal breeding is $\lambda(t) = \frac{1}{2}\lambda_0[1 + cos(\frac{2\pi t}{T})]$, where $T$ is the seasonal length measured in suitable time units (e.g. days), and $\lambda_0$ is the maximum breeding rate during a season.

**Age structure**. Let $n(a,t)$ be the density of the subpopulation of age $a > 0$ at time $t \geq 0$. The variable $n(0,t)$ is the density of newborn animals. Thus, if $\lambda(a)$ is the per-capita average birth rate of animals in the infintessimal age range $a$ to $a + da$, then

$$n(0,t) = \int_{a_m}^{\infty} \lambda(a) n(a,t) da, \tag{2.3}$$

where we have assumed that $\lambda(a) = 0$ for $a \leq a_m$, and $a_m > 0$ is the age at which sexual maturity is attained. For $a \leq a_m$, animals are juveniles. However, this does not necessarily imply that $\lambda(a) > 0$ for $a > a_m$, since young adult animals may be denied the opportunity to breed by older, more dominant adults, even though they could breed if given the chance.

Animals can only enter the class $n(a,t)$ with $a > 0$ by becoming older, whereas they can leave the class by dying. Thus, assuming that ecological time $t$ and age $a$ are measured in the same units, we have $da = dt$, from which it follows that the change $dn(a,t)$ in the class $n(a,t)$ in the infintessimal interval $t$ to $t + dt$ is

$$dn(a,t) = \frac{\partial n}{\partial t} dt + \frac{\partial n}{\partial a} da = -\rho(a) n(a,t) dt,$$

where $\rho(a)$ is the per-capita average death rate for animals of age $a$. We therefore obtain the equation

$$\frac{\partial n}{\partial t} + \frac{\partial n}{\partial a} = -\rho(a) n(a). \tag{2.4}$$

This is known as the *Von Foerster equation* [75]. It is realistic to assume that $n(a,t) = 0$ for $a \geq a_{max}$, where $a_{max}$ is an absolute upper bound for an animal's lifetime.

Of course, in a resource-limited environment, $\lambda(a)$ and/or $\rho(a)$ may depend on the total population density

$$N(t) = \int_0^\infty n(a,t)da,$$

again (usually) with $\lambda(a)$ a decreasing function and $\rho(a)$ an increasing function of $N$.

Write $X(a,t) = \frac{n(a,t)}{N(t)}$. Then, for each $t$, $\mathcal{X}(t) = \{X(a,t) : a \geq 0\}$ defines a probability density function on the interval $0 \leq a < \infty$. This density is known as the *age distribution*. If $X(a,t) \to X^*(a)$ as $t \to \infty$ for some time-independent density $X^*(a)$, then $\mathcal{X}^* = \{X^*(a) : a \geq 0\}$ is known as the *stable age structure*.

As well as being density-dependent as described above, it is also possible for $\lambda(a)$ and/or $\rho(a)$ to depend on the age structure $\mathcal{X}(t)$. For example, if older animals are dominant then they may deny breeding opportunities to younger animals, but the success with which they can do this may depend on how many older adults compared to younger adults there are in the population.

Equations (2.3) and (2.4) are generally difficult to solve analytically except in the simplest case in which $\lambda(a)$ (for $a > a_m$) and $\rho(a)$ are age-independent constants. It is therefore often more convenient to work with a finite, discrete set of (homogeneous) age classes connected by *maturation rates*. Thus, we assume age class densities, $N_0(t), N_1(t), ..., N_m(t)$, and maturation rates $\mu_1, \mu_2, ..., \mu_m$, where $\mu_i$ is the rate of transition from age class $i-1$ to age class $i$. Here, $N_0$ is the lowest age class (juveniles), which includes the newborns. The discrete versions of (2.3) and (2.4) then have the form

$$\begin{aligned} \frac{dN_0}{dt} &= \textstyle\sum_{i=1}^m \lambda_i N_i - \rho_0 N_0 - \mu_1 N_0, \\ \frac{dN_i}{dt} &= \mu_i N_{i-1} - \rho_i N_i - \mu_{i+1} N_i, \quad for \ 0 < i \leq m, \end{aligned} \tag{2.5}$$

where $\lambda_i$ is the birth rate and $\rho_i$ the death rate for age class $i$ (and $\mu_{m+1} = 0$).

The simplest example of such a system is when $m = 1$, and there are two age classes, *Juveniles*, $J = N_0$, and *Adults*, $A = N_1$. In this case it is more convenient to work with the total population density, $N = J + A$, and the adult frequency variable $x = \frac{A}{N}$. Equations (2.5) (for $m = 1$) then

separate into:

$$\begin{aligned} \frac{dN}{dt} &= r(x)N, \\ \frac{dx}{dt} &= \mu(1-x) - \rho_A x - r(x)x, \end{aligned} \tag{2.6}$$

where $r(x) = \lambda x - \rho_J(1-x) - \rho_A x$ is the (frequency-dependent) net reproductive rate. Thus, the second equation is autonomous in $x$, and its possible equilibria and their stability can be easily determined (subject to the constraint that $0 \leq x \leq 1$). In fact, the right hand side of (2.6) is a quadratic in $x$,

$$Q(x) = \mu + Ax - Bx^2,$$

where $A = \rho_J - \rho_A - \mu$ and $B = \lambda + \rho_J - \rho_A$. Since we would usually expect juveniles to have a higher death rate than adults ($\rho_J > \rho_A$), we can assume that $B > 0$. Clearly, $Q(0) = \mu > 0$ and $Q(1) = \mu + A - B = -\lambda < 0$, from which it follows that there is a *unique* equilibrium $x^*$ with $0 < x^* < 1$ and $Q(x^*) = 0$. Since $Q(x) > 0$ for $x < x^*$ and $Q(x) < 0$ for $x > x^*$ it follows from (2.6) that $x^*$ is asymptotically stable. Thus, $x^*$ is the stable age structure. With this age structure, the total population $N$ grows exponentially at rate $r^* = r(x^*)$.

The situation is more complicated if birth or death rates are density dependent; in a restricted environment the growth of any expanding population must eventually be limited by a shortage of resources [97]. For example, suppose juveniles are more strongly affected by population density than adults (e.g. they starve more readily through decreased food supply), say $\rho_0 = \rho_J + \varepsilon N$ with $\varepsilon > 0$. Then equations (2.6) are modified to

$$\begin{aligned} \frac{dN}{dt} &= r(x)N\Big(1 - \frac{N}{K(x)}\Big), \\ \frac{dx}{dt} &= \mu(1-x) - \rho_A x - r(x)x + \varepsilon x(1-x)N, \end{aligned} \tag{2.7}$$

where $r(x)$ is as before and $K(x) = \frac{r(x)}{\varepsilon(1-x)}$. Thus, if there is an asymptotically stable age structure $x^*$, then (after a long time) $N$ grows approximately logistically with intrinsic net reproductive rate $r^* = r(x^*)$ and carrying capacity $K^* = K(x^*)$.

**Males and females.** In most simple population models, such as the logistic (2.2), the population density is taken to be the density of females, since these produce offspring. This assumes that the sex ratio is fixed, usually at $1:1$, and that the male population density will therefore be proportional to the female population density. However, in situations where male life-history characteristics are significantly different from those of females, it is necessary to track the dynamics of both subpopulations.

An example of a simple model with sex ratio $s$ females to $1-s$ males is:

$$\begin{aligned} \frac{dM}{dt} &= (1-s)w\sigma P - \rho_M M, \\ \frac{dF}{dt} &= sw\sigma P + \sigma P - \pi P - \rho_F F, \\ \frac{dP}{dt} &= F - \sigma P - \rho_P P. \end{aligned} \tag{2.8}$$

Here, $M(t)$ is the population density of males, $F(t)$ is the density of non-pregnant females, and $P(t)$ is the density of pregnant females; $\pi$ is the rate at which females become pregnant, $\sigma$ is the rate at which pregnant females give birth (and then revert to being non-pregnant), $w$ is the litter size per birth event (strictly speaking the survivors to adulthood from a litter), and $\rho_M, \rho_F$ and $\rho_P$ are death rates. We assume that pregnant females face the same risks as non-pregnant females, but perhaps some additional risks also, so that $\rho_P \geq \rho_F$. The rate at which females become pregnant of course depends on the males present, at least for small densities, although it may not require many males before the maximum rate is achieved. For example, it would be reasonable to suppose that $\pi = \frac{\pi_0 M}{a+M}$, where $a > 0$ is small, and $\pi_0$ is the maximum pregnancy rate. The average gestation period is $\frac{1}{\sigma}$. However, the model (2.8) assumes that females can again become pregnant immediately after giving birth; a reasonable assumption for rabbits. Also, (2.8) assumes that newborns are immediately sexually mature, though it would be straightforward to add equations for sexually immature juveniles (male and female) after the manner of equations (2.5).

Notice that, apart from the possible dependence of $\pi$ on $M$, the second and third equations in (2.8) are independent of $M$. In particular, if $a$ is small, then it is a reasonable approximation to replace $\pi$ by the constant $\pi_0$, except when $M$ is very small. This shows the redundancy of male dynamics. However, this is only the case so long as the parameters are not density dependent. For example,

females may adjust their litter size in a density-dependent fashion, or fewer newborns may survive to maturity at high population densities. Thus, $w$ may depend on the total population density $N = M + F + P$. Another possibility is if there is competition amongst males to mate with females, so that males may practice infanticide either to bring females more readily into breeding condition (as in lions), or so that females will give preference to a male's own offspring with respect to the provision of resources. In either of these cases $w$ would be a decreasing function of $M$.

**Space.** The models discussed above are spatially homogeneous in that they assume that the population is randomly mixing and that each individual (in its relevant class) has the same access to resources as any other individual (in its class). Of course, in reality animals are dispersed in a spatial domain (2-dimensional for non-flying, non-burrowing terrestrial animals) and move from place to place within that domain. Dispersal effects and spatial heterogeneity can be modelled in two distinct ways: (1) treating space as continuous and animal movement as essentially diffusive; (2) treating space as discrete by representing it as a number of non-overlapping patches, each of which is homogeneous, and with migratory movement of animals between patches.

Continuous models usually take the form of reaction-diffusion equations, with the 'reaction' part of the process representing local birth-and-death (and perhaps other) processes, and the 'diffusive' part representing animal motion between locations. Thus, the single species model (2.1) can be extended to a spatial model of the form

$$\frac{\partial N}{\partial t} = \{\lambda(N,x) - \rho(N,x)\}N - \nabla \cdot [\mathbf{h}(x)N] + D\nabla^2 N, \tag{2.9}$$

where $x = (x_1, x_2)$ is a location in some 2-dimensional continuous spatial domain $\mathcal{D}$, $D$ is a (usually constant) diffusion coefficient, and $\mathbf{h}(x)$ is a vector field on $\mathcal{D}$ representing a preference bias in the direction of movement of animals from each site (taxis); $\nabla$ is the vector differential operator $\nabla = (\frac{\partial}{\partial x_1}, \frac{\partial}{\partial x_2})$ and $\nabla^2$ is the Laplace operator, $\nabla^2 = \frac{\partial^2}{\partial {x_1}^2} + \frac{\partial^2}{\partial {x_2}^2}$. Models of this kind are discussed in detail in [75], but we will not use this approach to spatial modelling in this thesis.

Instead we shall consider patch models. These models go back a long way (e.g. [64]), and versions of them have recently become very popular in the form of so-called *metapopulation models* ([56], [57],[58]). The versions we shall use will be more complicated than standard metapopulation models in that we represent within-patch growth processes explicitly, as well as migratory processes.

A simple version of this model form may be constructed as follows. We suppose space is represented

by a finite number of non-overlapping patches (or sites), $S_1, S_2, ..., S_n$, each of which is homogeneous in the sense that its resident population is randomly mixing and there is no resource heterogeneity within the site. However, sites may differ with respect to their favourability for animals of the given species (e.g. they may differ in carrying capacity). Spatial relationships with respect to possible migration between sites is represented by a *connectivity matrix*, $C = \{c_{ij}\}$, where $0 \leq c_{ij} \leq 1$. Thus, $c_{ij}$ is a measure of the direct accessibility of $S_j$ to animals emigrating from $S_i$. In particular, if $c_{ij} = 0$ then an animal cannot reach site $S_j$ directly from site $S_i$. We take $c_{ii} = 0$ so that an emigrating animal cannot return directly to its native site. A larger value of $c_{ij}$ means that $S_j$ is more easily accessible from $S_i$. For example, in many metapopulation models the form $c_{ij} = \chi_{ij} e^{-\alpha d_{ij}}$ is used, where $d_{ij}$ is a measure of the distance between $S_i$ and $S_j$, $\alpha > 0$ is a constant, and $\chi_{ij}$ is an accessibility index, equal to 1 if $S_j$ is directly accessible from $S_i$, and to 0 otherwise.

In addition, we assume given an *emigration rate*, $e_i$, which determines the rate at which animals leave $S_i$ and join the non-site-attached population of travellers. We also assume that emigrants are exposed to additional hazards while travelling between sites. These are represented by a global hazard rate $h$. Thus, if $N_i$ is the resident population density at $S_i$ and $E_i$ is the density of emigrants from $S_i$, then the population dynamics of this system is given by

$$\begin{aligned} \frac{dN_i}{dt} &= \{\lambda_i(N_i) - \rho_i(N_i)\}N_i - e_i N_i + \sigma \textstyle\sum_j c_{ji} E_j, \\ \frac{dE_i}{dt} &= e_i N_i - h E_i - \sigma c_i E_i, \quad for\ 0 < i \leq m, \end{aligned} \tag{2.10}$$

where $c_i = \sum_j c_{ij}$ and $\sigma$ is a measure of the rate of travel of migrating animals. Thus, $\sigma c_i$ is a measure of the rate at which animals emigrating from $S_i$ arrive at some other site.

This model assumes that animals arriving at a site are necessarily accepted as immigrants. In chapter 11 we shall consider extended versions of this type of model in which potential immigrants are denied admission to a site, and must then move on to search for somewhere more welcoming.

**Stochastic effects.** The models discussed above are all deterministic. Thus, animals all have "average" properties, and processes occur at average rates. In reality animals are subjects to much stochastic variation. This includes environmental variability (e.g. weather effects, resource stochasticity), as well as genetic and phenotypic variability between individuals with respect to life-history characteristics.

Stochastic models which take account of some (rarely all) sources of variability are usually *very* much more complicated than their deterministic counterparts, both with respect to analysis and simulation. In fact, only the most rudimentary stochastic models can by analysed successfully, and it is usually necessary to resort to simulation. This is because the long-run outcome of such a model is not an equilibrium population state (as in most deterministic models) but a stationary probability distribution over all possible population states. In particular, a single simulation run of such a model yields only one possible path along which the population could unfold, and to obtain the long-run stationary distribution it is necessary to execute many simulation runs and count the frequencies of possible outcomes. This can be very expensive in terms of computer running time (as well as data storage requirements). Nevertheless it is often important to understand the influence of stochastic effects.

As a compromise between determinism and a fully stochastic model, a useful approach is to attempt to identify the most important source of stochastic variability which might influence the population dynamics, and to model that while keeping other processes determinate. For example, recall that in the discussion of the logistic model (2.2) a density dependent death rate, $\rho = \rho_0 + \rho_1 N$, was assumed. Suppose that there is stochastic variability in resource availability (perhaps due to weather effects), which is experienced by the animals as changes in the intensity of intraspecific competition for these resources. Then variability in $\rho_1$ is the primary stochastic effect, and so we may treat $\rho_1$ as a random variable, say by assuming that $\rho_1(t)$ is drawn from a stationary lognormal distribution according to some Poisson temporal process. This will be our approach to climatic variability in chapter 4, where we discuss this representation in greater detail.

## 2.2 Modelling Disease Processes

The study of epidemics has a long history with a large variety of models and explanations for the cause and spread of disease outbreaks [75]. In fact, the earliest known model of the spread of infectious diseases was apparently that of Daniel Bernoulli in 1760 for the spread of smallpox. However, Bernoulli's treatment was premature due to the lack of any real understanding of the biophysical basis of infection. This lack discouraged further development until the beginning of the last century, when advances in biology and bacteriology had begun to shed light on disease mechanisms [129]. A classic reference is [60]. More up to date references are [2], [3], [5]. For a

modern approach to modelling smallpox, see [44].

There are now many mathematical models concerned with a number of diseases. For example, sexually transmitted diseases in humans such as AIDS, gonorrhea, chlamydia and syphillis, as well as non-sexually transmitted diseases such as malaria, mumps and measles. These models have sometimes been used to design vaccination programmes ([3] and [4]).

Spatial versions of disease models are less common, though becoming more so. Murray [75] reports an example of a simple model for the spatial spread of an epidemic applied to the Black Death in Europe between 1347 and 1350.

Though diseases affecting humans have been widely studied, models of animal diseases have also been developed. In particular, carnivore diseases play a significant role in species ecology and conservation. For example, *morbilliviruses* such as canine distemper virus (CDV) and phocid distemper virus (PDV), the canine *parvovirus* (CPV), bovine tuberculosis, mange and especially rabies have given rise to great concern recently since they have caused dramatic population declines with the consequent risk of extinction of some endangered species (such as the Medinyi arctic fox [50], the black-footed ferret [130] and the African wild dog [43] ) [42], [133]. Rabies is particularly important for wildlife conservation since it is caused by an RNA virus which is capable of infecting nearly all mammals. Murray [75] gives a detailed analysis of a temporal and spatial model of the spread of rabies amongst red foxes in Europe. For other spatial dynamic models of disease epidemics, see [52] and [53]. In general, the majority of extinctions or near extinctions is caused by generalist pathogens [42]. However, there are important specialist pathogens which have been extensively studied and modelled, in particular myxomatosis in rabbits (see [7], [37], [104], [108]).

In the remainder of this section we give a brief overview of the main principles involved in the mathematical modelling of disease epidemics.

We assume a disease agent (pathogen) which is a "microparasite" such as a virus or a bacterium. This means that the pathogen does not have a complex life history of its own, and that all pathogens are identical and form a single strain. In chapter 16 we shall relax this latter restriction and consider evolutionary effects arising from pathogen mutation between different strains.

Most epidemiological models follow the "$SI$-paradigm" and its elaborations. This assumes that the host population is divided into subclasses consisting of *susceptibles*, of density $S$, and *infecteds* (or sometimes *infectives*), of density $I$. Susceptibles are individuals who do not have the disease,

and infecteds are individuals who do. Elaborations of this model may include a class of *recovereds*, of density $R$, consisting of individuals who have recovered from the disease and have acquired immunity to it. Other possible subclasses are *latents*, who have the disease but do not yet exhibit symptoms. Latents may or may not be infective, depending on the particular disease. These elaborations lead to $SIR$ models or $SLIR$ models. In general, the total population density has the form $N = S + I +$ densities of other classes.

The key to understanding disease dynamics is to identify the route(s) of transmission from an infected (or infective) host to a susceptible. This may be by direct physical contact between hosts, or be mediated by contact between a vector and a host, or between a host and some environmental reservoir of pathogens. The most frequently used assumption in model construction is that the likelihood of infection is equal among members of a population, constant over space [61] and pathogens are passed on by *contact transmission* in a randomly mixing population. We discuss this process in general terms below.

**Contact transmission.** Choose a fixed, focal individual, say $a$, from a population $A$ and consider contacts between this individual and individuals from a population $B$ (which may or may not be the same as $A$). Let $e$ be the encounter rate between $a$ and some other individual from $B$. Thus, $e\delta t$ is the probability with which $a$ meets some other specified individual, say $b$, in the infintessimal time $\delta t$. Random mixing means that this probability is the same for all pairs of individuals $(a, b)$. Thus, the expected number of encounters that $a$ makes in time $\delta t$ is $\sum_{b\in B} e\delta t = e\delta t N_B$, where $N_B$ is the size of population $B$. In particular, the expected number of encounters that $a$ makes with infected individuals from $B$ is $\sum_{b\, infected} e\delta t = e\delta t I_B$, where $I_B$ is the number of infecteds in $B$. Thus, the expected number of encounters between a susceptible individual from population $A$ and an infected individual from population $B$ in time $\delta t$ is $\sum_{a\, susceptible} e\delta t I_B = e\delta t S_A I_B$, where $S_A$ is the number of susceptible individuals in $A$. Thus, if each encounter between a susceptible individual and an infected individual results in the transmission of the disease to the susceptible with probability $\tau$, then the expected *rate* of transmission of the disease from infecteds to susceptibles is $\beta S_A I_B$, where

$$\beta = \tau e. \tag{2.11}$$

By multiplying $e$ by a suitable factor population numbers can be converted into population densities, so that $S_A$ and $I_B$ can be taken to be densities in the above derivation. The resulting $\beta$ is known as the *contact transmission rate*. The resulting disease dynamics then takes the form

$$\begin{aligned} \frac{dS_A}{dt} &= -\beta S_A I_B + \text{other terms}, \\ \frac{dI_A}{dt} &= \beta S_A I_B + \text{other terms}, \end{aligned} \tag{2.12}$$

where $I_A$ is the density of infecteds in population $A$. Note that $e$, and hence $\beta$, can be density dependent. For example, in a spatially confined population, $e$ is likely to increase as the population size increases.

If $A = B$ then disease transmission is by direct physical contact. However, if $A$ is the host population and $B$ is a population of vectors, then transmission is via disease-carrying vectors (e.g. biting insects). In this case a contact process is also needed to describe transmission of the disease from an infected host to a susceptible vector. This will be described by a contact term of the form $\gamma I_A S_B$, where $\gamma = \sigma e$ with $\sigma$ the probability that a susceptible vector acquires the disease on contact with an infected host. Equations (2.12) are then supplemented by corresponding vector equations

$$\begin{aligned} \frac{dS_B}{dt} &= -\gamma I_A S_B + \text{other terms}, \\ \frac{dI_B}{dt} &= \gamma I_A S_B + \text{other terms}, \end{aligned} \tag{2.13}$$

Finally, $B$ may refer to the population of pathogens in an environmental reservoir. In this case, it is necessary to determine how this reservoir is stocked with pathogens. For example,

$$\frac{dI_B}{dt} = \theta - \delta I_B + \omega I_A, \tag{2.14}$$

where $\theta$ is the injection rate of pathogens into the environment from all independent external sources (if any), $\delta$ is the decay rate of pathogens in the environment and $\omega$ is the rate of discharge of pathogens into the environment from infected hosts. We will explore a model of this latter form for RCD in this thesis.

The "other terms" in (2.12) and (2.13) refer to other life-history processes. In particular, to additional disease effects such as disease-induced mortality of hosts, and possibly the loss of acquired immunity by recovered individuals. Vectors are assumed to be passive carriers of the disease and therefore do not suffer increased mortality.

Further complexities can arise in structured populations. For example, in an age structured population in which the disease is transmitted by direct physical contact, different age classes may have different susceptibilities to infection (different $\tau$'s in (2.11)), but they may also have different encounter rates, e.g. if juveniles are less mobile than adults or young adults have restricted access to older adults due to dominance hierarchies. This can result in encounter rates which are frequency dependent; i.e. depend on the population age structure. If the disease alters the age structure, then this may well have the secondary effect of altering the disease transmission characteristics.

The key determinant of whether an introduced disease will invade a disease-free population is the so-called *basic reproductive ratio* (sometimes, incorrectly, *rate*), denoted $R_0$. To illustrate this, consider the simple $SI$-model of a lethal disease (no recovery) incorporating transmission by direct physical contact between hosts:

$$\begin{aligned} \frac{dS}{dt} &= \lambda_0 N - (\rho_0 + \rho_1 N)S - \beta SI, \\ \frac{dI}{dt} &= \beta SI - (\alpha + \rho_0 + \rho_1 N)I, \end{aligned} \tag{2.15}$$

where $N = S + I$, there is a constant birth rate $\lambda_0$ and density dependent natural death rate $\rho = \rho_0 + \rho_1 N$ (as in the logistic model (2.2)), and $\alpha$ is the additional death rate of infecteds from the disease. The disease-free dynamics are obtained by setting $I = 0$, and are given by the logistic equation (2.2), having the stable equilibrium $N = K$, where $K = \frac{r}{\rho_1}$ is the carrying capacity. We wish to determine whether this disease-free equilibrium is stable with respect to the full disease dynamics (2.15). If it is, then the disease cannot invade the disease-free population; if it is unstable, then the disease can invade. Stability is determined by the eigenvalues of the linearized dynamics in a neighbourhood of the disease-free equilibrium. A simple analysis shows that these eigenvalues are both negative (the equilibrium is stable) if and only if $R_0 < 1$, where

$$R_0 = \frac{\beta K}{\alpha + \lambda_0}. \tag{2.16}$$

Thus, if $R_0 > 1$, then there is a positive eigenvalue, and the disease-free equilibrium is unstable.

For more complex models, the expression for $R_0$ in terms of the model parameters is more complicated (see chapter 16 for an example). However, the basic form is always

$R_0 =$ *transmission rate* $\times$ *disease free population size* $\times$ *expected survival time of infected.* (2.17)

This measures the expected number of susceptible individuals in the disease-free population which a single infected individual can infect before it ceases to be infective. In (2.16) the expected survival time of an infected is $T_{surv} = (\alpha + \lambda_0)^{-1}$.

Unfortunately, for complex models such as those for RCD we shall construct in subsequent chapters, it is impossible to find an explicit form for $R_0$.

Spatial extensions of epidemiological models may be developed using the patch dynamics approach (equations (2.10)), in which homogeneous models are used for within-patch processes, but the disease may be carried from patch to patch by migrating infected animals. This is the approach we develop in chapter 11.

## 2.3 Previous RCD Models

In the remaining sections of this chapter we shall review previously constructed models of RCD in rabbits. In fact before the present work, other studies and attempts to model the likely impact of RCD on the European Rabbit in Australia had been done by Barlow [10], Gobbet [49], Cooke [26], CSIRO's Climex model [137] and the Bureau of Rural Sciences Multivariate Statistical Model [140].

## 2.4 Barlow's Direct and Indirect Transmission Models

Barlow [10] built two continuous time models of the effects of RCD on a rabbit population. The models allowed for experimentation on both density dependence and direct and indirect transmission of the virus infecting a seasonally and non-seasonally varying rabbit population. The data on which the model was based was taken from a semi-arid New Zealand environment, where the rabbit population density is normally high and the disease found to be effective. He incorporated in the models the possibility of life immunity of juveniles if exposed to the virus. In his paper [10], he illustrates an analysis of the effects of varying the disease parameters on the outcome of the epidemic, especially in terms of intensity of the disease, its velocity and local persistence in the

environment.

The two models differentiate in that they follow two different assumptions about the disease transmission. The first is that transmission occurs directly between rabbits, from infected to susceptible rabbits, at a rate depending on the densities of both [10]. This is what Barlow [10] calls 'direct transmission' model; the alternative mechanism is that transmission occurs through free-living virus particles. These are assumed to be produced continuously by infected rabbits until they die or recover, and to decay exponentially in the environment with a specified half-life [10]. New infections are produced by susceptible rabbits encountering virus particles. The reason why two modes of transmission were considered by Barlow, is that free-living virus may have a much longer half-life than that of infected rabbits, which may increase the likelihood of persistence of disease in the model; even though epidemics mediated through indirect transmission will be slower than for direct transmission [10].

The direct transmission model, which includes density-dependent mortality, is outlined below:

$$\left.\begin{aligned} \frac{dS}{dt} &= a(N-I) - (b+cN)S - \beta IS; \\ \frac{dI}{dt} &= \beta IS - (b+cN)I - (\alpha+\nu)I; \\ \frac{dR}{dt} &= \nu I - (b+cN)R; \end{aligned}\right\} \tag{2.18}$$

where $S$ is the susceptible, $I$, the infective and $R$ the recovered class, and $N = S + I + R$ is the total population density. $a$ is the birth rate, $b$ the density-independent natural death rate and $c$ denotes the density-dependent mortality rate. $\alpha$, $\beta$ and $\nu$ are the rate of disease mortality, the RCD transmission coefficient and the recovery rate respectively.

The second model, which allows for indirect transmission, together with density dependent mortality and juvenile immunity was constructed as follows:

$$\left.\begin{aligned}
\frac{dJ}{dt} &= a(N-I) - (b+cN)J - hJ - \beta' FJ; \\
\frac{dS}{dt} &= hJ - (b+cN)S - \beta' FS; \\
\frac{dI}{dt} &= \beta' FS - (b+cN)I - (\alpha+\nu)I; \\
\frac{dR}{dt} &= \beta' FJ + \nu I - (b+cN)R; \\
\frac{dF}{dt} &= wI - mF;
\end{aligned}\right\} \tag{2.19}$$

where most of the parameters are the same as the direct transmission model, but this time there is an equation that governs the dynamic of the population density of juvenile rabbits $J$, and so $N = J + S + I + R$ and $\frac{1}{h}$ is the mean duration of the infant stage [10]. This model is based on the assumption that rabbits which become infected during the juvenile stage retain life immunity. $F$ is the density of free living virus; $w$ is the number of infective stages produced per infected rabbit per day, where for infective stages it is meant the unit of virus particle produced per day; $m$ is the proportion of infective stages which die per day and $\beta'$ is now the transmission rate per infective stage, i.e. the proportion of susceptible infected per unit of virus particle per day. These virus units are unknown and cannot be measured; but this is not important, what matters is their relative abundance [10].

Barlow included seasonality of the birth rate in his models by substituting the linear parameter $a$ by a sinusoidal function, namely $f(a,t) = a[1 + z\sin(\frac{2\pi t}{360})]$, where $a$ is now the mean reproductive rate and $1 \leq t \leq 360$ is the time of the year; $z = 0.80$, as a "default value" [10] (arbitrary value), denotes the amplitude of the sine wave as a fraction of $a$.

Some of these parameters were calculated from laboratory data and some from field data in Europe, Australia and New Zealand, while $w$ constitutes the only unknown parameter in the indirect transmission case, so it is mainly arbitrary and with units of free-living virus.

### 2.4.1 Barlow's Results

In his paper Barlow [10] analyzes the effect of juveniles immunity comparing an indirect transmission model which includes Juvenile immunity against one that simply consider one class of susceptible

rabbits, one of infected and one of recovered. For simplicity, the latter was not included in this description of Barlow's work, even though when the difference arisen it is mentioned.

¿From the above described models, Barlow [10] deduced that the basic reproductive rate of the disease, $R_0$, i.e. the expected number of new cases resulting from a single newly-infected rabbit in a susceptible population [10] is

$$R_0 = \frac{\beta K}{(\alpha + \nu + a)} \tag{2.20}$$

for the direct transmission case; while for the indirect transmission with juvenile immunity, $R_0$ is

$$R_0 = \frac{w\beta' K}{m(\alpha + \nu + a)(\frac{a}{h+1})} \tag{2.21}$$

These formulae for $R_0$ assume a density-dependent population with a pre-epidemic density equal to the carrying capacity. $R_0$ is the only quantity that determines the mortality caused by the epidemic, while its speed is related to both $R_0$ and the rate of loss of disease in the environment. In fact the speed of the epidemic is expressed as the reciprocal of the time in days (t) taken for susceptibles to decline by 50%; thus, for the direct transmission the speed of the epidemic varies as $(\alpha+\nu)(R_0-1)$, while for indirect transmission it is approximately related to $m(\alpha+\nu)(R_0-1)$ [10]. This implies that in the direct transmission case, for a given $\alpha$ and $\nu$ , the speed of an epidemic is directly related to the mortality it causes, whereas for indirect transmission the same mortality can be achieved by epidemics of varying speeds depending on the value of $m$. Barlow [10] shows how, in the indirect transmission case, the duration of the RCD epidemic, measured by the decline in rabbit density, increases when the lifespan of free-living virus is increased: this was achieved by reducing the value of $m$ while keeping the ratio $\frac{w}{m}$ constant in order that the final outcome of the epidemic remains the same [10].

The simulation of the long-term behaviour of the disease was carried out by keeping the value of all the parameters at their default value except $m$ and $w$ for the indirect transmission model [10]. The persistence of the disease was strictly determined by the parameter $m$, irrespective of whether juvenile immunity was included in the model or not, even though the latter enhanced the persistence of the disease and altered its dynamic behaviour, giving rise to yearly rather than biennial cycles for most combinations of $m$ and $R_0$. Barlow reached the conclusion that with the default parameters in the indirect transmission case, there is a high probability that if the disease

is to be introduced into a rabbit population, the population would recover over about 5 years after having suffered 92% of mortality, with subsequent epidemics being much smaller than the first one. The direct transmission model yielded the result that the disease either does not persist in time and invariably dies out or goes through 2-yearly cycles. In fact, with a constant or seasonally varying birth rate and a non-persistent RCD, the direct transmission model gives rapid, intense epidemic and recovery of the population in about 5 years. With persistent disease, there are 2-yearly epidemics with oscillations that are more sustained with the seasonally varying birth rate [10].

This suggests the need of a threshold population of susceptibles for the disease to persist in time; and above this threshold, the size of the outbreak, i.e. the proportion of the population affected, is dependent on the size of the susceptible population and hence on the time elapsed since the last outbreak [10]. According to Barlow, persistence in time of the disease seems to be possible only in the indirect transmission model, and only in the case in which the virus half-life is around 2 weeks, which means that the virus is moderately persistent. Then two possible cases will occur: if $R_0$ is very high, there will be a rapid epidemic and all animals remaining immune will reproduce and give life to a new susceptible population. While a low $R_0$ will yield a slow epidemic which will leave half the population susceptible, coexisting with free-living virus, and eventually will regain the threshold density for a new epidemic.

Moreover, Barlow [10] suggested that there is the possibility of a "spatial hide-and-seek" scenario, where the epidemics locally decay but first they infect more remote neighboring areas, which eventually will transmit back the disease to the original site, once the population of that site has reached again the threshold number of susceptibles, thus generating global persistence in the face of local extinction.

The introduction of infant immunity seems to bring a limitation on the efficiency of the disease, especially when this is not persistent, allowing for a faster recovery of the population. While for a persistent epidemic the average level of rabbit suppression is similar to that in the model without immunity [10].

Barlow's suggestion is that a spatial model should be developed, since even though the temporal one provides a good mean of investigation of the disease behaviour, a spatially explicit model might bring to a fuller understanding of the spatial pattern and patchiness of the dynamics of RCD.

## 2.5 Gobbet's Computer Model

Gobbet's aim in constructing and testing a model of the RCD dynamics is to test the model predictions against field observations through the analysis of the data collected through a computing iterative process and stochastic approach and treat of the parameters describing the disease [49]. In particular the aim is to clarify the importance of modes of transmission and weather the virus can persist in the field without the presence of carrier rabbits or sources of re-infection [49].

### 2.5.1 The One-Warren Model

The one-warren model simulates the progress of RCD through a single warren in order to understand what characterizes the progress of the disease. This model will in turn constitute a "sub-model" for incorporation into a spatial model of RCD [49]. The assumptions made in this model include:

- closed population of susceptible adult rabbits, i.e. no births, natural deaths, immigration or emigration;
- all rabbits in the population are assumed to be equally susceptible to RCD;
- the carcass continues to be infective after death: it contributes the same amount of infectious material to the system as a live infectious rabbit;
- mortality was set at 100%;

Gobbet allows for two modes of transmission, direct (from infectious rabbit to susceptible rabbit), depending on the number of infectious rabbit present; and indirect (from infectious rabbit, or its carcass, to the environment, to susceptible rabbit), determined by the amount of free living virus present. He assumes a certain probability that a susceptible rabbit can become infected in one day by defining a "transmission coefficient". Such probability is the sum of both the direct transmission coefficient, $\beta_D$, and indirect transmission coefficient, $\beta_I$, i.e. $\beta_D I + \beta_I V$, where $I$ is the number of infectious rabbits present and $V$ is the amount of free-living virus present. As soon as an infectious rabbit dies, the quantity of free-living virus starts to decay [49]. Gobbet suggested and tried two types of decay: linear and logarithmic. The result was that the linear decay seems to reproduce more closely the field trials modelled in his case. Thus the model simulates the possibility of both transmission patterns taking place in one susceptible population. Moreover it permits the

manipulation of various parameters, among which the initial number of rabbits, the half-life of free-living virus, i.e. the rate at which the free-living virus decays in the model, the number of rabbits inoculated, the direct and indirect transmission coefficients and the linear or logarithmic decay of free-living virus [49].

After determining the optimal values for the parameters, the model was run to find that the value of the indirect transmission coefficient is more influential on the model outcome than that of direct transmission; and that the impact of a field release may be patchy at any particular location since it varies between locations and size of the warren: in areas where the warrens are large, the impact may be more severe than where the warrens are small [49]. A longer virus half-life increases the duration and severity of the outbreak and decreases the proportion of the population that survives the disease.

### 2.5.2 The Multiple Warren Model

This model aimed to develop a computer simulation of RCD affecting a rabbit population incorporating a large number of rabbit warrens and inter-warren transmission, so to analyze the broad scale and long term effects of RCD on the rabbit population. It will allow the investigation of the possibility of persistence of the disease through spatial dynamics [49]. The single warren model indicates that the virus is not likely to persist for long periods (more than a few weeks) in any one warren, but in the field it has been reported that RCD reappears periodically since the initial outbreak. It is not yet known how the virus persists between epizootics, but the possibility of the existence of an "inactive" state has been brought forward. It could be that, between epizootics, the disease is still present but at low levels, maybe because the susceptible population density is not high enough for the disease to take off. Alternatively a mechanism of "spatial hide-and-seek" can explain persistence: spatial heterogeneity and spread [49] sustain the disease and allow its persistence.

The spatial dynamics of rabbit populations incorporates the "source-sink" concept: sources are areas of high productivity (higher birth rate due to the favourable environmental conditions) that may provide emigrants to areas with low or negative productivity (sinks) [49]. The single warren model predicts that larger warrens or denser populations are likely to be more severely affected by RCD. So it seems that "source" areas may be more affected than "sink" areas [49]. The persistence of the disease through "spatial hide-and-seek" [49] was investigated together with optimal timing

and methods of virus release. The assumptions made in this model include:

- all interactions are with immediately adjacent warrens only;
- each warren is at an equal distance from its neighbors;
- all rabbits occupy warrens;
- no new warrens are created;
- no spatial variation, except the differences created by various arrangements of warrens of different sizes;
- each rabbit has an age, which can be neonatal (0 to 42 days), juvenile (43 to 300 days) or adult;
- seasonal variability in birth and death;
- no difference in behaviour between male and female rabbits;
- each warren has a maximum number of rabbits that can occupy it, and it can be of only two sizes: small and large;
- dispersion is density dependent;
- mortality was set at 99%;
- any rabbit that recovers attains a life-long immunity;
- Neonatal immunity up till 6 weeks of age, and lifelong immunity if exposed to the disease;
- no inheritance of immunity;
- no changes in virulence in the virus;

Gobbet approached the concept of seasonal breeding differently from Barlow [10]. More than allowing for a seasonal variation of the breeding rate, he preferred to allow for variability in season quality, since reproduction in rabbits is closely linked to the availability of green feed [49]. So each month can be either "good" (green feed available) or "bad". Births occur in "good" months and death rates of the three age classes are higher in "bad" months.

Each warren in the model has a specific "size", that determines the maximum number of rabbits that may occupy it. According to Gobbet [49] rabbits that are 1 to 2 months old are more prompt to disperse together with older Subadults when the population density of the warren exceeds its "capacity". The death rates of this age class rabbits increase when they disperse, for the risk they suffer before getting established in a new warren. In the model warrens can be either of only 2 sizes [49]: big or small; and the spatial arrangement can be of uniform warren size or random distribution of small and large warrens [49].

In the multiple warren model, as in the single warren one, the parameters that seem to play the main role are the direct and the indirect transmission between warrens, and the virus half-life.

Gobbet [49], like Barlow, found that even though in field observations the disease seems to persist in a susceptible population, it does not behave likewise according to the model result; even though varying the virus half-life increases the duration of the disease in the environment. The model does not replicate the seasonality of disease outbreaks and the basic variation in population levels is more stable than in the field. This is probably due to the lack of understanding of inter-warren transmission dynamics. It may also be that the model population is below the "critical community size" which is the smallest population required for disease persistence [49]. Moreover, contrary to what observed in the infra-warren dynamics it seems that RCD has a stronger impact on larger warrens and denser populations, than smaller ones. The way of release seems not to affect the impact of the disease, while the timing might have an important effect on the proportion of immune rabbits in the population. High values of virus half-life do not have a dramatic effect on the impact and duration of the disease in the environment. No version of Gobbet's model has demonstrated the persistence of RCD through spatial dynamics [49].

To account for the lack of knowledge on inter-warren transmission, Gobbet introduced the possibility of a vector for the disease, namely the Spanish Flea. This seemed to be a way of clarifying the relationship between rabbit population density and contact transmission rates, but still did not account for the speed of spreading of the disease in space.

## 2.6 The CLIMEX Model

This model relates the rate of spread of RCD to climatic and seasonal factors, and explores the likely seasonal changes in the behaviour of the virus [137]; it is assumed that the spread of the

virus is limited at low temperatures (below $12^oC$), because vector activity is low, and at very high temperatures (above $30^oC$), because it does not survive long enough [137]. The results suggest that outbreaks occur and the disease seems to spread faster in spring and autumn and slower in summer. This "bimodal pattern" [26] seem to encourage the hypothesis that insects such as blow flies could be responsible for the spread of the virus since the seasonality of the abundance and activity of such insects is very similar to the one observed for RCD. The CLIMEX model uses parameters such as Temperature, Rainfall, Moisture, Cold Stress, Heat Stress, Wet stress and Dry Stress to predict a pattern for the spread of RCD that could closely match the observed data, and can be used to predict when, during the year, the disease is most likely to spread in any point in Australia. In fact the model takes into account the environmental factors that influence the presence and abundance of rabbits: the assumption being that the virus cannot survive without a susceptible population [137]. From the model results, which match closely the field observations, it is possible to argue against the hypothesis that direct contact transmission is a major mean of spread of RCD virus, and that movements of rabbits cannot account for such rates of spread of the virus [26]. Comparing the biology of the behaviour of bush flies with the prediction of the CLIMEX model, it seems that insects can be responsible for the pattern of virus spread, but they cannot totally account for it, since for example the abundance of bush flies is at its peak in summer, when it is normally too hot for the virus to survive. So there is not a very strong relation between the two phenomena, but insects remain a likely vector for the transmission of RCD to be investigated.

## 2.7 The Multivariate Statistical Model

The multivariate statistical model by CSIRO is another approach to the investigation of the impact of RCD on rabbits in Australia as related to environmental and habitat attributes. The general aim of statistical modeling is to derive a mathematical representation of the relationship between an observed variable and a number of explanatory variables and obtain a suitable frequency distribution for random error [140]. In particular, this type of modeling was used to explore the relationship between decline in rabbit abundance due to RCD and the environmental conditions of the site where the rabbit population considered lived. Such conditions were parameterized so to inspect the relative importance of climatic conditions such as temperature, rainfall and humidity (35 bioclimatic indices in all) in the effect of RCD on the site considered.

The model showed that rabbit abundance can be strongly related to the way in which RCD is introduced into the rabbit population at one particular site [140]; and that generally the virus proved to be more effective where it arrived naturally and was not intentionally released (by inoculation), even though this phenomenon must be considered together with the environmental conditions at release time. In fact the model highlights the environmental conditions, like temperature and humidity, that most strongly can affect the epidemic and endemic behaviour of RCD and strengthen its effectiveness of release [140].

# Chapter 3

# The Time Models

Before constructing a model encompassing both the temporal and spatial dynamics of an RCD epidemic affecting a population of susceptible rabbits in Australia, a simpler model is built to investigate the temporal dynamics solely. This model will then be used as a building block for the spatial model and it will reproduce the dynamics of a rabbit population in a single site, i.e. mimic the biology of a warren or a group of highly interconnected warrens in a homogeneous spatial region.

## 3.1 The Single Site Model

In the Single Site model the discrete variables are the population classes whose value is updated each day. Different possible stages in the life of the rabbit are considered as age classes, together with a class of pregnant females. This model will be described and analyzed first as a population dynamic model without any disease, and subsequently the disease will be incorporated. The reason behind this is to first build a model that can come the closest to represent the reality of the dynamics of a susceptible rabbit population and, after the values of relevant parameters have been estimated, the disease will be inserted and the outcome investigated.

### 3.1.1 The Single Site Model without the Disease

The model variables are the different age classes in the rabbit population at a given time $t$; these are: $S_J[t]$, the class of Susceptible Juveniles; $S_Y[t]$, the class of Susceptible Subadults; $S_{A_{M,F}}[t]$, the

class of Susceptible Adults (Male or Female); $S_P[t]$, the class of Susceptible Pregnant Females. The principal reason for this particular age division comes mainly from field data and the biology of RCD which is described in section 1.5.2. Most of the literature indicates that Juveniles are naturally immune to the disease up till 8 weeks of age, while Subadults are rabbits that can become infected with the disease but are not yet sexually mature. Fenner and Ratcliffe [37] affirm that a rabbit does not reach sexual maturity until 3 or 4 months of age [section 1.3.5], thus in this model it will be assumed that the Subadults class is formed by those rabbits that are not sexually mature but are susceptible to the disease, i.e. in the age between 8 weeks and 12 weeks (2 to 3 months of age). We prefer from now on to call this class Youngsters to avoid confusing notation. Those belonging to the adult classes are susceptible to the disease and sexually mature, while pregnant females are females from the adult female class that are pregnant. A diagram illustrating the class divisions used in this model is given in figure 3.1.

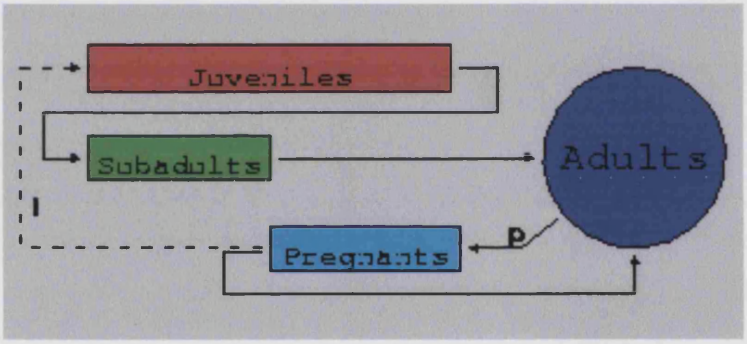


Figure 3.1: Block Diagram of life stages duration (p is the pregnancy rate).

In the following model there is no allowance for the existence of the disease as yet, but the variables are already denoted in a way which will make easier the distinction between classes once the disease is inserted (see equations (3.1)). Each class will be denoted by both an 'absolute' time and a 'counter' time that 'counts' the age of the animal and so determines when the rabbit switches class: for example $S_J[t]$ will now be $S_J[t,k]$: the members of class $S_J$ who have spent $k$ days in the Juvenile class at time $t$ ($t$ represents the absolute time and $k$ the counter), i.e. they entered the class $S_J$ on day $t-k$. The age counter, $k$, has range $1 \leq k \leq n_J$, where $n_J$ is the age at which a juvenile becomes a youngster. The same applies for the Youngster and Pregnant classes, with $n_Y$ and $n_P$ being the duration time of the Youngster and Pregnant class, respectively. In particular $S_J[t,0]$, $S_Y[t,0]$ and $S_P[t,0]$ are the new entrants to the indicated class on day $t$. A few

assumptions are made on the model (equations (3.1) below): Adults are of unspecified age, and thus do not have a $k$ counter or a class duration $n_A$; Youngsters become Adult males or females with probability $\frac{1}{2}$; and Pregnant females who have given birth, i.e. $S_P[t, n_P]$, return to the adult female class, but are available to become pregnant again on the next day. This last assumption is based on what reported in the literature (see section 1.3.2). The model has the form:

$$\left.\begin{aligned}
S_J[t+1,0] &= \lambda(1-m_A)S_P[t,n_P]; \\
S_J[t+1,k] &= (1-m_J)S_J[t,k-1]; \qquad (1 \le k \le n_J) \\
S_Y[t+1,0] &= (1-m_J)S_J[t,n_J]; \\
S_Y[t+1,k] &= (1-m_Y)S_Y[t,k-1]; \qquad (1 \le k \le n_Y) \\
S_{A_M}[t+1] &= (1-m_A)S_{A_M}[t] + \tfrac{1}{2}(1-m_Y)S_Y[t,n_Y]; \\
S_{A_F}[t+1] &= (1-m_A)((1-\bar{\pi})S_{A_F}[t] + S_P[t,n_P]) + \\
&\quad \tfrac{1}{2}(1-m_Y)S_Y[t,n_Y]; \\
S_P[t+1,0] &= \bar{\pi}(1-m_A)S_{A_F}[t]; \\
S_P[t+1,k] &= (1-m_A)S_P[t,k-1]; \qquad (1 \le k \le n_P)
\end{aligned}\right\} \qquad (3.1)$$

where

- $\lambda$ is the litter size of newborns per pregnant female,
- $\bar{\pi}$ is the fraction of Adult Females which become pregnant per day,
- $m_J$, $m_Y$ and $m_A$ are the natural death rate per day of Juveniles, Youngsters and Adults respectively. Pregnant females are assumed to have the same natural death rate as Adults.

A more detailed description of the parameters, what they represent and how their numerical values were derived from the biological data, is given in the section below.

### 3.1.2 The Basic Parameters

In this section we use data from the literature to estimate the parameters of the model (3.1).

- $\lambda = 4$ is the litter size per pregnant female. This value for $\lambda$ was taken from the data given by Williams et al. [131] (see section 1.3.2), who affirm that the mean litter of a large sample will fall between 3 and 7 young per female rabbit. A value below the average of these extremes was chosen since the field data [47] shows that females reach full litter size at 10 months of age, while the females in this model can become pregnant as young as 3 months, so their litter size will be smaller.

- $\bar{\pi}$ is the rate at which Adult Females become pregnant per day. Williams et al. [131] affirm that the gestation period is 30 days. The probability that a female can become pregnant is bound with the probability that it gives birth, in fact it has been observed that *post − partum oestrus* can stimulate a doe to mate again after it has given birth [see section 1.3.2]. Also note that $\bar{\pi}$ is not a constant rate but a function of the seasonal conditions during the year [see section 1.3.2]. The nature of this seasonal dependence will be discussed in chapter 4.

- $m_J$, $m_Y$ and $m_A$ represent the natural death rate per day of Juveniles, Youngsters and Adults respectively. They were calculated using data from Cowan's paper [31], which is reported in table 1 in the next page.

Table 1: Cowan's data showing the variation with sex in the numbers of juveniles at risk of dying during the age intervals, their mortality rates $q_x$, and their survival probabilities $l_x$.

| Age interval $(x-1) \to x$ (weeks) | Mortalily rate $(x-1) \to x$ $q_x$ | | Survival probability to age $x$ $l_{x-1}$ | |
|---|---|---|---|---|
| | m | f | m | f |
| 4-8 | 0.63 | 0.52 | 1.000 | 1.000 |
| 8-12 | 0.43 | 0.29 | 0.368 | 0.482 |
| 12-16 | 0.30 | 0.21 | 0.211 | 0.343 |
| 16-20 | 0.21 | 0.21 | 0.149 | 0.272 |
| 20-24 | 0.17 | 0.22 | 0.117 | 0.214 |
| 24-28 | 0.20 | 0.18 | 0.098 | 0.167 |
| 28-32 | 0.17 | 0.19 | 0.079 | 0.137 |
| 32-36 | 0.07 | 0.11 | 0.065 | 0.111 |
| 36-40 | 0.04 | 0.07 | 0.060 | 0.099 |
| 40-44 | 0.02 | 0.10 | 0.058 | 0.092 |
| 44-48 | 0.06 | 0.01 | 0.057 | 0.083 |
| 48-52 | 0.09 | 0.01 | 0.053 | 0.082 |
| $> 52$ | — | — | 0.048 | 0.080 |

Cowan gives a different value for the death rate of males and females of a particular age: the average between these two was used to calculate the death probability per day, since the model does not really differentiate between male and females, except in relation to pregnancy.

As it was assumed that the Juvenile age for a rabbit goes from 0 to 2 months following Williams et al. [131], the daily death rate of a juvenile was calculated using Cowan's [31] data in the following way:

The death probability from 4 to 8 weeks (Juvenile age), according to Cowan, is $\frac{1}{2}(0.63+0.52) = 0.575$ (see table 1, column 2); since no figure is given by Cowan for the period $0-4$ weeks, we take the death probability in such period to be 0. If we assume that young juveniles do not leave the nest till four weeks old, this means that all newborns are assumed to survive for

the first four weeks. Of those born on a particular day, 57.5% of them are dead by 8 weeks. Then the probability of survival to 8 weeks of age is

(probability of survival to age 4 weeks) $\times$ (probability of survival from 4 to 8 weeks of age), i.e.

$$1.0 \times (1 - 0.575) = 0.425$$

$$(1 - m_J)^{56} = 1 - 0.575 = 0.425$$

(see table 1); so the daily probability of death through the Juvenile phase, using Cowan's value for the survival probability, is:

$$m_J = 1 - (0.425)^{\frac{1}{56}} = 0.015$$

where $n_J = 56$ is the length in days of the Juvenile life stage.

In the same way $m_Y$ and $m_A$ were calculated and it was assumed that $m_P$=$m_A$, i.e. that the mortality rate for Pregnant Females is the same as the one for the Adult class from which they come from.

The Subadult, or Youngster, age for a rabbit is assumed to last 4 weeks ($n_Y = 28$) [see section 1.5.2]. The average death probability from 8 to 12 weeks (Youngster age), according to Cowan, is $\frac{1}{2}(0.43 + 0.29) = 0.36$ (see table 1, column 2), so the daily probability of survival through the Youngster phase is given by:

$$(1 - m_Y)^{28} = 1 - 0.36 = 0.064$$

where $n_Y = 28$ is the length in days of the Youngster life stage. It follows that

$$m_Y = 1 - (0.064)^{\frac{1}{28}} = 0.016$$

In order to calculate the Adult death rate, the Annual Survival Probability (ASP) [31] for rabbits older than one year will be used instead of the mortality rate. The notation we use is:

$$sp = ({s_A}^{x \to y})^z$$

where $s_A$ is the daily survival probability; $x \to y$ is the time interval for that survival probability, $z$ is the number of days in the interval $x \to y$, and $sp$ is the survival probability for the entire time interval considered.

¿From Table 1, the survival probability from 0 to 52 weeks (one year) of age is $({s_A}^{0 \to 1year})^{365} = \frac{1}{2}(0.048 + 0.080) = 0.064$ (see table 1, column 3); and the survival probability from 0 to 12 weeks (three months) of age is $({s_A}^{0 \to 3months})^{84} = \frac{1}{2}(0.211 + 0.343) = 0.277$ (see table 1, column 3); it follows that the daily survival probability from three months of age to one year is:

$$({s_A}^{3months \to 1year})^{365-84} = \frac{0.064}{0.277}$$

$$\Rightarrow ({s_A}^{3months \to 1year}) = (\frac{0.064}{0.277})^{\frac{1}{281}}$$

¿From Cowan [31] the average Annual Survival Probability for two-year-old rabbits, i.e. Adult individuals, is $\frac{1}{2}(0.36 + 0.47) = 0.415$; that is a one year old adult has a survival probability through its second year of 0.415.

It follows that the daily probability for a one year old rabbit to survive through the second year of its life is:

$$({s_A}^{1year \to 2years})^{365} = 0.415$$

$$\Rightarrow {s_A}^{1year \to 2year} = (0.415)^{\frac{1}{365}}$$

Then from Table 1 it is possible to calculate the daily survival probability from 3 months (= 12 weeks = 84 days)up to 2 years of age in the following way:

$$({s_A}^{3months \to 2years})^{281+365} = ({s_A}^{3months \to 1year})^{281}({s_A}^{1year \to 2years})^{365}$$

$$\Rightarrow {s_A}^{3months \to 2years} = (\frac{0.064}{0.277} \times 0.415)^{\frac{1}{281+365}} = 0.996377 \approx 0.996$$

Thus, the daily death rate for adults from 3 months to 2 years old is:

$$m_A = 1 - {s_A}^{3months \to 2years} = 1 - 0.996 = 0.004$$

It is assumed that the daily death rate will remain constant for the rest of the life span of the rabbit.

### 3.1.3 The Single Site Model with the Disease

Concerning the way RCD affects a susceptible rabbit population, there are two hypotheses. The first, asserts that Juveniles are immune for the first 2 months of their lives, during which time, if they contract the disease, they are carriers and can infect other individuals but do not die from the disease themselves and subsequently recover and retain life-time immunity. This is the basis of Barlow's model [10]. We will call this hypothesis the *Strong Juvenile Hypothesis* (or the Strong Hypothesis).

The second hypothesis, derived from Morisse [71], asserts that Juveniles are immune in the first month of their life, even though they can transmit the disease, and after the first month they remain immune for another month only if they were born to recovered does that have supplied them with maternal antibodies. Such "maternal immunity" decays in time until the rabbit becomes fully susceptible at the age of 8 weeks (see section 1.5.2 and figure 1.5). We will call this hypothesis the *Weak Juvenile Hypothesis* (or the Weak Hypothesis). That is, Juveniles are immune for half the time compared to the Strong hypothesis (if the Juveniles are not born to recovered does). The majority of authors who have written about the age susceptibility of RCD infection quote Morisse [71] as a main reference, but they consistently fail to follow Morisse's observations in his paper "Hepatitis of Viral Origin in Leporidae: introduction and aetiological hypotheses" (see section 1.5.2).

Most of the reported observations support one or the other of these two hypotheses, and since it is difficult to determine which comes closest to reality, two different models were developed to simulate what happens in each case.

A block diagram of the class division in the presence of the disease is illustrated in figure 3.2 at the end of this section and the model of the Strong Hypothesis is given by equations (3.2) on the following page.

$$
\begin{aligned}
S_J[t+1,0] &= \lambda(1-m_A)(S_P[t,n_P]+R_P[t,n_P]);\\
S_J[t+1,k] &= (1-m_J)(1-c_V)S_J[t,k-1];\\
I_J[t+1,k] &= (1-m_J)(c_V S_J[t,k-1]+(1-\nu_J)I_J[t,k-1]);\\
R_J[t+1,k] &= (1-m_J)(\nu_J I_J[t,k-1]+R_J[t,k-1]); \qquad (1\le k\le n_J)
\end{aligned}
$$

$$
\begin{aligned}
S_Y[t+1,1] &= (1-c_V)(1-m_J)S_J[t,n_J];\\
S_Y[t+1,k] &= (1-c_V)(1-m_Y)S_Y[t,k-1];\\
I_Y[t+1,1] &= (1-m_J)(c_V S_J[t,n_J]+(1-\nu_J)I_J[t,n_J]);\\
I_Y[t+1,k] &= (1-m_Y)(c_V S_Y[t,k-1]+(1-CM-\nu_Y)I_Y[t,k-1]);\\
R_Y[t+1,1] &= (1-m_J)(R_J[t,n_J]+\nu_J I_J[t,n_J]);\\
R_Y[t+1,k] &= (1-m_Y)(R_Y[t,k-1]+\nu_Y I_Y[t,k-1]); \qquad (2\le k\le n_Y)
\end{aligned}
$$

$$
\begin{aligned}
S_{A_M}[t+1] &= (1-c_V)((1-m_A)S_{A_M}[t]+\tfrac{1}{2}(1-m_Y)S_Y[t,n_Y]);\\
I_{A_M}[t+1] &= \tfrac{1}{2}(1-m_Y)(c_V S_Y[t,n_Y]+(1-CM-\nu_Y)I_Y[t,n_Y])+\\
&\quad (1-m_A)(c_V S_{A_M}[t]+(1-CM-\nu_A)I_{A_M}[t]);\\
R_{A_M}[t+1] &= (1-m_A)(R_{A_M}[t]+\nu_A I_{A_M}[t])+\\
&\quad \tfrac{1}{2}(1-m_Y)(R_Y[t,n_Y]+\nu_Y I_Y[t,n_Y]);
\end{aligned}
\tag{3.2}
$$

$$
\begin{aligned}
S_{A_F}[t+1] &= (1-c_V)(1-m_A)((1-\bar{\pi})S_{A_F}[t]+S_P[t,n_P])+\\
&\quad \tfrac{1}{2}(1-m_Y)(1-c_V)S_Y[t,n_Y];\\
I_{A_F}[t+1] &= \tfrac{1}{2}(1-m_Y)(c_V S_Y[t,n_Y]+(1-CM-\nu_Y)I_Y[t,n_Y])+\\
&\quad (1-m_A)(c_V(1-\bar{\pi})S_{A_F}[t]+c_V\textstyle\sum_{k=1}^{n_P}S_P[t,k]+(1-CM-\nu_A)I_{A_F}[t]);\\
R_{A_F}[t+1] &= (1-m_A)(R_P[t,n_P]+(1-\bar{\pi})R_{A_F}[t]+\nu_A I_{A_F}[t])+\\
&\quad \tfrac{1}{2}(1-m_Y)(R_Y[t,n_Y]+\nu_Y I_Y[t,n_Y]);
\end{aligned}
$$

$$
\begin{aligned}
S_P[t+1,1] &= (1-c_V)(1-m_A)\bar{\pi}S_{A_F}[t];\\
S_P[t+1,k] &= (1-c_V)(1-m_A)S_P[t,k-1];\\
R_P[t+1,1] &= \bar{\pi}(1-m_A)R_A[t];\\
R_P[t+1,k] &= (1-m_A)R_P[t,k-1]; \qquad (2\le k\le n_P)
\end{aligned}
$$

$$
W[t+1] = (1-m_V)W[t]+(\textstyle\sum_{k=1}^{n_J}I_J[t,k]+\sum_{k=1}^{n_Y}I_Y[t,k]+I_{A_M}[t]+I_{A_F}[t]);
$$

Some of the variables and parameters have been described in the previous sections. By inserting the disease, each age class, excluding the Pregnant Female class, is in turn divided into three subclasses: Susceptible, $S_a$, Infected, $I_a$ and Recovered, $R_a$, where $a$ indicates the age class they belong to; that is, $a = J$, $Y$, $A_M$, $A_F$ or $P$. The Susceptible class is formed by those individuals that have not yet caught the disease; the Infected class is formed by those individuals that have come into contact with the virus, have become infected and are then infective. Infected individuals can either survive or succumb to the disease; Recovereds are those individuals who have survived the disease and, it is assumed, will retain life-time immunity, following Barlow [10], since the literature reports that a recovered individual retains an immunity to the virus, but it is not clearly stated how long the immunity lasts, and it is not known whether they can become susceptible to a second infection [131] since their life span in the wild is relatively short. The Pregnant females are only divided into two subclasses: Susceptibles and Recovereds ($S_P$ and $R_P$). Here, it is assumed that the stress a pregnant female goes through when infected with RCD will cause a resorbtion *in uterum in toto* of the litter (see section 1.3.2). Thus, in the above model, a pregnant female who becomes infected with RCD will leave the Pregnant class during the subsequent day and join the Adult Female Infected class $I_{A_F}$. Note that the Recovered Pregnant Females are actually recovered adults that subsequently become pregnant.

Even though it has been shown that insect vectors could be one of the means of RHDV transmission in the field, we will not include in the model the specific dynamics of an insect vector. This is because of various issues: the activity of RCV is unlikely to be linked with a specific vector [141], so it would be necessary to include the seasonal dynamics of bushflies, mosquitoes and blowflies. In addition would have to take into account indeces of temperature and humidity for different geographical environments, because these affect the survival of the virus in flyspots (see section 1.5.2). This would result in the variability of the virus decay rate. This would complicate further an already complicated model, which would make it difficult to track back the contribution of the modellede variables. Since the surface-mechanical transmission of the virus is unlikely [9], the model assumes an indirect mode of transmission of the disease: we assumed the existence of a quantity of virus particles, or viral load, in the environment, quite similar to Barlow [10]'s assumption in his indirect transmission model (see section 2.1). These virus particles can be related to flyspots of viable virus [9] or conataminated faeces (see section 1.5.2). This viral load is represented in the model by the variable $W[t]$ and depends on the number of infected animals, which release viral particles. Free viral particles decay at a daily rate $m_V$. Since the value of the virus infectivity, $c_V$, cannot

be calculated from field data, due to the lack of knowledge of the means of virus transmission, it represents the only unknown parameter that bounds the effectiveness of the disease. Varying the value of $c_V$ in the different runs will allow an investigation of the possible outcomes of different strains of the disease on a susceptible rabbit population (see section 3.1.4 for an explanation of the disease parameters, and chapter 7 and 8 for the results).

Our second model, representing the Weak hypothesis, is set out in equations (3.3) on the following page.

The notation is slightly more complicated here since it has to allow for more than one class of susceptible juveniles. $S_J[t]$ is the class of Susceptible Juveniles born from Susceptible females; as a result they do not have maternal antibodies and are immune to the disease only up till one month of age. Subsequently they can catch the disease and then either die or recover. If they recover they remain immune for the rest of their lives. $S_{J\_}[t]$ is the class of Susceptible Juveniles that were born to Susceptible females, and so do not have maternal antibodies, and are older than one month of age. Individuals belonging to this class can catch the disease. Finally, $S_{J+}[t]$ is the class of Susceptible Juveniles born from Recovered females. These individuals are fully immune in the first month of age due to maternal antibodies, but their immunity decays slowly during the second month of age until they become fully susceptible to the disease on entering the Subadult class at 56 days (see section 3.1.4 for an explanation of the disease parameters, and chapter 9 and 10 for the results).

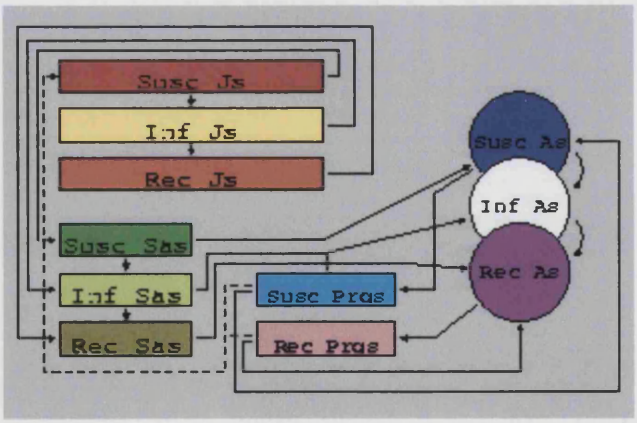


Figure 3.2: Block Diagram of life-stage duration with the disease. Js=Juveniles, Sas=Subadults, As=Adults, Prgs=Pregnants, Susc=Susceptible, Inf=Infected, Rec=Recovered.

$$
\begin{aligned}
S_J[t+1,0] &= \lambda(1-m_A)S_P[t,n_P];\\
S_J[t+1,k] &= (1-m_J)S_J[t,k-1]; \qquad (1\le k\le 28)\\
S_{J-}[t+1,1] &= (1-m_J)(1-c_V)S_J[t,28];\\
S_{J-}[t+1,k] &= (1-m_J)(1-c_V)S_{J-}[t,k-1]; \qquad (2\le k\le 28)\\
S_{J+}[t+1,0] &= \lambda(1-m_A)R_P[t,n_P];\\
S_{J+}[t+1,k] &= (1-m_J)S_{J+}[t,k-1]; \qquad (1\le k\le n_J)\\
I_J[t+1,1] &= (1-m_J)c_V S_J[t,28];\\
I_J[t+1,k] &= (1-m_J)(c_V S_{J-}[t,k-1]+(1-CM_- -\nu_J)I_J[t,k-1]); \qquad (2\le k\le 28)\\
R_J[t+1,k] &= (1-m_J)(R_J[t,k-1]+\nu_J I_J[t,k-1]); \qquad (2\le k\le 28)
\end{aligned}
$$

$$
\begin{aligned}
S_Y[t+1,1] &= (1-m_J)((1-c_V)S_{J-}[t,n_J]+S_{J+}[t,n_J]);\\
S_Y[t+1,k] &= (1-c_V)(1-m_Y)S_Y[t,k-1];\\
I_Y[t+1,1] &= (1-m_J)(c_V S_{J-}[t,28]+(1-CM_- -\nu_J)I_J[t,28]);\\
I_Y[t+1,k] &= (1-m_Y)(c_V S_Y[t,k-1]+(1-CM-\nu_Y)I_Y[t,k-1]);\\
R_Y[t+1,1] &= (1-m_J)(R_J[t,28]+\nu_J I_J[t,28]);\\
R_Y[t+1,k] &= (1-m_Y)(R_Y[t,k-1]+\nu_Y I_Y[t,k-1]); \qquad (2\le k\le n_Y)
\end{aligned}
$$

$$
\begin{aligned}
S_{A_M}[t+1] &= (1-c_V)((1-m_A)S_{A_M}[t]+\tfrac{1}{2}(1-m_Y)S_Y[t,n_Y]);\\
I_{A_M}[t+1] &= (1-m_A)(c_V S_{A_M}[t]+(1-CM-\nu_A)I_{A_M}[t])+\tfrac{1}{2}(1-m_Y)\\
&\quad (c_V S_Y[t,n_Y]+(1-CM-\nu_Y)I_Y[t,n_Y]);\\
R_{A_M}[t+1] &= (1-m_A)(R_{A_M}[t]+\nu_A I_{A_M}[t])+\tfrac{1}{2}(1-m_Y)(R_Y[t,n_Y]+\nu_Y I_Y[t,n_Y]);\\
S_{A_F}[t+1] &= (1-c_V)(1-m_A)((1-\bar{\pi})S_{A_F}[t]+S_P[t,n_P])+\tfrac{1}{2}(1-m_Y)(1-c_V)S_Y[t,n_Y];\\
I_{A_F}[t+1] &= \tfrac{1}{2}(1-m_Y)(c_V S_Y[t,n_Y]+(1-CM-\nu_Y)I_Y[t,n_Y])+(1-m_A)((1-CM-\nu_A)I_{A_F}[t]+\\
&\quad c_V(1-\bar{\pi})S_{A_F}[t]+c_V\textstyle\sum_{k=1}^{n_P}S_P[t,k]);\\
R_{A_F}[t+1] &= (1-m_A)(R_P[t,n_P]+(1-\bar{\pi})R_{A_F}[t]+\nu_A I_{A_F}[t])+\tfrac{1}{2}(1-m_Y)(R_Y[t,n_Y]+\nu_Y I_Y[t,n_Y]);\\
S_P[t+1,1] &= (1-c_V)(1-m_A)\bar{\pi}S_{A_F}[t];\\
S_P[t+1,k] &= (1-c_V)(1-m_A)S_P[t,k-1]; \qquad (2\le k\le n_P)\\
R_P[t+1,1] &= (1-m_A)\bar{\pi}R_{A_F}[t];\\
R_P[t+1,k] &= (1-m_A)R_P[t,k-1];\\
W[t+1] &= (1-m_V)W[t]+(\textstyle\sum_{k=1}^{28}I_J[t,k]+\sum_{k=1}^{n_Y}I_Y[t,k]+I_{A_M}[t]+I_{A_F}[t]);
\end{aligned}
\tag{3.3}
$$

### 3.1.4 The Parameters of the Disease

When a rabbit becomes infected with RCD, the possible outcomes from this "event" are death ($D$), recovery ($R$) or neither death nor recovery ($N$). The probabilities for each of these outcomes are $CM$, $\nu$ and $1 - CM - \nu$ respectively. Suppose an "event" like this takes place each day, and the process terminates when either $D$ or $R$ occurs. Then $e_D$, the probability that a rabbit will die after catching the disease, is

$$e_D = \sum_{n=1}^{\infty}(1 - CM - \nu)^{n-1}CM = \frac{CM}{CM + \nu} \tag{3.4}$$

while $e_R = 1 - e_D$, the probability that a rabbit will recover, is

$$e_R = \sum_{n=1}^{\infty}(1 - CM - \nu)^{n-1}\nu = \frac{\nu}{CM + \nu} \tag{3.5}$$

where $n$ is the number of days. For example, if 95% of infected animals eventually die, then $e_D = 0.95$ and $e_R = 0.05$. In particular,

$$\frac{e_R}{e_D} = \frac{\nu}{CM}. \tag{3.6}$$

The expected time to the first termination of process (either $D$ or $R$) is

$$\bar{T} = \sum_{n=1}^{\infty} n(1 - CM - \nu)^{n-1}(CM + \nu) = \frac{1}{CM + \nu} = \frac{e_D}{CM} \tag{3.7}$$

if this termination yields a death, then we can call $\bar{T} = \tau$ days (which occurs with probability $e_D$). That is, conditional on an infected animal eventually dying, we have

$$CM = \frac{1}{\tau}e_D. \tag{3.8}$$

$$\nu = \frac{1}{\tau}e_R. \tag{3.9}$$

- $c_V$ is the probability per day that a rabbit becomes infected with RCD. If we call $V[t]$ the viral load in the environment, we can write an expression for $V[t]$ in the following way:

$$V[t+1] = (1 - m_V)V[t] + \sum_{a,k} wI_a[t,k] \qquad (1 \leq k \leq n_a) \qquad (3.10)$$

where $m_V$ is the death rate of the virus; $a$ is the age class, so it can be $J$ for juveniles, $Y$ for youngsters or $A_{M,F}$ for adults; $w$ is the rate of production of virus per infected per day, and $I_a[t] = \sum_{k=1}^{n_a} I_a[t,k]$ is the infective population of class $a$ at time $t$.

We assume a function relating the viral load $V[t]$ to the probability of infection $c_V$ of the Michaelis-Menton form:

$$c_V = \frac{V[t]}{c + V[t]}$$

where $c > 0$ is a constant. $c_V$ is a saturated function with $c_V(0) = 0$ and $c_V \to 1$ as $V \to \infty$. Then $c$ is an inverse measure of the "virulence" of the virus strain in the sense that the smaller $c$ is, the lower the viral load $V[t]$ needs to be to attain any given probability of infection $c_V$.

We can now do a parameter reduction as follows: define $W = \frac{V}{w}$ and substitute in equation (3.10) by dividing both sides by $w$ to get

$$W[t+1] = (1 - m_V)W[t] + \sum_a I_a[t]$$

Then we can write

$$\begin{aligned} c_V &= \frac{V[t]}{c+V[t]} \\ &= \frac{wW[t]}{c+wW[t]} \\ &= \frac{W[t]}{\frac{c}{w}+W[t]} \\ &= \frac{W[t]}{b+W[t]} \end{aligned} \qquad (3.11)$$

where $b = \frac{c}{w}$. The new key parameter, $b$, now provides a measure of the strength of the virus; the smaller $b$ is, the stronger and more effective will be the virus at infecting susceptible rabbits (see figure 3.3).

- $\nu_J$, $\nu_Y$, $\nu_A$ are the probabilities (per day) of recovery from the disease. The values for these probabilities were calculated using equation (3.9); if we take $e_D = 0.95$, thus $e_R = 0.05$, and we allow for a life expectancy of 2 days after the disease is caught, i.e. $\tau = 2$, this yields $\nu_Y = \nu_A = \frac{1}{\tau} e_R = 0.025$. On the other hand, if only 50% of infected animals eventually die

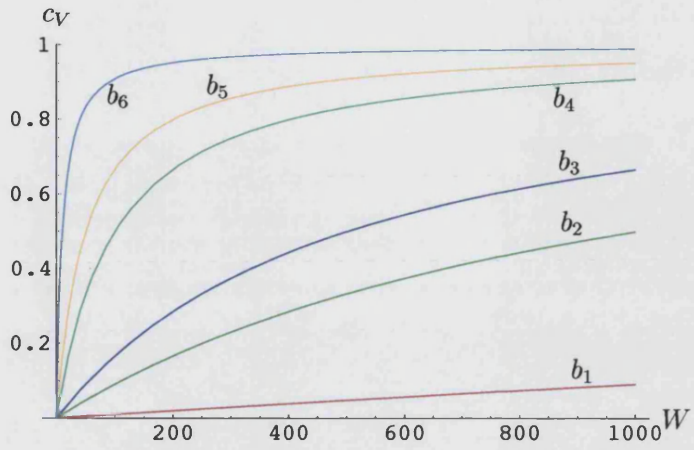


Figure 3.3: The infectivity $c_V$ for different values of b ($b_1 = 10000$, $b_2 = 1000$, $b_3 = 500$, $b_4 = 100$, $b_5 = 50$, $b_6 = 10$).

and 50% recover (i.e. for Juveniles in the Weak hypothesis case), then $e_D = e_R = 0.5$, which gives $CM_- = \nu_J = 0.25$ (from equation (3.8) and (3.9)), providing it is assumed again that $\bar{T} = \tau = 2$ days.

- $CM = 0.475$ is the case mortality of the disease, i.e. the mortality rate due to the disease. Even this value was calculated from equation (3.8) to yield a life expectancy of 2 days after the disease has been caught and keeping $e_D = 0.95$ fixed.

- $CM_- = 0.25$ is the case mortality for Juveniles that are born to susceptible pregnant females and are older than one month. This value was calculated using equation (3.8) with $e_D = 0.5$ (see Morisse [71]).

- $m_V = 0.066$ is the rate of virus decay in the environment. This value was calculated assuming that the persistence of free living virus in the environment lasts 15 days. Thus, $m_V = 0.066$ yields a virus life expectancy $\bar{T}_V = \frac{1}{m_V} = 15.1515$, and a virus half-life of approximately 10 days. Barlow [10] uses $m_V = 1.0\ day^{-1}$ in his model runs stating that a maximum half-life would be about two weeks giving a minimum value for $m_V$ of $0.05\ day^{-1}$; while Gobbet [49] uses a linear and a logarithmic decay for the virus, stating that the linear decay produces model results closer to the field data from Wardang Island; but he does not outline the field data in his research. He just affirms that the virus half life is 3 days using the linear decay

rate. The value for the decay rate of free-living virus used in this research is in between the values used by Barlow [10] and Gobbet [49].

# Chapter 4

# Seasonal and Stochastic Variation

## 4.1 Seasonal variation of the birth rate

The reproduction and breeding mode of the European wild rabbit has been illustrated in section 1.3.2. What emerges from observations and field data is the strong seasonal trend of rabbit breeding; in particular Gilbert et al. [47] have produced some data on the percentage of adult (more than nine months old) females pregnant at different sites in Australasia [see figure 1.1, section 1.3.2]. Using this data, a mathematical function can be found approximately reproducing the seasonality of rabbit breeding. We will fit a breeding function to the single site model in order to yield as results the breeding data available [47] (see section 1.3.2). We will initially obtain the best fit with an unbounded growing population, i.e. without density dependent effects. This baseline model fit will be compared to the results obtained from fitting the breeding function using density dependent effects (see section 4.3). We will show that it is possible to fit the data using a non density-dependent regulated model, as long as the population is growing at a constant average rate. Moreover we will see that the function we are fitting is independent of the population size because the date used for the fit consists of ratios of pregnant females to the total adult female population (see section 4.2).

We first chose an average value for $\lambda$. In the single site models, discussed in the previous sections, adult females can become pregnant when they are are as young as 3 months, while in the Gilbert et al. [47] data they are at least 9 months old. However, Gilbert et al. also say that females as young as three months can breed [47] (see section 1.3.2.), but that full litter size, between 3 and 7 newborns [131], is not attained until they are 10 months old. Since litter size increases with age up

to about 10 months, an "average" litter size in the low end of this range was chosen, to allow for the fact that females can become pregnant from three months onwards in our model. Hence the value $\lambda = 4$. In the case of the Subalpine region, $\lambda = 5$ was used in the model runs. We will see that this is because for the default value $\lambda = 4$ the population in Subalpine is not self-sustaining, but eventually crashes (section 6.1).

## 4.2 Fitting the breeding function $\bar{\pi}[t]$

Recall that $\bar{\pi} = \bar{\pi}[t]$ is the rate at which adult females become pregnant, and is seasonally varying. In this section we determine a suitable form for $\bar{\pi}[t]$ which fits the overall disease-free model (3.1) to the data of Gilbert et al. [47]. The data from Gilbert et al. represents the percentage of adult females pregnant at any given time through the year, which in our model is given by:

$$\wp[t] = \frac{S_P[t]}{S_{A_f}[t] + S_P[t]} \tag{4.1}$$

which expresses the ratio of pregnant females $S_P[t]$ to the total population of female rabbits, i.e. the sum of adult females which are not pregnant, $S_{A_f}[t]$, and those which are pregnant, $S_P[t]$. We chose a sine function to reproduce the seasonality of the breeding activity with the following form:

$$\bar{\pi}[t] = \begin{cases} \Pi^* Sin[\pi(\frac{t-n_0}{n_1-n_0})]; & n_0 \leq t \leq n_1 \\ \\ 0 & \text{otherwise} \end{cases} \tag{4.2}$$

$\bar{\pi}[t]$ is periodic with period 365 days, i.e. $\bar{\pi}[t + m\,365] = \bar{\pi}[t]$ ($m$ is an integer), and it is only non-zero during the breeding season, between days $n_0$ and $n_1$, where $0 \leq n_0 < n_1 \leq 365$. Note that we take $\bar{\pi}[t] = 1$ if $\Pi^* Sin[\pi(\frac{t-n_0}{n_1-n_0})] > 1$. The shape of such a function is illustrated in figure 4.1; it indicates the probability of transition per day from non-pregnant Adult female $S_{A_f}$ to Pregnant Adult female $S_P$.

The model was run using $\bar{\pi}[t]$ and the percentage of pregnant females was calculated using equation (4.1). The Least Square Method was then used to find the values of the sine function parameters, $\Pi^*$, $n_0$ and $n_1$, best fitting the data, i.e. minimizing the error between the model value (using the disease-free model (3.1) with parameter values described in section 3.1.2) and the data from

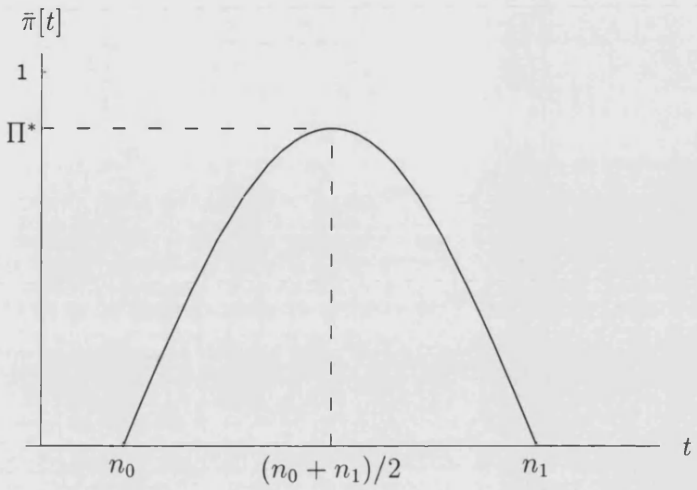


Figure 4.1: The function $\bar{\pi}[t]$ giving the time-dependent probability that an Adult female will become pregnant on a particular day ($t$ is the time in days).

Gilbert et al. On choosing values for the undetermined parameters $\Pi^*$, $n_0$ and $n_1$, the model then generates time series data for $\wp[t]$, $0 \leq t < 365$. The best fit values of $\Pi^*$, $n_0$ and $n_1$ are determined by minimising the mean-square error ($MSE$),

$$MSE = \frac{1}{K}\sum_{k=1}^{K}(\wp[t_k] - \hat{\wp}[t_k])^2,$$

where $\hat{\wp}[t_k]$, $1 \leq k \leq K$, are the real data values of $\wp[t]$ given by Gilbert et al. [47]. This was achieved by first guessing some values for the parameters which gave a reasonably good fit (as judged by eye) and then neighbouring values were tested with the Least Square method to find which would minimize the $MSE$. The neighbouring values were first taken to be 5 days before and 5 days after the guessed initial value for the parameters $n_0$ and $n_1$, while $\Pi^*$ neighbouring values were obtained by adding $\pm 0.1$. All combinations of these values were tested. This gave a "coarse filter" to select the range of the initially guessed values and choose those that minimize the error. Then a "fine filter" was used to search in a smaller range for the best fitting values for the parameters. This was achieved by trying values for $n_0$ and $n_1$ that are in the range of plus and minus 5 days, but trying every single day of the range; while for $\Pi^*$ neighbouring values for the second decimal place were tested. We tried different values of $\lambda$ in the range $3 - 6$ and still got the same $MSE$ to three decimal points. This is due to the fact that it is actually a ratio that is given in the data (4.1), which stabilizes at both high and low densities provided the population is either

growing steadily or declining steadily (and not too small), during the years for which the fitting was done. In fact we allowed the model to run for 5 years, so as to establish a constant growth, before attempting the fit in the $6^{th}$ year. Figure 4.2 shows the fit of the model to the data of the four Australian regions considered; the values of the parameters $\Pi^*$, $n_0$ and $n_1$ for each Australian region considered are the following:

- Subalpine: $(\Pi^*, n_0, n_1) = (0.064, 163, 330)$; $MSE = 0.400160$.
- Western NSW: $(\Pi^*, n_0, n_1) = (0.08, 81, 268)$; $MSE = 1.845470$.
- Riverina: $(\Pi^*, n_0, n_1) = (0.2, 59, 300)$; $MSE = 0.683245$.
- South-Western WA: $(\Pi^*, n_0, n_1) = (0.19, 80, 295)$; $MSE = 0.421849$.

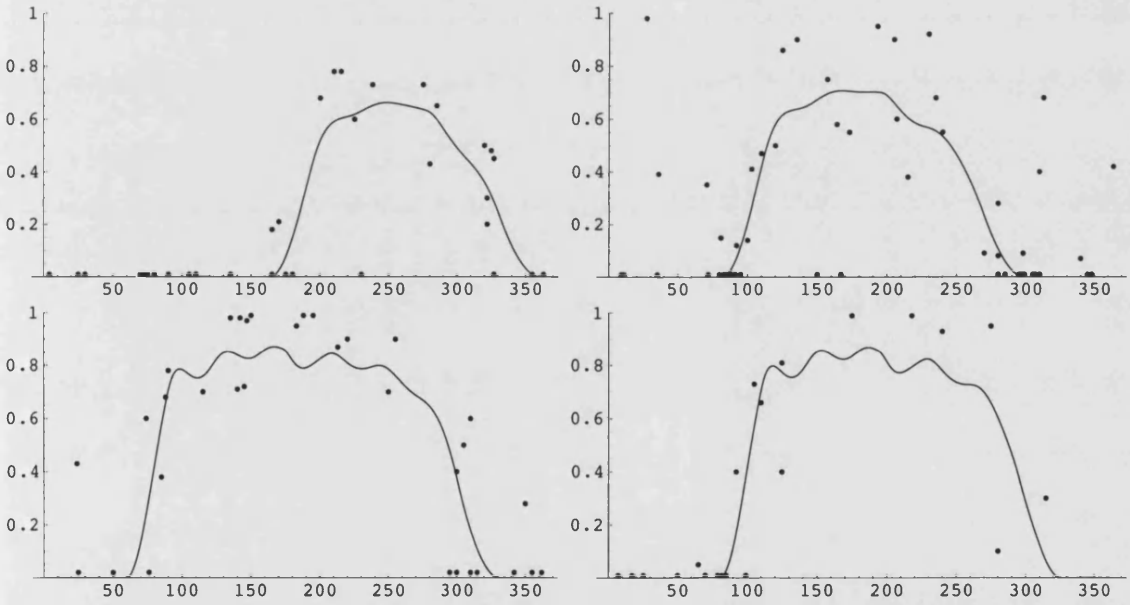


Figure 4.2: Best fit of model (3.1) to the data of Gilbert et al. [47]: proportion of pregnant females against time of the year in days. (a) Subalpine (top left). (b) Western NSW (top right). (c) Riverina (bottom left). (d) South-Western WA (bottom right). These fits were obtained with $\lambda = 4$, except for Subalpine, for which $\lambda = 5$ was used.

## 4.3 Density Dependent Regulation

The seasonal dependence of the birth rate alone does not allow for a realistic representation of the population dynamics of rabbits, since the way the model is constructed and run yields an infinite growth of the population density. Even though rabbits are a pest in many areas in the world, particularly in Australia, nevertheless infinite growth is not possible in a finite environment. This is behind the concept of carrying capacity.

### 4.3.1 $\lambda$ - Density Dependence

In section 1.3.2 we explained how there is the possibility that a pregnant doe can re-absorb the litters *in utero*, i.e. before they are born. This phenomenon results in the death of the embryos of many litters on, or about, the 11th-12th days of pregnancy. Brambell [15] observed that these embryos are re-absorbed rapidly: the resorption of the embryonic membranes and maternal placental tissues follows that of the embryos. CSIRO studies attempted to correlate this phenomenon with the social status of the does or with environmental stress, but these studies were on the whole inconclusive [37]. In particular in Australia, using Brambell's formula [15], it was found that $4-9\%$ of embryos might be lost, but whether this is more than basic loss due to genetic defects, or other phenomena, is unknown [28]. Nevertheless, resorption provides a possible mechanism for density-dependent population control through variation in breeding. We therefore explored the consequences for the model outcomes of introducing density dependence in the litter size $\lambda$.

We assume that when the population density is low, a female rabbit will tend to increase its litter size. On the other hand, at high density populations a rabbit will have a tendency to decrease its litter size in order to enhance the survival chances of its kittens in an overpopulated environment. A simple expression for $\lambda$ as a density dependent function is as follows:

$$\lambda(x) = 7 - 6.5\Big(\frac{x^l}{\hat{N}^l + x^l}\Big) \tag{4.3}$$

where $x$ is the population density. Clearly this function allows a variation of $\lambda$, between 0.5 to 7 kittens, that is bigger than is reported in the literature (see section 1.3.2). In fact $\lambda(0) = 7$ (kittens per litter), but for very high population density ($x \to \infty$), $\lambda \to 7-6.5 = 0.5$. It is therefore possible for the average pregnant female to produce less than one kitten. The threshold $\hat{N}$ is the population

density at which $\lambda(\hat{N}) = 7 - 6.5 \times 0.5 = 3.75$, slightly less than the average value of $\lambda = 4$ we have taken earlier (e.g. Figure 4.2) We take $l = 3$ to give the curve a reasonable steepness. Figure 4.3 shows how the function varies for different $\hat{N}$. The results from running the model with a density dependent $\lambda$ are discussed in section 6.2.1.

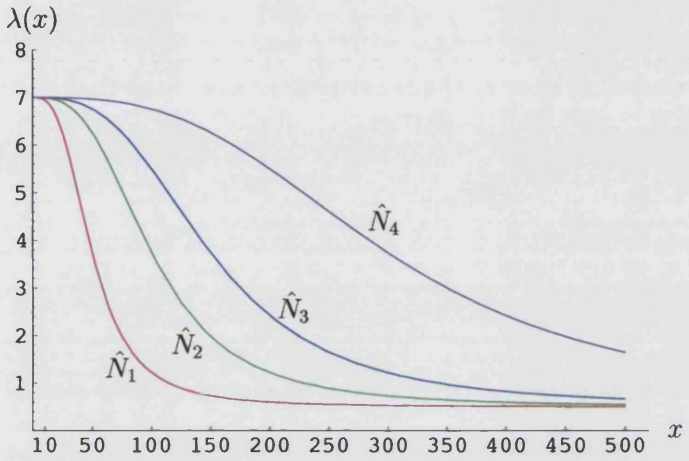


Figure 4.3: The density dependent function $\lambda(x)$ for different $\hat{N}$ ($x$ is the population density), and $l = 3$. $\hat{N}_1 = 50$, $\hat{N}_2 = 100$, $\hat{N}_3 = 150$, $\hat{N}_4 = 300$.

### 4.3.2 $m_J$ - Density Dependence

The literature [131], [47] and [31] (see section 1.3.3) suggests that the first to be affected in cases of overpopulation, with respect to the environment capacity, are younger rabbits: as the struggle to survive increases, the weakest are those most likely to succumb. High mortality of young rabbits can be caused by predation, seasonal conditions and myxomatosis; moreover, it varies according to when they are born relative to the beginning and end of the breeding season. Young born early or late in the season have low survival rates: the former face enhanced predation pressure and the latter declining food availability [131]. Gilbert et al. [47] affirm that population losses are almost all in the Juvenile population being due to lactation failure, social stress and predation. For this reason, it was decided that the Juvenile class should bear the weight of density dependent regulation through mortality. We modelled this by assuming that, when the population density exceeds a certain threshold, and the availability of food declines, the likelihood of death of Juveniles is increased. We therefore chose a density-dependent natural death-rate for Juveniles, as follows:

$$\Phi(x) = \begin{cases} m_{J_0} & \text{if } x \leq \hat{k} \\ \\ m_{J_0} + (1 - m_{J_0}) \frac{(x-\hat{k})^u}{(\hat{k})^u + (x-\hat{k})^u} & \text{if } x > \hat{k} \end{cases}$$

where $x$ is the population density, $m_{J_0}$ is the "default" natural death rate derived from the literature (see section 3.1.2) and $\hat{k}$ is the threshold value for the onset of density dependence. The value $u = 5$ was chosen to give a reasonably steep increase in Juvenile mortality rate once the threshold $\hat{k}$ has been passed. Figure 4.4 illustrates how the function varies with the threshold $\hat{k}$.

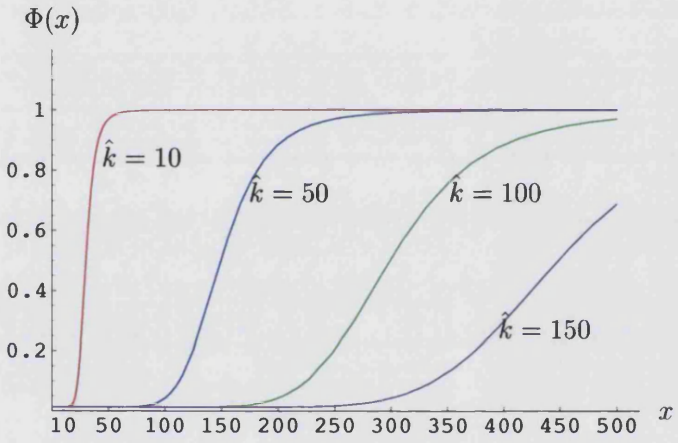


Figure 4.4: The density dependent function $\Phi(x)$ for different $\hat{k}$ ($x$ is the population density), and $u = 5$.

In the model simulations, the effects of varying the carrying capacity of the environment were investigated by varying the threshold $\hat{k}$. Thus the population dynamics of the rabbit could be explored in environments ranging from low sustainance availability ($\hat{k} = 10$ and $\hat{k} = 50$) to high capacity environments ($\hat{k} = 100$ and $\hat{k} = 500$).

### 4.3.3 Fitting the breeding function with density dependent $\lambda$ and $m_J$

The parameter values for the breeding function, fitted as shown in section 4.2, were fitted again with $\lambda$ and $m_J$ density dependent. We found that whether we let $\lambda$ be density dependent, or $m_J$, or both, the MSE remains of a similar magnitude and the best fit value of the parameters

is the same. This is because it is a ratio that is given in the data as we said in section 4.2. For example, in the Subalpine case when $\lambda$ is density dependent, for any threshold value, $\hat{N}$, we get that $MSE = 0.400298$ which is slightly worse than the non-density dependent fitting (see section 4.2). When a density dependent $m_J$ is included as well, we get that $MSE = 0.400306$ for $\hat{N} = 150$ and $\hat{k} = 100$. And for $\hat{N} = 300$ and $\hat{k} = 100$ we obtain $MSE = 0.400254$. In the Riverina case, when $\lambda$ is density dependent, for any threshold value, $\hat{N}$, we get that $MSE = 0.676247$ which is slightly better than the non-density dependent case (see section 4.2). When a density dependent $m_J$ is included as well, we get that $MSE = 0.678339$ for $\hat{N} = 150$ and $\hat{k} = 100$. And for $\hat{N} = 300$ and $\hat{k} = 100$ we obtain $MSE = 0.671404$. We obtained the same type of result for WNSW and SWWA. Hence, since the $MSE$ doesn't change significantly when density dependence effects are included, it is reasonable to use the best fit parameter values obtained with the non-density dependent fit as they do not vary with the threshold value of the density-dependent parameters.

## 4.4 Climate

Climatic conditions can influence the relative abundance of rabbits from year to year, or from season to season. This is an important factor for population regulation: for example a "bad" year or a "bad" season can affect the Juvenile rate of natural mortality, $m_J$, i.e. Juveniles are the first to suffer from unfavourable climatic conditions, like drought, or extreme cold, or excessive rainfall (see section 1.3.3). Moreover climate influences the availability of vegetation on which rabbits feed. Thus, it is reasonable to assume that climatic conditions may vary the carrying capacity of the environment hosting a rabbit population. Climatic variability was modelled as stochastic variation in the threshold $\hat{k}$ for Juvenile mortality. This is the principal determinant of carrying capacity in the model. Thus, $\hat{k}$ is treated as a random variable, distributed according to some continuous probability distribution. Since $\hat{k}$ is necessarily a positive variable, the distribution chosen was the lognormal distribution. The lognormal distribution is the distribution of a random variable whose logarithm is normally distributed [33]. In this research it will be used to reproduce the climatic variability during the year and through the years in different Australian environments.

The Lognormal distribution of a positive random variable $X$ with parameters $\mu$ and $\sigma^2$ is the distribution of $X$ when $Y = lnX$ is normally distributed with mean $\mu$ and variance $\sigma^2$. The two-parameter lognormal distribution is often denoted by $\Lambda(\mu, \sigma^2)$; the corresponding normal dis-

tribution is denoted by $N(\mu, \sigma^2)$ [33]. The probability density function of $\Lambda(\mu, \sigma^2)$ is

$$f(x) = \begin{cases} \frac{1}{\sqrt{2\pi\sigma^2}} \frac{1}{x} exp[-\frac{(lnx-\mu)^2}{2\sigma^2}] & \text{if } x > 0 \\ \\ 0 & \text{if } x \leq 0 \end{cases}$$

The mean of this distribution is $m = e^{\mu+\frac{\sigma^2}{2}}$ and its variance is $v = e^{2(\mu+\sigma^2)} - e^{2\mu+\sigma^2}$. Solving these expressions for $\mu$ and $\sigma^2$, we obtain $\mu = log\left(\frac{m}{\sqrt{1+\frac{v}{m^2}}}\right)$ and $\sigma^2 = log\left(1 + \frac{v}{m^2}\right)$.

Figure 4.5 illustrates how the probability density function of $\Lambda(\mu, \sigma^2)$ varies with $\sigma^2$.

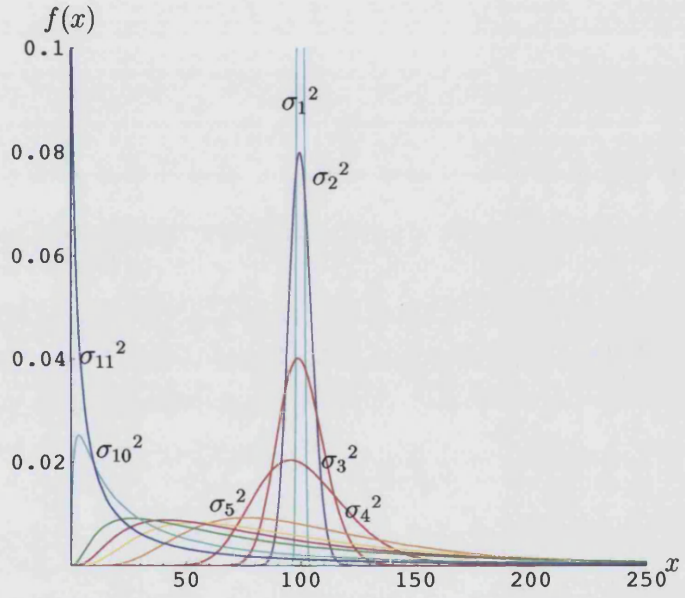


Figure 4.5: Probability density function of the Lognormal Distribution ($\mu = ln100 - \frac{\sigma^2}{2}$, ${\sigma_1}^2 = 0.0001$, ${\sigma_2}^2 = 0.0025$, ${\sigma_3}^2 = 0.01$, ${\sigma_4}^2 = 0.04$, ${\sigma_5}^2 = 0.25$, ${\sigma_{10}}^2 = 2.25$, ${\sigma_{11}}^2 = 4$).

A mean value $\hat{k}_0$ for the threshold capacity was first chosen, and then allowed to vary stochastically by using a random multiplicative factor to obtain the actual threshold capacity $\hat{k}$; i.e. $\hat{k} = x\hat{k}_0$, where $x$ is a lognormally distributed random variable with mean value $m = 1$. In this way a climatic change occurs in the model by changing the carrying capacity with a probability that is lognormally distributed. The main reason for choosing the Lognormal probability distribution as representing the probability density distribution of a climatic change taking place, is that it allows the representation of multiplicative events, as opposed to additive events, that are mostly

tribution is denoted by $N(\mu, \sigma^2)$ [33]. The probability density function of $\Lambda(\mu, \sigma^2)$ is

$$f(x) = \begin{cases} \frac{1}{\sqrt{2\pi\sigma^2}} \frac{1}{x} exp[-\frac{(lnx-\mu)^2}{2\sigma^2}] & \text{if } x > 0 \\ \\ 0 & \text{if } x \leq 0 \end{cases}$$

The mean of this distribution is $m = e^{\mu+\frac{\sigma^2}{2}}$ and its variance is $v = e^{2(\mu+\sigma^2)} - e^{2\mu+\sigma^2}$. Solving these expressions for $\mu$ and $\sigma^2$, we obtain $\mu = log\Big(\frac{m}{\sqrt{1+\frac{v}{m^2}}}\Big)$ and $\sigma^2 = log\Big(1 + \frac{v}{m^2}\Big)$.

Figure 4.5 illustrates how the probability density function of $\Lambda(\mu, \sigma^2)$ varies with $\sigma^2$.

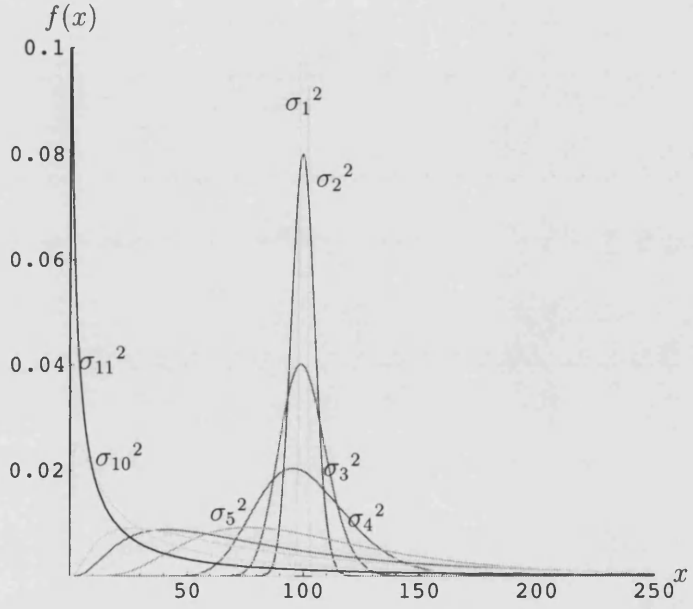


Figure 4.5: Probability density function of the Lognormal Distribution ($\mu = ln100 - \frac{\sigma^2}{2}$, ${\sigma_1}^2 = 0.0001$, ${\sigma_2}^2 = 0.0025$, ${\sigma_3}^2 = 0.01$, ${\sigma_4}^2 = 0.04$, ${\sigma_5}^2 = 0.25$, ${\sigma_{10}}^2 = 2.25$, ${\sigma_{11}}^2 = 4$).

A mean value $\hat{k}_0$ for the threshold capacity was first chosen, and then allowed to vary stochastically by using a random multiplicative factor to obtain the actual threshold capacity $\hat{k}$; i.e. $\hat{k} = x\hat{k}_0$, where $x$ is a lognormally distributed random variable with mean value $m = 1$. In this way a climatic change occurs in the model by changing the carrying capacity with a probability that is lognormally distributed. The main reason for choosing the Lognormal probability distribution as representing the probability density distribution of a climatic change taking place, is that it allows the representation of multiplicative events, as opposed to additive events, that are mostly

represented by the more common, not always positive, Normal distribution. The central limit theorem states that under fairly mild conditions the average of independent, but not necessarily identically distributed, random variables is asymptotically normally distributed [16]. Climatic events are represented by random variables, and hence their average would be normally distributed if they were not necessarily positive. In contrast a positive random variable is approximately lognormal if it is the geometric mean of "enough independent positive random variables". Thus, since in the model, the factors determining the climatic condition of a geographical area, such as humidity, rainfall and temperature, can be considered as independent events, the most suitable distribution appears to be the lognormal distribution, as it takes into account the effect of all climatic factors which contribute to the overall effect.

The effect of varying the variance $v$ of the lognormal distribution was investigated for the interval $0.01 \leq v \leq 10$ and three possible values for the variance, in this interval, were chosen and used in the simulations: low variance $v = 0.1$, intermediate variance $v = 1$ and high variance $v = 10$. Preliminary investigation showed that for $v < 0.1$ and $v > 10$ the results did not vary remarkably. Figure 4.5 shows the Lognormal distribution with the values of the variance selected for the simulation runs.

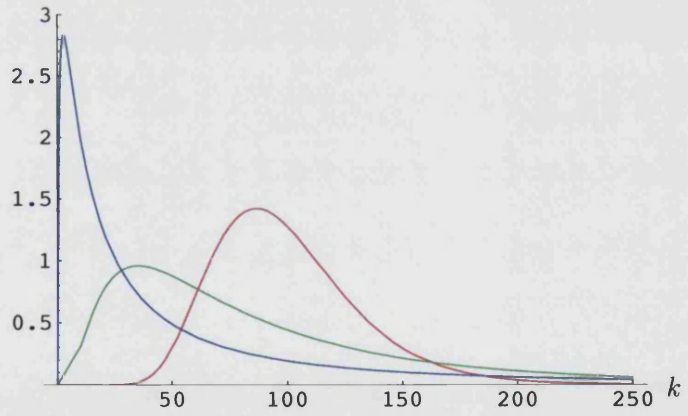


Figure 4.6: Probability density function of the random variable $k = x\hat{k}_0$ where $\hat{k}_0 = 100$ and $x$ is lognormally distributed with $m = 1$, $v = 0.1$ (red), $v = 1$ (green), $v = 10$ (blue).

The results were compared with the non-stochastic case where there is a constant density dependent regulation of the population (see previous section) and the variance of the distribution is zero.

The time of the year in which a climatic change (i.e. a random change in $\hat{k}$) occurs was not fixed but regulated by a Poisson probability distribution. The Poisson distribution with mean $\lambda t$ is defined as

$$p(k,t) = \frac{e^{-\lambda t}(\lambda t)^k}{k!}$$

for $k$=0,1,2,..., and is the probability that $k$ events occur in the time interval $[0,t)$. $\lambda$, the event frequency, i.e. the expected number of events per unit time, can be any positive real number [12]. In this case the unit of time is one day. The expected number of events in the interval $[0,t)$ is $\lambda t$; thus, $\lambda = \frac{r}{365}$ means that the expected number of events is $r$ per year.

We consider 4 cases of increasing frequency:

- $\lambda = \frac{1}{365}$: an average of 1 event per year;
- $\lambda = \frac{2}{365}$: an average of 1 event every 6 months;
- $\lambda = \frac{4}{365}$: an average of 1 event every season (3 months);
- $\lambda = \frac{12}{365}$: an average of 1 event every month.

On a given day, the probability that an event occurs is $\lambda e^{-\lambda}$, and the probability that no event occurs is $1 - \lambda e^{-\lambda}$. Define a random variable $X$ as follows:

$$X = \begin{cases} 1 & \text{if } x \leq \lambda e^{-\lambda} \quad \Rightarrow event\, occurs. \\ \\ 0 & \text{if } x > \lambda e^{-\lambda} \quad \Rightarrow no\, event\, occurs. \end{cases}$$

where $x \in [0,1]$ is a uniformly-distributed random number generated on each day.

The computational model allowed for varying the frequency of the climatic change as well as the time in which it could take place: the change takes place in a Poisson distributed manner and the frequency of the change could simply be set by varying the mean of the Poisson distribution.

# Chapter 5

# Emigration

To build a model that incorporates the possibility of a rabbit to disperse from a warren, the data from Parer [88] (see section 1.3.5) on the time and age of dispersion was used to determine the probability that any given rabbit in a warren might disperse at any given time in the year and at any given age. It is important to notice that the field trials from which Parer collected his data were located at Urana in New South Wales. In particular, Urana is in the Riverina region, thus the birth rate function used in the model will be the one relating to the Riverina region only (Gilbert [47] data, figure 1.1); emigration in the other geographical regions will not be investigated due to lack of data.

¿From the literature (see section 1.3.5) we know that age, social position, season and population density are the factors influencing the possibility that a rabbit might leave the warren it inhabits to look for a new residence. Parer [88] in particular has published some data on the time of dispersal, the dispersal distances and the age of the dispersing rabbits, the data is reported in table 1, 2 and 3, section 1.3.5.

In order to build a model that gives results close to the observed data, probability distributions for the age and seasonality of the emigration were tested and used in a version of the single site model that allows for emigration. Moreover we built a suitable probability distribution to make emigration depend on population density, a factor that can prompt a rabbit to leave its site to search for a site with less competitive conditions to live in. Emigration in the single site model is conceived as an individual leaving the site to a non-specified destination; the hazard this individual faces after it leaves the site is of no interest at this stage: it will be considered later in the spatial

model. The guessed probabilities were used in the model to find the values of the parameters that would best fit the data, i.e. the model was run initially with a set of parameters for the probability function whose values were guessed graphically from the data; then the model results were tested against the field data to find which value of the parameters yields the smallest difference with the field data.

## 5.1 Age of Emigration

The data from Parer [88] (see Table 3, section 1.3.5) represents the number of rabbits of different age classes which dispersed yearly; it is then possible to find a yearly probability distribution for the age class of the dispersing animal. In table 3 the age of the dispersing rabbits is split into 40 day intervals and it is assumed that no animals younger than 20 days emigrate as there is no data reported on this. This assumption holds in our model.

Plotting the data on the age of the dispersing animals, we guessed that a decaying exponential can be a suitable probability distribution function for the age of an emigrating individual. This function represents the probability that an emigrating individual has a certain age as it follows:

$$D(a) = \begin{cases} 0 & \text{if } 0 \leq a \leq 20. \\ \\ \alpha e^{-\alpha(a-20)} & \text{if } a > 20. \end{cases} \tag{5.1}$$

where $a$ is the age of the animal in days and $\alpha$ is the exponential decay rate. Note that $D(a) = 0$ for $0 < a < 20$ since in Parer's [88] data no animal younger than 20 days emigrates. Hence $D(a)$ is a probability distribution defined on the interval $0 \leq a < \infty$; i.e.

$$\int_0^\infty D(a)da = 1$$

It follows that $\int_{a_1}^{a_2} D(a)da$ is the probability that an emigrating animal has age between $a_1$ and $a_2$.

$\alpha$ is the only parameter to be determined and $\alpha = 0.014527$ is the best fit value. This value was found by minimizing the mean-square error function between data and model values with the Least Square method (see appendix to this chapter). The fitted values were obtained by integrating the probability distribution (5.1) in the same age intervals in which the data was taken. Figure 5.1 shows both the data and the model points using the best fit value found for $\alpha$.

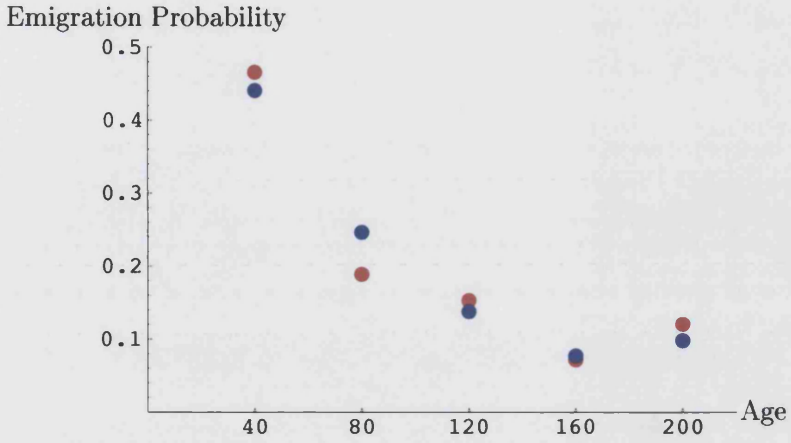


Figure 5.1: Age of Emigration Probability: red dots represent the real data, blue dots the fitted data.

Using $D(a)$ it is possible to determine with what probability an emigrating animal belongs to one of the age classes used in our models, namely Juvenile (0 to 56 days old), Youngster (57 to 84 days old) or Adult (85 days onwards). This is obtained by integrating $D(a)$ in the respective age class intervals, i.e. from 20 to 56 days, from 56 to 84 days and from 84 days to infinity respectively. The result is illustrated in figure 5.2. below:

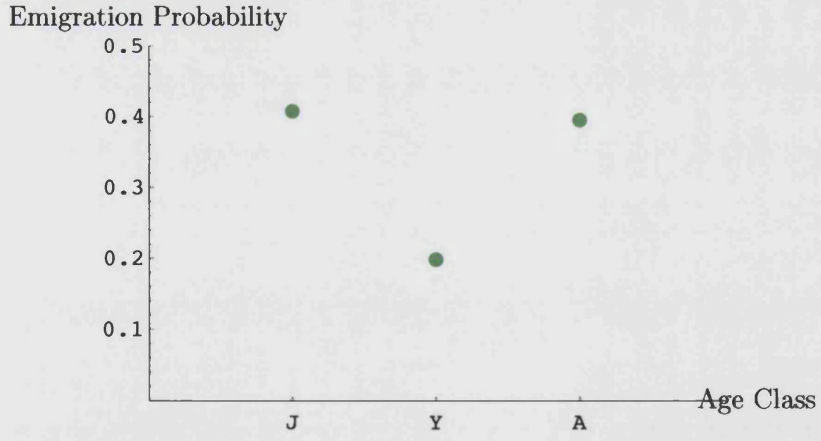


Figure 5.2: Emigration Probability for each age class.

It can be observed that Juveniles and Adults emigrate with roughly the same probability, while

Subadults emigrate with much lower probability. However, the Juveniles have a much narrower age spun during which they emigrate ($56 - 20 = 36$ days) than do adults (remaining lifetime from age 84 days onwards).

Since in the single site model the variables are iterated daily, it is necessary to find a daily probability distribution for the age of the emigrating animal; i.e. a daily distribution that would yield the yearly distribution outlined in figure 5.2 above.

A suitable function representing the daily age distribution for emigrating animals is shown in figure 5.3 below. There is an equal probability that an emigrating rabbit is between 20 to 83 days old, i.e. it belongs to part of the Juvenile ($> 20$ days old) and the Youngster class; and an exponentially decaying probability that it belongs to the adult class. In fact in the literature, adult animals are described to be more and more sedentary as they grow older, while most immigrants are younger rabbits (see section 1.3.5). This function was chosen to be quite simple, but it proves to give good results.

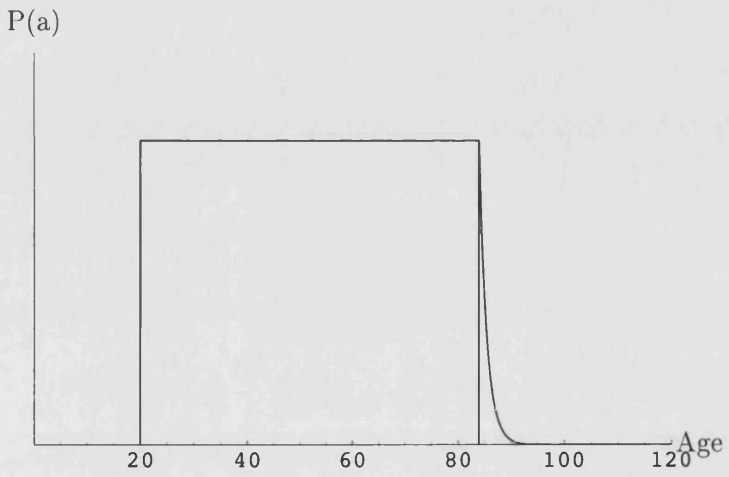


Figure 5.3: Daily Probability Distribution for the age of an emigrating rabbit.

This is a two parameter probability function, with the parameters being the height of the box and the decay rate of the exponential; however, it is possible to make it a single parameter function by expressing the height of the box as a function of the decay rate of the exponential in the following way:

$$h(\delta) = \frac{1}{(l + \frac{1}{\delta})}$$

where $\delta$ is the exponential decay parameter, $h(\delta)$ is the height of the box and $l$ is the width of the box which is set to be 63 days to include the Juveniles ($> 20$ days old) and Youngster class (up to 83 days old). Thus the daily probability distribution of the age of an emigrating rabbit is:

$$P(a) = \begin{cases} 0 & \text{if } 0 \leq a < 20. \\ h(\delta) & \text{if } 20 \leq a \leq 84. \\ h(\delta)e^{-\delta(a-84)} & \text{if } a > 84. \end{cases} \tag{5.2}$$

where $a$ is the age of the rabbit and $h$ and $\delta$ have been specified above. The exponential decay refers to the adult class, so it starts on the $84^{th}$ day. This is the daily probability distribution used in the model to fit the data of Parer [88] of the yearly age distribution of the emigrating animals. The only unknown parameter is $\delta$; the emigration model used is illustrated in section 5.4 and the method used to fit the model to data is described in detail in section 5.7.1 in the appendix to this chapter.

We can then define $\epsilon_J$, $\epsilon_Y$ and $\epsilon_A$ as the age dependent emigration rate for the Juvenile, Youngster and Adult class respectively; their value is obtained by integrating $P(a)$ in the relevant class age interval as follows:

$$\begin{aligned} \epsilon_J &= \int_{20}^{56} P(a)\,\mathrm{d}a; \\ \epsilon_Y &= \int_{56}^{84} P(a)\,\mathrm{d}a; \\ \epsilon_A &= \int_{84}^{\infty} P(a)\,\mathrm{d}a; \end{aligned} \tag{5.3}$$

These will be used in the emigration model outlined in section 5.4.

## 5.2 Season of Emigration

The data from Parer [88], outlined in Table 1 (see section 1.3.5), on the time (in months) of emigration during the year is in figure 5.4.

It is necessary to fit a distribution function to the data in order to have a probability for each day

of the year that an individual will emigrate. A suitable function could be the one illustrated in figure 5.5, where $t$ is the time in days. The form of the function in figure 5.5 is based on the data in figure 5.4: it is assumed that there is an approximately constant background rate of emigration throughout the year, with a seasonal surge during a particular period (southern-hemisphere spring-beginning of summer). This surge is related to social reorganisation prior to the breeding season (see section 1.3.5).

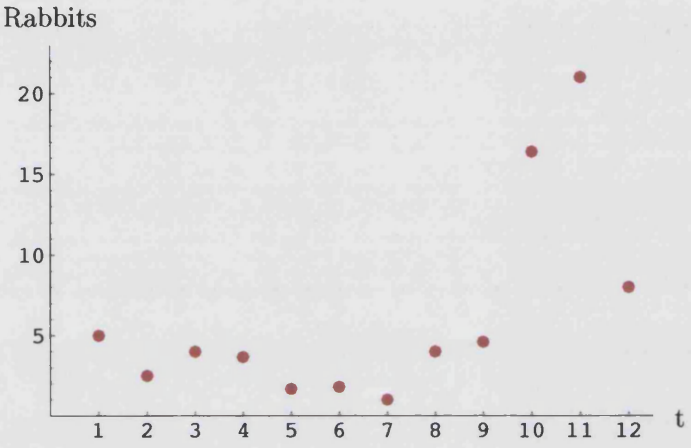


Figure 5.4: Time (in months) of dispersal of young male and female rabbits [month 1= January] (see Parer [88]).

It can be observed that such a function must be characterised by several parameters, namely, the background emigration level, the amplitude of the main emigration wave, the time when the main emigration starts and when it ends. The equation of the function in figure 5.5 has the form:

$$\sigma(t) = \begin{cases} A(\frac{1}{2}(1+b_g) - \frac{1}{2}(1-b_g)cos[\frac{2\pi(t-e_0)}{e_1-e_0}]), & e_0 \leq t \leq e_1 \\ \\ A\,b_g & \text{otherwise} \end{cases} \tag{5.4}$$

where $\sigma(t)$, assumed periodic with period 1 year, is the emigration probability for day $t$, $e_0$ and $e_1$ are the days of the year between which the main seasonal emigration takes place, $A$ is the maximum value of the emigration probability between $e_0$ and $e_1$, $A\,b_g$ is the background level of emigration, where $0 \leq b_g < 1$; i.e. a constant rate of emigration taking place during the year outside the main emigration season between $e_0$ and $e_1$. This function then represents the probability that a rabbit

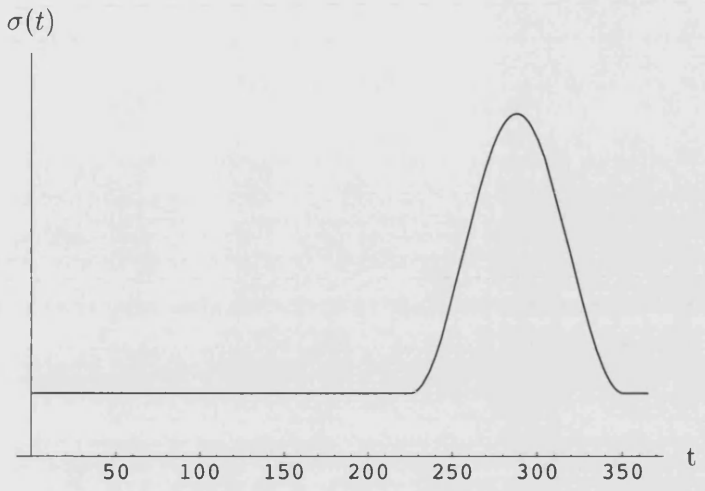


Figure 5.5: Daily Probability distribution for seasonal emigration.

would emigrate at a certain day during the year: the best fit value for the parameters $A$, $b_g$, $e_0$ and $e_1$ can be found by using Newton's method (see section 5.7.1 in the appendix) to minimize the Mean Square Error between the model result, using $\sigma(t)$ as seasonal emigration rate, and Parer's data. These parameters are estimated simultaneously, in order to obtain simultaneous best fit to the data in figure 5.4 and the "derived" data of figure 5.2. The model used to find the best fit values for the seasonal probability distribution is outlined in section 5.4.

## 5.3 Density-dependent Emigration

An alternative approach to the one discussed above is to consider emigration as a purely density dependent phenomenon, rather than seasonal; i.e. animals emigrate only in response to high population density [32], with no specifically seasonal component in their behaviour. To investigate this hypothesis and compare it to the data of Parer, it is necessary to find a probability function that a rabbit will emigrate depending on the local population density. A threshold function like the one illustrated in figure 5.6 is suitable for this purpose. In order to compare the density-dependent emigration probability and the seasonal emigration probability and determine which yields the best fit to the field data, it is necessary that the two probabilities have the same number of parameters to be fitted. Since the seasonal probability function is characterised by four parameters, we need to build a probability function depending on density also characterised by four parameters. Thus,

an equation for the probability that a rabbit would emigrate given the density, $R$, of the warren which he inhabits can be as follows:

$$\sigma(R) = Ab_g + A(1 - b_g)\frac{R^u}{(x^u + \tau^u)} \tag{5.5}$$

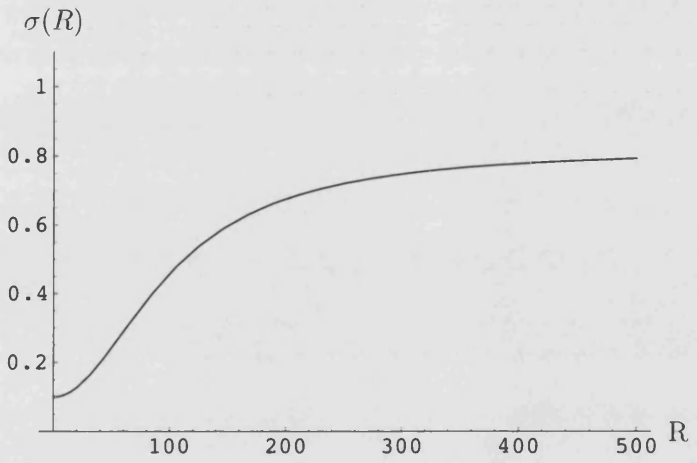


Figure 5.6: Probability distribution for density-dependent emigration (threshold=100); $R$= Rabbit Density.

A threshold function like the one in figure 5.6 depends on the threshold value, $\tau$, the background level, $Ab_g$, which is a constant level of emigration taking place even without high densities, the steepness, $u$, of the curve at the threshold value, and the asymptotic probability, $A$, i.e. the maximum emigration probability for very high densities.

To find the best fit values of the parameters that minimise the Mean Square Error between the model result using $\sigma(R)$ as density-dependent emigration rate and Parer's data, the Gradient Descent Method will be used. The procedure is explained in section 5.7.2 in the appendix.

## 5.4 The Emigration Model

It is necessary to modify the single site model to allow for emigration of the individuals of the relevant classes; a suitable model is the following:

$$
\begin{aligned}
S_J[t+1,0] &= \lambda(1-m_A)S_P[t,n_P];\\
S_J[t+1,k] &= (1-\epsilon_J[k-1]\sigma[T])(1-m_J)S_J[t,k-1];\\
E_{S_J}[t,k-1] &= \epsilon_J[k-1]\sigma[T](1-m_J)S_J[t,k-1];\\
E_{S_J}[t,n_J] &= \epsilon_J[n_J]\sigma[T](1-m_J)S_J[t,n_J]; \qquad (1 \le k \le n_J)
\end{aligned}
$$

$$
\begin{aligned}
S_Y[t+1,1] &= (1-\epsilon_J[n_J]\sigma[T])(1-m_J)S_J[t,n_J];\\
S_Y[t+1,k] &= (1-\epsilon_Y[k-1]\sigma[T])(1-m_Y)S_Y[t,k-1];\\
E_{S_Y}[t,k-1] &= \epsilon_Y[k-1]\sigma[T](1-m_Y)S_Y[t,k-1];\\
E_{S_Y}[t,n_Y] &= \epsilon_Y[n_Y]\sigma[T](1-m_Y)S_Y[t,n_Y]; \qquad (2 \le k \le n_Y)
\end{aligned}
\tag{5.6}
$$

$$
\begin{aligned}
S_{A_M}[t+1] &= (1-\epsilon_A\sigma[T])(1-m_A)S_{A_M}[t]+\\
&\quad \tfrac{1}{2}(1-\epsilon_Y[n_Y]\sigma[T])(1-m_Y)S_Y[t,n_Y];\\
S_{A_F}[t+1] &= (1-m_A)((1-\epsilon_A\sigma[T])(1-\pi)S_{A_F}[t]+S_P[t,n_P])+\\
&\quad \tfrac{1}{2}(1-\epsilon_Y[n_Y]\sigma[T])(1-m_Y)S_Y[t,n_Y];\\
E_{S_{A_{M,F}}}[t] &= (1-m_A)\epsilon_A\sigma[T]((1-\pi)S_{A_F}[t]+S_{A_M}[t]);
\end{aligned}
$$

$$
\begin{aligned}
S_P[t+1,1] &= \pi(1-m_A)S_{A_F}[t];\\
S_P[t+1,k] &= (1-m_A)S_P[t,k-1]; \qquad (2 \le k \le n_P)
\end{aligned}
$$

Most of the variables and parameters are the same as the single site model given in equations (3.1). However, this model includes the possibility that rabbits from the Juvenile, Youngster and Adult classes can emigrate from the site; only pregnant females do not emigrate. This probability is determined by the distribution functions described in the previous section: $\epsilon_J$, $\epsilon_Y$ and $\epsilon_A$ are the age dependent emigration rate for the Juvenile, Youngster and Adult class respectively as defined in equation (5.3); $\sigma$ is the emigration probability, which can depend either on the season, then $T$ is the day of the year and $\sigma$ is defined by equation (5.4); or on the total population density, then $T = R(t)$ is the population density on day $t$ and $\sigma$ is defined by equation (5.5). $E_{S_J}$, $E_{S_Y}$ and $E_{S_A}$ are the particular age fractions of the total emigrating population. At this point of the research it is not of interest to know what happens to the emigrating population, after it leaves the site. Instead, we shall use the model (5.6) to estimate the best fit values for the unknown parameters in the functions $\sigma[T]$ (equation (5.4) or (5.5)) using the field data from Parer's observations [88]. Newton's method is used to get the best fit for the seasonal emigration parameters; while the Gradient descent method

is used to find the best fit for the density-dependent emigration parameters. The reason why two methods had to be used is that while Newton's method is much better and faster, it is sometimes unstable; so to find a good fit for the density-dependent emigration, the Gradient Descent proved more useful.

## 5.5 Seasonal emigration parameters.

Results using Newton's method with no density-dependent regulation of $m_J$.

Newton's method (see appendix) yielded that the best fit values for the parameters using the model, with a 5 year run, with no density dependent regulation of $m_J$, are $\delta = 1.132$, which is the age parameter (see equation (5.2)), $A = 0.122$, $b_g = 0.184$, $e_0 = 208$ and $e_1 = 296$, which are the seasonal parameters (see equation (5.4)). Then

$$\hat{\mathbf{p}} = \{1.132, 0.122, 0.184, 208, 296\}.$$

and the mean-square-error (MSE) is 0.00010999, which is the sum of the MSE's associated with figures 5.8 and 5.9.

The following figures show the model result using these best fit parameter values; in figure 5.7, the blue dots represent the proportion of emigrating animals of a particular age (in days) out of the total emigrating population. In figure 5.8 the blue dots are the proportion of all emigrating Juveniles, Youngsters and Adult respectively out of the total emigrating population. Figure 5.9 represents the sasonal probability that a rabbit emigrates given the time of the year using the best fit values of the parameters.

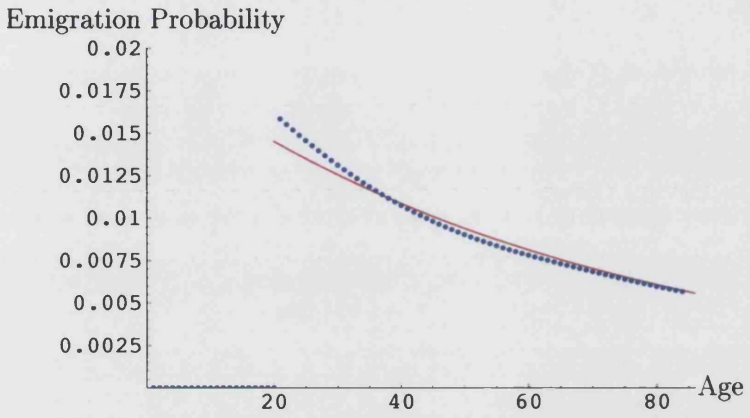


Figure 5.7: Age of Emigration Probability: the exponential curve (red is the curve 5.1) with best fit value $\alpha = 0.014527$ obtained from Parer's data (see figure 5.1). The blue dots are the age-at-emigration data derived from the model (5.6).

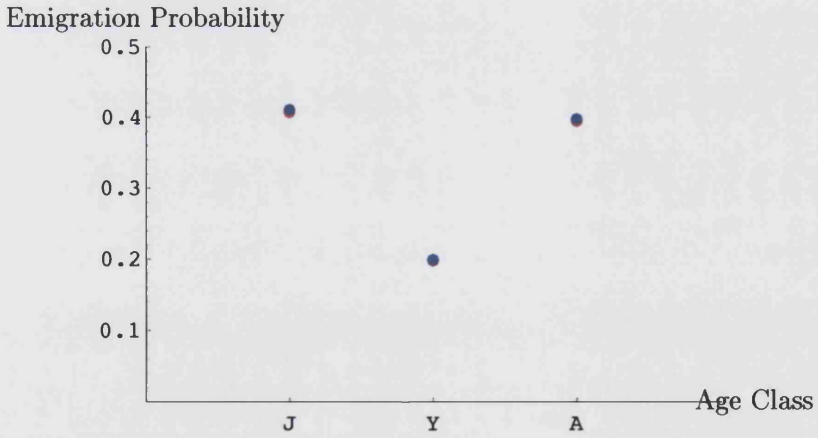


Figure 5.8: Emigration Probability for each age class: red dots represent the fit to Parer's data as in figure 5.2. The blue dots represent the model result.

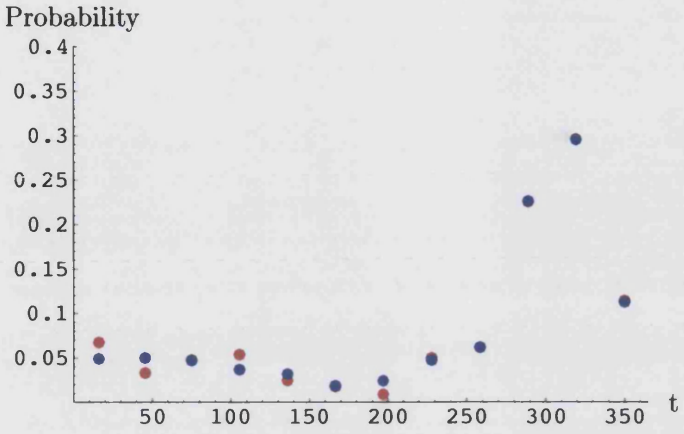


Figure 5.9: Probability distribution for seasonal emigration: red dots represent Parer's data as in figure 5.4. The blue dots represent the model result.

Results using Newton's method with density-dependent regulation of $m_J$.

The same procedure was carried out to find the best fit for the parameter values using natural density dependence regulation acting on the Juvenile mortality, $m_J$, with different threshold values for the carrying capacity: $\hat{k} = 10, 50, 100, 500$.

The best fit parameter values, found using Newton's method, are $\delta = 1.247$, $A = 0.651$, $b_g = 0.133$, $e_0 = 206$ and $e_1 = 305$; i.e.

$$\hat{\mathbf{p}}_{(10,50,100,500)} = \{1.247, 0.651, 0.133, 206, 305\}.$$

These values are independent of the density threshold $\hat{k}$. The parameter values that best fit the available data are the same for any threshold capacity used as they yield the same MSE, $MSE = 0.000581698$ for any of the values of the threshold capacity tried, except for $\hat{k} = 500$ for which $MSE = 0.000581803$: in this case the model simulation was run for 10 years instead of 5 to allow for the density regulation to have an effect on the population size. The MSE for $\hat{k} = 500$ would certainly be the same if we had run the model for longer. The size of the MSE shows that when there is no density dependent regulation, Newton's method provided a better fit to the data; it is not clear why. It could suggest that emigration is not a phenomenon bound to the population density of any particular site/warren, but more a social phenomenon connected to the seasonal conditions. Or maybe Parer's data was collected from a site which was very favourable and not

strongly density regulated.

The figures below illustrate the results; in figure 5.10, the blue dots represent the proportion of emigrating animals of a particular age (in days) out of the total emigrating population. In figure 5.11 the blue dots are the proportion of all emigrating Juveniles, Youngsters and Adult respectively out of the total emigrating population.

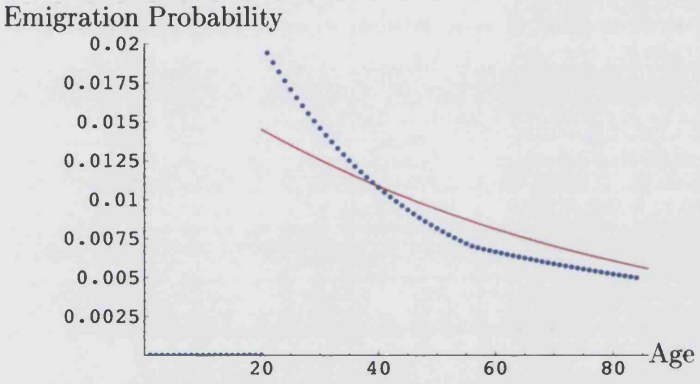


Figure 5.10: Age of Emigration Probability ($\hat{k} = 10$): the exponential curve (red is the curve 5.1) with best fit value $\alpha = 0.014527$ obtained from Parer's data (see figure 5.1). The blue dots are the age-at-emigration data derived from the model (5.6).

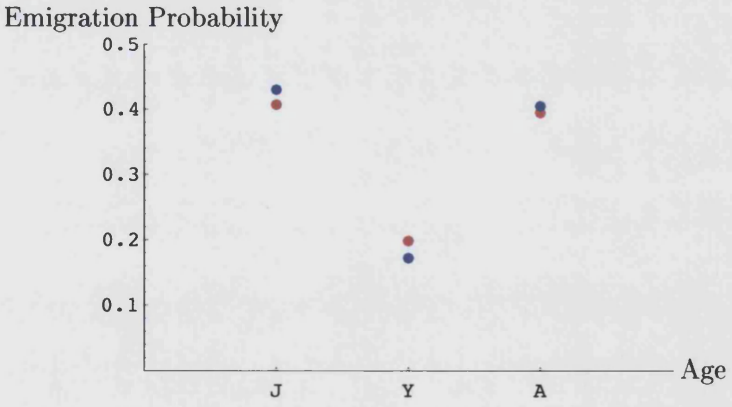


Figure 5.11: Emigration Probability for each age class ($\hat{k} = 10$): red dots represent the fit to Parer's data, blue dots represent the model result.

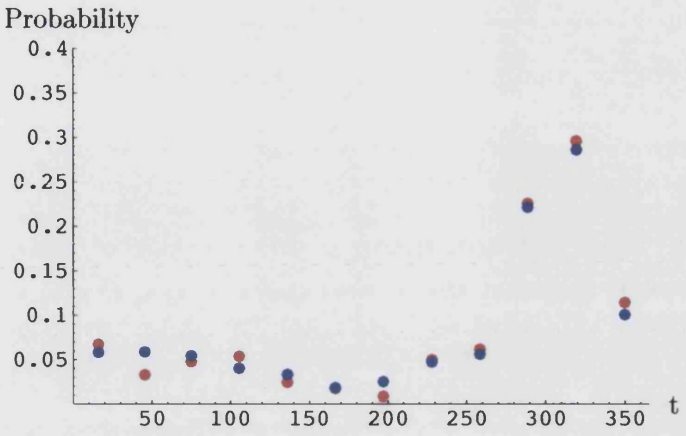


Figure 5.12: Probability distribution for seasonal emigration ($\hat{k} = 10$): red dots represent Parer's data, blue dots represent the model result.

## 5.6 Density-dependent emigration parameters.

Results using the Gradient Descent method with no density-dependent regulation of $m_J$.

The Gradient Descent method (see appendix) yielded the best fit values for the density-dependent emigration parameters again by minimising the total MSE: for the non-density dependent $m_J$ case, the parameters values are: $\delta = 1.0$, $A = 0.16$, $b_g = 0.008$, $u = 2.3$ and $\tau = 5000$, i.e.

$$\hat{\mathbf{p}} = \{1.0, 0.16, 0.008, 2.3, 5000\}.$$

with $MSE = 0.00408283$. Figures 5.13, 5.14 and 5.15 show the model results, using this set of parameters, against Parer's data.

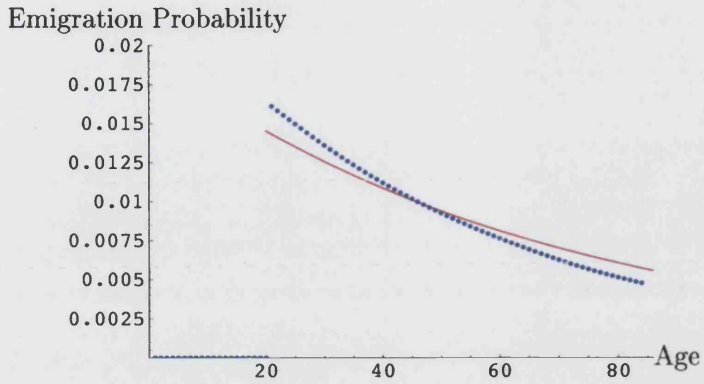


Figure 5.13: Age of Emigration Probability: the exponential curve (red is the curve 5.1) with best fit value $\alpha = 0.014527$ obtained from Parer's data (see figure 5.1). The blue dots are the age-at-emigration data derived from the model (5.6).

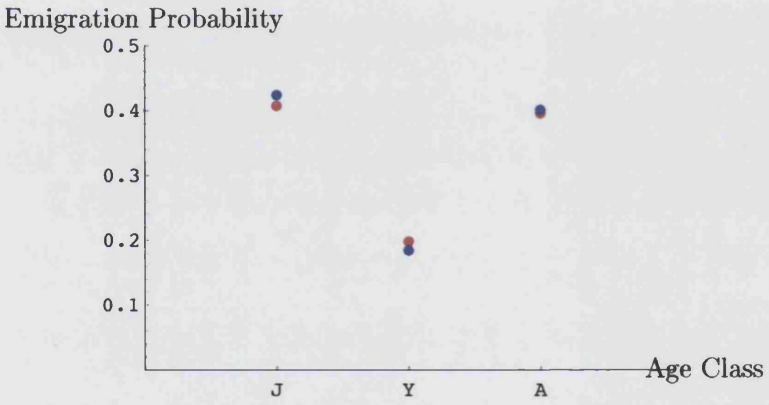


Figure 5.14: Emigration Probability for each age class: red dots represent the fit to Parer's data, blue dots represent the model result.

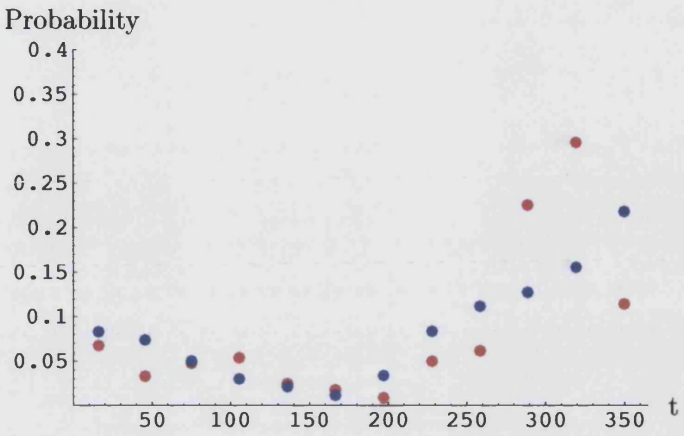


Figure 5.15: Probability distribution for density-dependent emigration: red dots represent Parer's data, blue dots represent the model result.

Results using the Gradient Descent method with density-dependent regulation of $m_J$.

When density-dependent regulation of $m_J$ was included, with $\hat{k} = 100$, the Gradient descent method yielded the following results for the best fit parameter values: $\delta = 0.99$, $A = 0.99$, $b_g = 0.08$, $s_t = 3.73$ and $\tau = 220$, i.e.

$$\hat{\mathbf{p}} = \{0.99, 0.99, 0.08, 3.73, 220\}.$$

with $MSE = 0.0054515$. Figures 5.16, 5.17 and 5.18 illustrate the model results, by using these parameter values in the emigration function, against Parer's data.

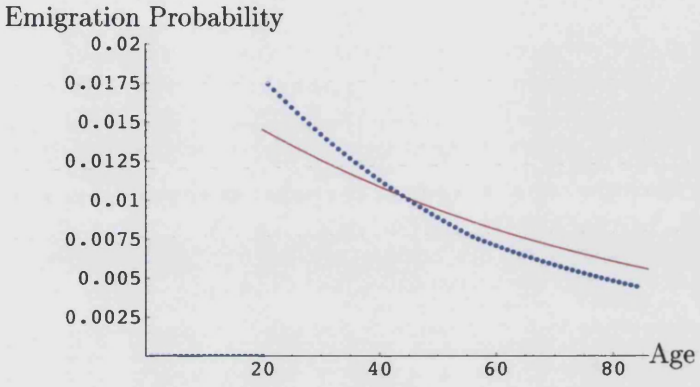


Figure 5.16: Age of Emigration Probability ($\hat{k} = 100$): the exponential curve (red is the curve 5.1) with best fit value $\alpha = 0.014527$ obtained from Parer's data (see figure 5.1). The blue dots are the age-at-emigration data derived from the model (5.6).

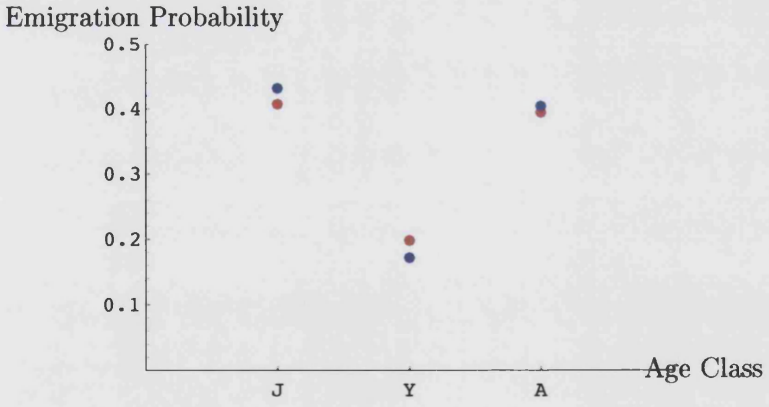


Figure 5.17: Emigration Probability for each age class ($\hat{k} = 100$): red dots represent the fit to Parer's data, blue dots represent the model result.

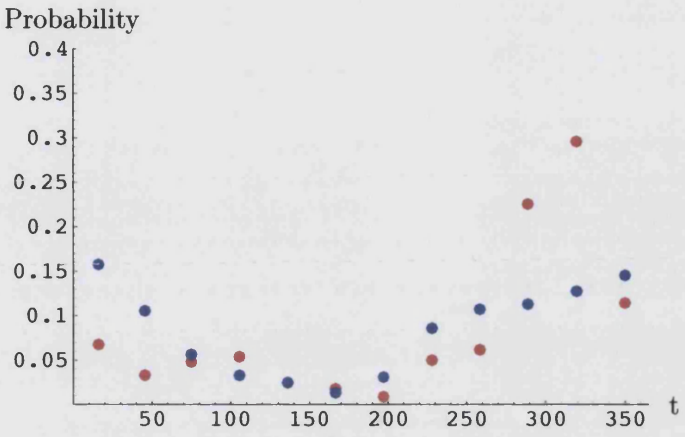


Figure 5.18: Probability distribution for density-dependent emigration ($\hat{k} = 100$): red dots represent Parer's data, blue dots represent the model result.

Even in this case, with the non-density dependence of $m_J$, we found that the model fits the real data better than when density dependence of Juvenile mortality is included. But it is obvious from the MSE values, as well as from inspection of the figures, that a seasonal emigration yields a better fit than a density dependent one. This seems to suggest that what might prompt rabbits to leave their site/warren for another one is the seasonal conditions more than how densely inhabited is the warren they are leaving. Therefore, in the spatial model, seasonal dependent emigration will be used to investigate the relation between the disease and the spatial configuration of the environment rabbits live in.

## 5.7 Appendix. Fitting model to data: Least Squares theory.

Newton's method and the Gradient Descent method are used to find the values for the unknown model parameters that minimize a mean-square-error (MSE) function. That is, we are given a sequence of data points, like the ones in Parer's data,

$$d_1, d_2, ..., d_N \in \Re$$

(usually, but not necessarily indexed by time), and a deterministic theoretical "model", like the emigration model illustrated in equations (5.6), which, it is proposed, generates this data (up to stochastic fluctuations). The model depends on the values of parameters $\mathbf{p} = (p_1, ..., p_n)$, and associated with any (allowable) set of parameter values is an output set of model values

$$m_1(\mathbf{p}), m_2(\mathbf{p}), ..., m_N(\mathbf{p}) \in \Re$$

indexed by the same indexing set as the given data. Then, we seek to find the parameter values which minimize the MSE function defined below

$$S(\mathbf{p}) = \frac{1}{N}\sum_{k=1}^{N}(m_k(\mathbf{p}) - d_k)^2. \tag{5.7}$$

In this research $n = 5$ is the length of the vector $\mathbf{p}$, $m_k(\mathbf{p})$ are the emigration model output and $d_k$ is Parer's data.

### 5.7.1 Newton's method

Newton's method considers that for $S(\mathbf{p})$ to be a minimum, it is necessary to find a value of $\mathbf{p}$ for which $\nabla S = \mathbf{0}$; where the gradient is taken with respect to $p_i$. If applied to the seasonal emigration model ($\sigma[T] = \sigma[t]$ as in equation (5.4)), the unknown parameter vector is

$$\mathbf{p} = (\delta, A, b_g, e_0, e_1).$$

Let $\mathcal{P}$ be the set of biologically allowable parameter values and set $\mathbf{f} = \nabla S$. Then $\mathbf{f} : \mathcal{P} \longrightarrow \Re^n$ is a vector-valued function of $n$ variables, $\mathbf{p} = (p_1, ..., p_n)$. A minimum of $S$ will occur at a value $\hat{\mathbf{p}}$ for which $\mathbf{f}(\hat{\mathbf{p}}) = \mathbf{0}$, where $\hat{\mathbf{p}} \in \mathcal{P}$ and $\hat{S} = S(\hat{\mathbf{p}})$ is a local minimum (and hopefully a global minimum).

We begin with a starting value $\mathbf{p}_0$ for which $\| \mathbf{f}(\hat{\mathbf{p}}_0) \|$ is already "small". This starting value could be found using a trial-and-error search method or the gradient descent method. Consider the Taylor expansion

$$\mathbf{f}(\mathbf{p}_0 + \mathbf{h}) = \mathbf{f}(\mathbf{p}_0) + D\mathbf{f}(\mathbf{p}_0)\mathbf{h} + terms\, of\, order \parallel \mathbf{h} \parallel^2, \tag{5.8}$$

where $\mathbf{h} = (h_1, ..., h_n) \in \Re^n$ is a vector with $\| \mathbf{h} \|$ small, and

$$D\mathbf{f}(\mathbf{p}_0) = \left(\frac{\partial f_i}{\partial p_j}(\mathbf{p}_0)\right) = \left(\frac{\partial^2 S}{\partial p_i \partial p_j}\right),$$

is the matrix of partial derivatives at $\mathbf{p}_0$. It is then assumed that $\mathbf{h}$ is chosen so that $\mathbf{p}_1 = \mathbf{p}_0 + \mathbf{h}$ is actually a zero of $\mathbf{f}$, and also that $\| \mathbf{h} \|$ is so small that the terms of order $\| \mathbf{h} \|^2$ in (5.8) are negligible. From (5.8), we therefore obtain

$$\mathbf{h} = -[D\mathbf{f}(\mathbf{p}_0)]^{-1}\mathbf{f}(\mathbf{p}_0), \tag{5.9}$$

provided the matrix $D\mathbf{f}(\mathbf{p}_0)$ is invertible. In general we cannot hope that the value of $\mathbf{h}$ given by (5.9) yields an *exact zero*, i.e. $\mathbf{p}_1 = \mathbf{p}_0 + \mathbf{h}$, because of the neglected terms of order $\| \mathbf{h} \|^2$. But by iterating this procedure the hope is to find a sequence $\mathbf{p}_0, \mathbf{p}_1, ..., \mathbf{p}_m, ...$, of increasingly better approximations to a true zero. When $\| \mathbf{f}(\mathbf{p}_m) \| \approx 0$ to some appropriate degree of accuracy, then we take $\hat{\mathbf{p}} = \mathbf{p}_m$.

This method is fast but it has the disadvantage that it is not always guaranteed to work. For example if $\mathbf{p}_0$ is not well chosen, then it is possible that $D\mathbf{f}(\mathbf{p}_0)$ is not invertible (or to have a very small eigenvalue). Moreover, even if $D\mathbf{f}(\mathbf{p}_0)$ is well-behaved, it can still be the case that $\mathbf{p}_1$ is actually a worse approximation to a zero of $\mathbf{f}$ than was $\mathbf{p}_0$.

To apply the method to a least-square fit, we take $\mathbf{f} = \nabla S$. Then

$$D\mathbf{f} = \left(\frac{\partial^2 S}{\partial p_i \partial p_j}\right) = D^2 S, \tag{5.10}$$

and (5.9) gives,

$$\mathbf{h} = \mathbf{p}_1 - \mathbf{p}_0 = -[D^2 S(\mathbf{p}_0)]^{-1} \nabla S(\mathbf{p}_0),$$

and

$$\mathbf{p}_1 = \mathbf{p}_0 - [D^2 S(\mathbf{p}_0)]^{-1} \nabla S(\mathbf{p}_0), \tag{5.11}$$

The problem is how to compute both the first and second derivatives of $S$ at $\mathbf{p}_0$, as well as $S(\mathbf{p}_0)$, from the given model. Since $\frac{\partial^2 S}{\partial p_j \partial p_i} = \frac{\partial^2 S}{\partial p_i \partial p_j}$, this gives $1 + n + \frac{1}{2}n(n+1) = \frac{1}{2}(n+1)(n+2)$ distinct objects to calculate.

It is usually impossible to find analytic expressions for the first and second derivatives, and $S(\mathbf{p})$ can only be computed numerically. To do this, we choose a set of "small" positive numbers

$$\mathbf{h} = (h_1, ..., h_n), \tag{5.12}$$

with $0 < h_k < 1$, and which are fixed once and for all. We then use for the first derivatives the approximations

$$\frac{\partial S}{\partial p_k}(\mathbf{p}) \approx \frac{S(\mathbf{p} + h_k \mathbf{e}_k) - S(\mathbf{p})}{h_k}, \tag{5.13}$$

where $\mathbf{e}_k = (0, ..., 1, ..., 0) \in \Re^n$ is the basis vector with 1 in the $k^{th}$ coordinate and 0 elsewhere. The sizes of the $h_k$ are chosen to reflect the sensitivity of $S$ to small changes in $\mathbf{p}$, and we try to choose them so that the approximations (5.13) have at most order 1. Of course this will depend on the region of parameter space from which $\mathbf{p}$ is chosen.

For the second derivatives, we begin with the Taylor expansion

$$S(\mathbf{p}_0 + h_k \mathbf{e}_k) = S(\mathbf{p}_0) + \frac{\partial S}{\partial p_k}(\mathbf{p}_0) h_k + \frac{1}{2}\frac{\partial^2 S}{\partial p_k^2}(\mathbf{p}_0) h_k^2 + terms\, of\, order\, h_k^3,$$

$$S(\mathbf{p}_0 - h_k \mathbf{e}_k) = S(\mathbf{p}_0) - \frac{\partial S}{\partial p_k}(\mathbf{p}_0) h_k + \frac{1}{2}\frac{\partial^2 S}{\partial p_k^2}(\mathbf{p}_0) h_k^2 + terms\, of\, order\, h_k^3.$$

Adding these and neglecting higher order terms then gives the approximation

$$\frac{\partial^2 S}{\partial p_k^2}(\mathbf{p}_0) \approx \frac{S(\mathbf{p}_0 + h_k \mathbf{e}_k) - 2S(\mathbf{p}_0) + S(\mathbf{p}_0 - h_k \mathbf{e}_k)}{h_k^2} \tag{5.14}$$

To obtain the cross-derivatives, $\frac{\partial^2 S}{\partial p_j \partial p_k}$,for $j \neq k$, we use the 2-variable Taylor expansions

$$S(\mathbf{p}_0 + h_j\mathbf{e}_j + h_k\mathbf{e}_k) = S(\mathbf{p}_0) + \frac{\partial S}{\partial p_j}(\mathbf{p}_0)h_j + \frac{\partial S}{\partial p_k}(\mathbf{p}_0)h_k + \frac{1}{2}\left(\frac{\partial^2 S}{\partial p_j^2}(\mathbf{p}_0)h_j^2 + 2\frac{\partial^2 S}{\partial p_j \partial p_k}(\mathbf{p}_0)h_j h_k + \frac{\partial^2 S}{\partial p_k^2}(\mathbf{p}_0)h_k^2\right) + \mathcal{O}[\| \mathbf{h} \|^3],$$

$$S(\mathbf{p}_0 - h_j\mathbf{e}_j - h_k\mathbf{e}_k) = S(\mathbf{p}_0) - \frac{\partial S}{\partial p_j}(\mathbf{p}_0)h_j - \frac{\partial S}{\partial p_k}(\mathbf{p}_0)h_k + \frac{1}{2}\left(\frac{\partial^2 S}{\partial p_j^2}(\mathbf{p}_0)h_j^2 + 2\frac{\partial^2 S}{\partial p_j \partial p_k}(\mathbf{p}_0)h_j h_k + \frac{\partial^2 S}{\partial p_k^2}(\mathbf{p}_0)h_k^2\right) + \mathcal{O}[\| \mathbf{h} \|^3].$$

Adding these two and neglecting higher order terms, we obtain

$$\frac{\partial^2 S}{\partial p_j^2}(\mathbf{p}_0)h_j^2 + 2\frac{\partial^2 S}{\partial p_j \partial p_k}(\mathbf{p}_0)h_j h_k + \frac{\partial^2 S}{\partial p_k^2}(\mathbf{p}_0)h_k^2 \approx S(\mathbf{p}_0 + h_j\mathbf{e}_j + h_k\mathbf{e}_k) - 2S(\mathbf{p}_0) + S(\mathbf{p}_0 - h_j\mathbf{e}_j - h_k\mathbf{e}_k),$$

and substituting from (5.14) then gives

$$\frac{\partial^2 S}{\partial p_j \partial p_k}(\mathbf{p}_0) \approx \frac{1}{2h_j h_k}\{[S(\mathbf{p}_0 + h_j\mathbf{e}_j + h_k\mathbf{e}_k) - S(\mathbf{p}_0 + h_j\mathbf{e}_j) - S(\mathbf{p}_0 + h_k\mathbf{e}_k)] + 2S(\mathbf{p}_0) + [S(\mathbf{p}_0 - h_j\mathbf{e}_j - h_k\mathbf{e}_k) - S(\mathbf{p}_0 - h_j\mathbf{e}_j) - S(\mathbf{p}_0 - h_k\mathbf{e}_k)]\}. \quad (5.15)$$

In order to implement the method, it follows from (5.13), (5.14) and (5.15), that it is necessary to compute $S(\mathbf{p}_0)$, $S(\mathbf{p}_0 + h_k\mathbf{e}_k)$, $S(\mathbf{p}_0 - h_k\mathbf{e}_k)$, $S(\mathbf{p}_0 + h_j\mathbf{e}_j + h_k\mathbf{e}_k)$ and $S(\mathbf{p}_0 - h_j\mathbf{e}_j - h_k\mathbf{e}_k)$ for $1 \leq k \leq n$ and $1 \leq j < k$. This gives $1 + 2n + n(n-1) = 1 + n + n^2$ quantities to be computed for each step of the process. In our model, as $n = 1, 2, 3, 4, 5$, there are $3, 7, 13, 21, 31$ quantities.

### 5.7.2 Gradient Descent method

The Gradient Descent method is used to minimise the MSE function when the set of parameters are the density-dependent parameters in the function $\sigma[R]$ (equation (5.5)). The parameter vector in the density-dependent emigration function is:

$$\mathbf{p} = (\delta, A, b_g, u, \tau)$$

where $\delta$ is the exponential decay parameter of the age probability of emigration (equation (5.2)), and $A$, $b_g$, $s_t$ and $\tau$ have been described in section 5.3.

In this case Newton's method was not stable enough to yield satisfying results. Instead we used the much slower, but more reliable, Gradient Descent Method, which is described below.

Let $\mathbf{p}_0$ be a starting value chosen using a trial and error method and let

$$\nabla S(\mathbf{p}) = (\frac{\partial S}{\partial p_1}, ..., \frac{\partial S}{\partial p_n})$$

be the gradient of $S$ with respect to $\mathbf{p}$. We can define a function

$$f(s) = S(\mathbf{p}_0 - s\nabla S(\mathbf{p}_0)) - S(\mathbf{p}_0). \tag{5.16}$$

where $s \geq 0$ is a real variable. Then $f(0) = 0$, and

$$f'(0) = - \parallel \nabla S(\mathbf{p}_0) \parallel^2 = -\sum_{k=1}^{n} (\frac{\partial S}{\partial p_k}(\mathbf{p}_0))^2. \tag{5.17}$$

If $\mathbf{p}_0$ is not a local minimum of S, then $\nabla S(\mathbf{p}_0) \neq \mathbf{0}$, and hence $f'(0) < 0$; i.e. there is an interval, $0 < s < s_0$, in which $f(s)$ is strictly decreasing, or $0 = f(0) > f(s) > f(s_0)$. Hence it is possible to find an $s_1 > 0$ for which $f(s_1) < 0$. Taking $\mathbf{p}_1 = \mathbf{p}_0 - s_1 \nabla S(\mathbf{p}_0)$, we therefore conclude that

$$S(\mathbf{p}_1) < S(\mathbf{p}_0). \tag{5.18}$$

This procedure can now be iterated to construct a sequence, $\mathbf{p}_0, \mathbf{p}_1, ..., \mathbf{p}_m ...$, with $S(\mathbf{p}_0) > S(\mathbf{p}_1) > ...S(\mathbf{p}_m) > ....$ The process can be terminated when $\parallel \nabla S(\mathbf{p}_m) \parallel \approx 0$ to some appropriate margin of error (some specified number of decimal places). Then the required minimising value is $\hat{\mathbf{p}} = \mathbf{p}_m$.

A systematic way to search an appropriate value of $s_1$ for which (5.18) holds is the following. A suitable $s^{(0)} > 0$ is fixed (once and for all)- usually a power of 2- and we consider the decreasing sequence: $s^{(0)} > s^{(1)} > ...s^{(r)} > ... > 0$, where $s^{(r+1)} = \frac{1}{2}s^{(r)}$. These values are then tested in turn by taking $s_1 = s^{(r)}$ for $r = 0, 1, ...$, until the first value is found for which (5.18) holds. The theory illustrated above guarantees the existence of such value. Obviously it is preferable to choose $s^{(0)}$ so that not too many trials are needed before $s_1$ is found, i.e. it should not be too large. On the other hand, the larger $s_1$ can be chosen, the faster the descent process will proceed. Using this method we face the same problem as in Newton's method, i.e. in complicated applications (such as those considered) it is not usually possible to find analytic expressions for the derivatives $\frac{\partial S}{\partial p_k}$. Indeed there is generally no analytic expression for $S(\mathbf{p})$, and its value must be generated numerically from the given model. To use the method we therefore have to numerically approximate the derivatives.

It can be done in the same way explained in the previous section (section 5.5.1), by approximating the first derivatives as in (5.12) and (5.13). Moreover, for a more sophisticated implementation of this method, one can have adaptable $h_k$; i.e. different possible values of the $h_k$ can be tested to ensure that the approximate derivatives have consistent magnitudes. Unfortunately, this method bears the disadvantage of being very slow, and an adaptable $\mathbf{h}$ only enhances this problem. None of our implementations incorporate this feature, but the method has nevertheless proved reliable in our applications.

# Chapter 6

# Results: Disease-free environment

## 6.1 Seasonality

The model was run (for 25 years) using the values for the parameters derived in section 3.1.2, and the breeding functions derived in section 4.2. Initially the outcome was investigated not using any density dependence regulation or stochastic climatic variation in order to provide a baseline of behaviour in each geographical region.

We observed that the population explodes for all the different Australian regions considered, even though at a different rate. In the Subalpine and Western NSW environment (shown in figure 6.1) the take off of the population size is much slower then for the Riverina and South-Western Western Australia regions (not shown). Moreover in the Subalpine case, it was chosen to take a higher litter size $\lambda$ than for the other 3 regions, since the population was not able to sustain itself with the "default" value $\lambda = 4$; $\lambda = 5$ was used instead. It was confirmed that Subalpine is a marginal environment [27], so the fact that the model behaviour reflects this was encouraging. The oscillations are the seasonal breeding effect on the population. The reason why we do not show the behaviour of the total population density with time for Riverina and South-Western WA is that their time scale for the population to explode is remarkably smaller than for Subalpine and Western NSW. For example, in Riverina, the population reaches a density of $8 \times 10^5$ after 8 years, and in South-Western WA the population reaches a density of $8 \times 10^5$ after 11 years.

In the next section the outcome of a model simulation using the density regulating function explained in section 4.3 is discussed.

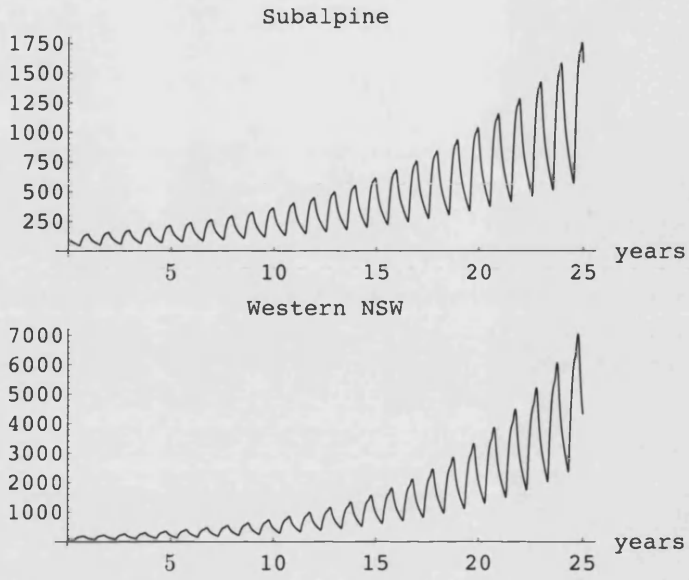


Figure 6.1: Rabbit population density with no density dependence against time (years). $\lambda = 5$ for Subalpine, $\lambda = 4$ for Western NSW.

## 6.2 Seasonality with density dependence

### 6.2.1 $\lambda$- Density Dependence

The model was run for 15 years using a density dependent litter size $\lambda$ for different threshold values $\hat{N}$ (see equation 4.3). The threshold value only determines the average stable equilibrium value of the population density. In fact the population goes to an equilibrium value after about 5 years, but still we ran the model for 15 years to allow it to become completely stable before recording results.

Figure 6.2 illustrates the variation of $\lambda$ in one year for the four Australian environments considered. No $m_J$ density dependent is present at this stage. It can be observed that even though $\lambda$ has no effect outside the breeding season, $\lambda(x)$ is growing for $n \leq n_0$ because no breeding is taking place and the population density is declining. When the breeding season starts at the $n_0$ day of the year, after a small time delay, $\lambda$ starts decreasing as the population increases beyond the threshold. A $\lambda$-value smaller than the breeding season average tends to persist for more than half of the breeding season, until the end of the breeding season. After the $n_1^{th}$ day of the year, $\lambda$ starts increasing again after a small time delay (see figure 6.2). Thus the pattern of breeding shows a rapid spurt at the

beginning of the breeding season, with does producing large litter sizes, followed by a relatively long interval in which does produce lower than average litter sizes. This kind of behaviour can be observed for all the Australian regions considered; what varies between them is the time interval of the breeding season and the average value of $\lambda$ during the breeding season. In fact Riverina and SWWA have much longer breeding seasons, and we expect the population to grow exponentially very fast (see section 6.1). This is why the average value of $\lambda$ for these two regions is much lower than that for Subalpine and WNSW. From the model runs, we obtain an average value of $\lambda = 4.97$ for Subalpine, $\lambda = 4.11$ for WNSW, $\lambda = 2.15$ for Riverina and $\lambda = 2.48$ for SWWA, regardless of the threshold value for the $\lambda$ function.

Figure 6.3 illustrates how $\lambda$ varies as a function of the threshold level $\hat{N}$ when $m_J$ density dependence is present (see section 4.3.2 for a discussion of $m_J$ density dependence). We do not know how the $m_J$ threshold level $\hat{k}$ and the $\lambda$ threshold level $\hat{N}$ are related. Thus, we kept $\hat{k} = 100$ fixed (as this will be the value of $\hat{k}$ most used throughout this research) and observed the average value of $\lambda$ in the breeding season for different $\hat{N}$ for the four Australian regions. We can then see in figure 6.3 that for Subalpine and WNSW, $\lambda$ is constant for $\hat{N} \leq \hat{k}$, since $\lambda$ density dependence controls the population and the $m_J$ density dependence doesn't play any role for a population smaller than $\hat{k}$. On the other hand for Riverina and SWWA $\lambda$ starts to increase for $\hat{N} < \hat{k}$. This is because for these two environments, the average stable population is a value somewhat bigger than the $\lambda$ function threshold value. Thus, for $\hat{N} = \hat{k}$ the average stable population density is bigger than $\hat{N}$, and hence bigger than $\hat{k}$. As a consequence the $m_J$ density-dependent control mechanism starts to lower the population density value and $\lambda$ increases. This case is similar to the density dependent cases described in figure 6.2. When $\hat{N} > \hat{k}$, the $m_J$ density dependent control is regulating the population keeping it at an average value somewhat above $\hat{k}$. This implies that the population density is less than $\hat{N}$, and this allows the value of $\lambda$ to rise. So we observe that $\lambda$ increases as $\hat{N}$ inreases beyond $\hat{k}$ (figure 6.3). Even though $\lambda$ behaves similarly in all the environments, we notice that for marginal environments (Subalpine and WNSW) the average value of $\lambda$ for $\hat{N} \leq 100$ is higher than in Riverina and SWWA. We expect this since $\lambda$ has to have a higher value to sustain the population in a marginal environment, i.e. one with a shorter breeding season.

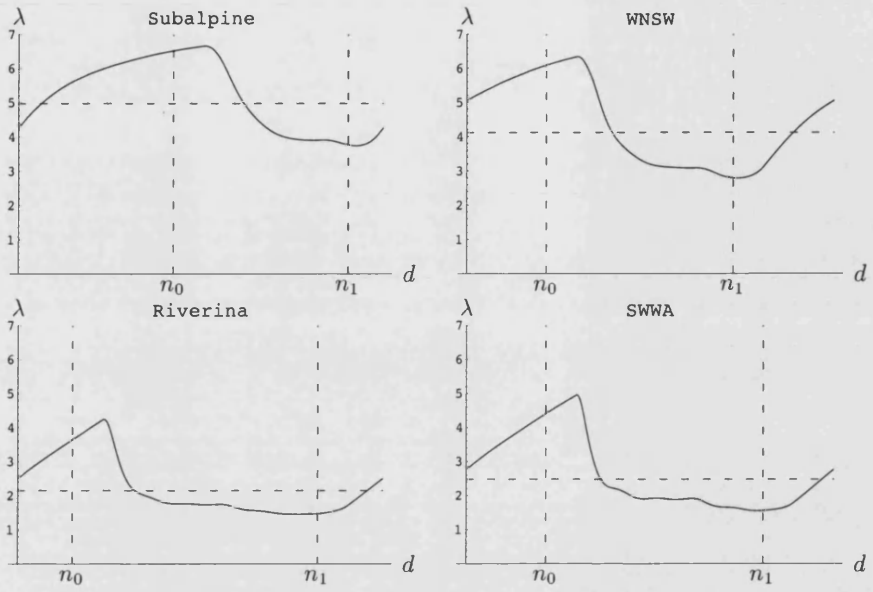


Figure 6.2: $\lambda$ variation during one year ($d$=days). The horizontal dotted line represents the average value of $\lambda$ during the breeding season, i.e. between $n_0$ and $n_1$ (vertical dotted lines).

### 6.2.2 $m_J$- Density Dependence

Density dependence was included in the model to investigate the effect of different environmental capacities as represented by the density effect on Juvenile mortality as discussed in section 4.3.2. Figure 6.4 illustrates the effect of using the $m_J$ density dependent regulating function for different threshold capacities, $\hat{k}$, in the four Australian regions considered.

The population growth is regulated yielding a stable oscillation around the average annual population size, which is somewhat above the threshold capacity value: this holds for any threshold capacity chosen. The oscillations are an effect of the seasonal periodicity of the birth rate. This shows that it is realistic to assume that any environment can sustain only a certain population density, and that the model can represent the real dynamics of rabbits in the wild when it incorporates a density regulation. Note that, unlike in the unregulated cases of figure 6.1, the density-regulated populations behave in a very similar fashion for all the regions.

In the simulations to come in the course of this research we will use a constant $\lambda$ since $m_J$ density regulation is enough to control the population from exploding and we have more literature (see

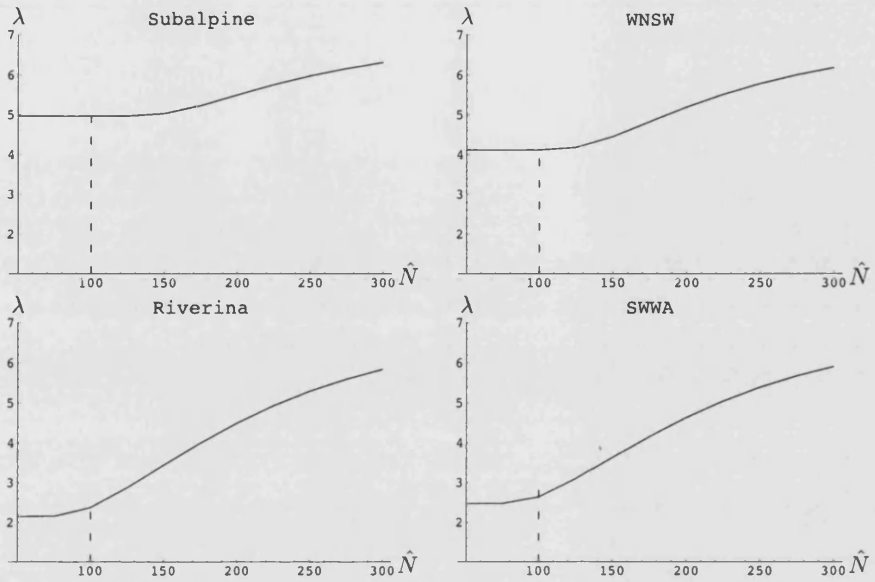


Figure 6.3: $\lambda$ versus the threshold level $\hat{N}$ when $m_J$ density dependence is included ($\hat{k} = 100$). The vertical dashed line is at $\hat{k}$, the $m_J$ density-dependent threshold.

sections 1.3.3 and 4.3.2) to show that in high density populations, it is the Juveniles that suffer an increased death rate; while there is no strong evidence for variation in $\lambda$ under environmental stress [28]. Thus, we will use $\lambda = 4$ for WNSW, Riverina and SWWA, which is the average value of the litter size as reported in the literature (see section 1.3.2). In fact in figure 6.3 we see that for these 3 environments, for any $\lambda \geq 4$, the $m_J$ density dependent effects will be dominant. However, for Subalpine $\lambda \geq 5$ must be chosen for the $m_J$ density dependence to be dominant (see figure 6.3), and to avoid the population from collapsing, i.e. for Subalpine we will use a value of $\lambda$ close to the breeding season average as shown in figure 6.2.

## 6.3 Climatic Variability

To investigate the effect of different climatic conditions, the model was run allowing for the threshold capacity $\hat{k}$ to change through time as a Poisson distributed process, and the possible values of the threshold capacity to be randomly distributed according to a lognormal distribution, as discussed in section 4.4. This was carried out for all the four Australian regions for which seasonal data was

available; results are shown in figures 6.3, 6.4, 6.5, 6.6; note that the dots are annual averages, which in turn have been averaged over three independent runs (variance not shown). It can be observed that the higher the Poisson frequency, the less variable the population is from year to year.

The total population density for the non-stochastic density dependent case is marked in black: this helps to make a comparison against which to evaluate the effect of stochastic regulation on the population. The other colours each indicate a different variance for the lognormal distribution, and these changes are tried for different Poisson frequencies.

The introduction of stochastic variation clearly alters the outcome of the model: the population size from year to year varies with unstable oscillations. Such oscillations are dampened as the frequency of the climate change becomes higher, and at the same time the population size becomes lower. This seems to indicate that varying the threshold capacity through time keeps the population density down.

The same kind of phenomenon is observed in all the four regions considered, even though the effects are more intensive in the Subalpine and Western NSW regions, since these regions are more marginal and climatic variation more disastrous for rabbits as their breeding season is shorter than for Riverina or South-Western Western Australia (figure 4.2).

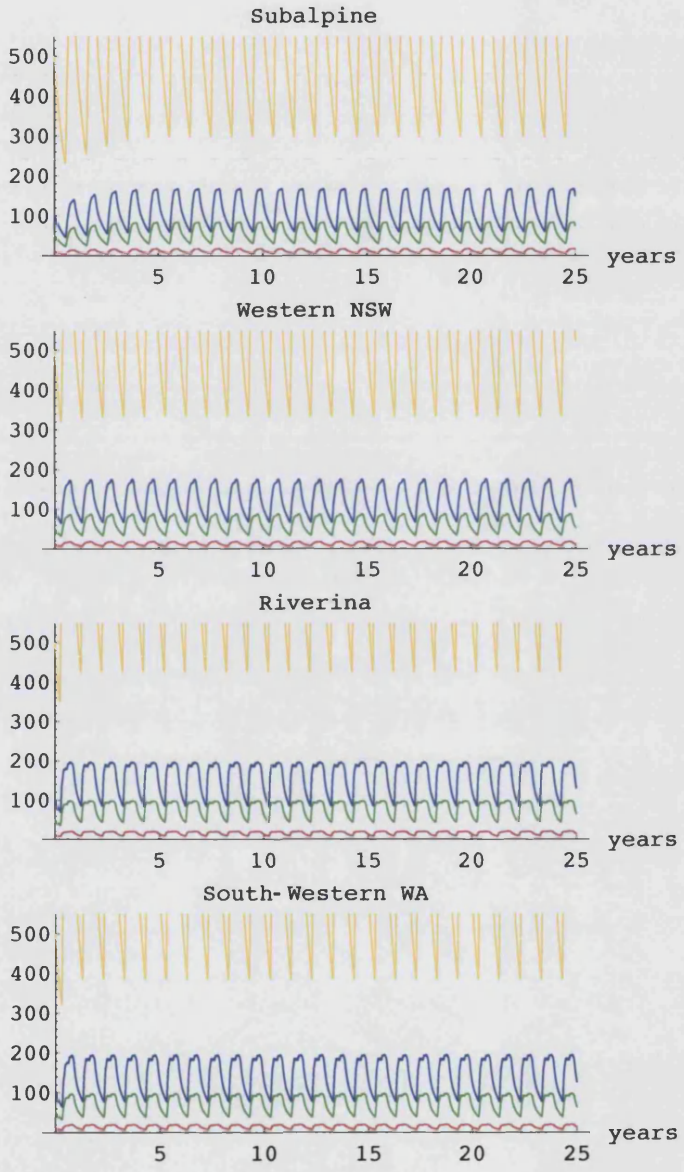


Figure 6.4: The effect of varying the carrying capacity $\hat{k}$ ($\hat{k} = 10$ (red), $\hat{k} = 50$ (green), $\hat{k} = 100$ (blue), $\hat{k} = 500$ (yellow)).

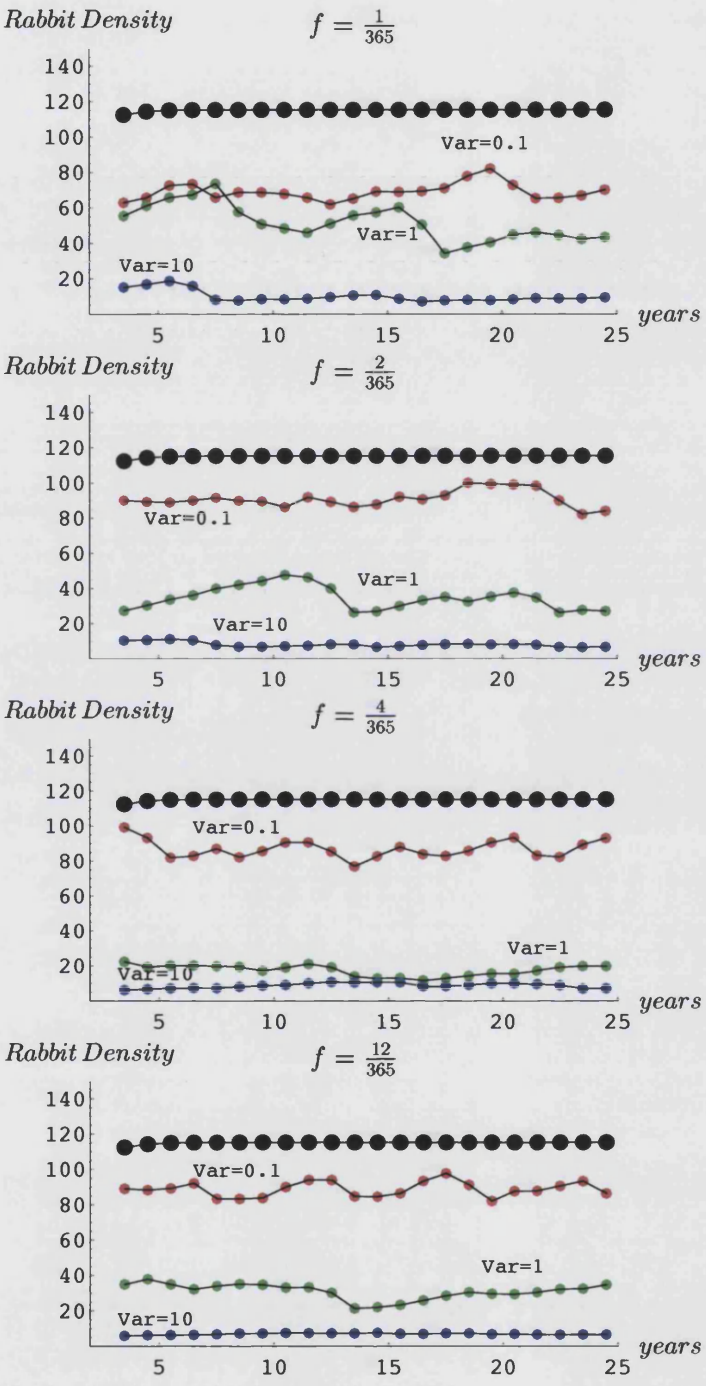


Figure 6.5: The effect of climatic variability in the Subalpine region (black large-dotted line is the non-stochastic case). $f$ =Poisson frequency.

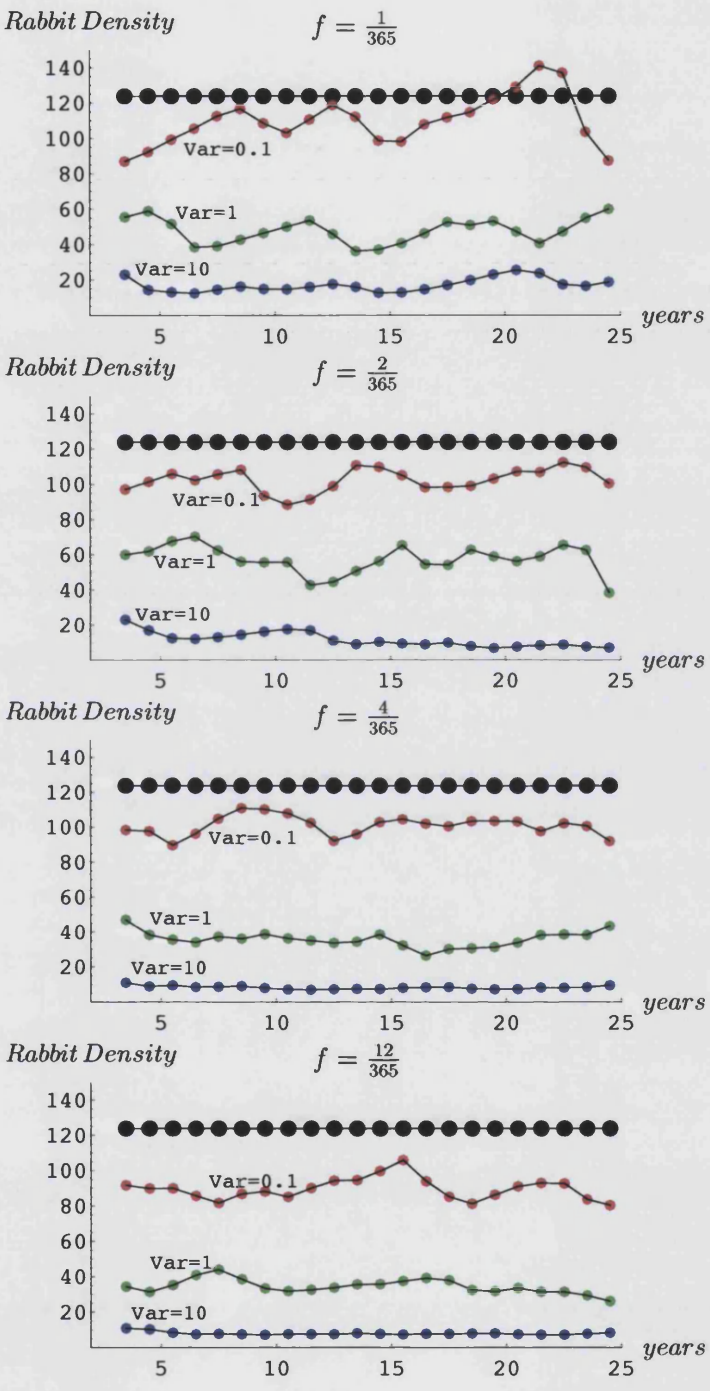


Figure 6.6: The effect of climatic variability in the Western NSW region (black large-dotted line is the non-stochastic case). $f$ =Poisson frequency.

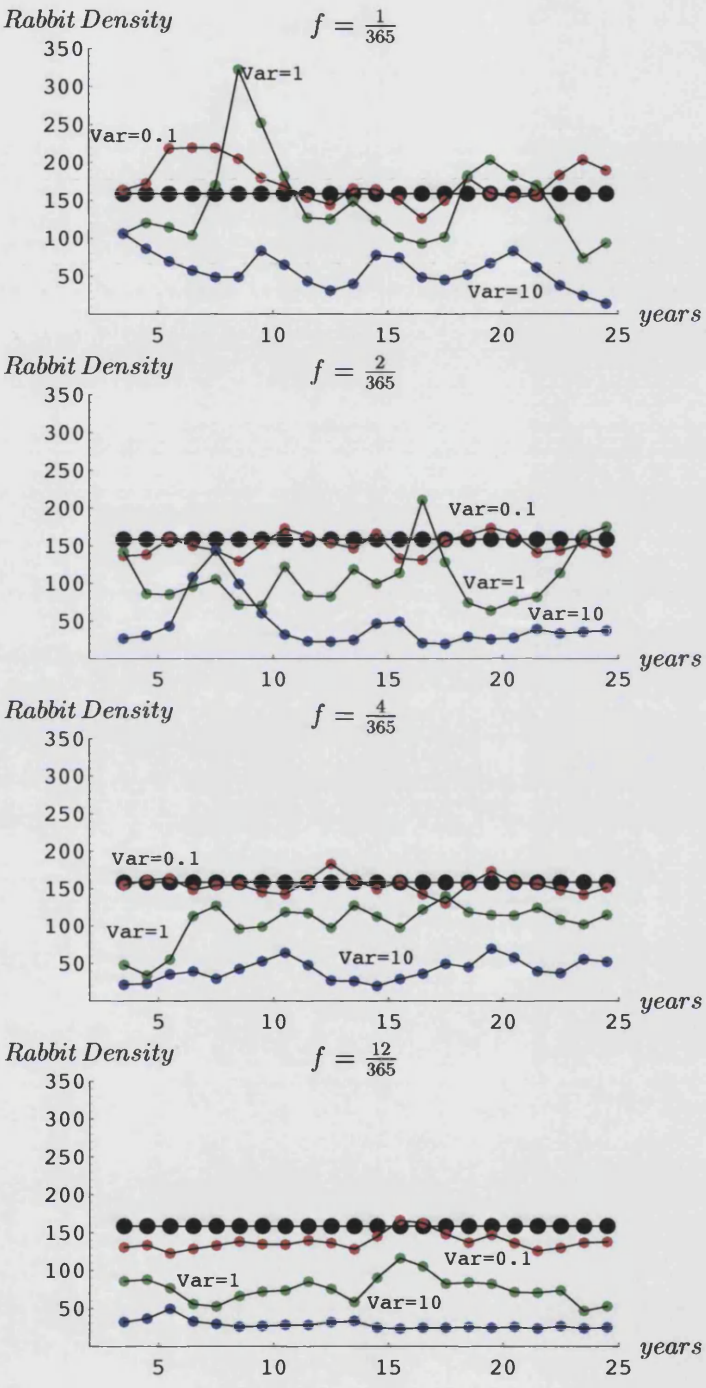


Figure 6.7: The effect of climatic variability in the Riverina region (black large-dotted line is the non-stochastic case). $f$ =Poisson frequency.

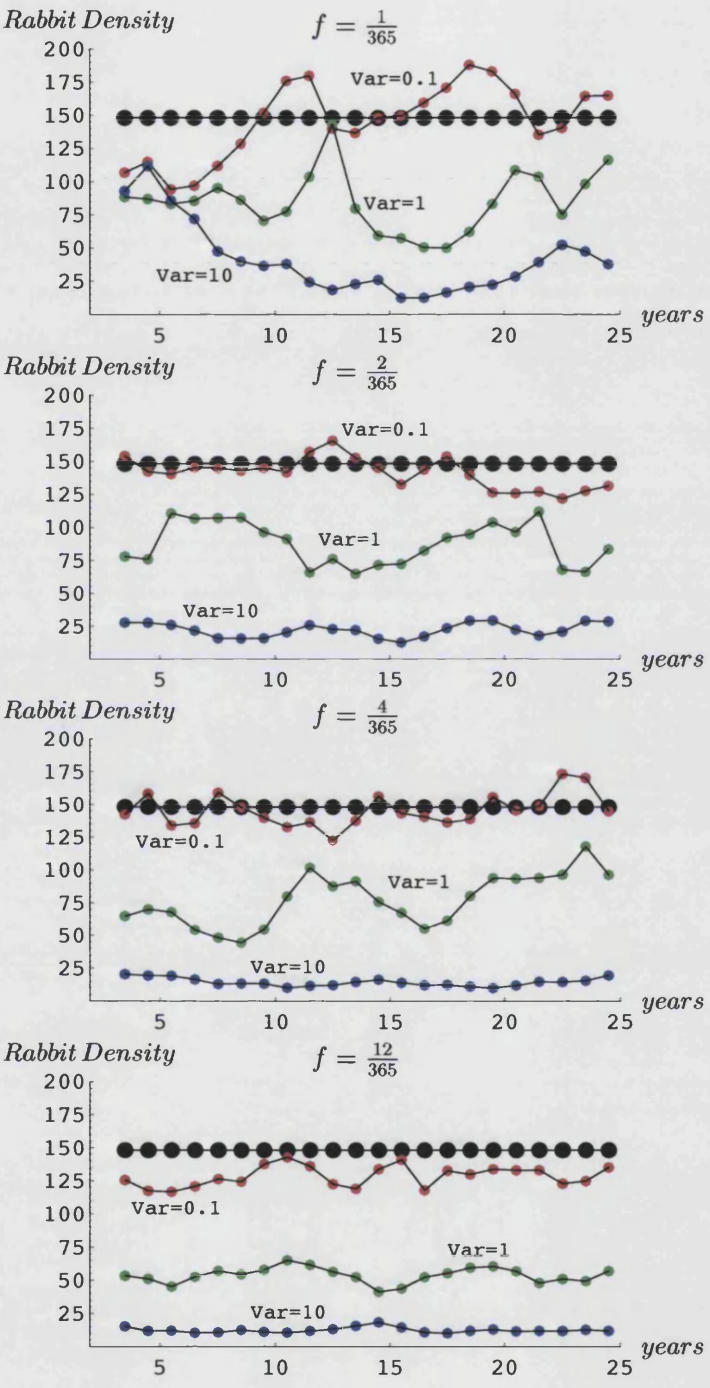


Figure 6.8: The effect of climatic variability in the South-Western Western Australia region (black large-dotted line is the non-stochastic case). $f$ =Poisson frequency.

# Chapter 7

# Adding the Disease using the Strong hypothesis: non stochastic results.

In the investigation of the effects of the disease on the population, the model representing the Strong hypothesis (equation (3.2)) was run for 5 years without any disease, to avoid any possible dependence on the initial conditions, and subsequently an environmental viral load of 2 units ($W = 2$) was introduced. The total run time was 25 years. Initially the disease model was tested using no stochastic variability, but only density dependent regulation, with $\hat{k} = 100$ being the threshold capacity value; in this manner it has been possible to select the appropriate and significant range of the virulence parameter $b$ (section 3.1.4) to be used to investigate further the outcome of the interaction between rabbits and RCD in the model. Since the infectivity, $c_V$, and the decay rate in the environment, $m_V$, are the main characteristics of the disease, and are yet unknown, the effect of varying them was analised. $c_V$ was varied by changing the value of $b$. This can be thought of as representing different virus strains. Thus $b$ can be used as the indication for virus strain, and, by varying $b$, it is possible to see which strain is most effective in terms of controlling the population density. Below are some examples of the effect of using different values of the virulence parameter $b$ in the equation for $c_V$ (3.11) for each Australian region for which data is available.

## 7.1 Subalpine

Figures 7.1 to 7.7 show that the disease becomes effective only for values of $b \leq 3000$. For $b = 5000$ the population remains unchanged by the disease and the disease strain does not persist after the initial outbreak. For $b = 4000$, the disease persists for the entire run but still does not significally affect the population size. The disease has recurrent outbreaks but the viral load never goes over 3 units; the rabbit population recovers easily from a weak strain. On the other hand, for $b = 3000$ the disease persists with 2 substantial outbreaks, about 12 years apart, that affect the population, which recovers to pre-outbreak values only after $10 - 12$ years, when a new outbreak occurs (Figure 7.1). Figure 7.2 shows the dynamics of the population of each age class, which can help to understand what is happening in figure 7.1. We can observe that there are very few Infected Juveniles appearing about one year after the outbreak and lasting for less than a year. The Recovered Adults are partly coming from the Recovered Subadult class and partly Adults that have survived and recovered from the disease. Note that there is a very small number of infected since the virulence of the virus is quite low. For $3000 < b < 600$, the population size is constantly reduced by a persistent disease, it never regains pre-disease size and it is kept at low values (less than 50 individuals) throughout the run of 20 years (post-disease) (Figure 7.3). For $b = 100$ (Figure 7.4), the population size collapses and remains very low after the first outbreak for the entire run, with the disease persisting at low values, but already a new trend in the disease outbreaks can be observed; the outbreaks have a cyclical reappearance that coincide with the seasonal trend of the reproduction rate of the rabbit. This is due to the fact that the disease kills all the susceptibles and the youngster and adult population consists of recovered juveniles that survive the disease, remain immune for life (the Strong hypothesis) and mature to be the adult class (See figure 7.5). The virus keeps the population to very low levels, since it lets a new susceptible population build up after about 12 years from disease outbreak which can then be dominated by the virus. While for $b \leq 80$, a totally new scenario appears as, even though the disease persists, towards the end of the run the population size recovers almost to pre-disease levels through the recovered population (see figure 7.7), with an exponential growth that is rippled by the seasonal fluctuations due to the reproductive rate, i.e. "availability" of juveniles that can become immune (figure 7.6). This indicates that the transition from $b = 100$ to $b = 80$ is a turning point in the disease success to control the population. Later on we will show that this phenomenon occurs when using the Strong hypothesis, but not in the Weak hypothesis case.

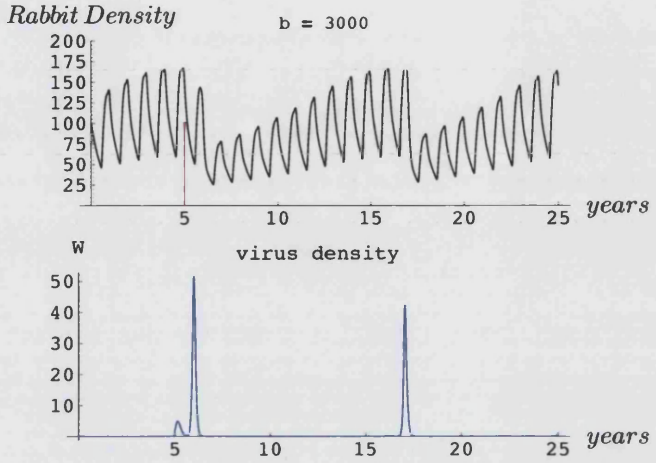


Figure 7.1: Effect of RCD on a rabbit population in Subalpine($b = 3000$).

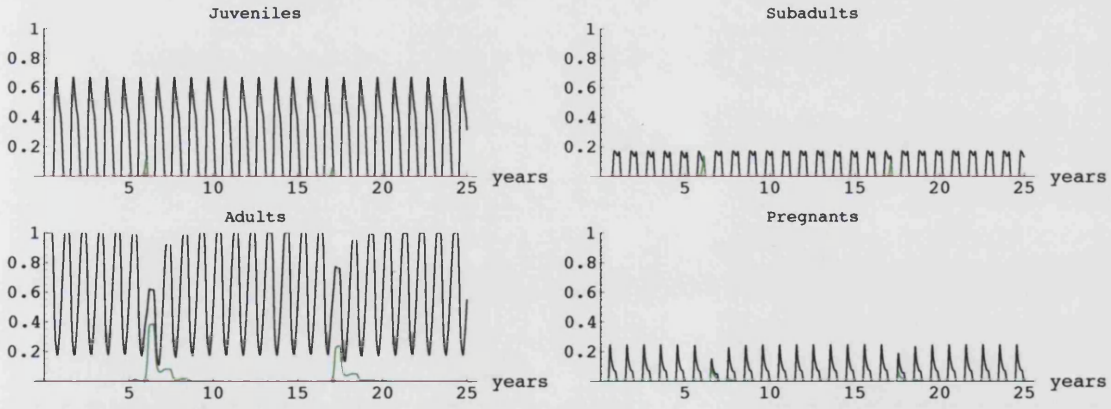


Figure 7.2: Proportion of the age classes against time (Black=Susceptible, Red=Infected, Green=Recovered), ($b = 3000$).

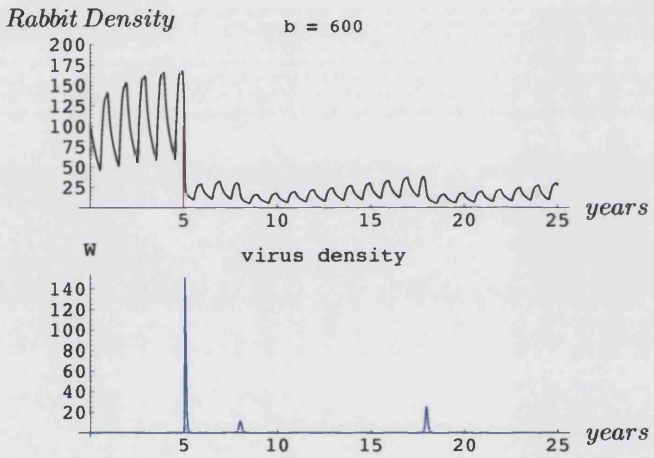


Figure 7.3: Effect of RCD on a rabbit population in Subalpine($b = 600$).

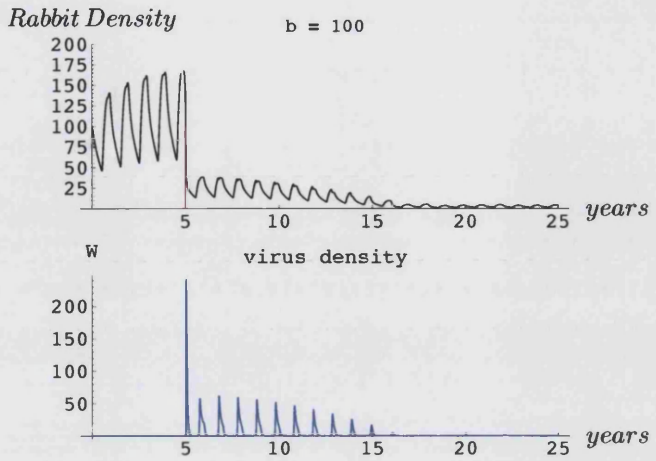


Figure 7.4: Effect of RCD on a rabbit population in Subalpine($b = 100$).

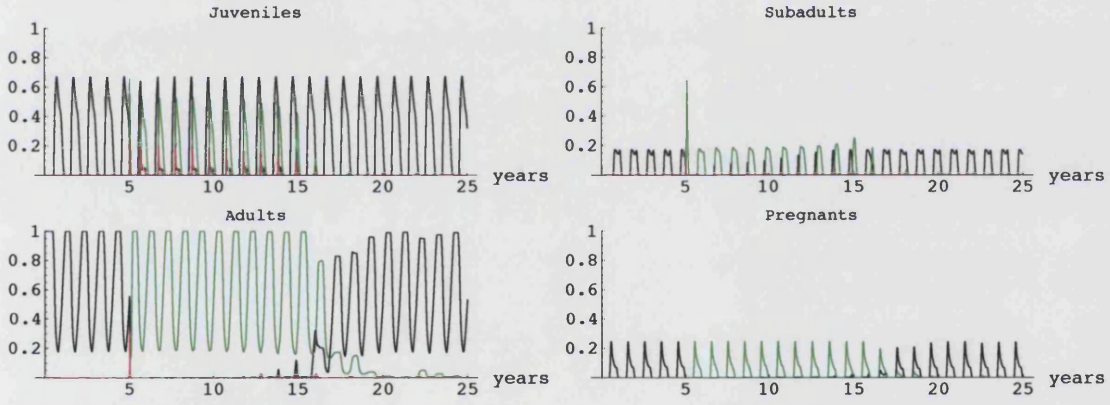


Figure 7.5: Proportion of the age classes against time (Black=Susceptible, Red=Infected, Green=Recovered), ($b = 100$).

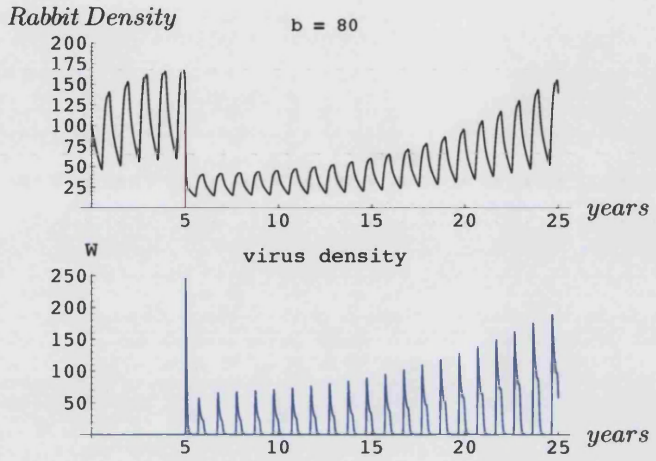


Figure 7.6: Effect of RCD on a rabbit population in Subalpine($b = 80$).

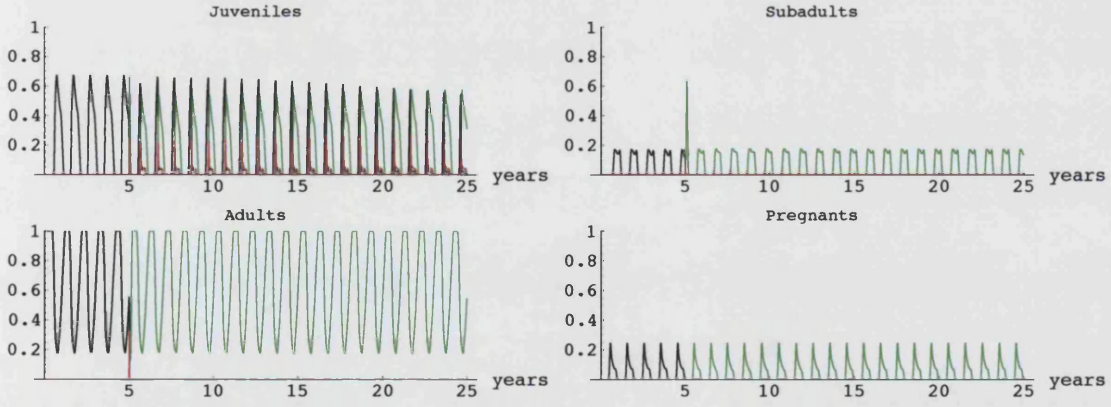


Figure 7.7: Proportion of the age classes against time (Black=Susceptible, Red=Infected, Green=Recovered), ($b = 80$).

## 7.2 Western NSW

The following figures illustrate the effect of different virus strains on a population living in the other marginal environment considered: Western NSW. The variation in population size according to the value of $b$ (virus strain) is quite similar to the Subalpine region.

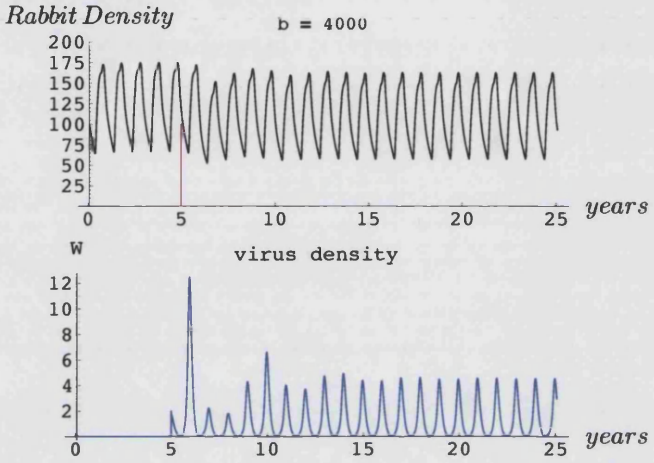


Figure 7.8: Effect of RCD on a rabbit population in Western NSW ($b = 4000$).

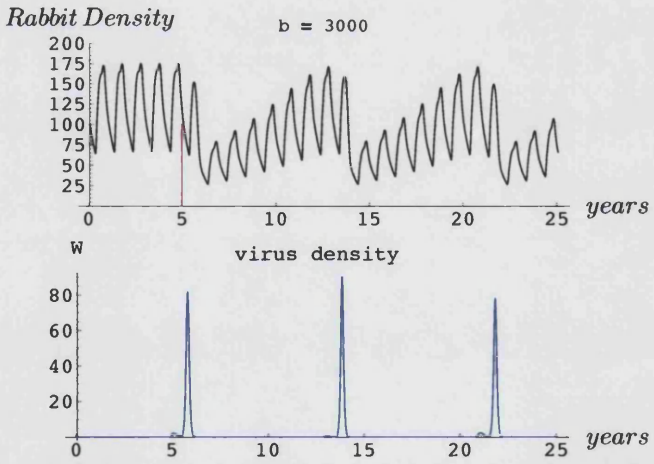


Figure 7.9: Effect of RCD on a rabbit population in Western NSW ($b = 3000$).

For $b$ to have an effect on the population size, its value should be around 3000 since for $b = 4000$, even though the disease persists with yearly outbreaks, the population size is only slightly affected

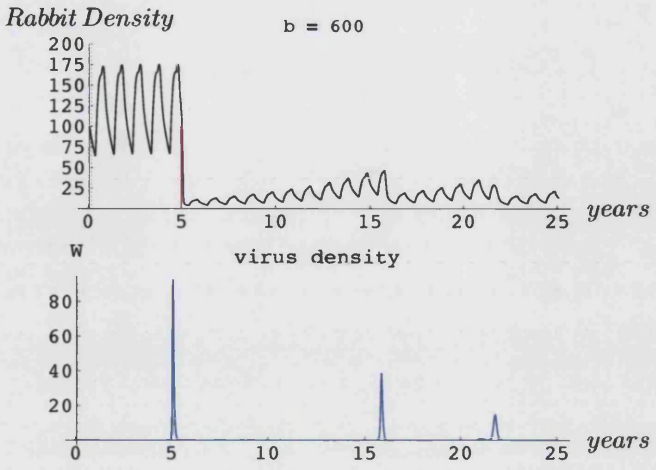


Figure 7.10: Effect of RCD on a rabbit population in Western NSW ($b = 600$).

at the end of the $6^{th}$ year, and it returns to almost non-disease levels during the following year, which it maintains for the rest of the run (Figure 7.8). Above $b = 4000$, the disease has no effect on the population and does not persist after the initial introduction. For $b = 3000$ the disease persists with regular outbreaks every 8 years, during which the population size builds up exponentially until a new outbreak occurs (Figure 7.9). The same outcome can be observed for values of $b$ as low as 200, even though intervals between outbreaks become shorter. As $b$ decreases the population size can build up, but to much lower values, until for $b = 200$ there is no more growth between successive outbreaks, and the population size is kept to very low values, with oscillations due to seasonal effects. The virus is so infectious that an initial outbreak is enough to maintain the population at very low values for the rest of the run: the subsequent outbreaks occur with very low value levels of viral load, due to the very small population size. The disease persists but at very low values, probably it is maintained amongst Juveniles, which are not killed. This scenario is the same for all values of $b$ from 200 down to 40. For $b = 30$ (figure 7.11), the disease starts to persist with regular outbreaks every year, but at the same time the population slowly recovers. After its introduction, it brings the population size to very low values, but after about the $15^{th}$ year, the population starts to grow exponentially again. The population consists mostly of recovered individuals, and only the juveniles catch the disease, recover and remain immune, survive and mature to become Subadults and Adults. All the Adult and Subadult individuals are recovered Juveniles that have matured. No Susceptibles other than Juveniles are present in the population. The virus persists through the

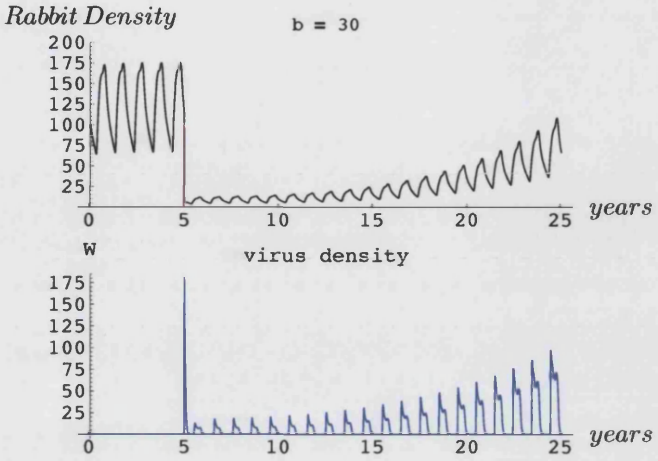


Figure 7.11: Effect of RCD on a rabbit population in Western NSW ($b = 30$).

juveniles that do not die from it, but the disease is not present among Subadults or Adults. The same outcome is observed for $b \leq 30$.

## 7.3 Riverina

For the non-stochastic case, according to the model results, a rabbit population living in the Riverina region is not remarkably affected by the disease for any value of $b$. This can be observed in figures 7.12 to 7.17. For values of $b > 6000$ the disease does not persist, and even when it persists for $b \leq 6000$, it does not significantly reduce the population size, but regains the initial size after 7 years ($b = 2000$, figures 7.15-7.16) or 5 years ($b = 1000$, figure 7.17). In fact the breeding period in the Riverina region is much longer than for the Marginal environments. So during the year there will always be Juveniles that will carry the disease, even though they remain immune and will preserve their immune state as they mature into Youngsters and Adults; the disease will not have an impact on the population but it will persist among the Susceptible Juveniles (see figure 7.16).

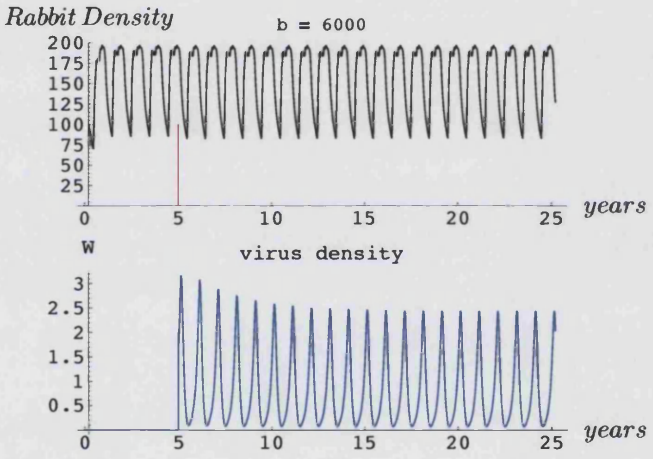


Figure 7.12: Effect of RCD on a rabbit population in Riverina ($b = 6000$).

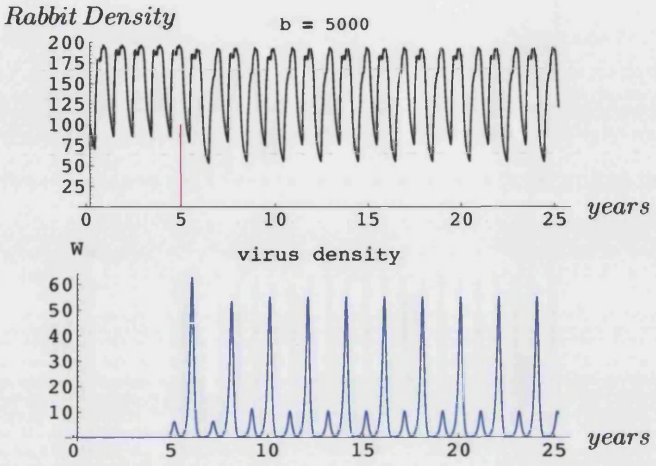


Figure 7.13: Effect of RCD on a rabbit population in Riverina ($b = 5000$).

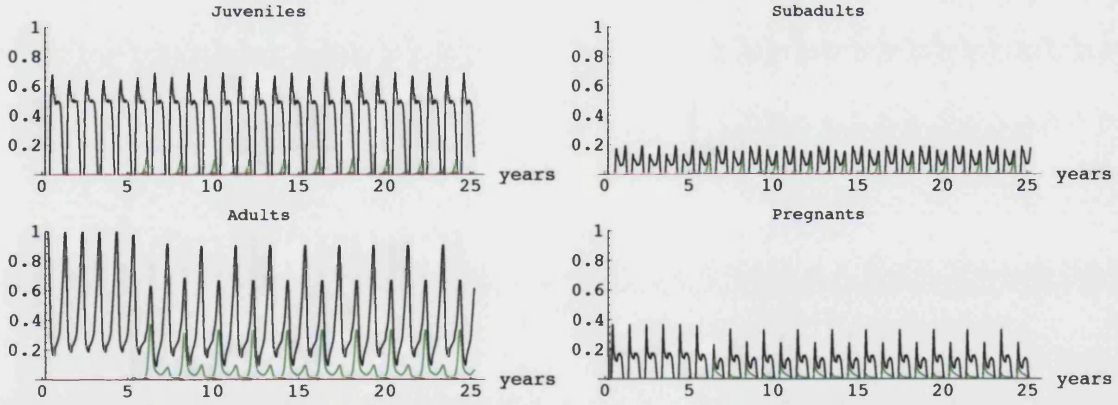


Figure 7.14: Proportion of the age classes against time (Black=Susceptible, Red=Infected, Green=Recovered), ($b = 5000$).

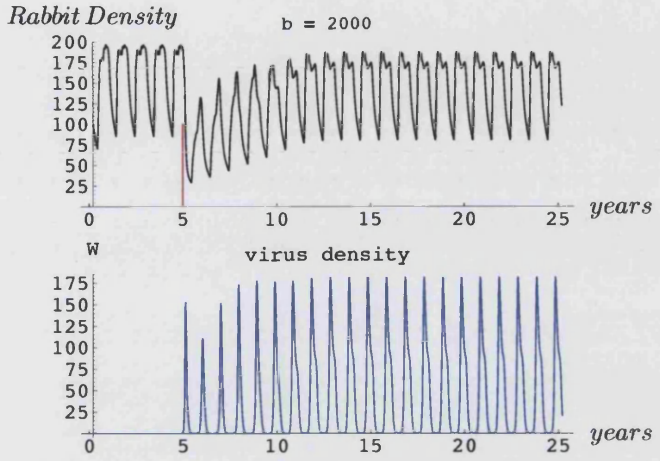


Figure 7.15: Effect of RCD on a rabbit population in Riverina ($b = 2000$).

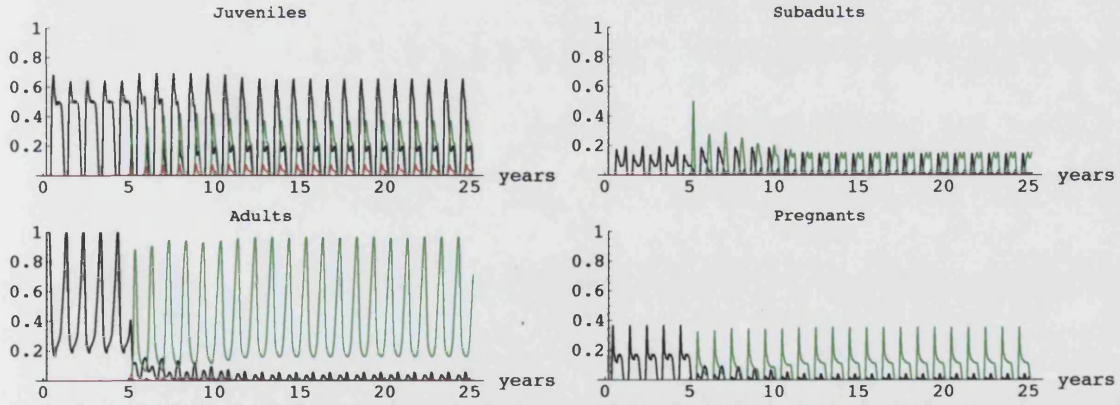


Figure 7.16: Proportion of the age classes against time (Black=Susceptible, Red=Infected, Green=Recovered), ($b = 2000$).

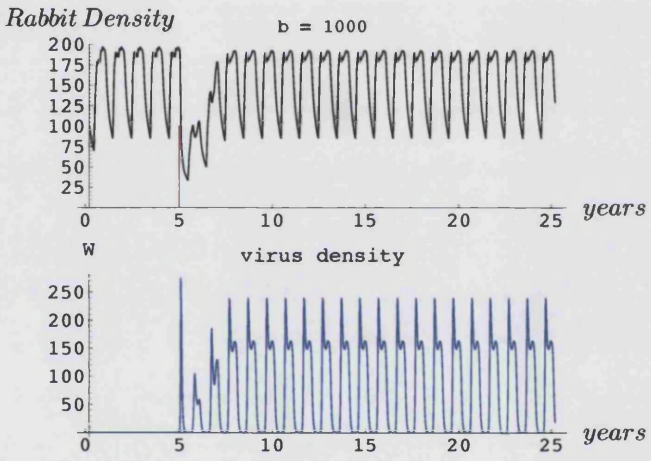


Figure 7.17: Effect of RCD on a rabbit population in Riverina ($b = 1000$).

## 7.4 South-Western WA

A more interesting outcome is observed when the disease is introduced in a rabbit population in South-Western WA. Figures 7.18 to 7.24 below illustrate the results. It can be seen that for $b > 1000$, the outcome is very similar to the Riverina case, where the disease starts to persist but is ineffective. But for $b = 1000$ (figure 7.20), the disease controls the population quite well, and this can be observed for decreasing values of $b$ up till $b = 300$ (figure 7.22), where the population density is kept at values of less than 25. For $b = 200$ (figure 7.23), the population regains its original size after 18 years from the first outbreak, and even though the disease persists, it starts to be present only in the immune population that originated from Juveniles that caught the disease, survived and became immune. Even though South-Western WA has a long breeding season compared to the more marginal regions of Subalpine and Western NSW, it is much more affected by the disease compared to the Riverina region: it can be observed that the population is hardly ever affected by the disease in the Riverina region, while in the South-Western WA region the disease controls the population for $1000 \leq b \leq 300$. This is probably due to the fact that in Riverina, rabbits have the longest breeding season compared to the other regions considered (see figure 4.2).

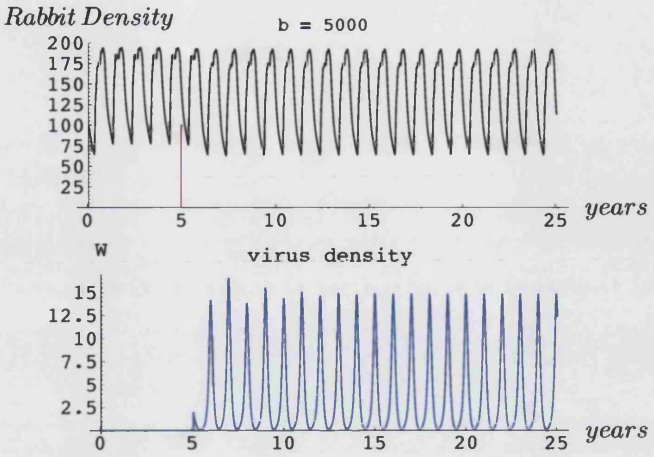


Figure 7.18: Effect of RCD on a rabbit population in South-Western WA ($b = 5000$).

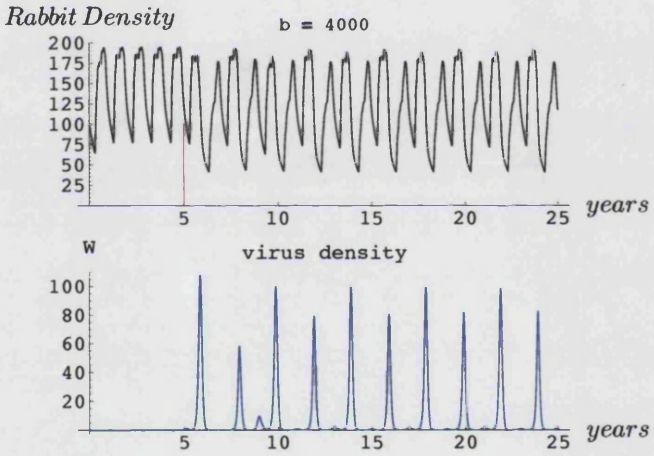


Figure 7.19: Effect of RCD on a rabbit population in South-Western WA ($b = 4000$).

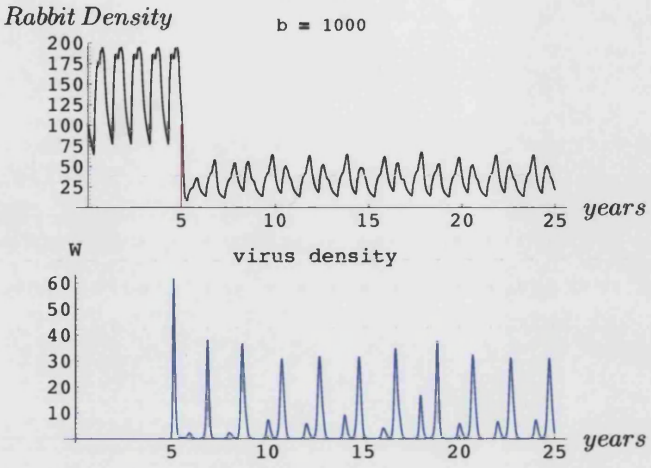


Figure 7.20: Effect of RCD on a rabbit population in South-Western WA ($b = 1000$).

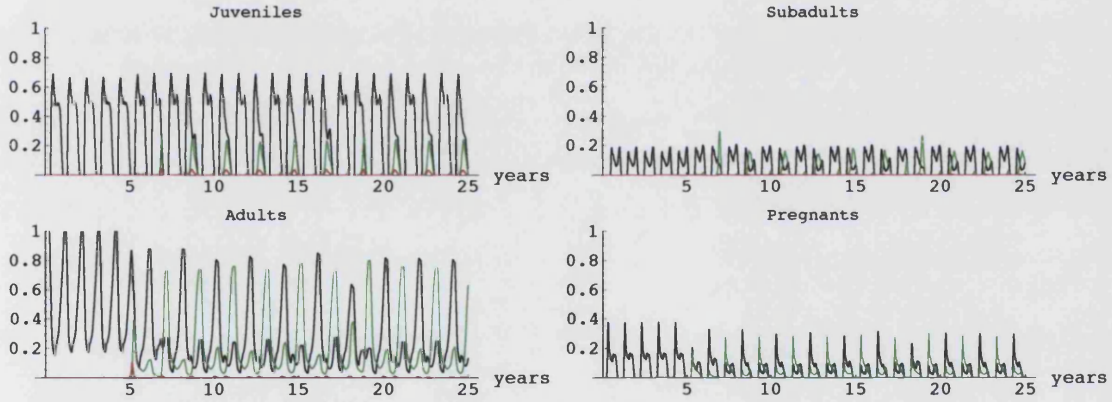


Figure 7.21: Proportion of the age classes against time (Black=Susceptible, Red=Infected, Green=Recovered), ($b = 1000$).

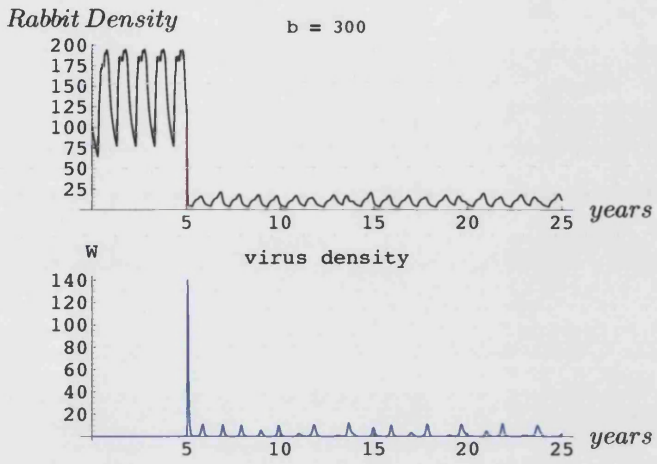


Figure 7.22: Effect of RCD on a rabbit population in South-Western WA ($b = 300$).

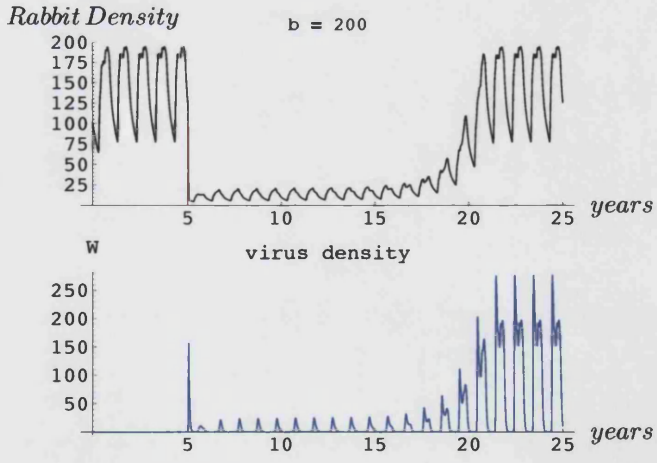


Figure 7.23: Effect of RCD on a rabbit population in South-Western WA ($b = 200$).

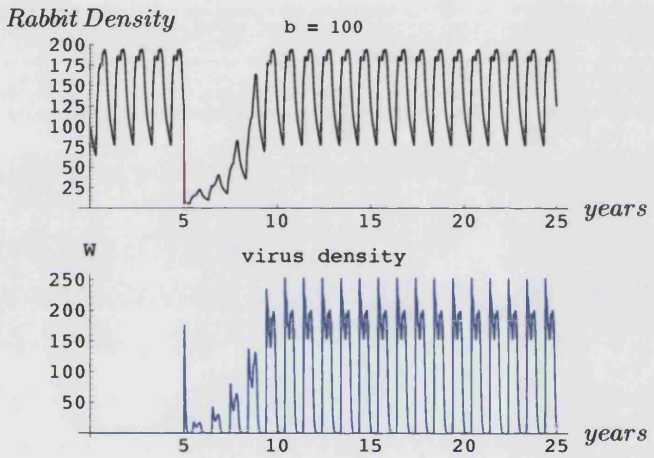


Figure 7.24: Effect of RCD on a rabbit population in South-Western WA ($b = 100$).

# Chapter 8

# Adding the disease using the Strong hypothesis: stochastic results.

An investigation into the outcome of the interaction between the disease and a rabbit population in the four Australian regions considered was carried out using stochastic variation of the climatic conditions as discussed in section 6.3. The procedure for varying the virus strain is the same as in the previous section (see chapter 7). All the data points in the graphs in this chapter represent annual averages, averaged in turn over three independent runs. $f$ is the Poisson event frequency.

## 8.1 Subalpine

The following figures should be compared to figure 6.5, which shows the effect of climatic variability on a rabbit population in a disease-free environment in the Subalpine region. The disease starts to have an effect for values of $b \leq 3000$: for $b = 3000$ (figure 8.1), the disease influence is more dramatic in the non-stochastic case (heavy-dotted black line); the stochastic effects seem to dominate the disease effects as a population control mechanism, especially for high frequencies of the climatic change. As the value of $b$ decreases, the disease starts to win over climatic variability in controlling the population size, until for $b = 600$ (figure 8.2) the population does not regain the pre-disease size even though it "ripples" as it tries to increase. In this case the climatic variability smoothes the "rippling", co-working with the disease. Decreasing $b$ to $b = 200$ (figure 8.3), the population is controlled mostly by the disease; in fact the non-stochastic and the stochastic cases are barely

distinguishable. This means that the disease completely dominates the stochastic effects as a population control mechanism. For $b = 100$ (figure 8.4), the highly virulent disease delays the suppression of the population for about 10 years. After this, the population is essentially wiped out. The delay is due to the fact that the virus starts to survive only through Juveniles and immune individuals, since it is so infective that it kills its host too fast for it to infect another individual. This is because the persistence of the virus is now bound to the presence of Juveniles, that eventually become immune adults (compare to figure 7.5). For $b = 80$ (figure 8.5), the population grows exponentially after an initial decrease in the absence of stochastic effects, and tends to regain pre-disease size. The stochastic climatic factors delay or suppress this effect, especially for high frequencies of change and a high variance of the Lognormal distribution.

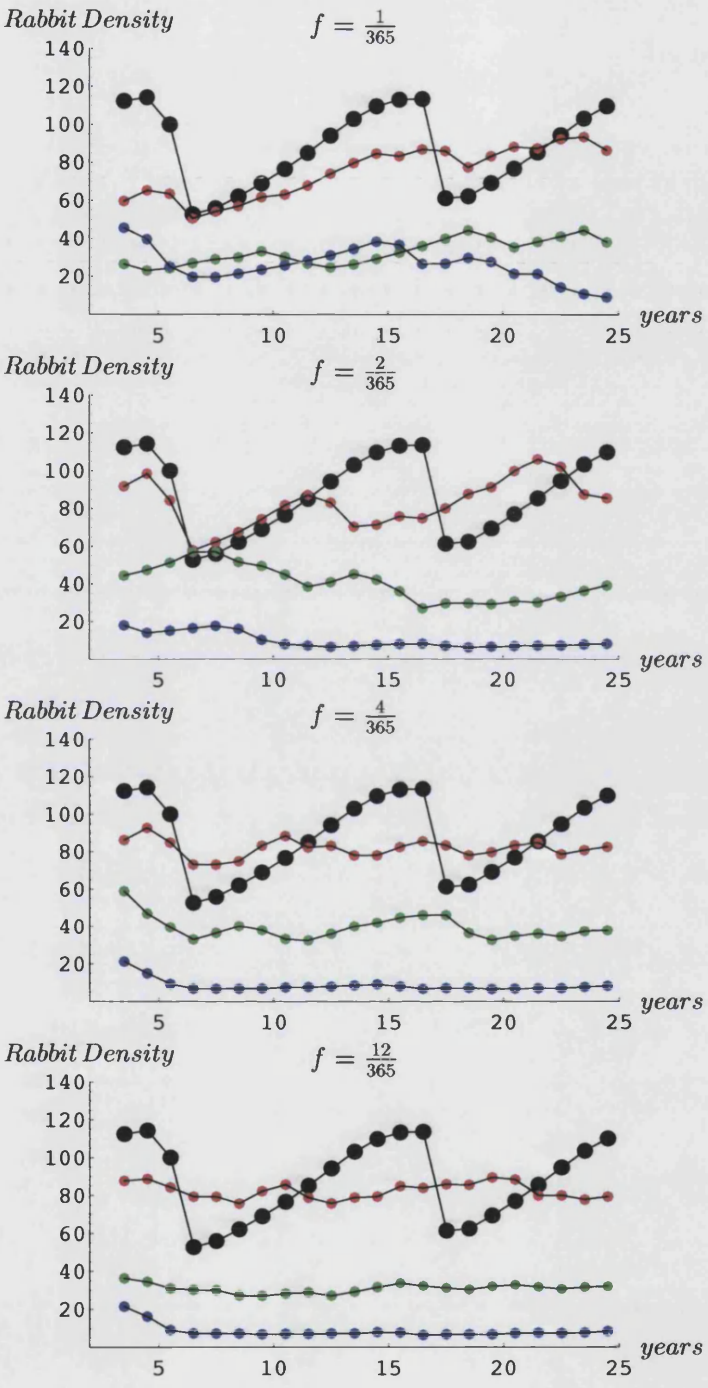


Figure 8.1: Disease and climatic variability in the Subalpine region (b=3000) for different variances (var) of the Lognormal Distribution: var=0.1(red), var=1(green), var=10(blue); heavy-dotted black line is the non-stochastic case.

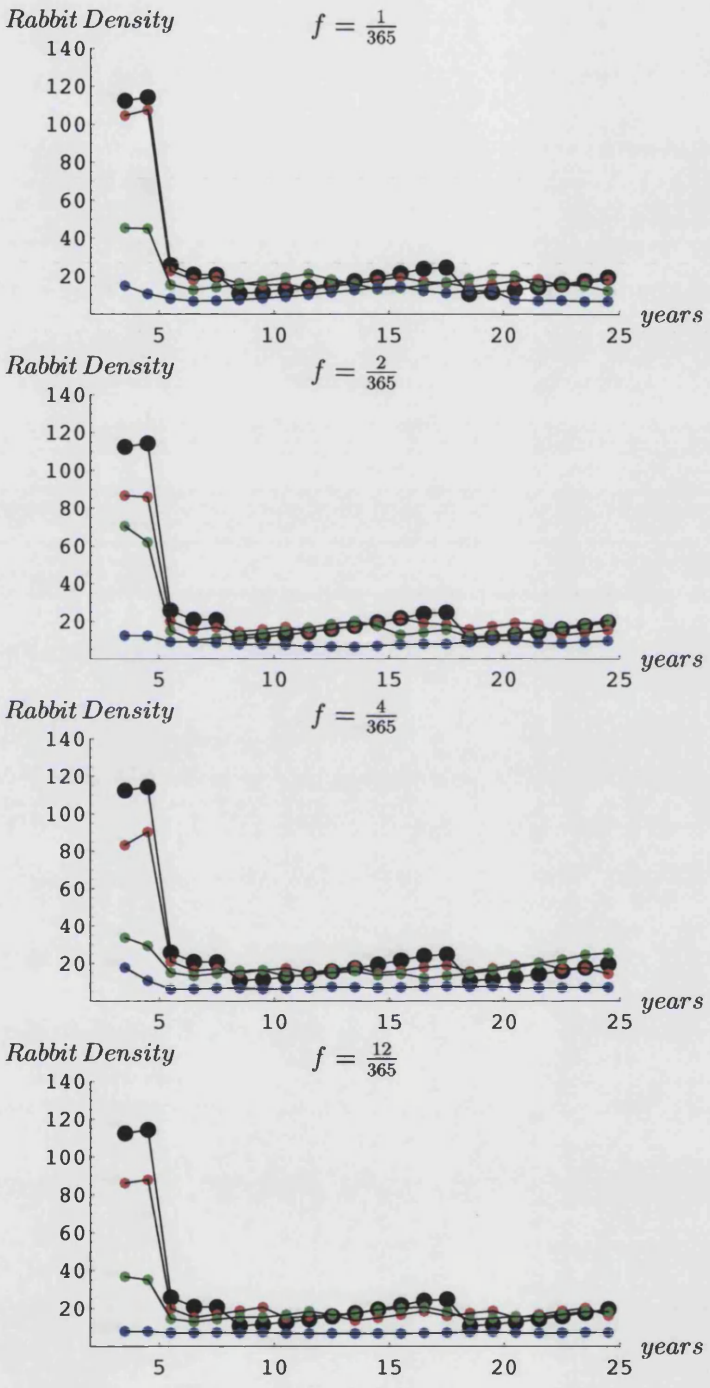


Figure 8.2: Disease and climatic variability in the Subalpine region (b=600) for different variances (var) of the Lognormal Distribution: var=0.1(red), var=1(green), var=10(blue); heavy-dotted black line is the non-stochastic case.

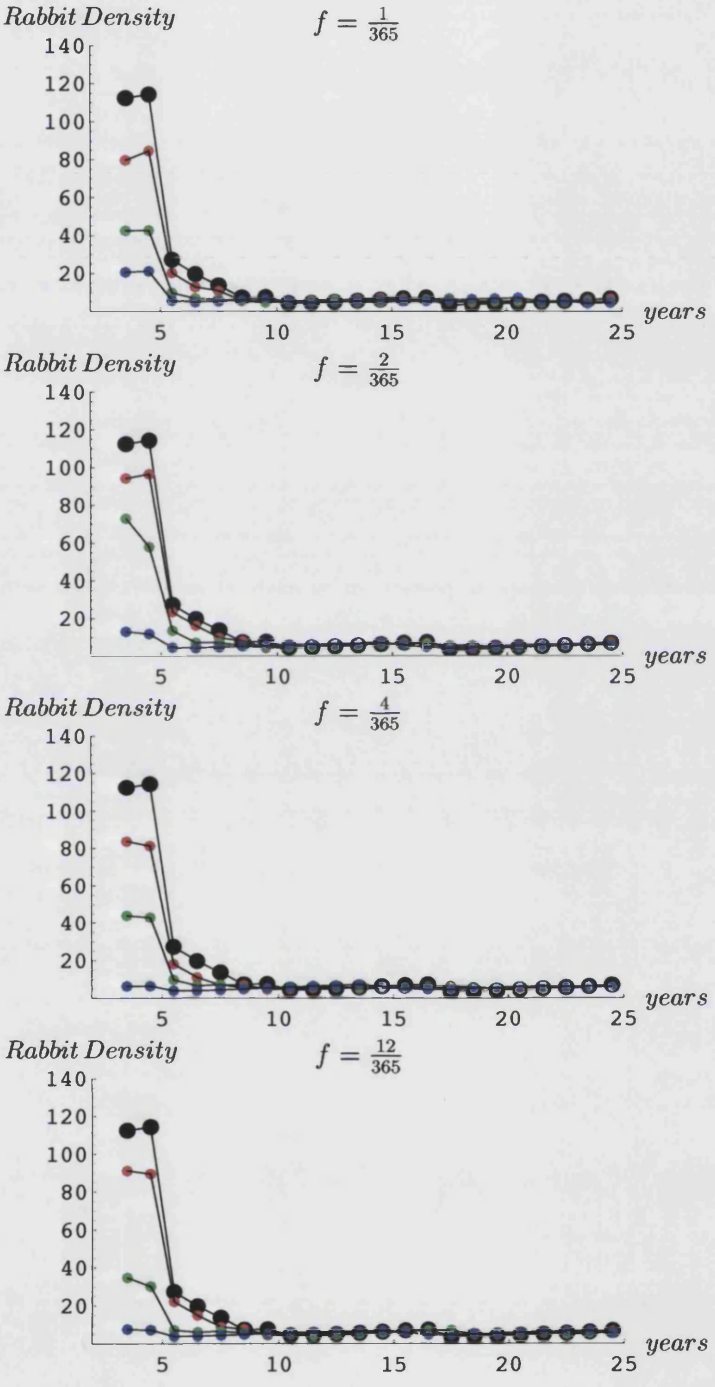


Figure 8.3: Disease and climatic variability in the Subalpine region (b=200) for different variances (var) of the Lognormal Distribution: var=0.1(red), var=1(green), var=10(blue); heavy-dotted black line is the non-stochastic case.

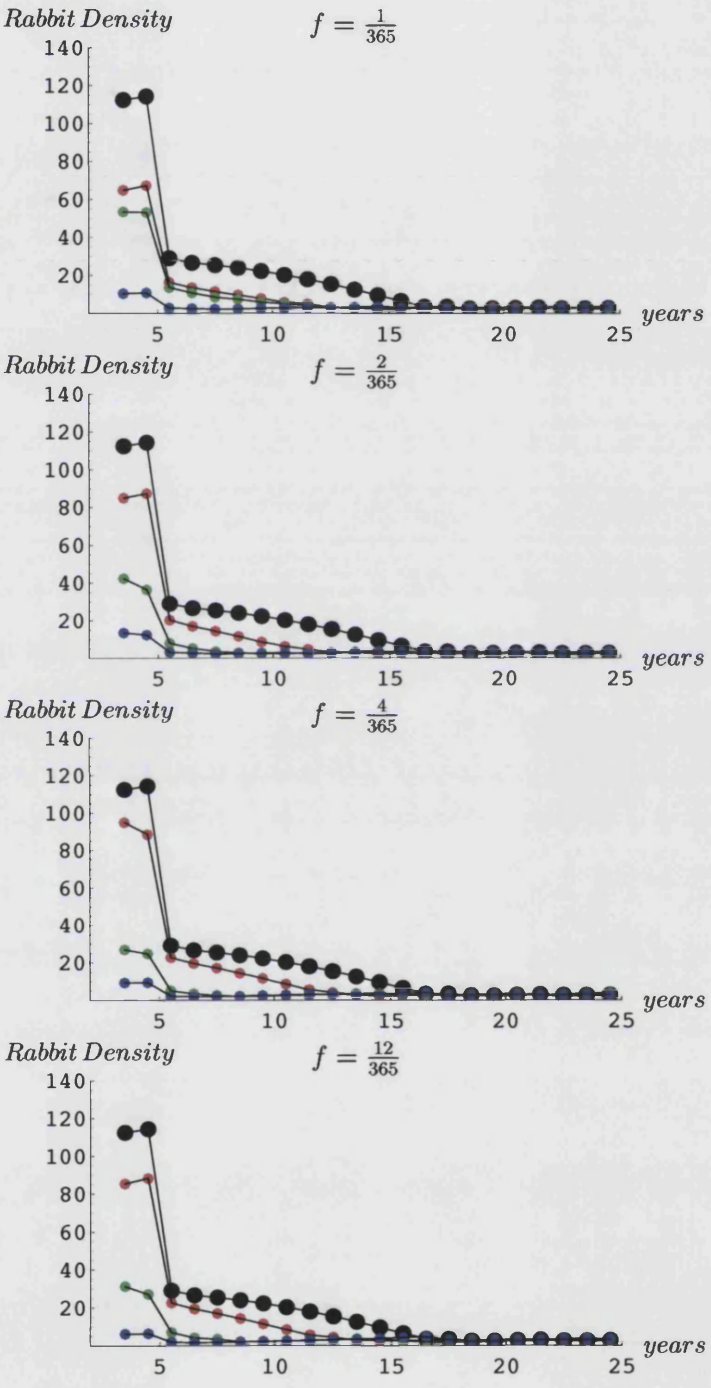


Figure 8.4: Disease and climatic variability in the Subalpine region (b=100) for different variances (var) of the Lognormal Distribution: var=0.1(red), var=1(green), var=10(blue); heavy-dotted black line is the non-stochastic case.

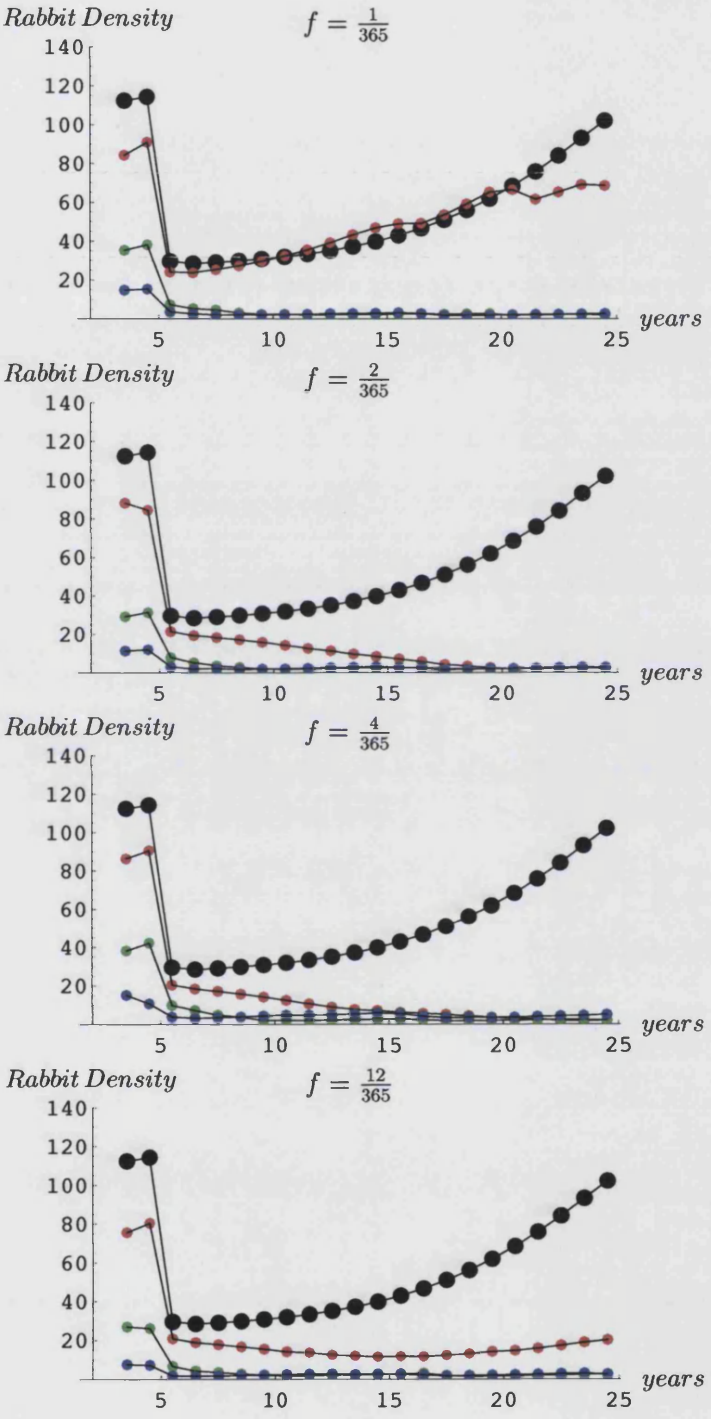


Figure 8.5: Disease and climatic variability in the Subalpine region (b=80) for different variances (var) of the Lognormal Distribution: var=0.1(red), var=1(green), var=10(blue); heavy-dotted black line is the non-stochastic case.

## 8.2 Western NSW

Figures 8.6 to 8.9 should be compared to figure 6.6, which shows the effect of climatic variability on a rabbit population in a disease-free environment in Western NSW. For high values of $b$ ($b = 4000$), the disease does not affect the population size very strongly and climatic variability is more the factor controlling the population growth. The scenario is quite similar to the non-disease case (figure 6.6). As $b$ decreases, the effect of the disease becomes more dominant in the interplay between climatic variability and disease invasion. The strong fluctuations in the non-stochastic case ($b = 3000$) are dampened or suppressed by the climatic conditions, especially for higher variances, but the disease starts to be the main factor controlling the population (figure 8.6). This becomes very evident for $b = 600$ and $b = 200$ (figures 8.7 and 8.8), where the disease totally controls the population density and climatic variability doesn't have much of an effect on the population size. For very low values of $b$ ($b = 30$, figure 8.9), the disease starts to persist only among individuals that have become immune and so does not control the population so efficiently, climatic variability delays the natural population recovery, if compared to the non-stochastic case (heavy-dotted black line).

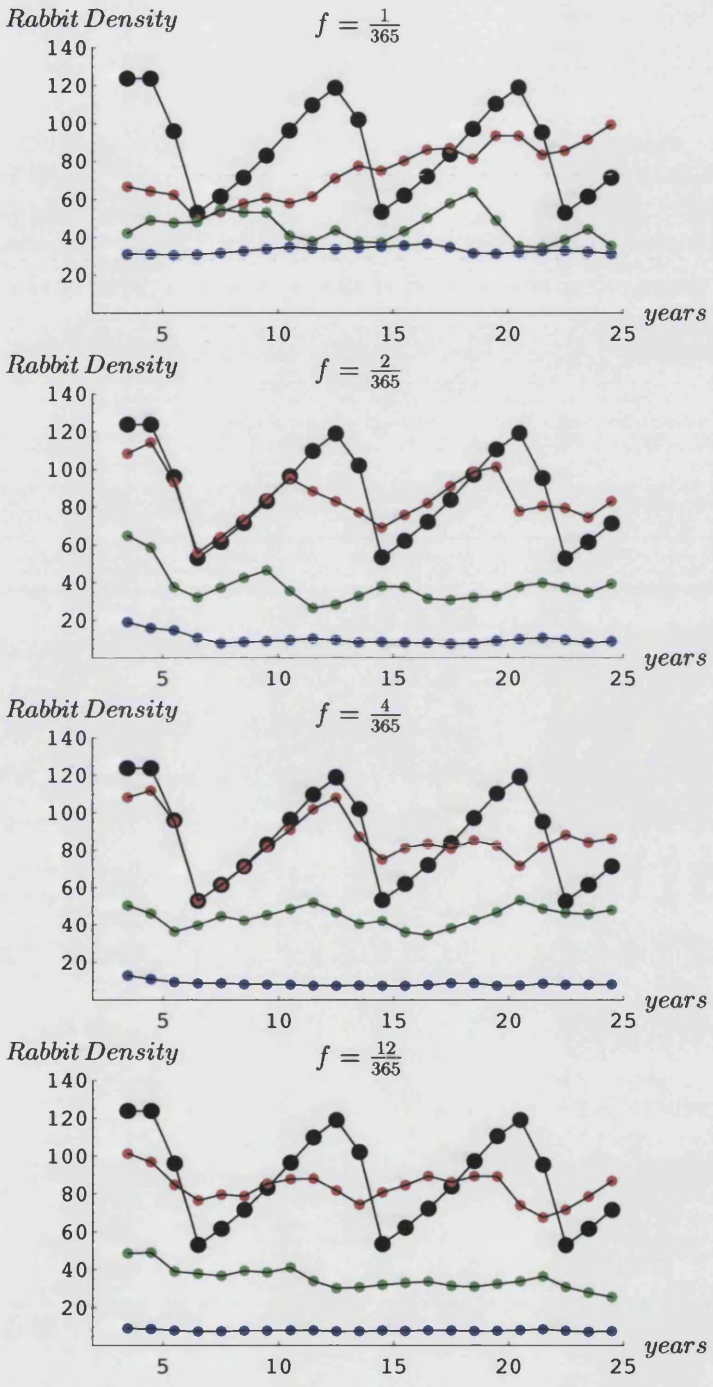


Figure 8.6: Disease and climatic variability in the Western NSW region (b=3000) for different variances (var) of the Lognormal Distribution: var=0.1(red), var=1(green), var=10(blue); heavy-dotted black line is the non-stochastic case.

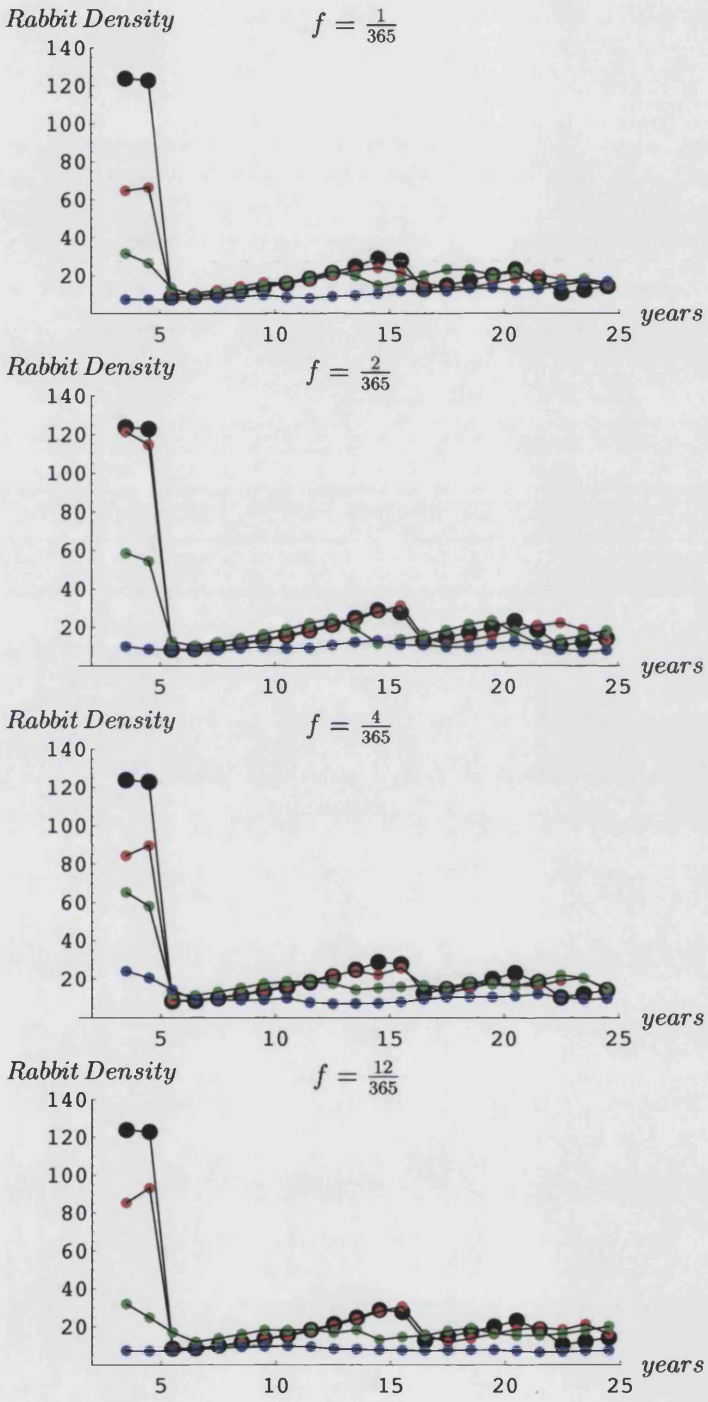


Figure 8.7: Disease and climatic variability in the Western NSW region (b=600) for different variances (var) of the Lognormal Distribution: var=0.1(red), var=1(green), var=10(blue); heavy-dotted black line is the non-stochastic case.

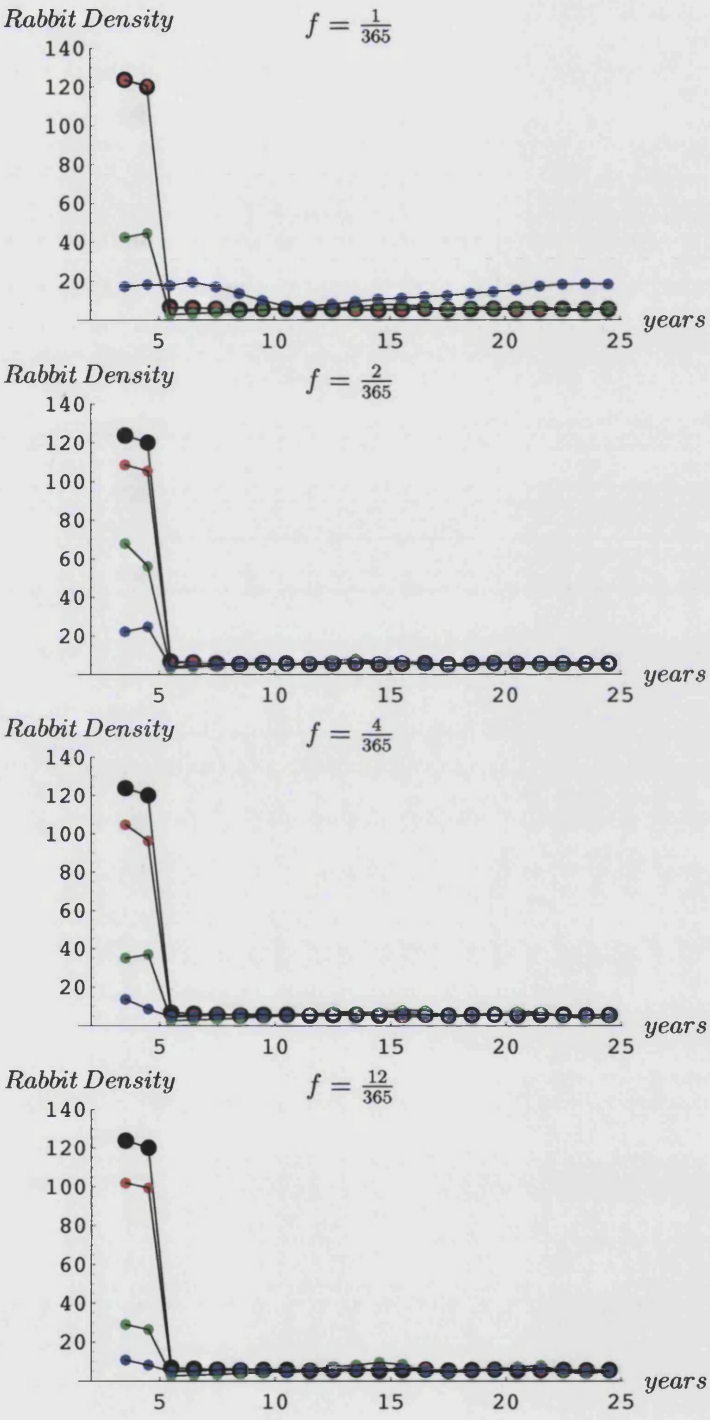


Figure 8.8: Disease and climatic variability in the Western NSW region (b=200) for different variances (var) of the Lognormal Distribution: var=0.1(red), var=1(green), var=10(blue); heavy-dotted black line is the non-stochastic case.

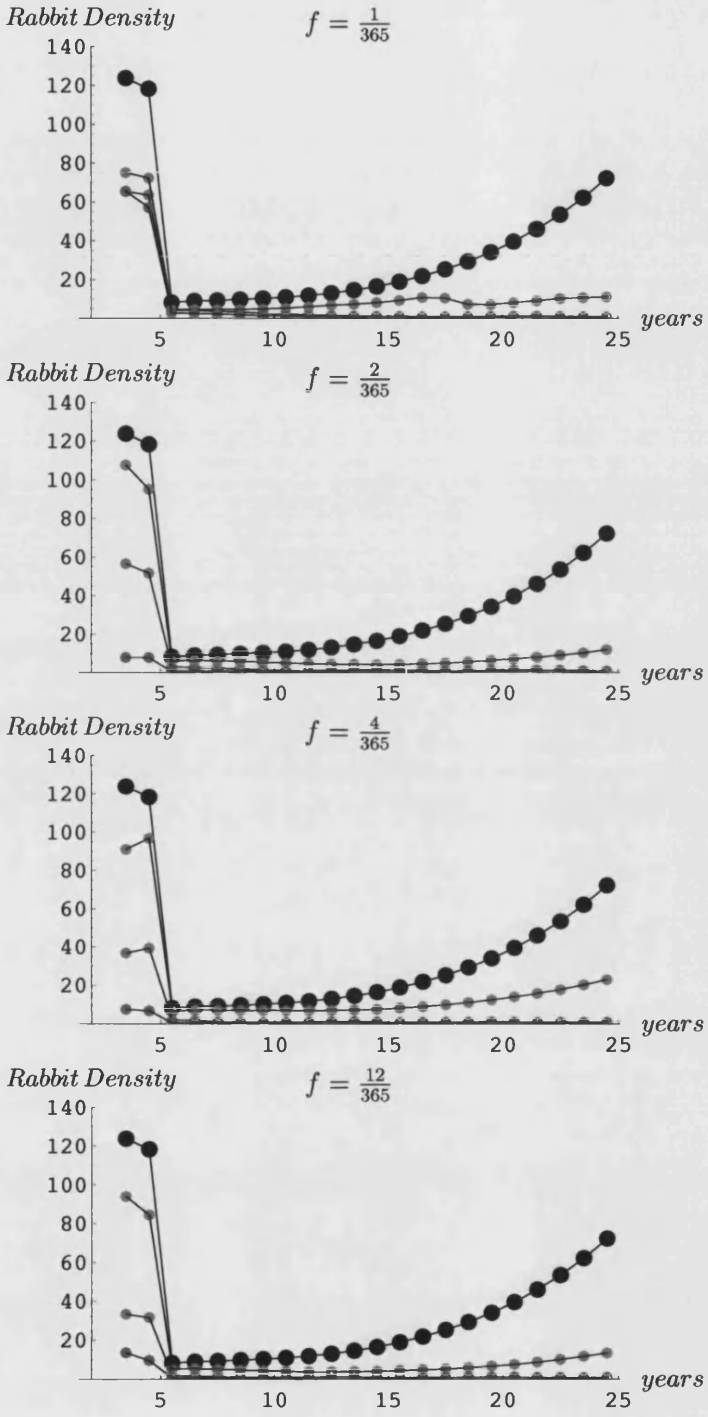


Figure 8.9: Disease and climatic variability in the Western NSW region (b=30) for different variances (var) of the Lognormal Distribution: var=0.1(red), var=1(green), var=10(blue); heavy-dotted black line is the non-stochastic case.

## 8.3 Riverina

The following figures should be compared to figure 6.7, which shows the effect of climatic variability on a rabbit population in a disease-free environment in the Riverina region. For $b > 5000$, the disease has no visible effect on the population density. The size of the rabbit population is mainly controlled by climatic variability and the two scenarios, with and without disease, appear very similar. A different outcome is observed for $b = 5000$ (figure 8.10), where the disease has a conspicuous impact on the population, especially for the stochastic cases with low frequency of climatic change ($f = \frac{1}{365}$). For changes of climate happening once a month ($f = \frac{12}{365}$), the "rippling", i.e. the seasonal effects, is smoothed out, especially at high variances. The virus lowers the population density but never significantly, as for example for $b = 2000$ (figure 8.12), where the disease impact lasts for about 5 years during which the population size rebuilds to pre-disease number through the large number of immune Juveniles that mature into Subadults and Adults. In fact Riverina is the most favourable environment out of the four regions considered in this work: this is due to the very long breeding season (figure 4.2(c)) and, consequently, the continuing presence of Juveniles that can become immune if exposed to the disease. The disease never really controls the population in both the stochastic and non-stochastic cases. For $b < 2000$, the disease effects tend to disappear as the population recovers faster and faster to pre-disease levels through the immune individuals.

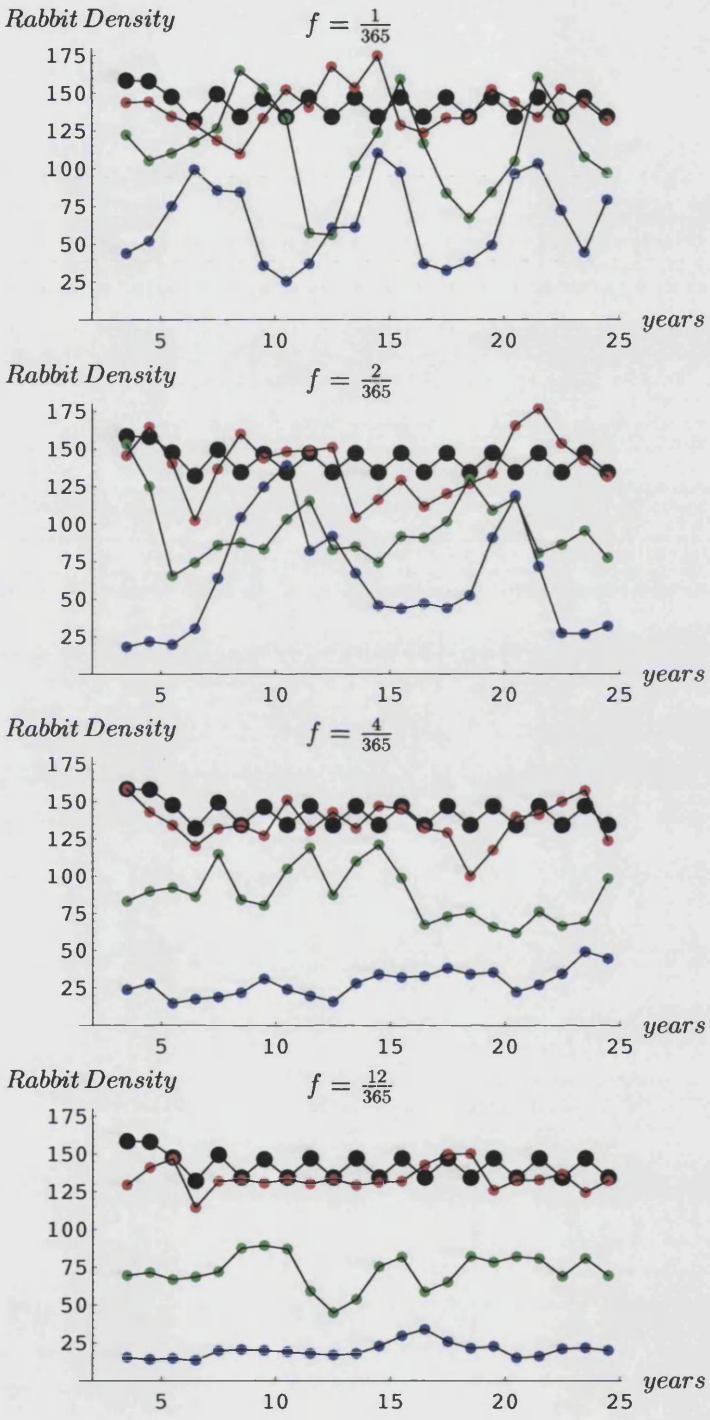


Figure 8.10: Disease and climatic variability in the Riverina region (b=5000) for different variances (var) of the Lognormal Distribution: var=0.1(red), var=1(green), var=10(blue); heavy-dotted black line is the non-stochastic case.

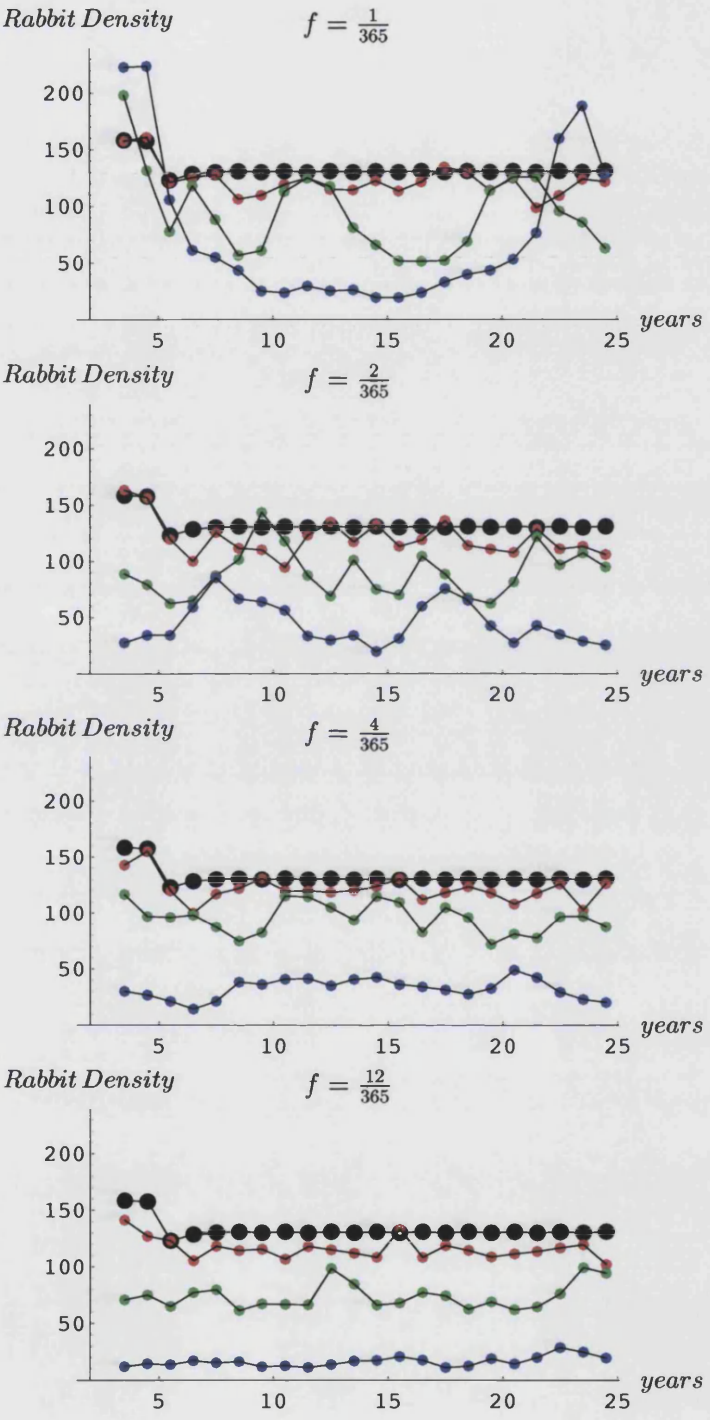


Figure 8.11: Disease and climatic variability in the Riverina region (b=4000) for different variances (var) of the Lognormal Distribution: var=0.1(red), var=1(green), var=10(blue); heavy-dotted black line is the non-stochastic case.

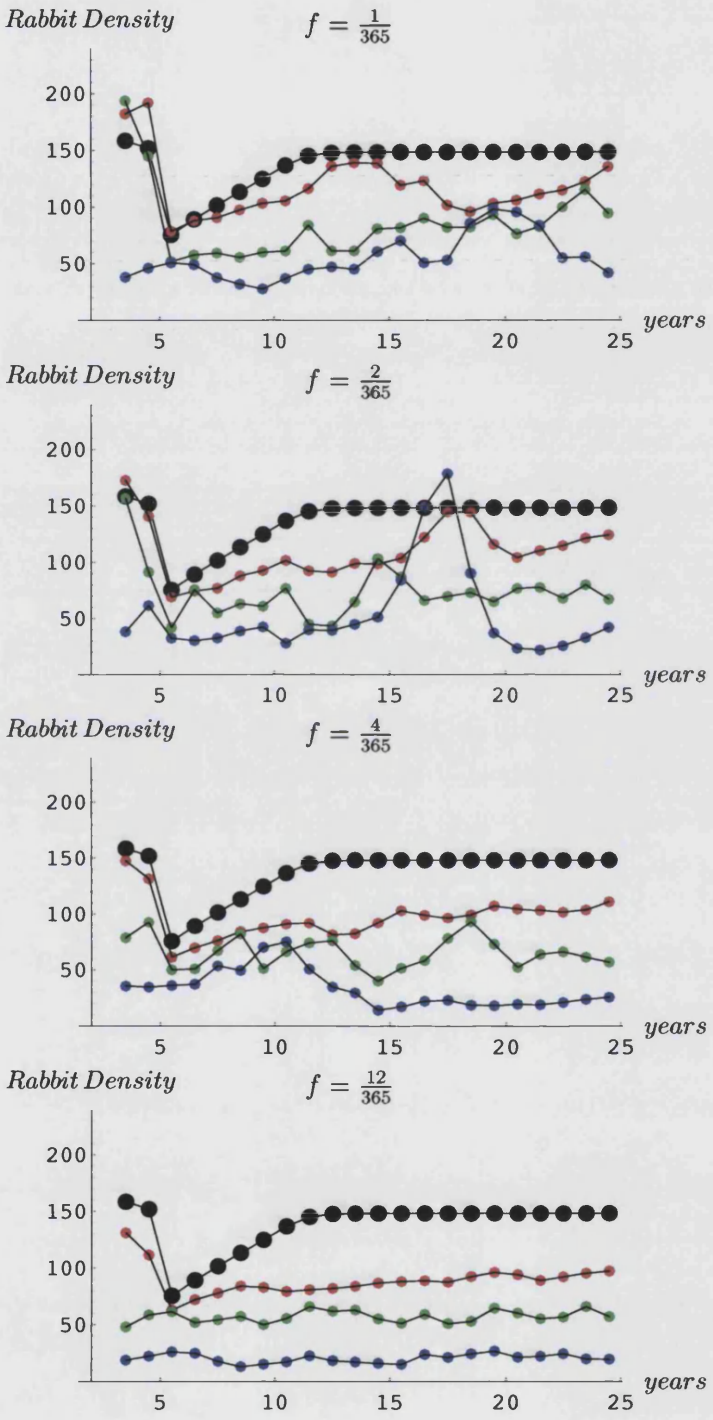


Figure 8.12: Disease and climatic variability in the Riverina region (b=2000) for different variances (var) of the Lognormal Distribution: var=0.1(red), var=1(green), var=10(blue); heavy-dotted black line is the non-stochastic case.

## 8.4 South-Western WA

The following figures should be compared to figure 6.8, which shows the effect of climatic variability on a rabbit population in a disease-free environment in the South-Western WA region. According to the model results, the disease starts having an effect for $b = 4000$ (figure 8.13;, for values larger than this, the climatic variation controls the population more than the disease. South-Western WA is a favourable environment for rabbits, like Riverina, with a long breeding season compared to the more marginal Subalpine and Western NSW. Nevertheless, for values of $1000 > b > 300$ (figure 8.14 and 8.15) the disease controls the population, which is kept at low values (with a density of less than 25 individuals for $b = 300$) and never regains the pre-disease size. For $b = 200$ (figure 8.16), the disease crashes the population initially but, for the non-stochastic case the population starts to grow again as immunity in the population increases, until after about 17 years from disease introduction it regains the original density. For the stochastic case it remains at low values throughout the run, though there is a tendency to recover for lower stochastic variance. As $b$ decreases, the virus only diminishes the population for few years after the initial outbreak and then it grows back, even though the climatic variation delays this phenomenon, or suppresses the population at very high variance level ($var = 10$) as shown in figure 8.17.

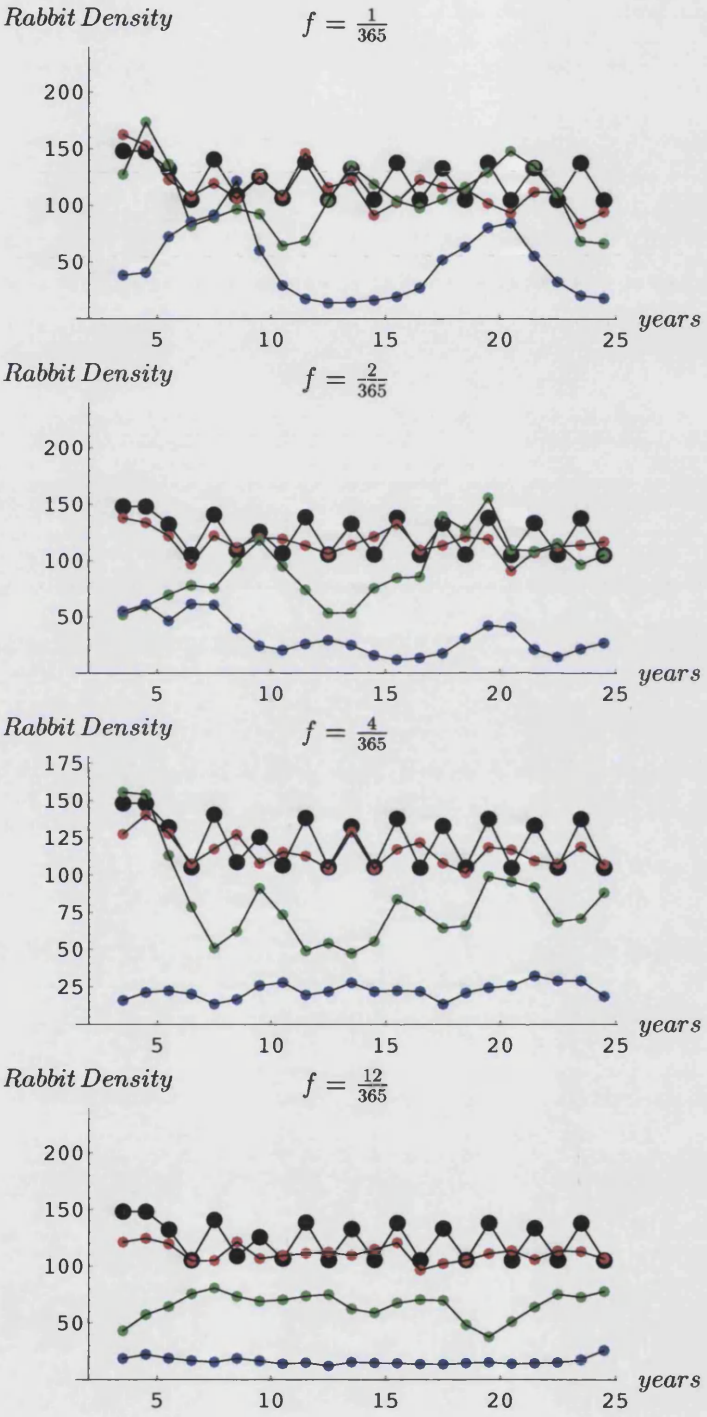


Figure 8.13: Disease and climatic variability in the South-Western WA region (b=4000) for different variances (var) of the Lognormal Distribution: var=0.1(red), var=1(green), var=10(blue); heavy-dotted black line is the non-stochastic case.

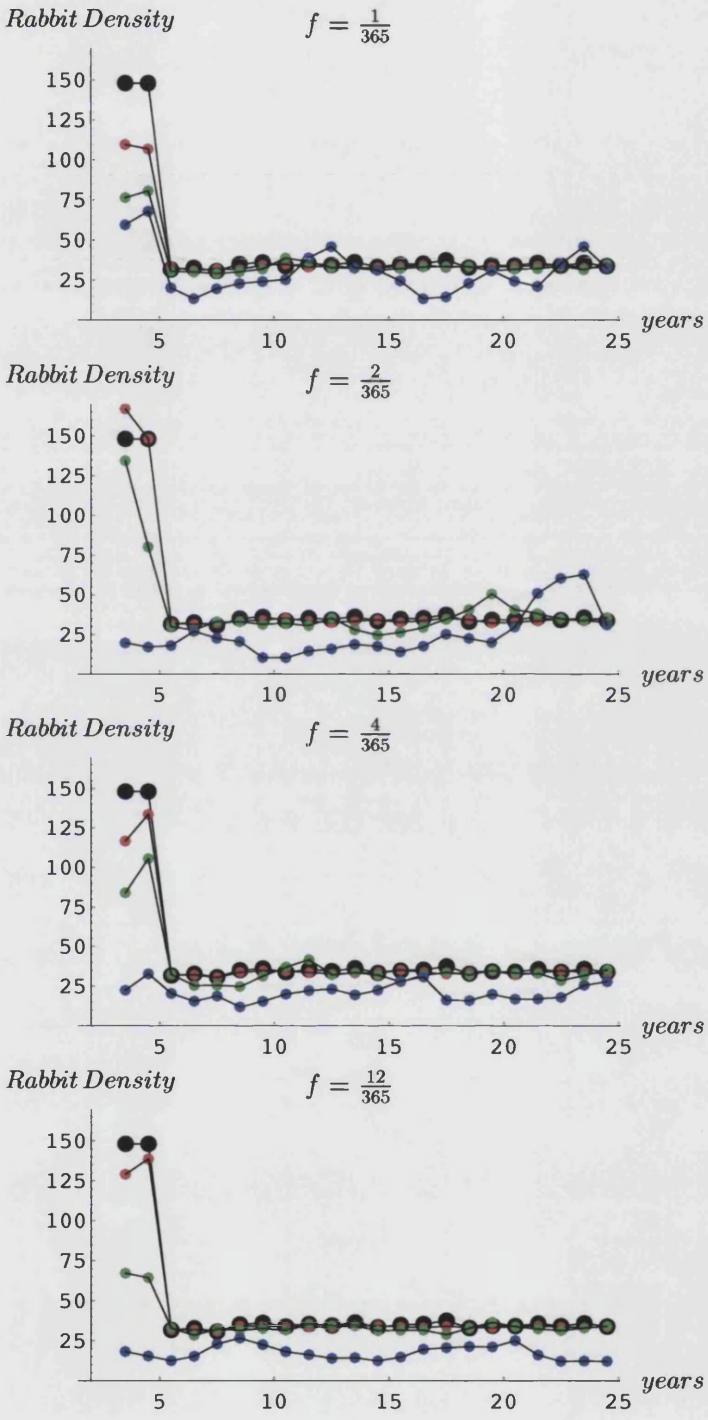


Figure 8.14: Disease and climatic variability in the South-Western WA region (b=1000) for different variances (var) of the Lognormal Distribution: var=0.1(red), var=1(green), var=10(blue); heavy-dotted black line is the non-stochastic case.

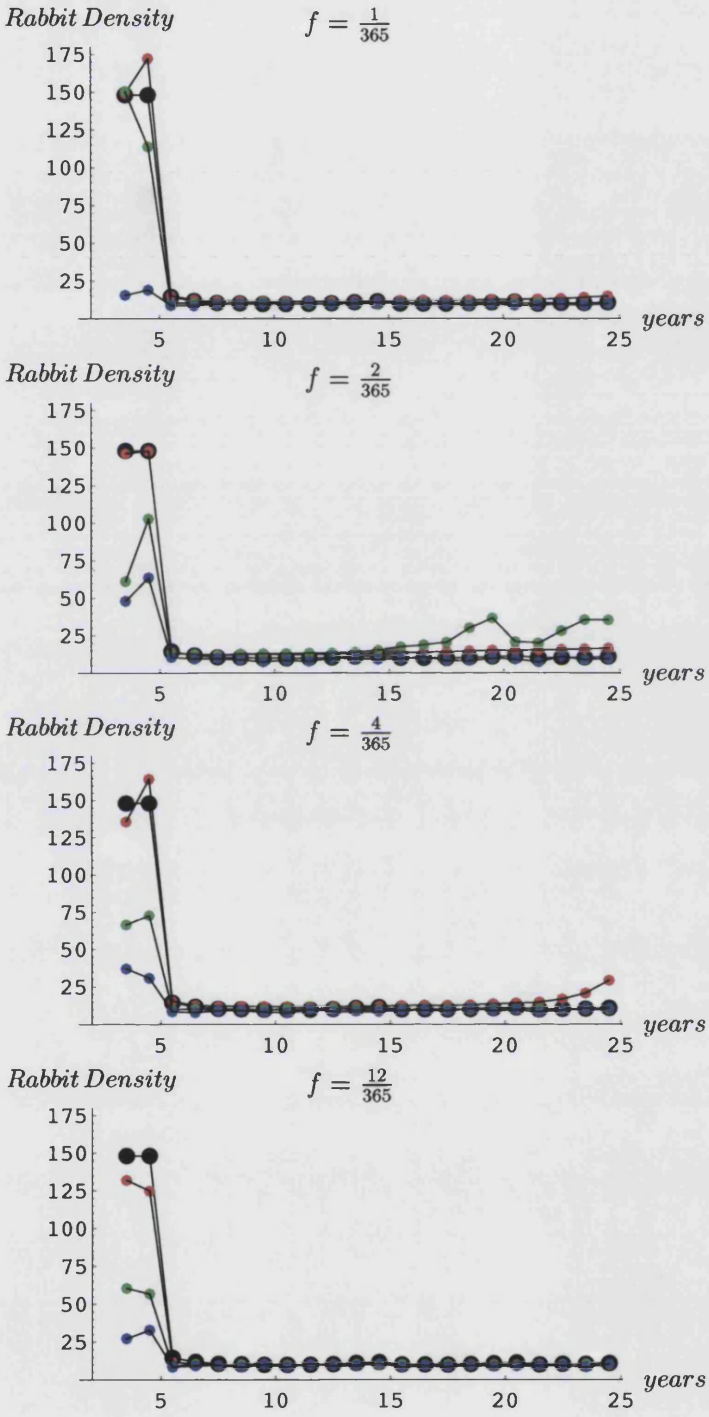


Figure 8.15: Disease and climatic variability in the South-Western WA region (b=300) for different variances (var) of the Lognormal Distribution: var=0.1(red), var=1(green), var=10(blue); heavy-dotted black line is the non-stochastic case.

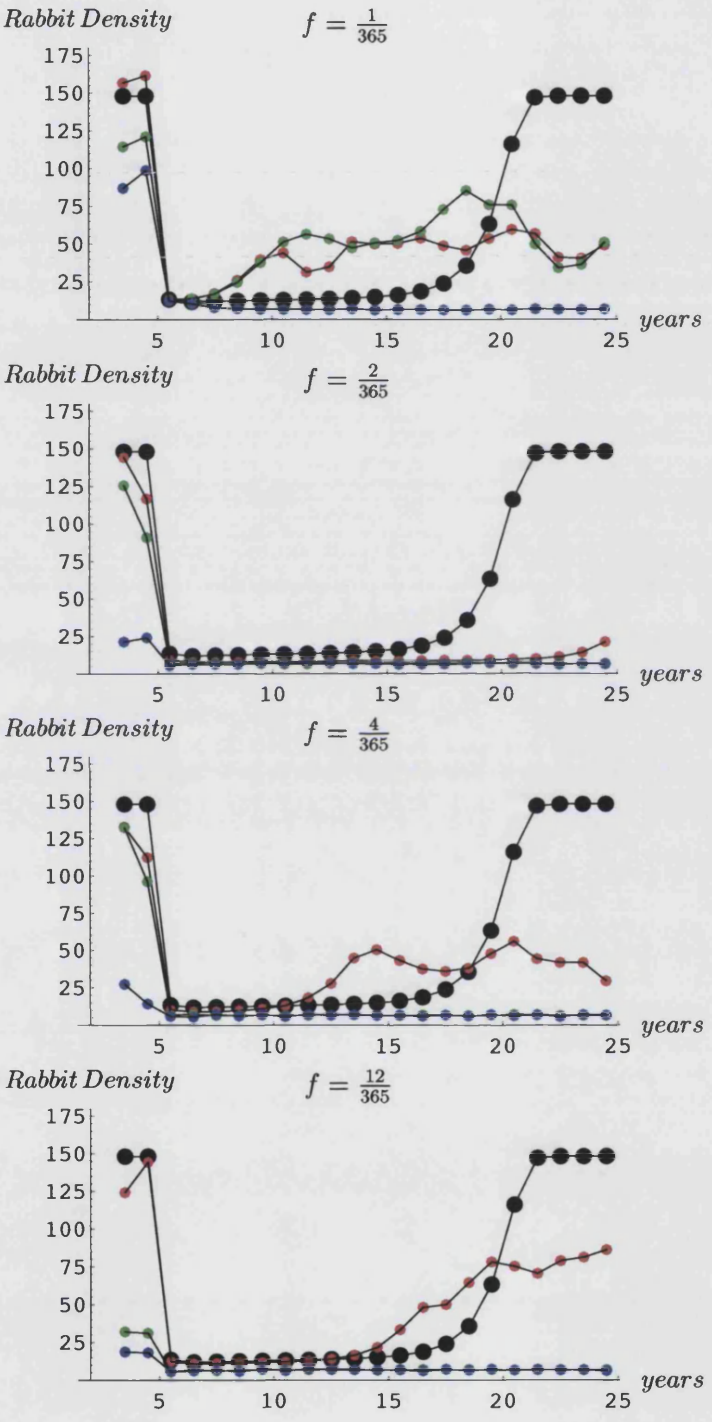


Figure 8.16: Disease and climatic variability in the South-Western WA region (b=200) for different variances (var) of the Lognormal Distribution: var=0.1(red), var=1(green), var=10(blue); heavy-dotted black line is the non-stochastic case.

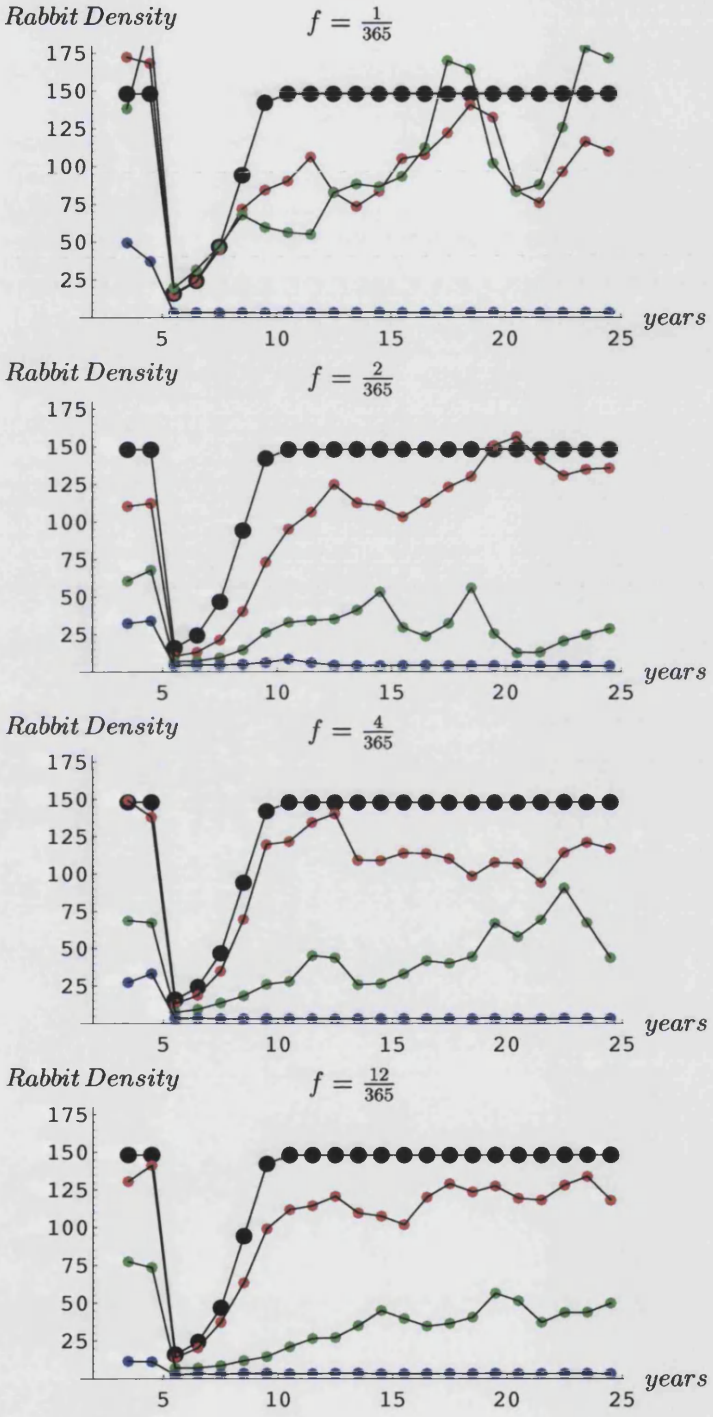


Figure 8.17: Disease and climatic variability in the South-Western WA region (b=100) for different variances (var) of the Lognormal Distribution: var=0.1(red), var=1(green), var=10(blue); heavy-dotted black line is the non-stochastic case.

# Chapter 9

# Adding the Disease using the Weak hypothesis: Non-stochastic Results.

It can be expected that using the Weak hypothesis about the way that RCD affects a susceptible rabbit population (section 1.5.2), the disease will be more effective, since the time span for which Juveniles can acquire life-long immunity is much shorter than in the Strong hypothesis: in fact it is half; except for the Juveniles who receive maternal antibodies and are then immune until they reach Subadulthood. However, unlike in the Strong hypothesis, these new Subadults are then completely Susceptible. It can be noticed from the figures of the dynamics of the different population classes that in this case Juveniles do not carry the disease as much as in the Strong hypothesis case: only those that are less than 28 days and are not born from Recovered mothers can carry the disease and remain immune for life. So there are a lot less Recovered Juveniles that eventually become recovered Subadults and Adults. In particular in the favourable environments, the disease is remarkably more effective than in the Strong hypothesis since the presence of Juveniles for a large part of the year becomes less important and the Juveniles cannot build up to an immune adult population (see figures 9.16, 9.18 and 9.20) as has been seen in the the Strong hypothesis case (chapter 7). Some Juveniles will still become immune. However the newly Susceptible Subadults who had maternal antibodies as Juveniles, are now vulnerable to being killed by the disease, and so have a lower chance of recovery and subsequent immunity.

## 9.1 Subalpine

In the Subalpine area, the disease becomes effective only for values of $b \leq 2000$: for $b = 2000$ (figure 9.1-9.2) two outbreaks occur in the simulation time, with recovery to pre-disease size after about 10 years, when another outbreak occurs; the disease persists but it is not yet very effective. In the Strong hypothesis the same behaviour is observed for a higher value of $b$, namely $b = 3000$ (see figure 7.1). For $b = 1000$ (figure 9.3-9.4), the population does not regain pre-disease size before the end of the run; only the initial outbreak occurs in the simulation time, but the virus titre is higher ($W = 80$). The disease is probably persistent though, in fact for $b = 700$ (figure 9.5-9.6) a similar trend can be observed but towards the end of the run a new smaller outbreak ($W = 50$) occurs which lowers the population just as the initial outbreak ($W = 110$), probably because the population does not reach pre-disease size before the second viral outbreak takes place. A similar behaviour is observed for lower values of $b$, with the disease persisting with smaller outbreaks that keep the population density very low. The initial outbreak is very high ($W = 200$) and the population seem to be almost zero for some part of the run ($b = 10$, figure 9.9). In the Strong hypothesis the disease becomes ineffective for values of $b \leq 80$, because of the immune individuals that caught the disease in the Juvenile life stage. In the Weak hypothesis, however, the disease is more and more effective as the value of $b$ decreases.

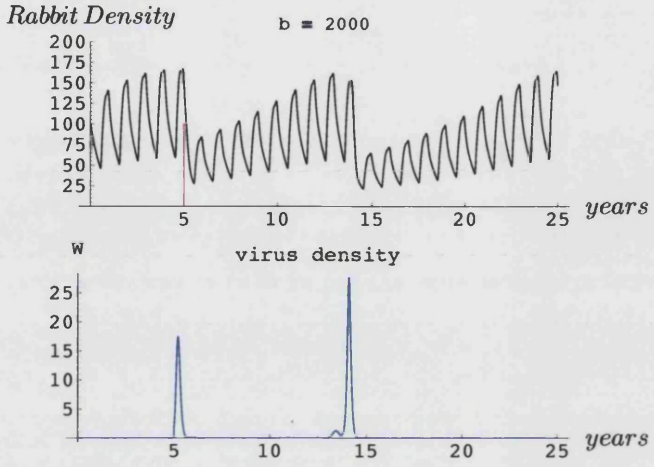


Figure 9.1: Effect of RCD on a rabbit population in Subalpine ($b = 2000$).

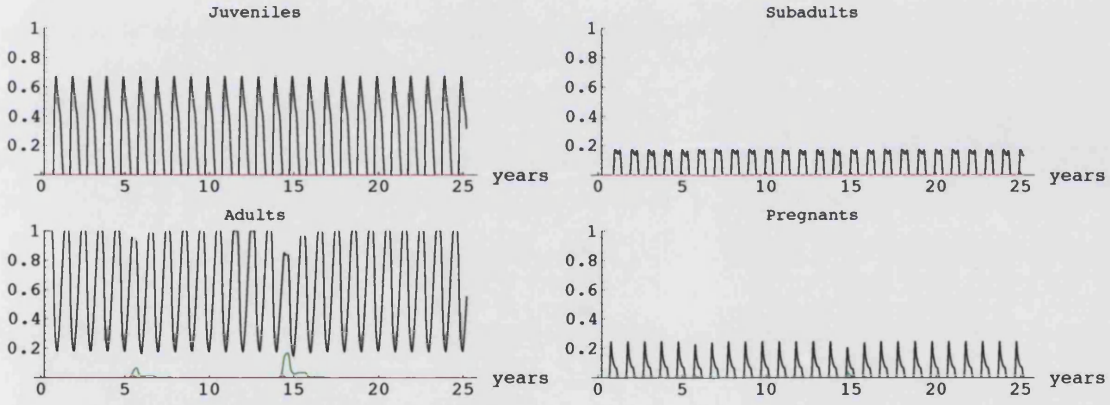


Figure 9.2: Proportion of the age classes against time (Black=Susceptible, Red=Infected, Green=Recovered), ($b = 2000$).

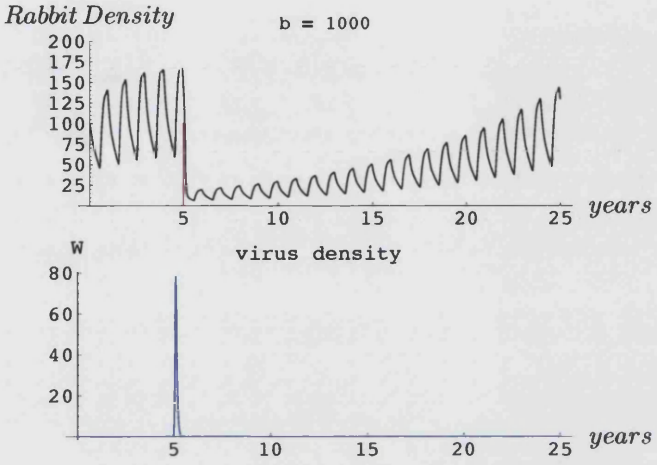


Figure 9.3: Effect of RCD on a rabbit population in Subalpine ($b = 1000$).

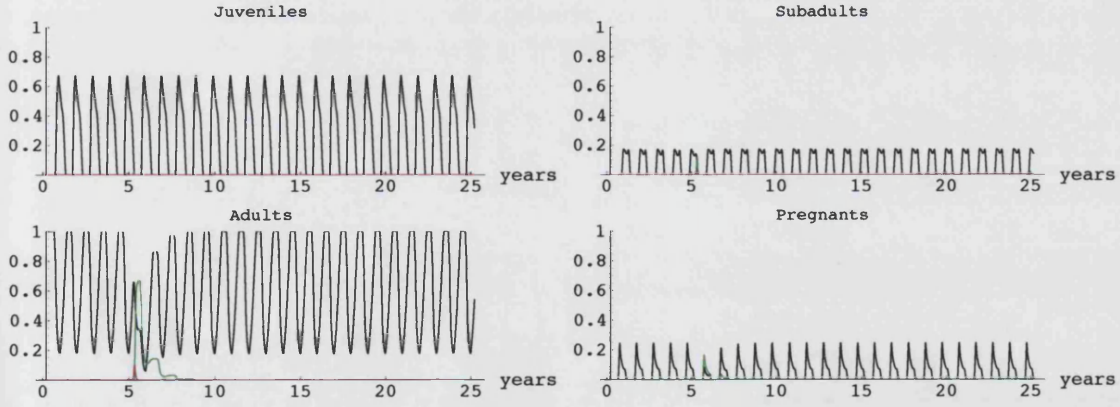


Figure 9.4: Proportion of the age classes against time (Black=Susceptible, Red=Infected, Green=Recovered), ($b = 1000$).

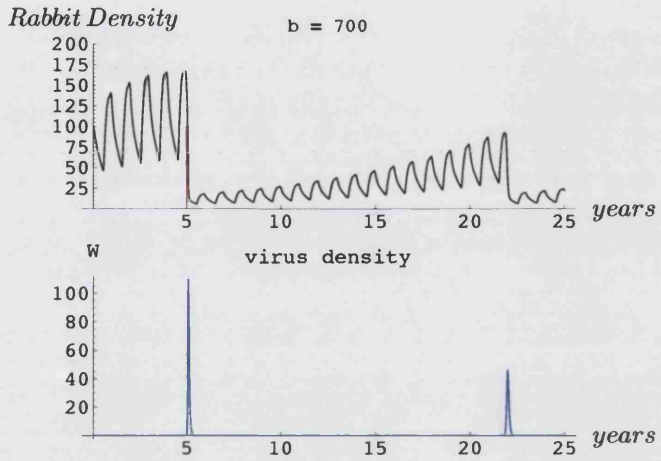


Figure 9.5: Effect of RCD on a rabbit population in Subalpine ($b = 700$).

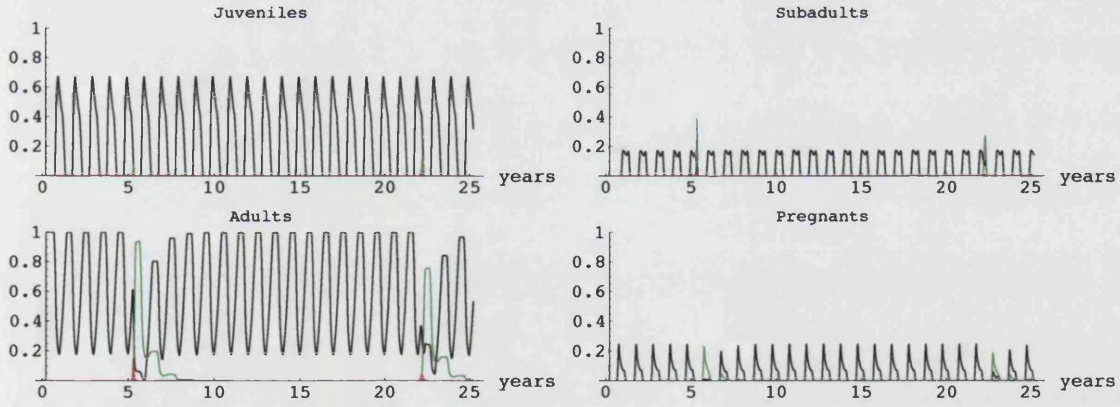


Figure 9.6: Proportion of the age classes against time (Black=Susceptible, Red=Infected, Green=Recovered), ($b = 700$).

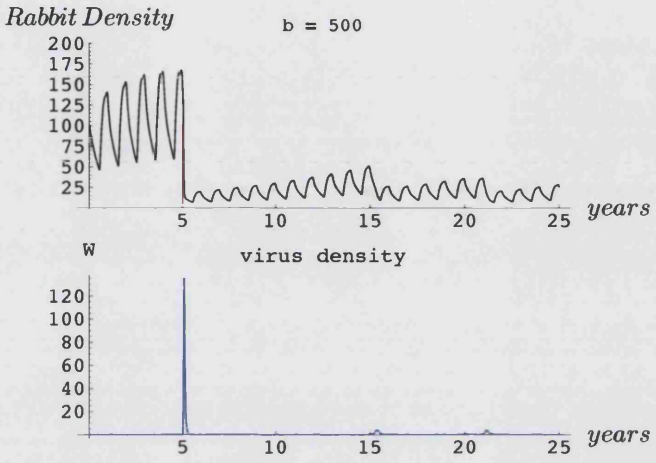


Figure 9.7: Effect of RCD on a rabbit population in Subalpine ($b = 500$).

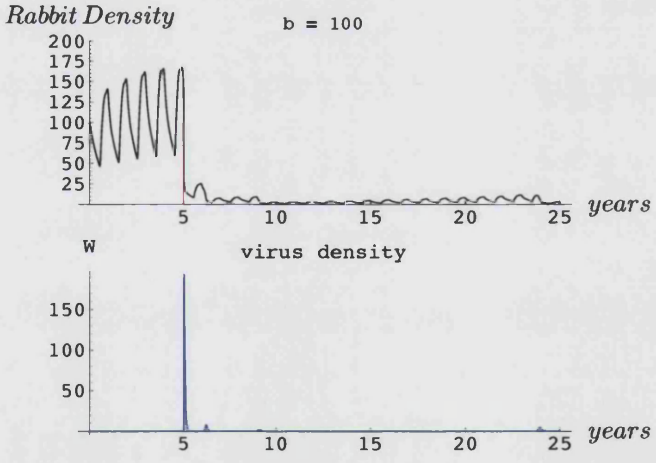


Figure 9.8: Effect of RCD on a rabbit population in Subalpine ($b = 100$).

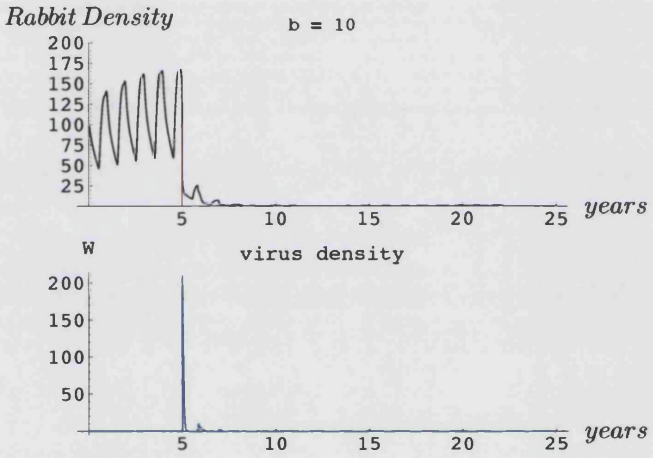


Figure 9.9: Effect of RCD on a rabbit population in Subalpine ($b = 10$).

## 9.2 Western NSW

The disease remains ineffective for $b \geq 3000$, even though it persists with dying oscillations throughout the run. For $b = 2000$ (figure 9.10), the disease persists with sharper peaks that periodically reduce the population, which then grows back to high densities after about 5 years from the outbreak. A similar trend is observed in this region for $b = 3000$ using the Strong hypothesis (figure 7.9). This seems to indicate that for very high values of $b$ (low virulence) the disease is more effective in the Strong hypothesis case, but that in the Weak hypothesis case, the range of $b$ for which the virus controls the population very effectively, is much larger. In the Weak hypothesis case, at $b = 200$ (figure 9.12) the population remains at very low values (density$< 20$) throughout the run, just as in the Strong hypothesis case, but for $b = 30$ the population is essentially wiped out (figure 9.13), while in the Strong hypothesis case (figure 7.11) it starts to grow back slowly exponentially. As in Subalpine, the disease remains extremely effective even for very low values of $b$.

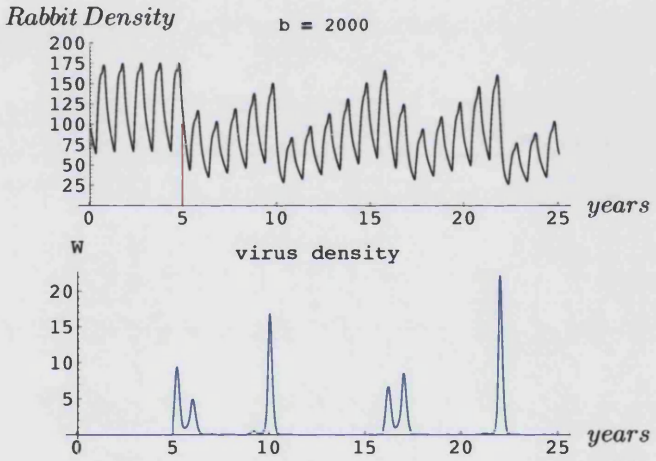


Figure 9.10: Effect of RCD on a rabbit population in Western NSW ($b = 2000$).

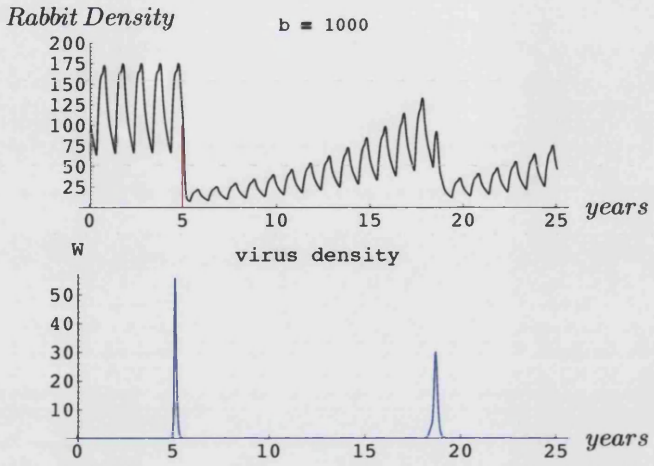


Figure 9.11: Effect of RCD on a rabbit population in Western NSW ($b = 1000$).

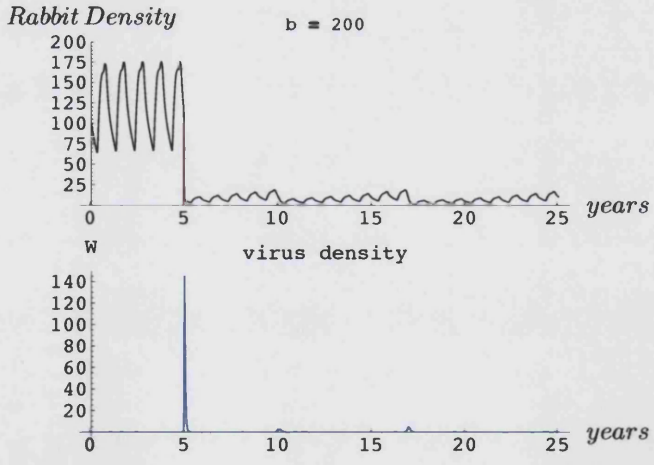


Figure 9.12: Effect of RCD on a rabbit population in Western NSW ($b = 200$).

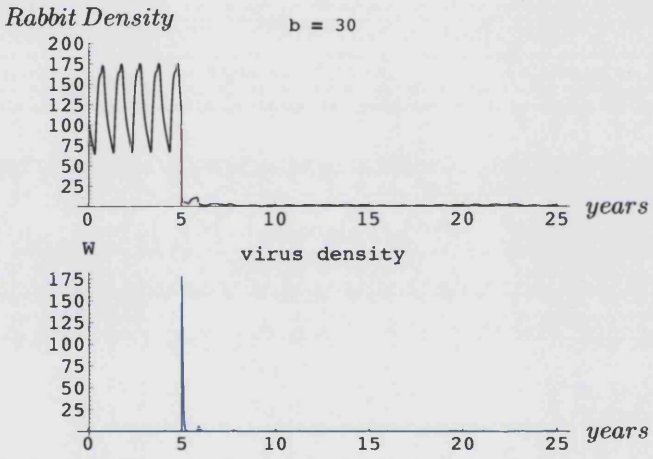


Figure 9.13: Effect of RCD on a rabbit population in Western NSW ($b = 30$).

## 9.3 Riverina

In the Riverina region, the disease persists for $b \leq 3000$ but it affects the population size only for $b \leq 2000$, where the virus breaks out periodically every 2 years with $W = 50$ (figure 9.15). The population starts to be controlled for $b = 1000$ (figure 9.17-9.18), while in the Strong hypothesis case, the disease is never really effective in this region because of the large number of Juveniles always available during the year. In the Weak hypothesis case, the disease almost crashes the population for very low values of $b$, like $b = 10$ (figure 9.21). Probably the Weak hypothesis is more effective then the Strong hypothesis because of the highly vulnerable class of susceptible Subadults who were immune due to the maternal antibodies they inherited as Juveniles. Since the surviving Adults will mostly be Recovereds (see figure 9.20 especially), their offspring will all be in the maternal antibody class, and hence will become vulnerable as Subadults. The population is then mainly sustained by the small number of Subadults who recover to become Recovered Adults.

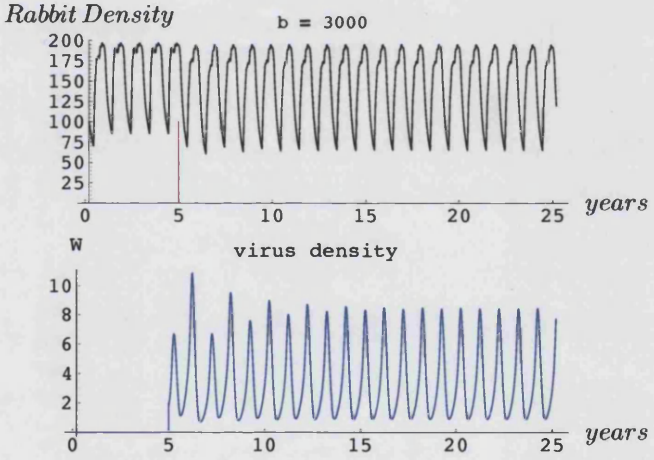


Figure 9.14: Effect of RCD on a rabbit population in Riverina ($b = 3000$).

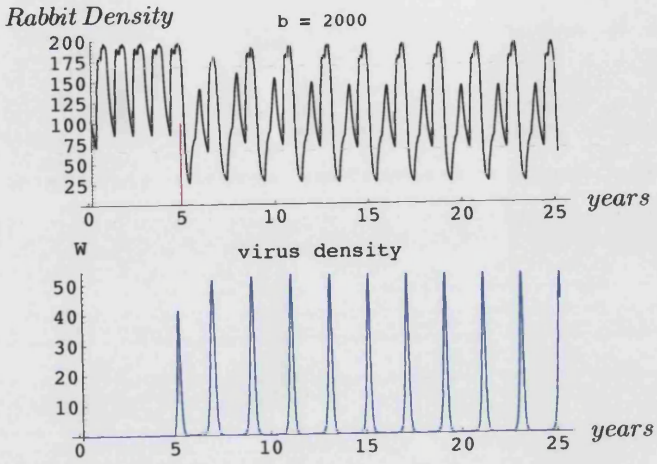


Figure 9.15: Effect of RCD on a rabbit population in Riverina ($b = 2000$).

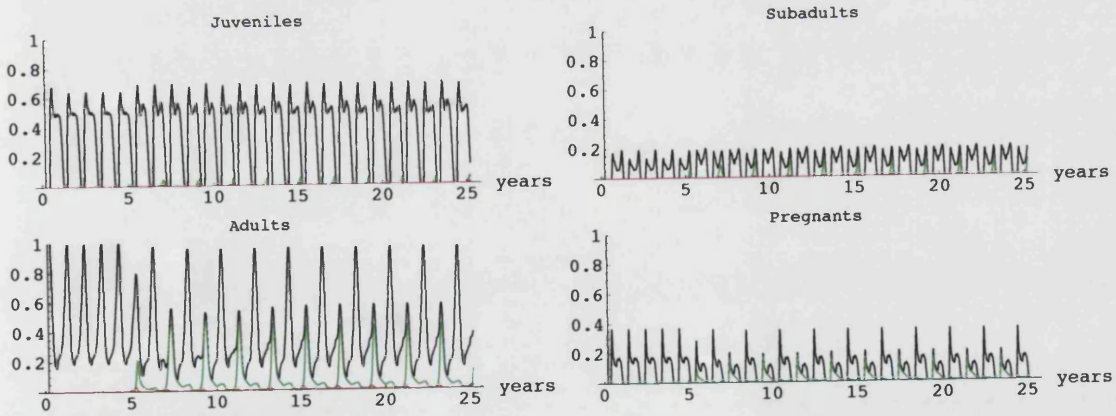


Figure 9.16: Proportion of the age classes against time (Black=Susceptible, Red=Infected, Green=Recovered), ($b = 2000$).

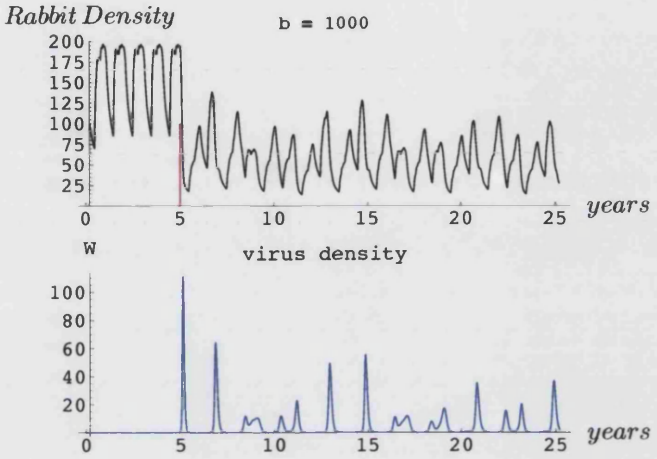


Figure 9.17: Effect of RCD on a rabbit population in Riverina ($b = 1000$).

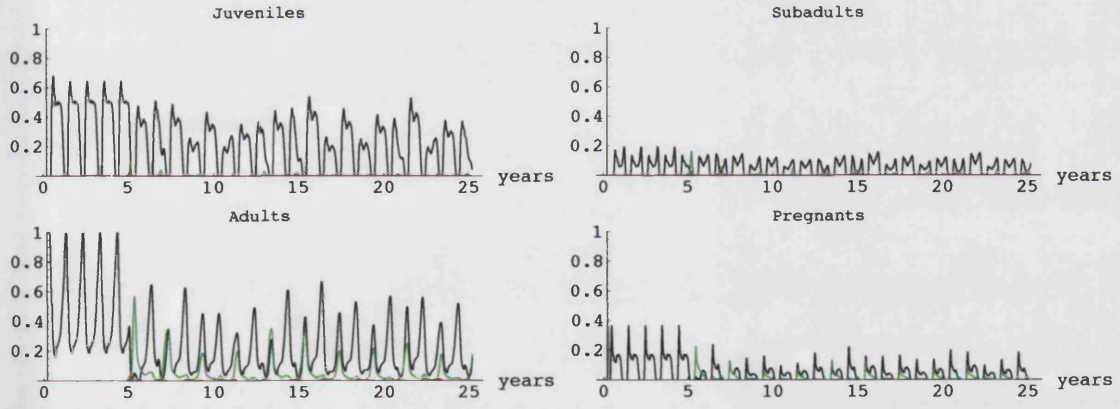


Figure 9.18: Proportion of the age classes against time (Black=Susceptible, Red=Infected, Green=Recovered), ($b = 1000$).

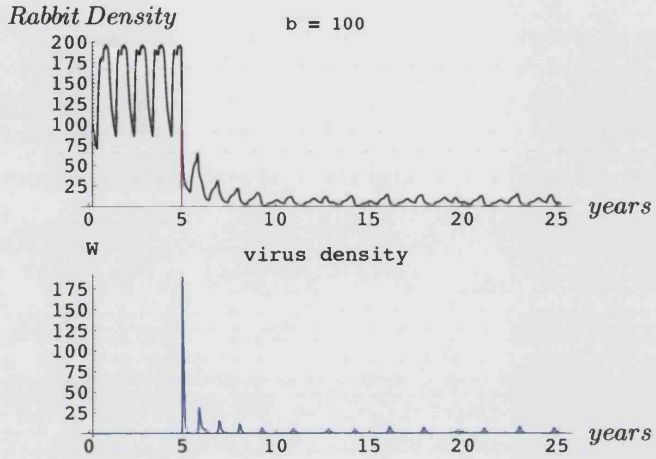


Figure 9.19: Effect of RCD on a rabbit population in Riverina ($b = 100$).

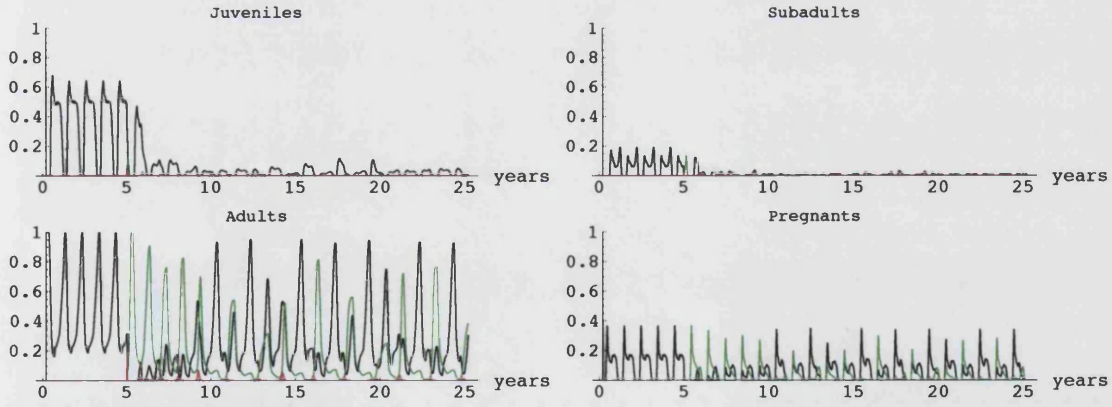


Figure 9.20: Proportion of the age classes against time (Black=Susceptible, Red=Infected, Green=Recovered), ($b = 100$).

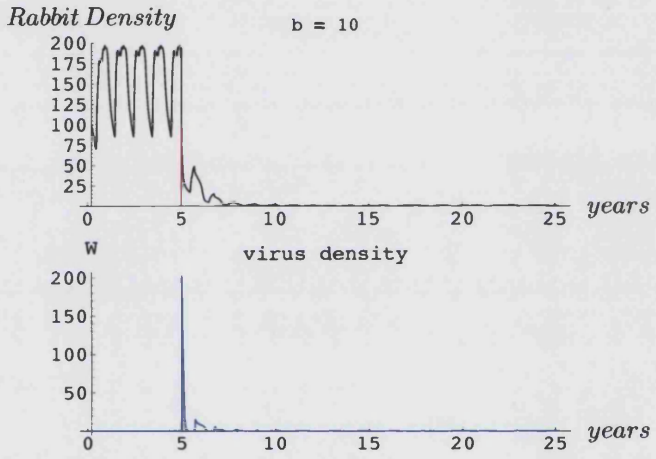


Figure 9.21: Effect of RCD on a rabbit population in Riverina ($b = 10$).

## 9.4 South-Western WA

In the Weak hypothesis case, South-Western WA rabbit populations are affected very similarly to Riverina, while for the Strong hypothesis the effect in South-Western WA was much greater (the population is controlled for a small range of $b$, $1000 < b < 300$) than in Riverina, where the population was never really controlled. In the Weak hypothesis the population is affected in the same way for the range $1000 < b < 300$, but for $b \leq 300$ the disease keeps on being very effective and keeping the rabbit number very low, in contrast to the Strong hypothesis, where the population recovers for very low $b$.

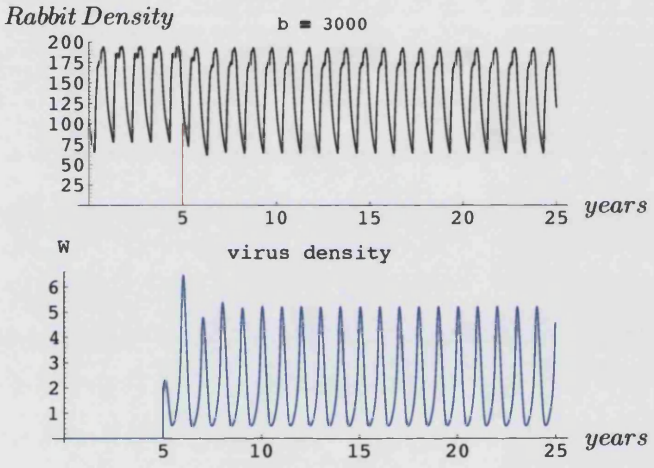


Figure 9.22: Effect of RCD on a rabbit population in South-Western WA ($b = 3000$).

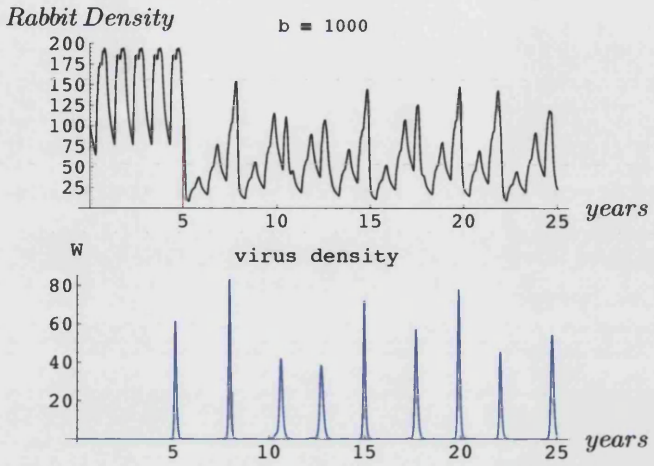


Figure 9.23: Effect of RCD on a rabbit population in South-Western WA ($b = 1000$).

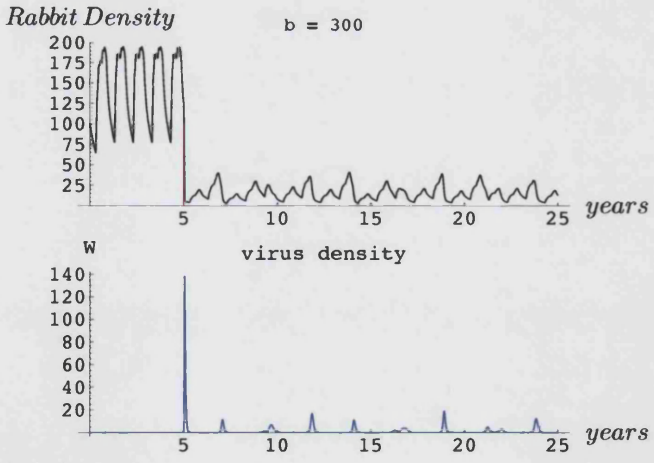


Figure 9.24: Effect of RCD on a rabbit population in South-Western WA ($b = 300$).

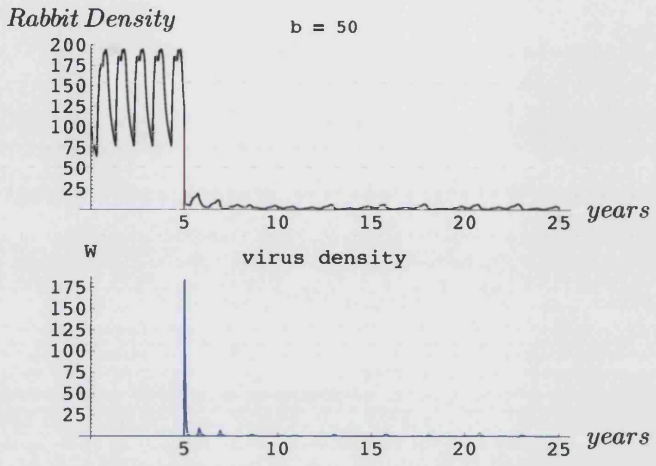


Figure 9.25: Effect of RCD on a rabbit population in South-Western WA ($b = 50$).

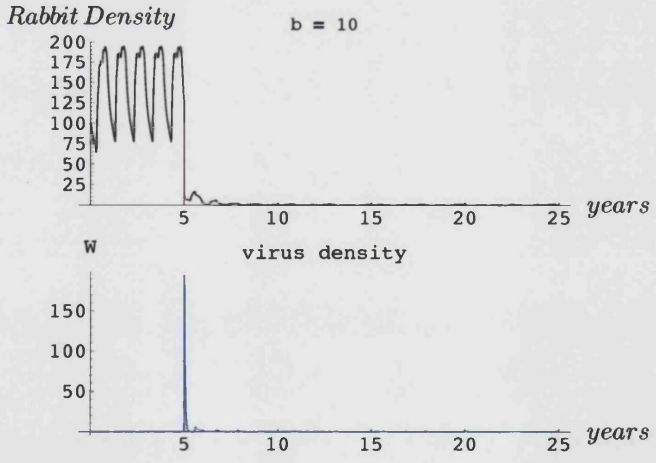


Figure 9.26: Effect of RCD on a rabbit population in South-Western WA ($b = 10$).

# Chapter 10

# Adding the Disease using the Weak hypothesis: Stochastic Results.

## 10.1 Subalpine

If the figures 10.1 to 10.7, describing the model result of introducing RCD using the Weak hypothesis in a susceptible rabbit population in a Subalpine type of environment, are compared to figures 8.1 to 8.5, it is possible to notice the difference in outcome between the Strong hypothesis approach and the Weak hypothesis approach regarding Juvenile immunity in the case where climatic variability is included in the model. It is found that the disease is not effective until $b = 2000$ (figure 10.2), for higher values of $b$ the stochastic effects are dominant in controlling the population. This behaviour is different in the Strong hypothesis where the disease is already effective for $b = 3000$ (compare figures 8.1 with 10.1) and dominant over the climatic variability. As $b$ decreases, the disease controls the population more effectively; for $b = 500$ the Weak hypothesis and the Strong hypothesis give similar outcomes: the two hypothesis yield similar results for values of $500 \leq b \leq 100$. When $b < 100$ the behaviours start to differ in that the disease becomes more and more deadly in the Weak hypothesis case (see figures 10.6 and 10.7); while the population tends to rebuild through the recovered individuals in the Strong hypothesis case (see figures 8.4 and 8.5). It will be noted that this kind of behaviour repeats for the whole range of $b$ in the other geographic areas considered in the next sections. Also note that for very high stochastic variance ($var = 10$), the population is effectively controlled, with or without the disease.

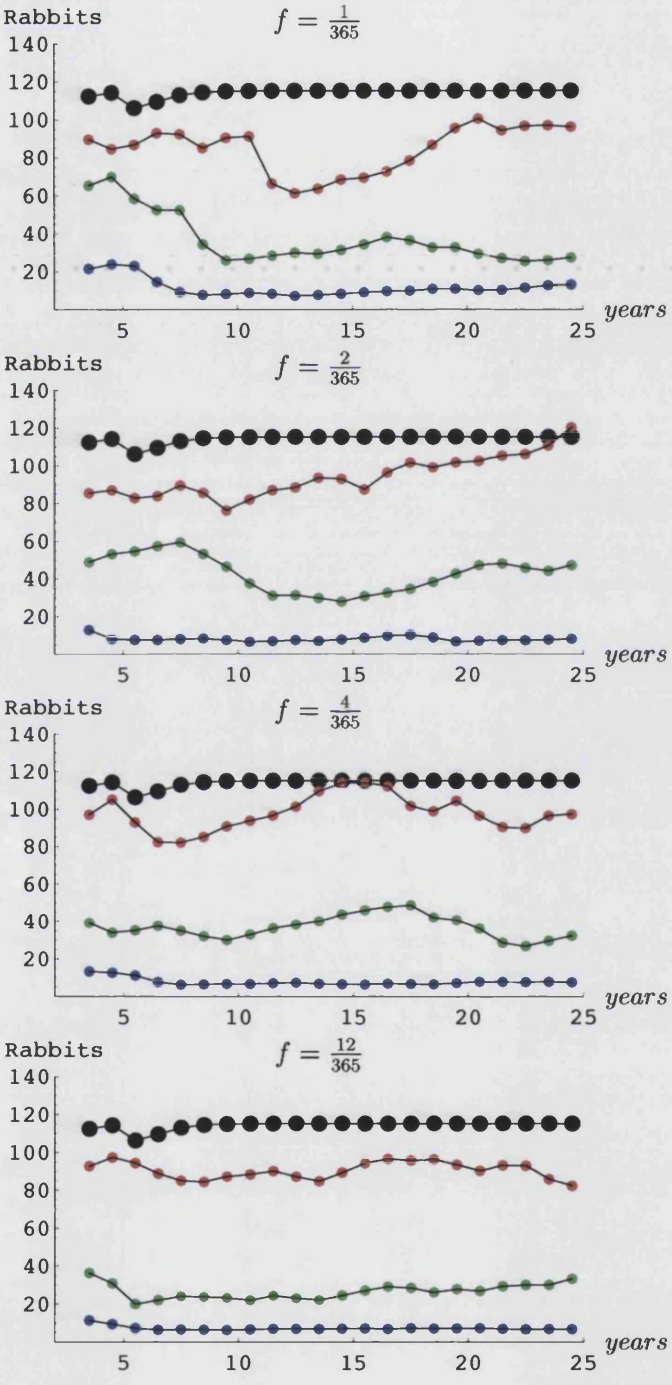


Figure 10.1: Disease and climatic variability in the Subalpine region (b=3000) for different variances (var) of the Lognormal Distribution: var=0.1(red), var=1(green), var=10(blue); heavy-dotted black line is the non-stochastic case.

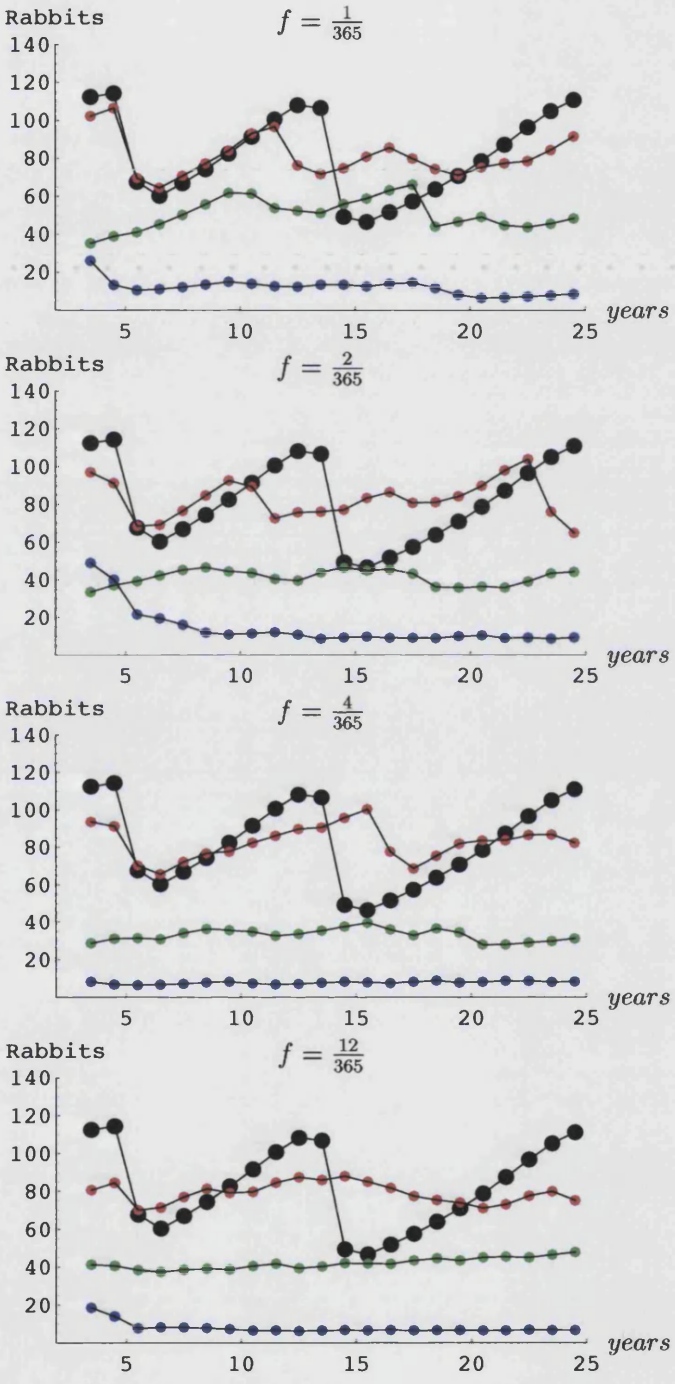


Figure 10.2: Disease and climatic variability in the Subalpine region (b=2000) for different variances (var) of the Lognormal Distribution: var=0.1(red), var=1(green), var=10(blue); heavy-dotted black line is the non-stochastic case.

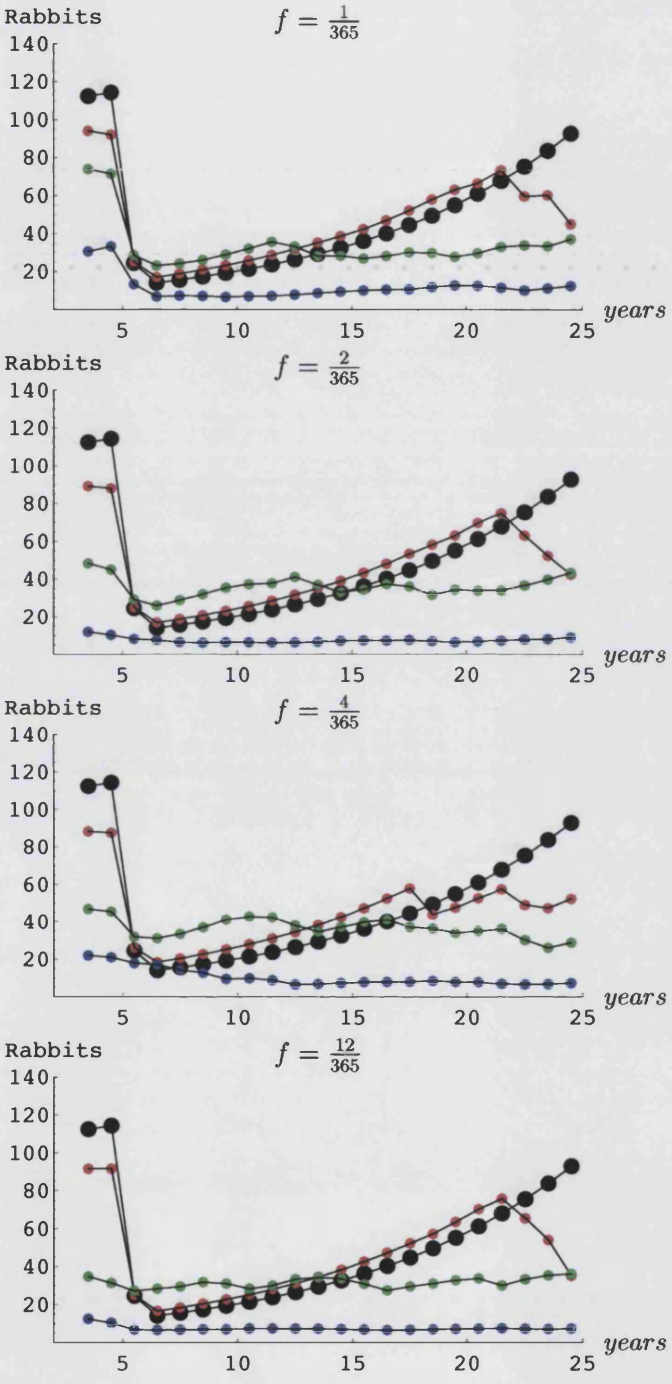


Figure 10.3: Disease and climatic variability in the Subalpine region (b=1000) for different variances (var) of the Lognormal Distribution: var=0.1(red), var=1(green), var=10(blue); heavy-dotted black line is the non-stochastic case.

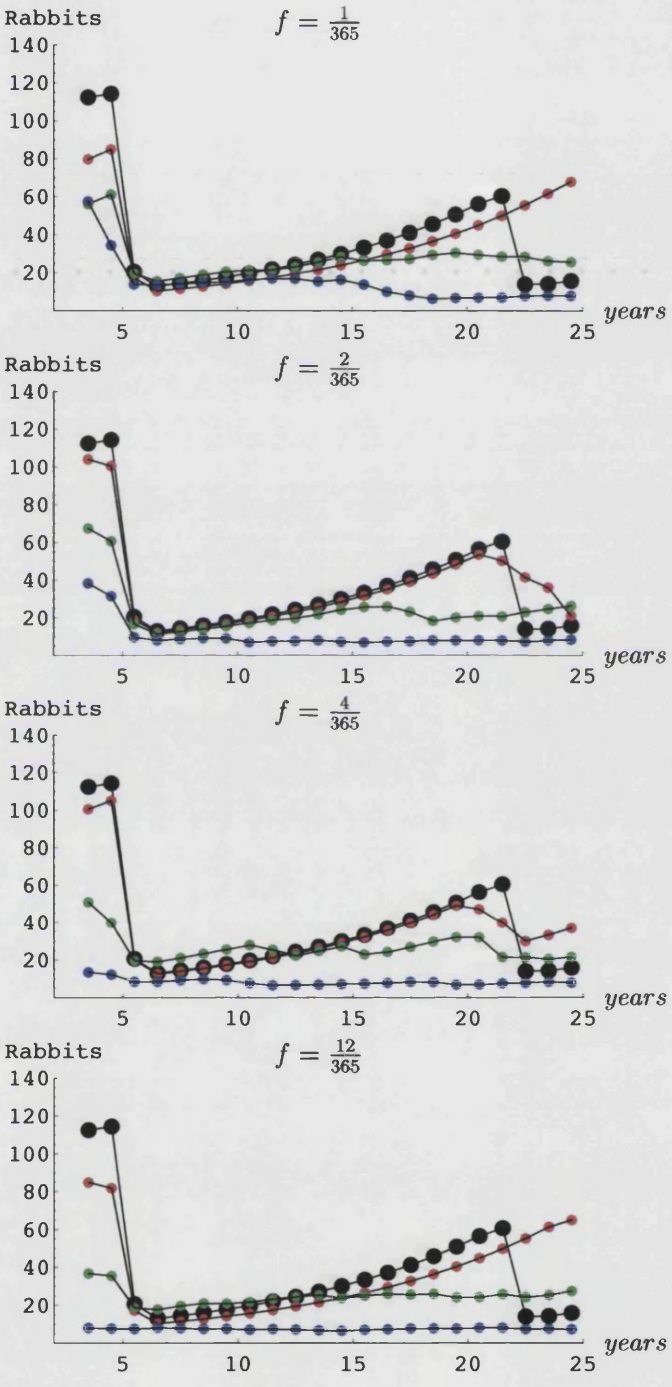


Figure 10.4: Disease and climatic variability in the Subalpine region (b=700) for different variances (var) of the Lognormal Distribution: var=0.1(red), var=1(green), var=10(blue); heavy-dotted black line is the non-stochastic case.

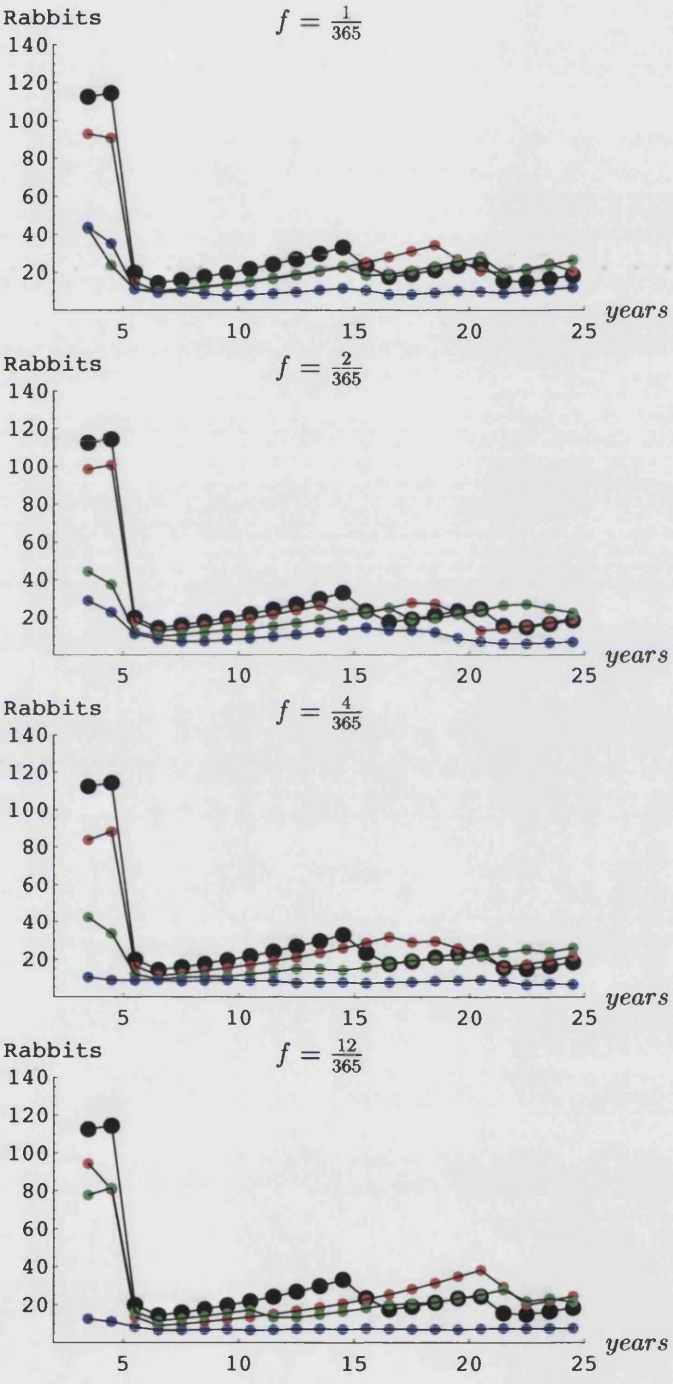


Figure 10.5: Disease and climatic variability in the Subalpine region (b=500) for different variances (var) of the Lognormal Distribution: var=0.1(red), var=1(green), var=10(blue); heavy-dotted black line is the non-stochastic case.

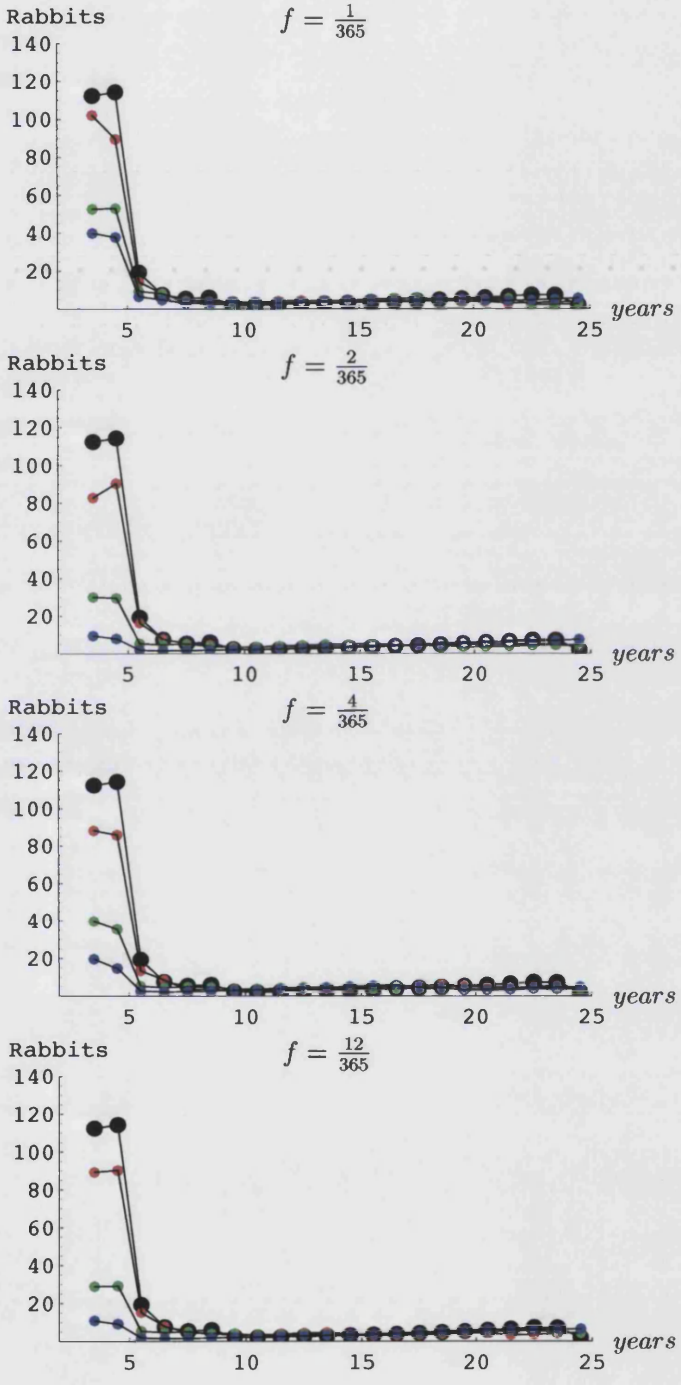


Figure 10.6: Disease and climatic variability in the Subalpine region (b=100) for different variances (var) of the Lognormal Distribution: var=0.1(red), var=1(green), var=10(blue); heavy-dotted black line is the non-stochastic case.

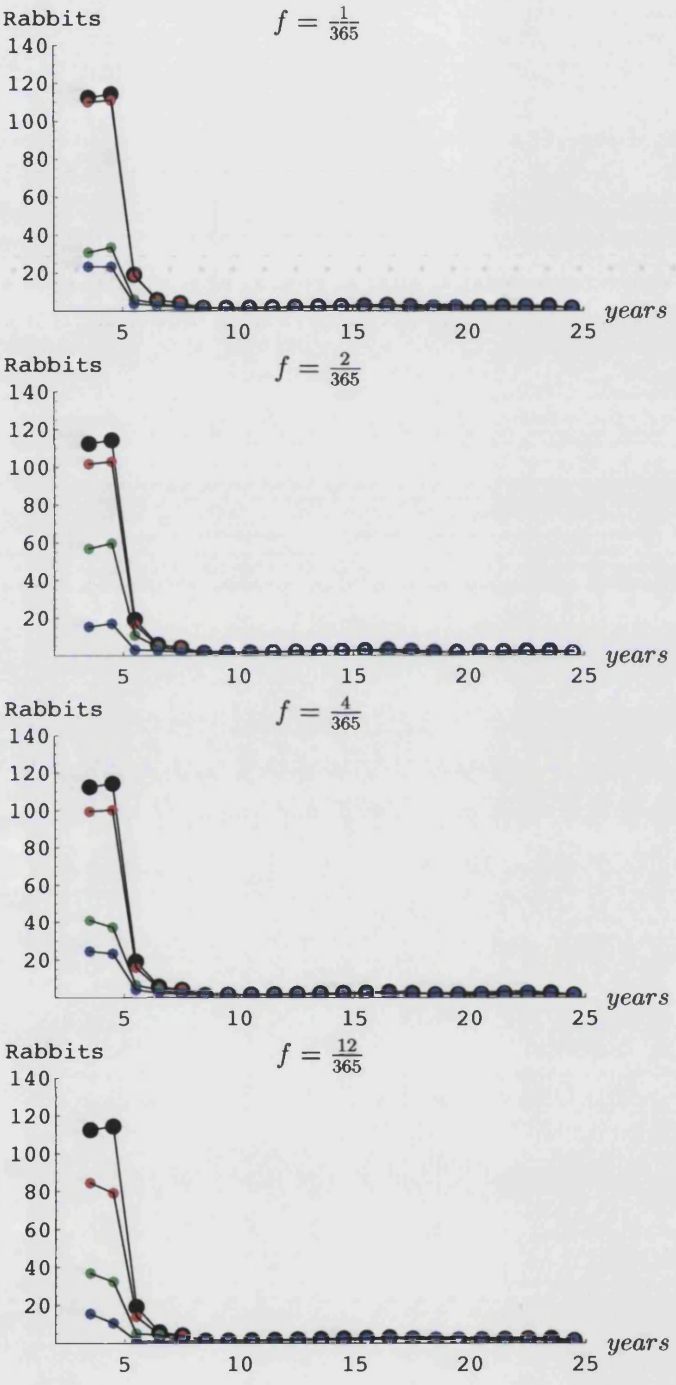


Figure 10.7: Disease and climatic variability in the Subalpine region (b=50) for different variances (var) of the Lognormal Distribution: var=0.1(red), var=1(green), var=10(blue); heavy-dotted black line is the non-stochastic case.

## 10.2 Western NSW

Figures 10.8 to 10.12 illustrate the model outcome of introducing the disease in a population of susceptible rabbits in Western NSW using the Weak hypothesis. The results can be compared with figures 8.6 to 8.9 which outline the results from the model using the Strong hypothesis. In the Strong hypothesis case the disease starts to have an effect for higher values of $b$ than in the Weak hypothesis case: for $b = 3000$ the outcome in the Weak hypothesis case is quite similar to the non disease case and the population is mainly controlled by the stochastic effects (figure 10.8), while in the Strong hypothesis case, for the same value of $b$ (figure 8.6), the disease lowers the population size and subsequently the rabbit number starts to increase until a new outbreak of the disease occurs, especially for low variances of the lognormal distribution. For lower values of $b$ there is less difference between the Weak hypothesis and the Strong hypothesis; for example for $b = 200$ (see figures 8.8 and 10.11). However, as $b$ becomes smaller the disease is more and more effective in the Weak hypothesis case; for the Strong hypothesis case it has been observed to become less effective. For example $b = 30$ (see figure 8.9), where the population starts to recover towards the end of the run with stochastic effects delaying the growth in the Strong hypothesis case; while in the Weak hypothesis case the population crashes and never recovers for values as low as $b = 10$. The stochastic effects play the same role in both cases; that is they are dominant for high values of $b$ with respect to the disease, and help the disease in controlling the population when the virus becomes more effective at lower values of $b$. In fact for high stochastic variance the population is effectively controlled with or without the disease.

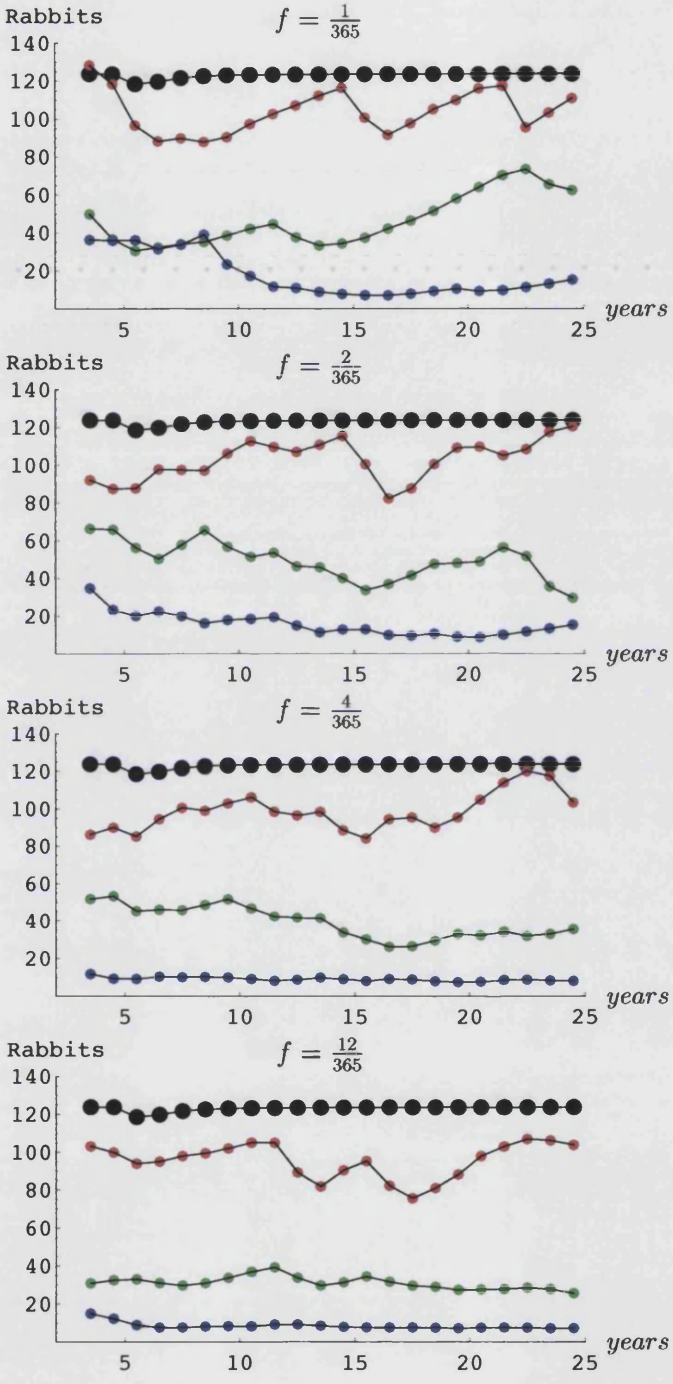


Figure 10.8: Disease and climatic variability in the Western NSW region (b=3000) for different variances (var) of the Lognormal Distribution: var=0.1(red), var=1(green), var=10(blue); heavy-dotted black line is the non-stochastic case.

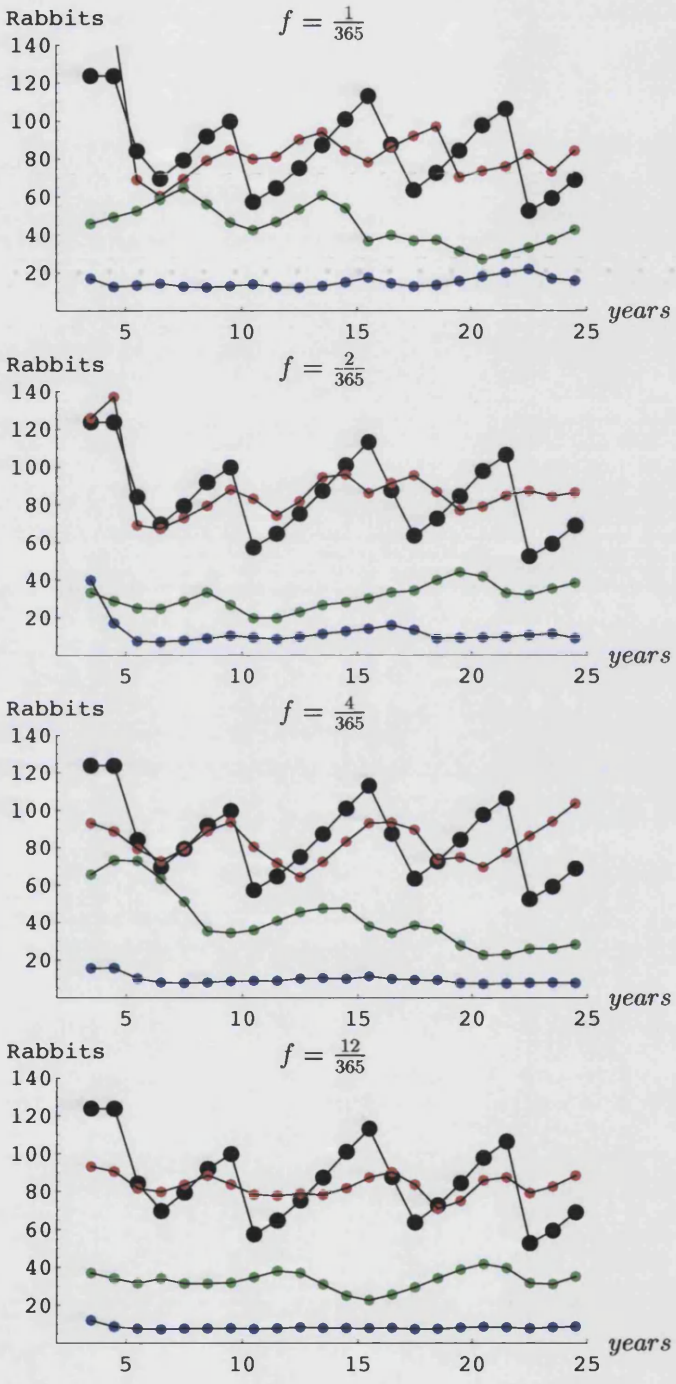


Figure 10.9: Disease and climatic variability in the Western NSW region (b=2000) for different variances (var) of the Lognormal Distribution: var=0.1(red), var=1(green), var=10(blue); heavy-dotted black line is the non-stochastic case.

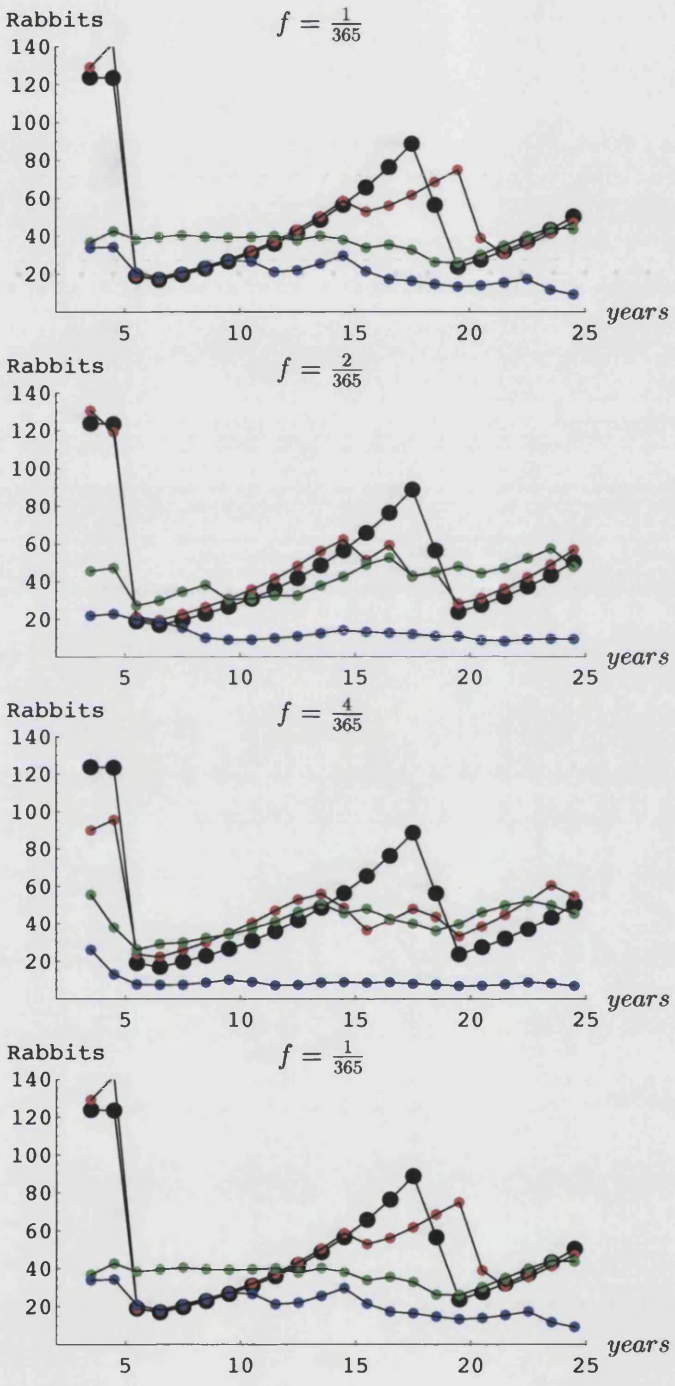


Figure 10.10: Disease and climatic variability in the Western NSW region (b=1000) for different variances (var) of the Lognormal Distribution: var=0.1(red), var=1(green), var=10(blue); heavy-dotted black line is the non-stochastic case.

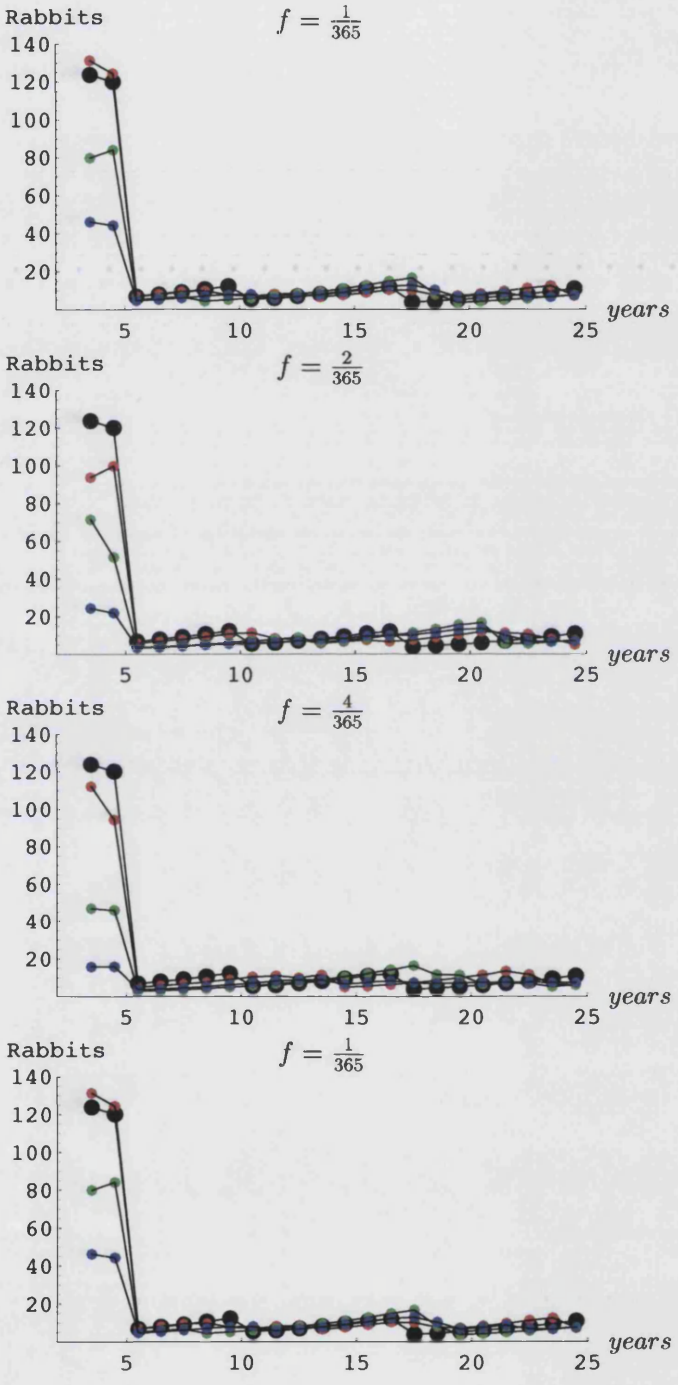


Figure 10.11: Disease and climatic variability in the Western NSW region (b=200) for different variances (var) of the Lognormal Distribution: var=0.1(red), var=1(green), var=10(blue); heavy-dotted black line is the non-stochastic case.

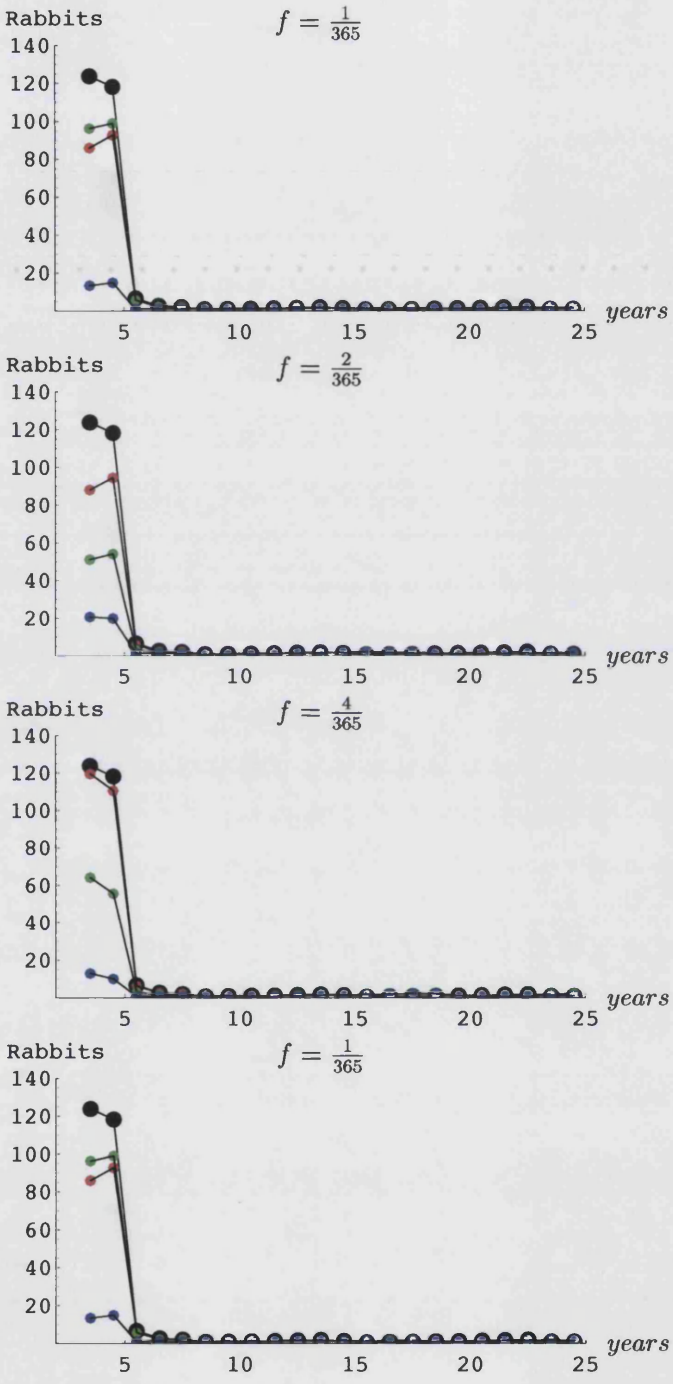


Figure 10.12: Disease and climatic variability in the Western NSW region (b=30) for different variances (var) of the Lognormal Distribution: var=0.1(red), var=1(green), var=10(blue); heavy-dotted black line is the non-stochastic case.

## 10.3 Riverina

Figures 10.13 to 10.16 give the model results obtained from introducing RCD in a susceptible rabbit population in the Riverina region using the Weak hypothesis. If these figures are compared to figures 8.10 to 8.12, it is possible to observe the differences between this hypothesis and the Strong hypothesis; especially in this geographical region, the difference is quite pronounced. In the Strong hypothesis case, the disease never really has a dramatic effect on the population size; while in the figures below the disease clearly controls the population starting from $b = 1000$ (figure 10.15), though it has a significant effect at $b = 2000$, especially in the non-stochastic case (figure 10.14). For decreasing values of $b$ the population is totally controlled to the point in which the average annual population density is less than 20 ($b = 100$ figure 10.16). The disease has a greater impact with decreasing values of $b$, as observed in all cases related to the Weak hypothesis. The difference between the stochastic and non-stochastic cases follows the same trend as in the marginal environments; i.e.. for high values of $b$, when the disease is not so effective, the stochastic effects are dominant in keeping the population size down, but as $b$ decreases, the disease becomes dominant and the trend of the population size follows the non-stochastic case.

## 10.4 South-Western WA

The model results (figures 10.17 to 10.20) for the South-Western WA region using the Weak hypothesis follow the same pattern as for the previous regions when compared to the results in the Strong hypothesis case (figures 8.13 to 8.17): the disease has a delayed effect relative to the Strong hypothesis case, and its impact on the population size becomes significant at $b = 1000$ (see figure 10.18), while in the Strong hypothesis case the disease already controls the population for $b = 4000$ (see figure 8.13), and for $b = 1000$ the population is stably kept at values lower than an annual average density of 40 (see figure 8.14). However, in the Strong hypothesis case for $b \leq 200$ (see figure 8.16 and 8.17) the population rebuilds to pre-disease size after the initial impact, but in the Weak hypothesis case the disease becomes more effective with decreasing values of $b$ (see figures 10.19 and 10.20): the stochastic effects become secondary control agents with respect to the disease, while they play the role in population control for high values of $b$.

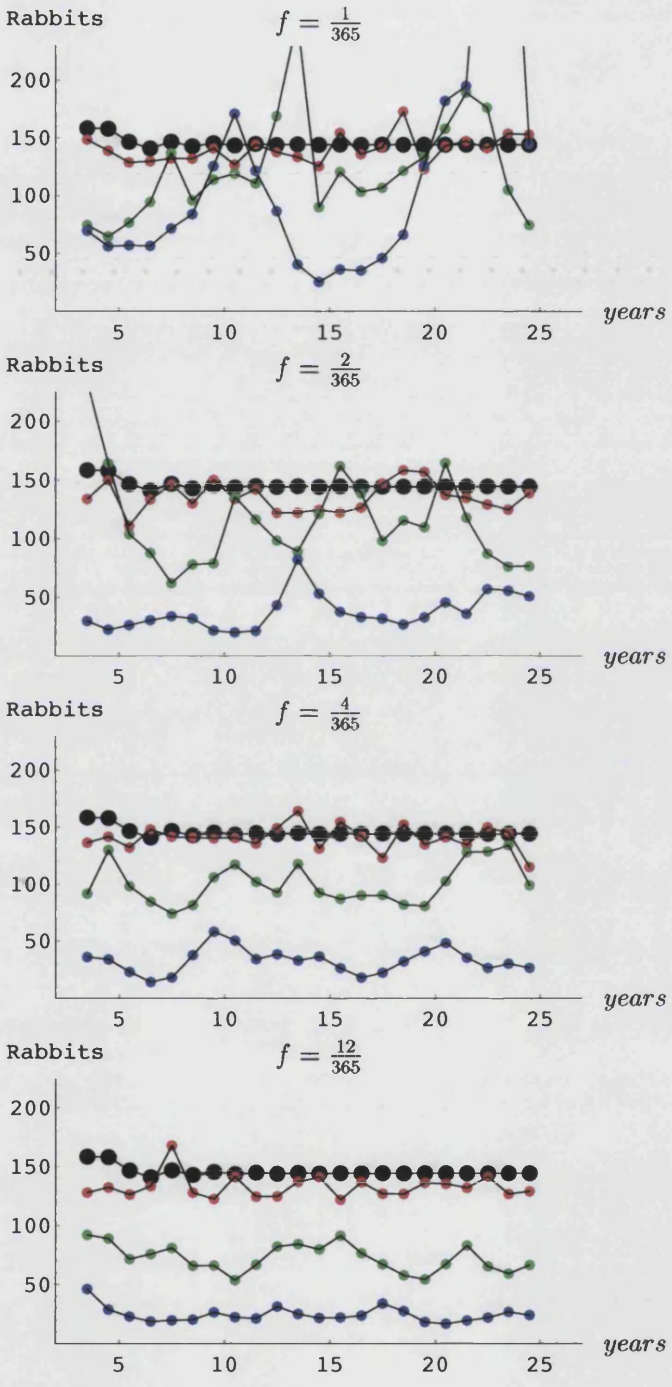


Figure 10.13: Disease and climatic variability in the Riverina region (b=3000) for different variances (var) of the Lognormal Distribution: var=0.1(red), var=1(green), var=10(blue); heavy-dotted black line is the non-stochastic case.

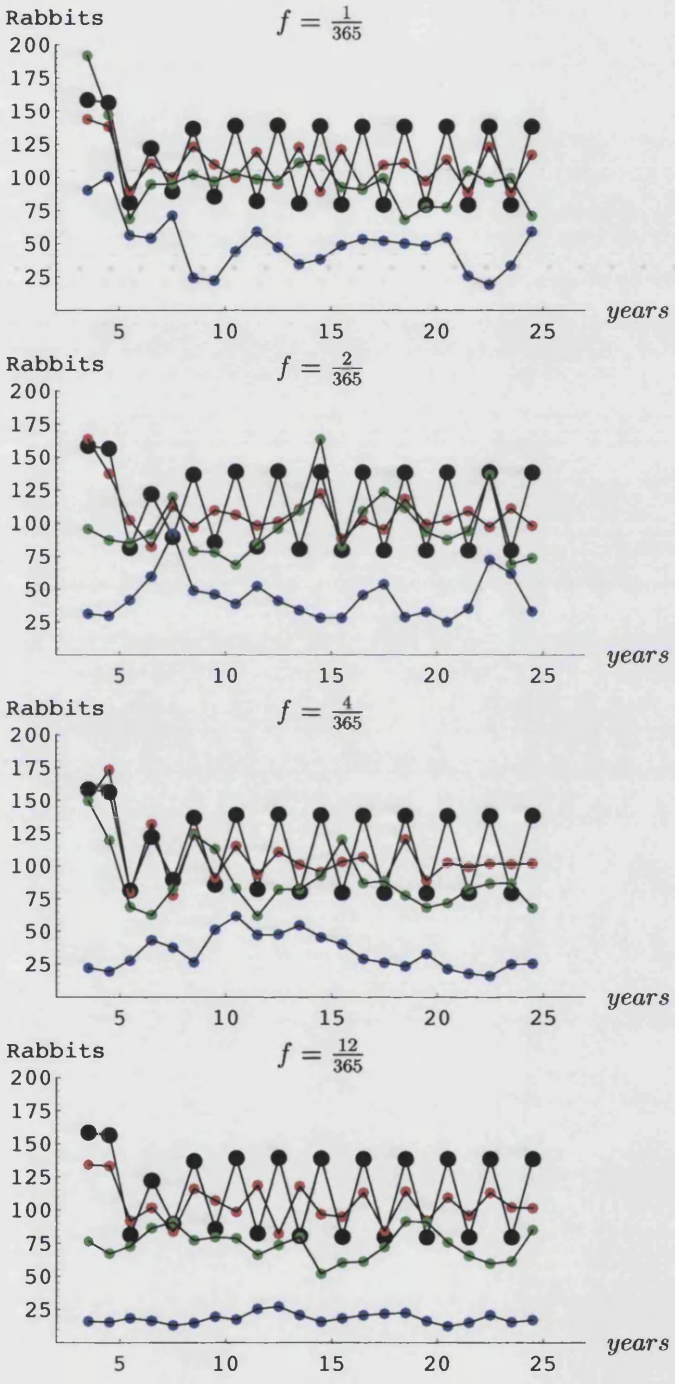


Figure 10.14: Disease and climatic variability in the Riverina region (b=2000) for different variances (var) of the Lognormal Distribution: var=0.1(red), var=1(green), var=10(blue); heavy-dotted black line is the non-stochastic case.

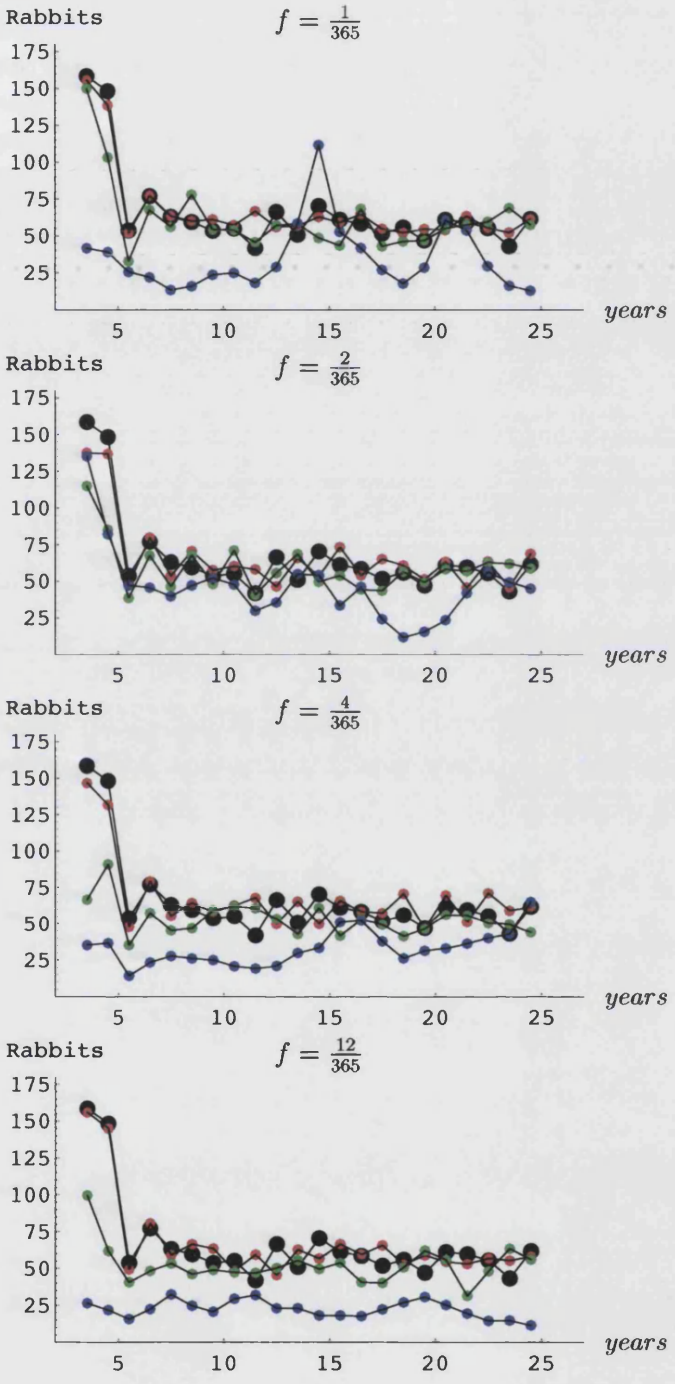


Figure 10.15: Disease and climatic variability in the Riverina region (b=1000) for different variances (var) of the Lognormal Distribution: var=0.1(red), var=1(green), var=10(blue); heavy-dotted black line is the non-stochastic case.

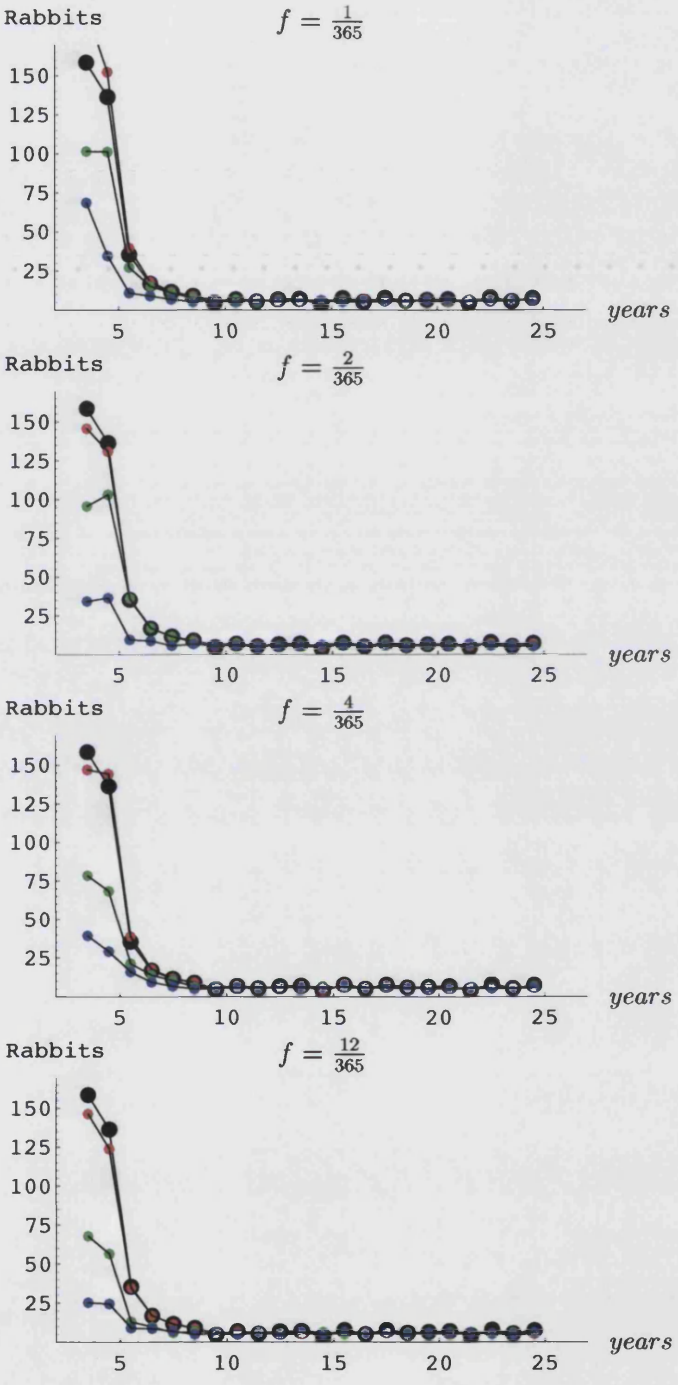


Figure 10.16: Disease and climatic variability in the Riverina region (b=100) for different variances (var) of the Lognormal Distribution: var=0.1(red), var=1(green), var=10(blue); heavy-dotted black line is the non-stochastic case.

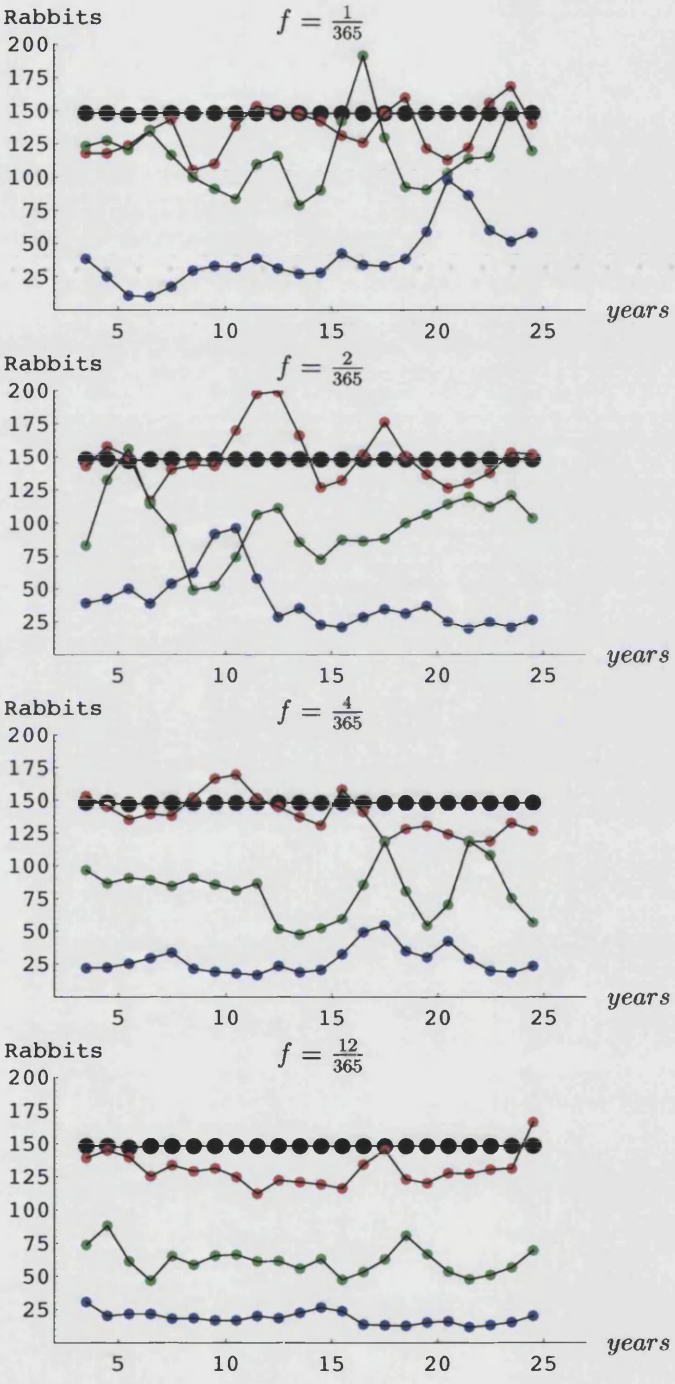


Figure 10.17: Disease and climatic variability in the South-Western WA region (b=4000) for different variances (var) of the Lognormal Distribution: var=0.1(red), var=1(green), var=10(blue); heavy-dotted black line is the non-stochastic case.

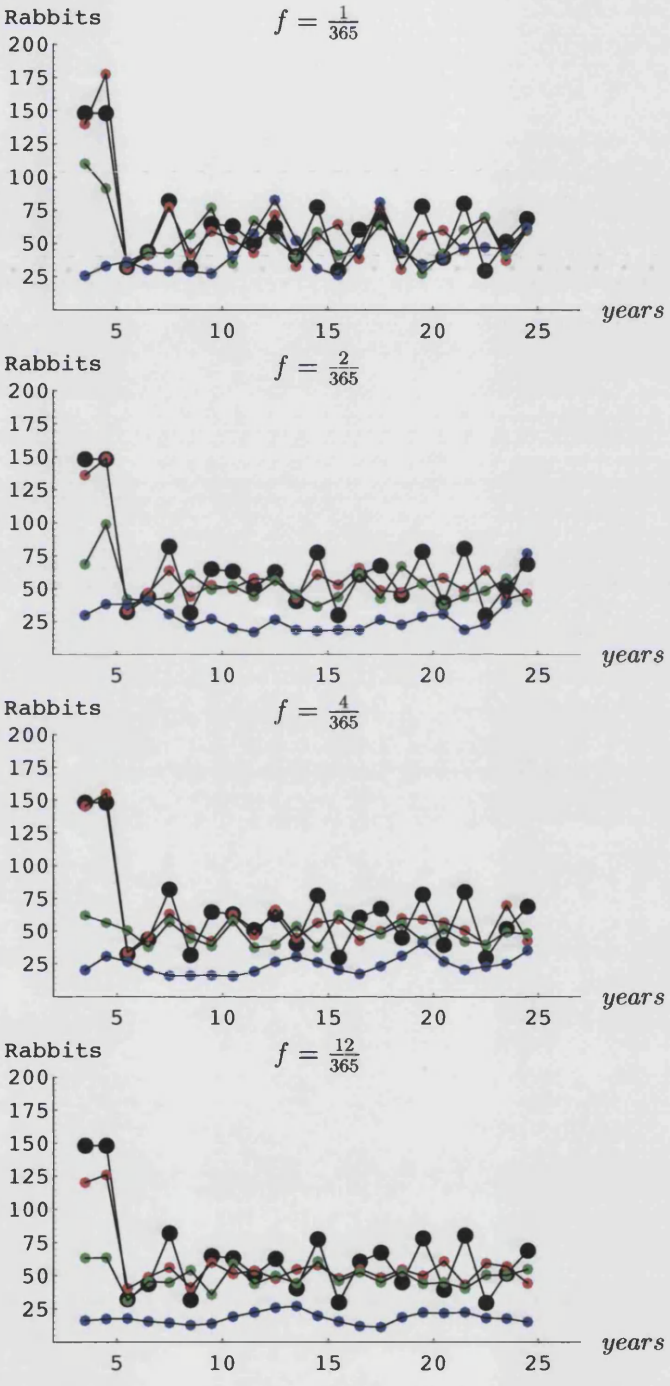


Figure 10.18: Disease and climatic variability in the South-Western WA region (b=1000) for different variances (var) of the Lognormal Distribution: var=0.1(red), var=1(green), var=10(blue); heavy-dotted black line is the non-stochastic case.

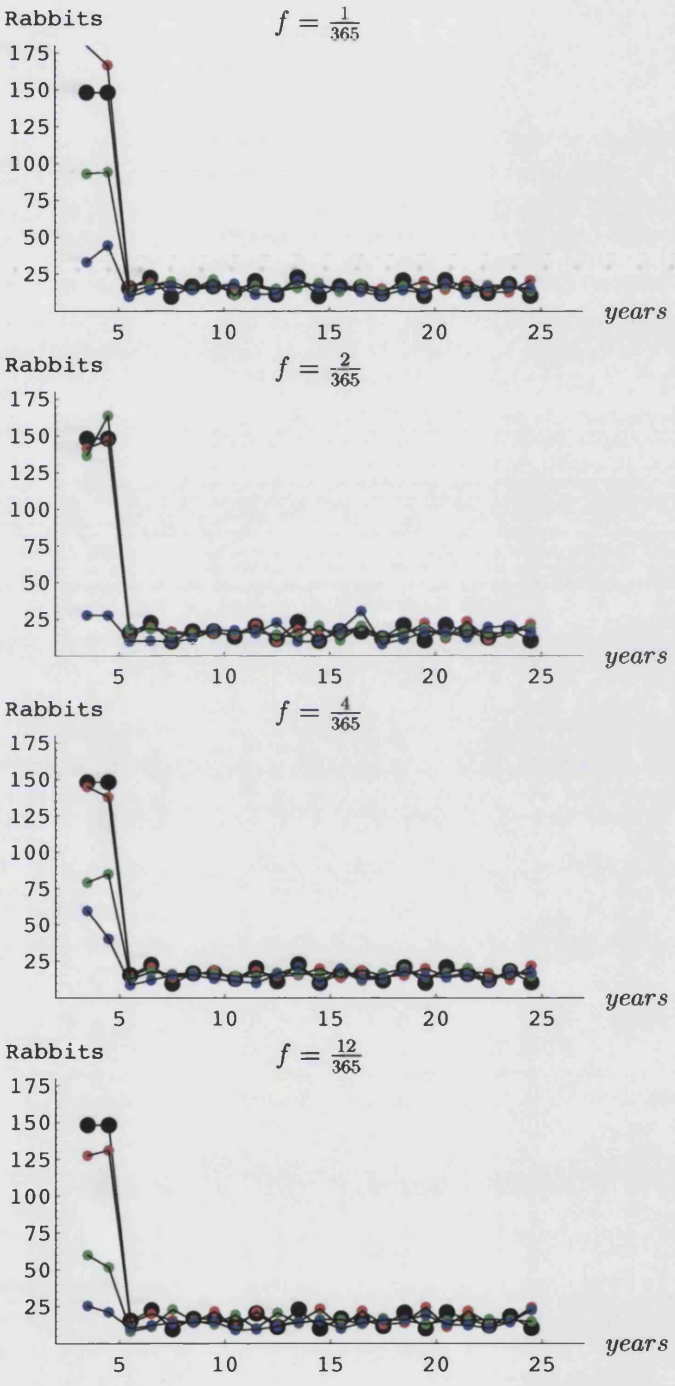


Figure 10.19: Disease and climatic variability in the South-Western WA region (b=300) for different variances (var) of the Lognormal Distribution: var=0.1(red), var=1(green), var=10(blue); heavy-dotted black line is the non-stochastic case.

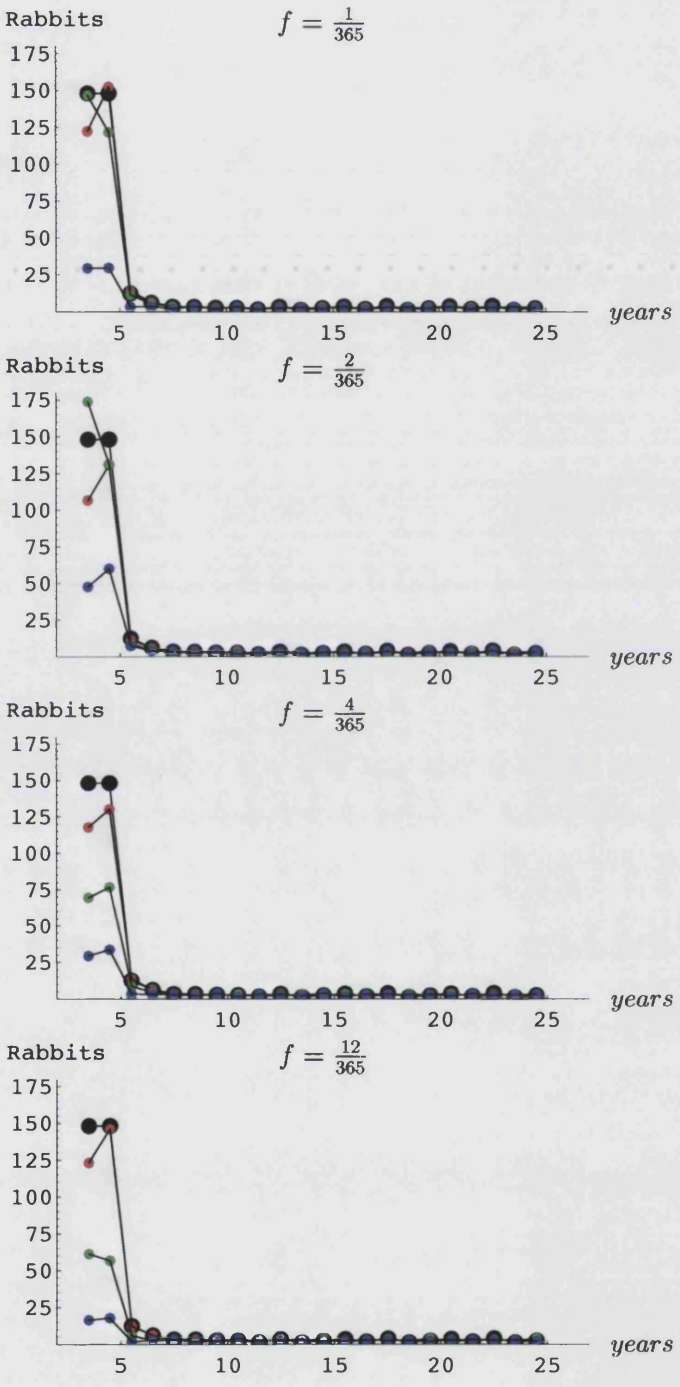


Figure 10.20: Disease and climatic variability in the South-Western WA region (b=50) for different variances (var) of the Lognormal Distribution: var=0.1(red), var=1(green), var=10(blue); heavy-dotted black line is the non-stochastic case.

# Chapter 11

# The Multiple Site Model

To construct a model that incorporates the spatial and temporal dynamics of a population of susceptible rabbits infected with RCD, it is necessary to account for that part of the resident population leaving the site to join another site, where by "site" we mean a set of closely-related warrens. In the emigration model (see chapter 5) devised to find the best fit parameter values to the data, we did not consider what happens to the emigrating population, where it goes to and what hazards it faces in transit to another site. The multiple site model, which we discuss in this chapter, accounts for the full dynamics of the emigrating population and for the interaction between sites distributed in specific spatial configurations. These configurations allow for the manipulation of several variables such as:

- site carrying capacity;
- the "connectivity" between sites, which makes certain environments more or less favourable for rabbits and allows the investigation of the "Hide-and-Seek" [49] concept;
- the site(s) at which the disease is introduced;
- homogeneous and non-homogeneous spatial distribution of the site interaction;
- transit hazard;
- probability of acceptance at an end site.

The spatial model can be thought of as the dynamics resulting from the interaction of three populations associated with each site: an emigrant, an immigrant and a resident population. The

equations governing the dynamics of each of these populations are given in the appendix to this chapter (section 11.4). A schematic representation of the interactions is illustrated in figure 11.1 and a description of the general concept behind the spatial dynamics will follow.

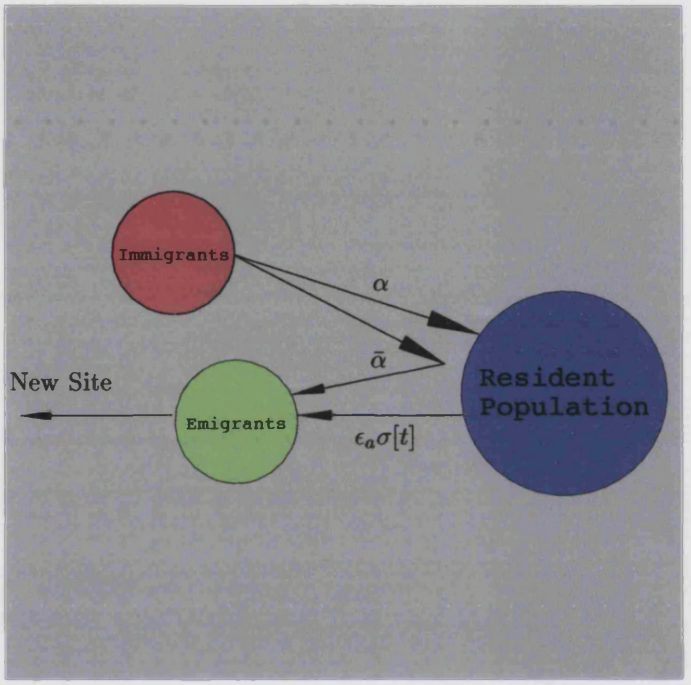


Figure 11.1: Dynamics of the three populations.

The dynamics for the resident population (see section 11.4.1) is described by equations very similar to those for the single site model, but when accounting for the interaction between sites, an emigration probability for the resident population and an "acceptance" or "non-acceptance" probability for an immigrating population must be included. The emigration probability of an individual emigrating from the site it inhabits is expressed by the term $\epsilon_a\sigma[t]$, where $\epsilon_a$ is the age dependent emigration rate, $a$ is the class of the individual, i.e. $J, Y, A_M$ or $A_F$; and $\sigma[t]$ is the seasonal emigration probability ($t$ is the day of the year). This term has already been explained in chapter 5. Moreover the dynamics of the resident population will be dependent on the immigrating population into that site. From the rabbits trying to immigrate and become established in the site, only some proportion will be accepted. The acceptance probability is given by a probability $\alpha$ and the non-acceptance by $\bar{\alpha} = 1 - \alpha$. The acceptance probability $\alpha$ depends on the population density at the site of immigration, in a manner explained in section 11.1 below. We assume that pregnant

females are sedentary to the site in which they became pregnant. Thus, pregnant females do not emigrate and no proportion of the immigrating population will join the pregnant female class.

The dynamics of the Immigrant population is described by the equations in section 11.4.2. A new parameter, $h$, is introduced, which represents the hazard to which rabbits in transit between sites are exposed; that is $h$ is the probability per day that an emigrating animal will die, in addition to the normal mortality rate. This is due to factors such as additional exposure to predators, and maybe hunger and thirst. In the model simulations $h$ is kept as a constant, namely $h = 0.6$. This means that an emigrating rabbit is 60% more likely to die on a given day, than a resident rabbit. The connectivity and the site-specific threshold capacity, which determines the population threshold at which density dependent Juvenile mortality clicks in, are the stochastic elements that allow for spatial variation. The connectivity determines the spatial interaction between the sites; that is, how the sites are connected: it is explained in more detail in section 11.2. The Immigrant population can be viewed as the proportion of the total Emigrant populations from all other sites that has survived the hazard, the disease and natural death, has arrived at a given site and then tries to gain acceptance into the site.

The dynamics of the Emigrant population is described by the equations in section 11.4.3. Once they leave their site, emigrants will try to immigrate into neighbouring sites, the probability that an emigrant from site $i$ will end in any neighbouring site $j$ is expressed by a connectivity matrix whose entries give the probability per day that an emigrant from site $i$ will arrive at site $j$ (if it survives). The emigrants from site $i$ who try to immigrate into site $j$, but are refused, then join the class of emigrants from site $j$ for the subsequent day.

## 11.1 The Acceptance and Non-Acceptance Probability Functions

We have discussed in section 1.3.5 how the literature reports that there are several factors that might influence a rabbit's decision to emigrate from its resident site: these factors include age, social status, season and population density of the resident site. When a rabbit leaves the site it resides in, it will seek to establish itself in more favourable conditions, ideally a new site with low population density and high food abundance. If the new site has a high population density, the immigrant will be hindered in becoming established there. We therefore assume that the probability of acceptance of an individual into a site is a decreasing function of the population density of the

site into which the individual is trying to immigrate: the bigger the population density of the site, the harder it is to be accepted. A suitable mathematical function that exhibits this behaviour is the following:

$$\alpha = 1 - \frac{N^u}{\hat{N}^u + N^u}; \tag{11.1}$$

where $N$ is the population density and $\hat{N}$ is a threshold capacity of the site which determines the density at which an immigrant animal has a 50 : 50 chance of being accepted. Graphs of this function for various $u$ are shown in figure 11.2. For low values of $u$ more immigrants will be accepted after the site populations overcomes the threshold. While for higher values of $u$ the probability of acceptance decays more sharply after the threshold is overcome by the population site. In the model $\hat{N}$ is chosen to be 100 and $u$ is chosen to be 5 as an intermediate shape for the probability. It might have been better to choose $\hat{N}$ to be proportional to the carrying capacity of the receiving site. That would have made it different for each site. It was chosen to be constant for simplicity in the modelling.

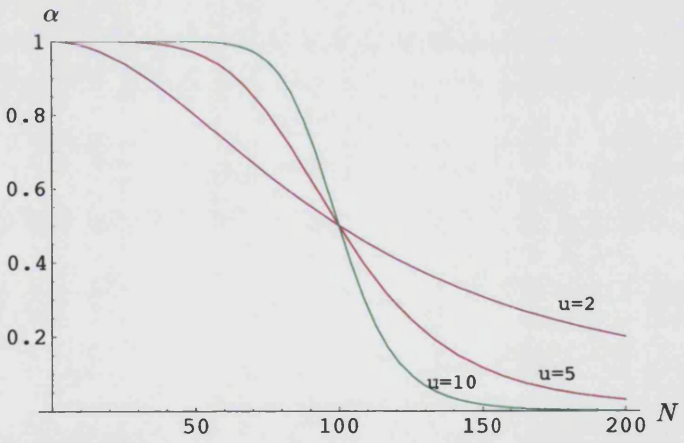


Figure 11.2: Density-dependence probability of acceptance $\alpha$ of an immigrating individual into a site. $\alpha$ is shown for different values of $u$.

It follows that the probability that an emigrating individual is not accepted into another site is:

$$\bar{\alpha} = 1 - \alpha = \frac{N^u}{\hat{N}^u + N^u}. \tag{11.2}$$

## 11.2 The Connectivity

The site-to-site "connectivity" is one of the main concepts in the spatial modelling: it is a matrix whose elements describe both the spatial configuration and the spatial interaction between the sites.

In the connectivity matrix the row index indicates the site from which a rabbit is emigrating and the column index indicates the site to which the rabbit is immigrating. Thus, the $(i,j)^{th}$ element $\chi_{ij}$ is the probability per day that a rabbit coming from site $i$ will arrive at site $j$. Moreover it is assumed that $\chi_{ij} = \chi_{ji}$, that is, it is just as likely that an emigrant from site $j$ will arrive at site $i$, as that an emigrant from site $i$ will arrive at site $j$, on any given day. Therefore such a matrix will always be a square matrix, since all the sites must allow for both emigration and immigration, and diagonal entries are equal to zero as it is assumed that an emigrating individual does not immigrate back into the site from which it emigrated in the same day. Some examples are given below to illustrate how the connectivity matrix "creates" spatial variation.

The general connectivity matrix for any spatial configuration consisting of 5 sites is the following:

$$\begin{pmatrix} 0 & \chi_{1,2} & \chi_{1,3} & \chi_{1,4} & \chi_{1,5} \\ \chi_{2,1} & 0 & \chi_{2,3} & \chi_{2,4} & \chi_{2,5} \\ \chi_{3,1} & \chi_{3,2} & 0 & \chi_{3,4} & \chi_{3,5} \\ \chi_{4,1} & \chi_{4,2} & \chi_{4,3} & 0 & \chi_{4,5} \\ \chi_{5,1} & \chi_{5,2} & \chi_{5,3} & \chi_{5,4} & 0 \end{pmatrix},$$

If $\chi_{ij}$ is large, it means that $i$ and $j$ are close neighbours; while if $\chi_{ij}$ is small, it means that $i$ and $j$ distant from each other, or otherwise difficult to reach.

First one dimensional configurations were tested. The linear spatial configurations are illustrated in figures 11.3, 11.4 and 11.5. Note that the colours used in these figures correspond to the colour coding used in the results outlined in chapter 12 and 14, so the population size of each site will be tracked in the colour of the site used in figures 11.3, 11.4 and 11.5. In the first figure, figure 11.3, the connectivity between the sites is the same throughout, i.e. the probability that one rabbit moves from one site to another is the same whichever site it is in. The end sites are connected only to one neighbouring site. In figure 11.4 the connectivity increases going from site 1 to site 5. The length of the arrows indicate the connectivity in such way that a longer arrow means that the two sites are weakly connected, while as the arrows become shorter, the connectivity between the sites

becomes stronger ($\chi_{i,i+1}$ increases). Figure 11.5 shows decreasing connectivity going from site 1 to site 5.

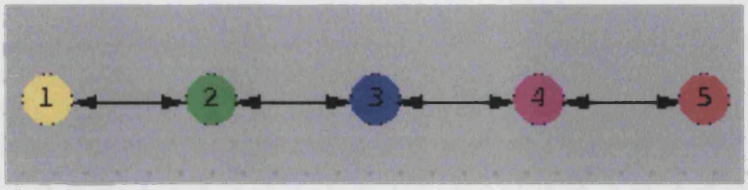


Figure 11.3: Linear spatial configuration: Constant connectivity between all the sites.

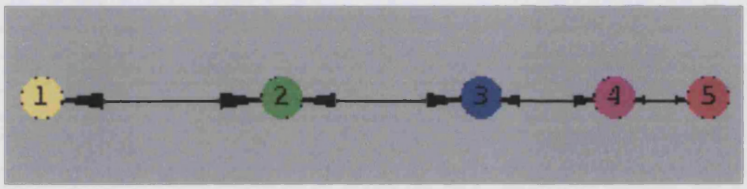


Figure 11.4: Linear spatial configuration: Increasing connectivity from site 1 to site 5.

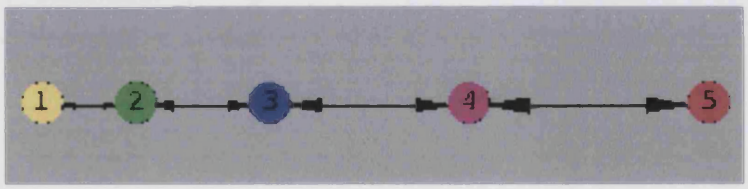


Figure 11.5: Linear spatial configuration: Decreasing connectivity from site 1 to site 5.

It is assumed that a rabbit from any site can only go to a neighbouring site and that each site has one or two neighbours. The connectivity matrix for the linear spatial configuration in figures 11.3, 11.4 and 11.5 has the form:

$$\begin{pmatrix} 0 & \chi_{1,2} & 0 & 0 & 0 \\ \chi_{2,1} & 0 & \chi_{2,3} & 0 & 0 \\ 0 & \chi_{3,2} & 0 & \chi_{3,4} & 0 \\ 0 & 0 & \chi_{4,3} & 0 & \chi_{4,5} \\ 0 & 0 & 0 & \chi_{5,4} & 0 \end{pmatrix}$$

where in the constant connectivity case (figure 11.3), $\chi_{ij} = \chi$ is independent of $i$ and $j$. In the

increasing connectivity case $\chi_{i,i+1}$ increases as $i$ increases, and in the decreasing connectivity case it decreases.

The simplicity with which the connectivity matrix allows the manipulation of spatial configurations permits experimentation with a wide range of complex configurations. In this research we consider two simple two-dimensional spatial configurations, illustrated in figures 11.6 and 11.7.

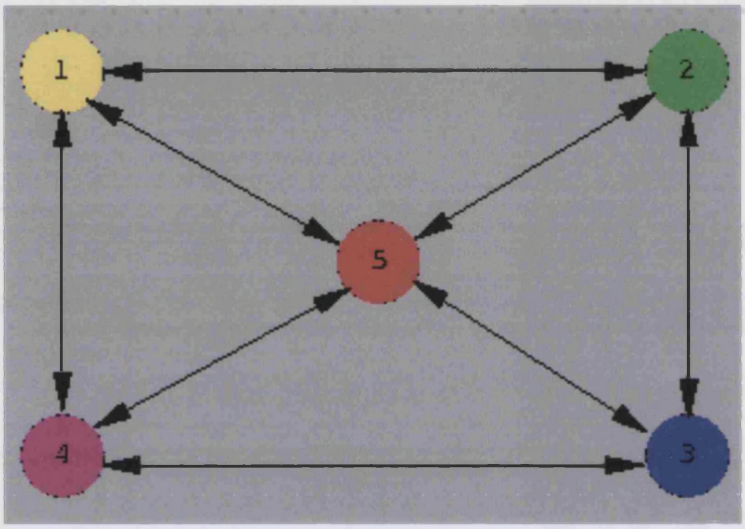


Figure 11.6: 2-Dimensional spatial configuration: constant connectivity.

In the two dimensional cases we consider it is assumed that a rabbit emigrating from any site can only reach a neighbouring site (in one day). The connectivity matrix for the 2-dimensional spatial configuration in figure 11.6 is:

$$\begin{pmatrix} 0 & \chi_{1,2} & 0 & \chi_{1,4} & \chi_{1,5} \\ \chi_{2,1} & 0 & \chi_{2,3} & 0 & \chi_{2,5} \\ 0 & \chi_{3,2} & 0 & \chi_{3,4} & \chi_{3,5} \\ \chi_{4,1} & 0 & \chi_{4,3} & 0 & \chi_{4,5} \\ \chi_{5,1} & \chi_{5,2} & \chi_{5,3} & \chi_{5,4} & 0 \end{pmatrix}$$

Figure 11.7 shows a non-symmetric spatial configuration which involves 7 sites, with sites 3 and 6 connected to 3 neighbouring sites and the others connected to only one or two sites. The connectivity matrix is therefore 7-dimensional of the following form:

$$\begin{pmatrix} 0 & \chi_{1,2} & 0 & 0 & 0 & 0 & 0 \\ \chi_{2,1} & 0 & \chi_{2,3} & 0 & 0 & 0 & 0 \\ 0 & \chi_{3,2} & 0 & \chi_{3,4} & 0 & \chi_{3,6} & 0 \\ 0 & 0 & \chi_{4,3} & 0 & 0 & 0 & 0 \\ 0 & 0 & 0 & 0 & 0 & \chi_{5,6} & 0 \\ 0 & 0 & \chi_{6,3} & 0 & \chi_{6,5} & 0 & \chi_{6,7} \\ 0 & 0 & 0 & 0 & 0 & \chi_{7,6} & 0 \end{pmatrix}$$

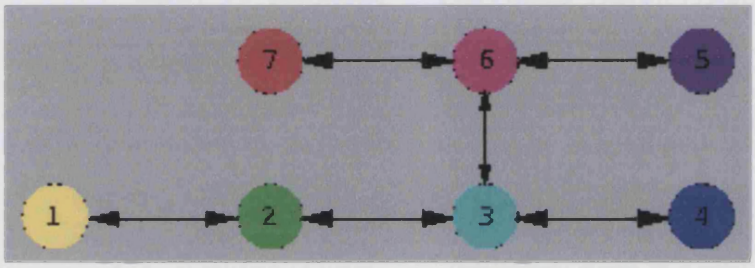


Figure 11.7: 2-Dimensional asymmetric spatial configuration.

## 11.3 Varying the threshold capacity $\hat{k}$

Another important aspect of this spatial model is that it allows for the variation of the threshold capacity of each site, i.e. the population size that a site can sustain. Over the threshold capacity value, density dependent mechanisms will be activated. In our model the Juvenile death rate is increased in response to a high population density exceeding the threshold capacity (see section 4.3). Thus the environment can also be made heterogeneous by choosing different threshold capacities for different sites. Biologically this means that some areas (sites) are more favourable for rabbits and can sustain a larger population while others are less favourable. An investigation into the source-sink concept can be carried out, together with spatial Hide-and-Seek of the disease in the interaction between different sites. Some possible spatial variations of the threshold capacity of the sites are shown in figures 11.8 and 11.9. Here, the size of the sites indicates which ones have a bigger threshold capacity and hence a higher carrying capacity. The colour coding is the same as will be used to present the results in chapters 13 and 15.

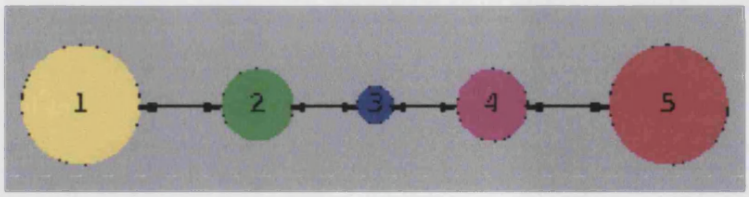


Figure 11.8: Linear heterogeneous spatial configuration: favourable borders. End sites have high capacity, declining through sites 2 and 4 to a very low capacity central site: site 3.

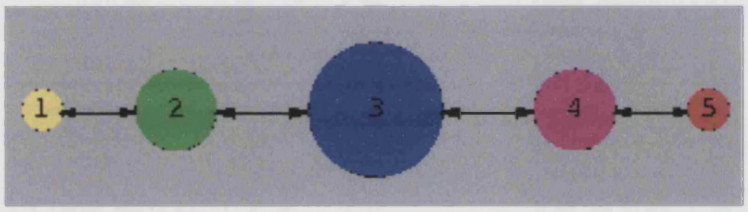


Figure 11.9: Linear heterogeneous spatial configuration: non-favourable borders. The reverse of the figure 11.8 configuration.

Figures 11.8 and 11.9 relate to the linear model (figures 11.3, 11.4 and 11.5) while figures 11.10 and 11.11 show the 2-dimensional spatial configurations of figure 11.6 with varying threshold capacity for the different sites. The configuration in figure 11.10 represents an environment with marginal borders (smaller threshold capacity) around a central favourable area, while figure 11.11 represents a non-favourable patch surrounded by four more suitable sites. For the configuration outlined in figure 11.7, four distinct cases where analysed: (i) both connectivity and threshold capacity where kept constant, (ii) the threshold capacity was kept constant while the connectivity was varied randomly, (iii) the connectivity was kept constant while the threshold capacity was varied randomly and (iv) both connectivity and threshold capacity where varied randomly.

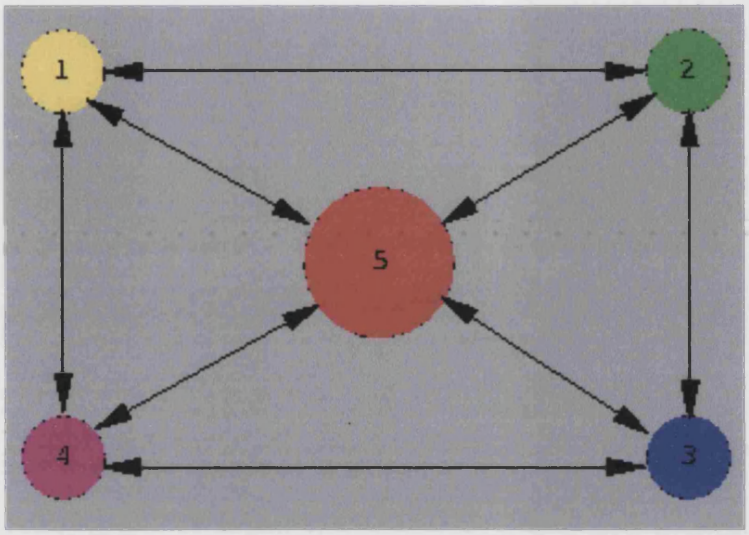


Figure 11.10: 2-Dimensional spatial configuration: varying $\hat{k}$. Unfavourable borders, favourable centre.

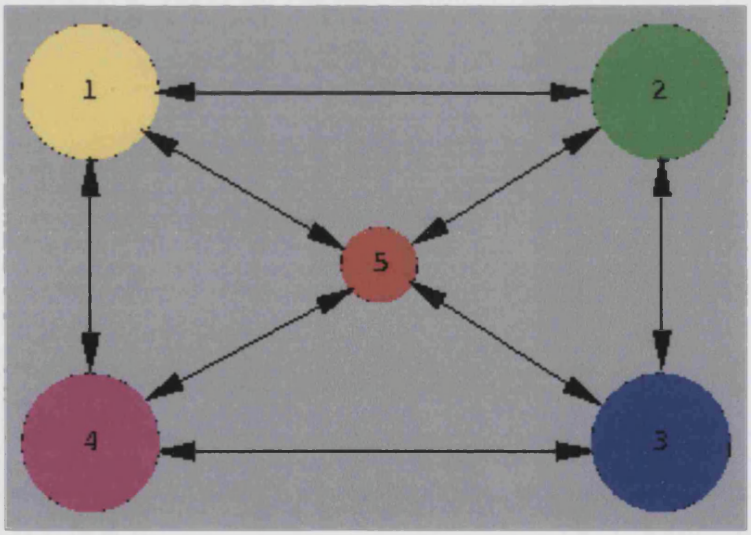


Figure 11.11: 2-Dimensional spatial configuration: varying $\hat{k}$. Favourable borders, unfavourable centre.

## 11.4 Appendix: The General Model

### 11.4.1 Resident population (site $x$)

$$
\begin{aligned}
S_J[t+1,0,x] &= \lambda(1-m_A)(S_P[t,n_P,x]+R_P[t,n_P,x];\\
S_J[t+1,k,x] &= (1-\epsilon_J[k-1]\sigma[t])(1-m_J)(1-c_V)S_J[t,k-1,x]+\\
&\quad \alpha M_{S_J}[t,k-1,x]; && (1\le k\le n_J)\\
I_J[t+1,1,x] &= 0;\\
I_J[t+1,k,x] &= (1-\epsilon_J[k-1]\sigma[t])(1-m_J)(c_V S_J[t,k-1,x]+(1-\nu_J)I_J[t,k-1,x])+\\
&\quad \alpha M_{I_J}[t,k-1,x]; && (2\le k\le n_J)\\
R_J[t+1,1,x] &= 0;\\
R_J[t+1,k,x] &= (1-\epsilon_J[k-1]\sigma[t])(1-m_J)(\nu_J I_J[t,k-1,x]+R_J[t,k-1,x])+\\
&\quad \alpha M_{R_J}[t,k-1,x]; && (2\le k\le n_J)\\
S_Y[t+1,1,x] &= (1-\epsilon_J[n_J]\sigma[t])(1-m_J)(1-c_V)S_J[t,n_J,x];\\
S_Y[t+1,k,x] &= (1-\epsilon_Y[k-1]\sigma[t])(1-m_Y)(1-c_V)S_Y[t,k-1,x]+\\
&\quad \alpha M_{S_Y}[t,k-1,x]; && (2\le k\le n_Y)\\
I_Y[t+1,1,x] &= (1-\epsilon_Y[n_J]\sigma[t])(1-m_J)(c_V S_J[t,n_J,x]+(1-\nu_J)I_J[t,n_J,x]);\\
I_Y[t+1,k,x] &= (1-\epsilon_Y[k-1]\sigma[t])(1-m_Y)(c_V S_Y[t,k-1,x]+(1-CM-\nu_J)I_Y[t,k-1,x]+\\
&\quad \alpha M_{I_Y}[t,k-1,x]; && (2\le k\le n_Y)\\
R_Y[t+1,1,x] &= (1-\epsilon_J[n_J]\sigma[t])(1-m_J)(\nu_J I_J[t,n_J,x]+R_J[t,n_J,x]);\\
R_Y[t+1,k,x] &= (1-\epsilon_Y[k-1]\sigma[t])(1-m_Y)(\nu_Y I_Y[t,k-1,x]+R_Y[t,k-1,x])+\\
&\quad \alpha M_{R_Y}[t,k-1,x]; && (2\le k\le n_Y)\\
S_{A_M}[t+1,x] &= (1-\epsilon_A[t]\sigma[t])(1-m_A)(1-c_V)S_{A_M}[t,x]+\\
&\quad \tfrac{1}{2}(1-\epsilon_Y[n_Y]\sigma[t])(1-m_Y)(1-c_V)S_Y[t,n_Y,x]+\\
&\quad \alpha M_{S_{A_M}}[t,x];\\
I_{A_M}[t+1,x] &= (1-\epsilon_A[t]\sigma[t])(1-m_A)(c_V S_{A_M}[t,x]+(1-CM-\nu_A)I_{A_M}[t,x])+\\
&\quad \tfrac{1}{2}(1-\epsilon_Y[n_Y]\sigma[t])(1-m_Y)(c_V S_Y[t,n_Y,x]+(1-CM-\nu_Y)I_Y[t,n_Y,x])+\\
&\quad \alpha M_{I_{A_M}}[t,x];\\
R_{A_M}[t+1,x] &= (1-\epsilon_A[t]\sigma[t])(1-m_A)(\nu_A I_{A_M}[t,x]+R_{A_M}[t,x])+\\
&\quad \tfrac{1}{2}(1-\epsilon_Y[n_Y]\sigma[t])(1-m_Y)(\nu_Y I_Y[t,n_Y,x]+R_Y[t,n_Y,x])+\\
&\quad \alpha M_{R_{A_M}}[t,x];
\end{aligned}
$$

$$
\begin{aligned}
S_{A_F}[t+1,x] &= (1-m_A)(1-c_V)((1-\epsilon_A\sigma[t])(1-\pi)S_{A_F}[t,x]+S_P[t,n_P,x])+\\
&\quad \tfrac{1}{2}(1-\epsilon_Y[n_Y]\sigma[t])(1-m_Y)(1-c_V)S_Y[t,n_Y,x]+\\
&\quad \alpha M_{S_{A_F}}[t,x];\\
I_{A_F}[t+1,x] &= (1-m_A)((1-\epsilon_A\sigma[t])(1-CM-\nu_A)I_{A_F}[t,x]+\\
&\quad (1-\epsilon_A\sigma[t])c_V(1-\pi)S_{A_F}[t,x]+c_V S_P[t,n_P,x])+\\
&\quad \tfrac{1}{2}(1-\epsilon_Y[n_Y]\sigma[t])(1-m_Y)(c_V S_Y[t,n_Y,x]+(1-CM-\nu_Y)I_Y[t,n_Y,x])+\\
&\quad \alpha M_{I_{A_F}}[t,x];\\
R_{A_F}[t+1,x] &= (1-m_A)((1-\epsilon_A\sigma[t])(1-\pi)R_{A_F}[t,x]+(1-\epsilon_A\sigma[t])\nu_A I_{A_F}[t,x]+R_P[t,n_P,x])+\\
&\quad \tfrac{1}{2}(1-\epsilon_Y[n_Y]\sigma[t])(1-m_Y)(\nu_Y I_Y[t,n_Y,x]+R_Y[t,n_Y,x])+\\
&\quad \alpha M_{R_{A_F}}[t,x];\\
S_P[t+1,1,x] &= \pi(1-m_A)(1-c_V)S_{A_F}[t,x];\\
S_P[t+1,k,x] &= (1-m_A)(1-c_V)S_P[t,k-1,x]; \qquad (2\le k\le n_P)\\
R_P[t+1,1,x] &= \pi(1-m_A)R_{A_F}[t,x];\\
R_P[t+1,k,x] &= (1-m_A)R_P[t,k-1,x]; \qquad (2\le k\le n_P)\\
W[t+1,k,x] &= (1-m_V)W[t,x]+(I_J[t,k-1,x]+I_Y[t,k-1,x]+I_{A_M}[t,x]+I_{A_F}[t,x]);
\end{aligned}
$$

where $\epsilon_a[k]$, with $a = J, Y, A$, is the age dependent emigration probability for the three age classes considered ($A = A_M$ or $A_F$) (see section 5.1); $\sigma[t]$ is the seasonal emigration probability (see section 5.2); $\alpha$ is the acceptance probability; $M_{S_a,I_a,R_a}[t,x]$, with $a = J, Y, A_M, A_F$, are the immigrating population which has been accepted with probability $\alpha$ in site $x$. It is a new variable with respect to the emigration model (5.4). Note that the equations for the dynamics of the pregnant females does not include an emigration or immigration term, since they are assumed sedentary as explained at the beginning of this chapter.

### 11.4.2 Immigrant population

$$
\begin{aligned}
M_{S_J}[t+1,0,x] &= 0;\\
M_{S_J}[t+1,k,x] &= (1-h)(1-m_J)\textstyle\sum_j \chi_{j,x} E_{S_J}[t,k-1,j]; \qquad (1 \le k \le n_J)\\
M_{I_J}[t+1,0,x] &= 0;\\
M_{I_J}[t+1,k,x] &= (1-h)(1-m_J)(1-\nu_J)\textstyle\sum_j \chi_{j,x} E_{I_J}[t,k-1,j]; \qquad (1 \le k \le n_J)\\
M_{R_J}[t+1,0,x] &= 0;\\
M_{R_J}[t+1,k,x] &= (1-h)(1-m_J)\textstyle\sum_j \chi_{j,x}(\nu_J E_{I_J}[t,k-1,x] + E_{R_J}[t,k-1,j]);\\
&\qquad (1 \le k \le n_J)\\
M_{S_Y}[t+1,1,x] &= (1-h)(1-m_J)\textstyle\sum_j \chi_{j,x} E_{S_J}[t,n_J,j];\\
M_{S_Y}[t+1,k,x] &= (1-h)(1-m_Y)\textstyle\sum_j \chi_{j,x} E_{S_Y}[t,k-1,j]; \qquad (2 \le k \le n_Y)\\
M_{I_Y}[t+1,1,x] &= (1-h)(1-m_J)(1-\nu_J)\textstyle\sum_j \chi_{j,x} E_{I_J}[t,n_J,j];\\
M_{I_Y}[t+1,k,x] &= (1-h)(1-m_Y)(1-CM-\nu_Y)\textstyle\sum_j \chi_{j,x} E_{I_Y}[t,k-1,j];\\
&\qquad (2 \le k \le n_Y)\\
M_{R_Y}[t+1,1,x] &= (1-h)(1-m_J)\textstyle\sum_j \chi_{j,x}(\nu_J E_{I_J}[t,n_J,j] + E_{R_J}[t,n_J,j]);\\
M_{R_Y}[t+1,k,x] &= (1-h)(1-m_Y)\textstyle\sum_j \chi_{j,x}(\nu_Y E_{I_Y}[t,k-1,j] + E_{R_Y}[t,k-1,j]);\\
&\qquad (2 \le k \le n_Y)\\
M_{S_{A_M}}[t+1,x] &= (1-h)\textstyle\sum_j \chi_{j,x}(\frac{1}{2}(1-m_Y)E_{S_Y}[t,n_Y,j] + (1-m_A)E_{S_{A_M}}[t,j]);\\
M_{I_{A_M}}[t+1,x] &= (1-h)\textstyle\sum_j \chi_{j,x}(\frac{1}{2}(1-m_Y)(1-CM-\nu_Y)E_{I_Y}[t,n_Y,j]+\\
&\quad (1-m_A)(1-CM-\nu_A)E_{I_{A_M}}[t,j]);\\
M_{R_{A_M}}[t+1,x] &= (1-h)\textstyle\sum_j \chi_{j,x}(\frac{1}{2}(1-m_Y)(\nu_Y E_{I_Y}[t,n_Y,j] + E_{R_Y}[t,n_Y,j])+\\
&\quad (1-m_A)(\nu_A E_{I_{A_M}}[t,j] + E_{R_{A_M}}[t,j]));\\
M_{S_{A_F}}[t+1,x] &= (1-h)\textstyle\sum_j \chi_{j,x}(\frac{1}{2}(1-m_Y)E_{S_Y}[t,n_Y,j] + (1-m_A)E_{S_{A_F}}[t,j]);\\
M_{I_{A_F}}[t+1,x] &= (1-h)\textstyle\sum_j \chi_{j,x}(\frac{1}{2}(1-m_Y)(1-CM-\nu_Y)E_{I_Y}[t,n_Y,j]+\\
&\quad (1-m_A)(1-CM-\nu_A)E_{I_{A_F}}[t,j]);\\
M_{R_{A_F}}[t+1,x] &= (1-h)\textstyle\sum_j \chi_{j,x}(\frac{1}{2}(1-m_Y)(\nu_Y E_{I_Y}[t,n_Y,j] + E_{R_Y}[t,n_Y,j])+\\
&\quad (1-m_A)(\nu_A E_{I_{A_F}}[t,j] + E_{R_{A_F}}[t,j]));
\end{aligned}
$$

where $h$ is the hazard taken per day; $E_{S_a,I_a,R_a}[t,k,j]$, with $a = J, Y, A_M, A_F$, is the emigrating population of age $k$ from site $j$ which tries to immigrate into site $x$ and $\chi_{j,x}$ is the probability that a rabbit coming from a site $j$ will arrive at site $x$ (see section 11.2).

### 11.4.3 Emigrant population

$$
\begin{aligned}
E_{S_J}[t+1,0,x] &= \epsilon_J[0]\sigma[t](1-m_J)S_J[t,0,x];\\
E_{S_J}[t+1,k,x] &= (1-h)(1-m_J)(1-\zeta_x)E_{S_J}[t,k-1,x]+\\
&\quad \epsilon_J[k-1]\sigma[t](1-m_J)(1-c_V)S_J[t,k-1,x]+\bar{\alpha}M_{S_J}[t,k-1,x];\\
&\quad (1\le k\le n_J)\\
E_{I_J}[t+1,0,x] &= 0;\\
E_{I_J}[t+1,k,x] &= (1-h)(1-m_J)(1-\nu_J)(1-\zeta_x)E_{I_J}[t,k-1,x]+\\
&\quad \epsilon_J[k-1]\sigma[t](1-m_J)(c_V S_J[t,k,x]+(1-\nu_J)I_J[t,k,x])+\bar{\alpha}M_{I_J}[t,k-1,x];\\
&\quad (1\le k\le n_J)\\
E_{R_J}[t+1,0,x] &= 0;\\
E_{R_J}[t+1,k,x] &= (1-h)(1-m_J)(1-\zeta_x)(\nu_J E_{I_J}[t,k-1,x]+E_{R_J}[t,k-1,x])+\\
&\quad \epsilon_J[k-1]\sigma[t](1-m_J)(\nu_J I_J[t,k-1,x]+R_J[t,k-1,x])+\bar{\alpha}M_{R_J}[t,k-1,x];\\
&\quad (1\le k\le n_J)\\
E_{S_Y}[t+1,0,x] &= (1-h)(1-m_J)(1-\zeta_x)E_{S_J}[t,n_J,x]+\\
&\quad \epsilon_Y[k-1]\sigma[t](1-m_Y)(1-c_V)S_Y[t,k-1,x]; \qquad (1\le k\le n_Y)\\
E_{S_Y}[t+1,k,x] &= (1-h)(1-m_Y)(1-\zeta_x)E_{S_Y}[t,k-1,x]+\\
&\quad \epsilon_Y[k-1]\sigma[t](1-m_Y)(1-c_V)S_Y[t,k-1,x]+\bar{\alpha}M_{S_Y}[t,k-1,x];\\
&\quad (1\le k\le n_Y)\\
E_{I_Y}[t+1,0,x] &= (1-h)(1-m_J)(1-\nu_J)(1-\zeta_x)E_{I_J}[t,n_J,x]+\\
&\quad \epsilon_Y[k-1]\sigma[t](1-m_Y)(c_V S_Y[t,k-1,x]+(1-CM-\nu_Y)I_Y[t,k-1,x]);\\
&\quad (1\le k\le n_Y)\\
E_{I_Y}[t+1,k,x] &= (1-h)(1-m_Y)(1-CM-\nu_Y)(1-\zeta_x)E_{I_Y}[t+1,k-1,x]+\\
&\quad \epsilon_Y[k-1]\sigma[t](1-m_Y)(c_V S_Y[t,k-1,x]+(1-CM-\nu_Y)I_Y[t,k-1,x])+\\
&\quad \bar{\alpha}M_{I_Y}[t,k-1,x]; \qquad (1\le k\le n_Y)\\
E_{R_Y}[t+1,0,x] &= (1-h)(1-m_J)(1-\zeta_x)(\nu_J E_{I_J}[t,n_J,x]+E_{R_J}[t,n_J,x])+\\
&\quad \epsilon_Y[k-1]\sigma[t](1-m_Y)(R_Y[t,k-1,x]+\nu_Y I_Y[t,k-1,x]); \qquad (1\le k\le n_Y)\\
E_{R_Y}[t+1,k,x] &= (1-h)(1-m_Y)(1-\zeta_x)(\nu_Y E_{I_Y}[t,k-1,x]+E_{R_Y}[t,k-1,x])+\\
&\quad \epsilon_Y[k-1]\sigma[t](1-m_Y)(R_Y[t,k-1,x]+\nu_Y I_Y[t,k-1,x])+\bar{\alpha}M_{R_Y}[t,k-1,x];\\
&\quad (1\le k\le n_Y)
\end{aligned}
$$

$$
\begin{aligned}
E_{S_{A_M}}[t+1,x] &= (1-h)(1-\zeta_x)((1-m_A)E_{S_{A_M}}[t,x] + \tfrac{1}{2}(1-m_Y)E_{S_Y}[t,n_Y,x])+ \\
&\quad \epsilon_A[k-1]\sigma[t](1-m_A)(1-c_V)S_{A_M}[t,x] + \bar{\alpha}M_{S_{A_M}}[t,x]; \\
E_{I_{A_M}}[t+1,x] &= (1-h)(1-\zeta_x)((1-CM-\nu_A)(1-m_A)E_{I_{A_M}}[t,x]+ \\
&\quad \tfrac{1}{2}(1-CM-\nu_Y)(1-m_Y)E_{I_Y}[t,n_Y,x])+ \\
&\quad \epsilon_A[k-1]\sigma[t](1-m_A)c_V S_{A_M}[t,x] + \bar{\alpha}M_{I_{A_M}}[t,x]; \\
E_{R_{A_M}}[t+1,x] &= (1-h)(1-\zeta_x)(\nu_A(1-m_A)E_{I_{A_M}}[t,x] + \tfrac{1}{2}\nu_Y(1-m_Y)E_{I_Y}[t,n_Y,x])+ \\
&\quad \epsilon_A[k-1]\sigma[t](1-m_A)(\nu_A I_{A_M}[t,x] + R_{A_M}[t,x]) + \bar{\alpha}M_{R_{A_M}}[t,x]; \\
E_{S_{A_F}}[t+1,x] &= (1-h)(1-\zeta_x)((1-m_A)E_{S_{A_F}}[t,x] + \tfrac{1}{2}(1-m_Y)E_{S_Y}[t,n_Y,x])+ \\
&\quad \epsilon_A[k-1]\sigma[t](1-m_A)(1-c_V)S_{A_F}[t,x] + \bar{\alpha}M_{S_{A_F}}[t,x]; \\
E_{I_{A_F}}[t+1,x] &= (1-h)(1-\zeta_x)((1-CM-\nu_A)(1-m_A)E_{I_{A_F}}[t,x]+ \\
&\quad \tfrac{1}{2}(1-CM-\nu_Y)(1-m_Y)E_{I_Y}[t,n_Y,x])+ \\
&\quad \epsilon_A[k-1]\sigma[t](1-m_A)c_V(1-\pi)S_{A_F}[t,x] + \bar{\alpha}M_{I_{A_F}}[t,x]; \\
E_{R_{A_F}}[t+1,x] &= (1-h)(1-\zeta_x)(\nu_A(1-m_A)E_{I_{A_F}}[t,x] + \tfrac{1}{2}\nu_Y(1-m_Y)E_{I_Y}[t,n_Y,x])+ \\
&\quad (1-h)(1-\textstyle\sum_x \zeta_{j,x})((1-m_A)E_{R_{A_F}}[t,x] + \tfrac{1}{2}(1-m_Y)E_{R_Y}[t,n_Y,x])+ \\
&\quad \epsilon_A[k-1]\sigma[t](1-m_A)(\nu_A I_{A_F}[t,x] + (1-\pi)R_{A_F}[t,x]) + \bar{\alpha}M_{R_{A_F}}[t,x];
\end{aligned}
$$

where $\zeta_x = \sum_j \chi_{x,j}$ is the probability that a rabbit emigrating from site $x$ will end up somewhere. Hence $1-\zeta_x$ is the probability that a rabbit emigrating from site $x$ will not have arrived at any other site on a given day.

# Chapter 12

# Results: 1-Dimensional Spatial Model (the Strong Hypothesis)

The colour coding of the figures in this chapter is the same throughout, where site 1 is represented by yellow, site 2 is represented by green, site 3 is represented by blue, site 4 is represented by magenta and site 5 is represented by red. If more than one site has the same population dynamics, the graph might have only one colour to represent more than one site (the dominant colour, like red, for example.) See figures 11.3, 11.4, 11.5, 11.8 and 11.9 for the associated spatial configurations. The disease is always introduced into site 1 after 5 years, at the beginning of the year, by adding a small amount of virus into the environment. All the figures report the average annual population size versus time (in years).

## 12.1 Varying the connectivity value without the disease.

For the constant connectivity case, several values of the connectivity where tested, namely $\chi_{i,j} = 0.001, 0.005, 0.01, 0.05, 0.1, 0.5$. These were chosen because the model outcome seemed to be more sensitive to this range of values. Outside this range the system behaves like single sites totally unconnected with each other. In fact it will be observed later that in general the system is not very sensitive to the connectivity value especially when there is no disease present or the disease is not effective. In the case where no disease is present, each site rapidly behaves as a single site (see figure 12.1) and the model outcome is the same for all values of the connectivity range considered.

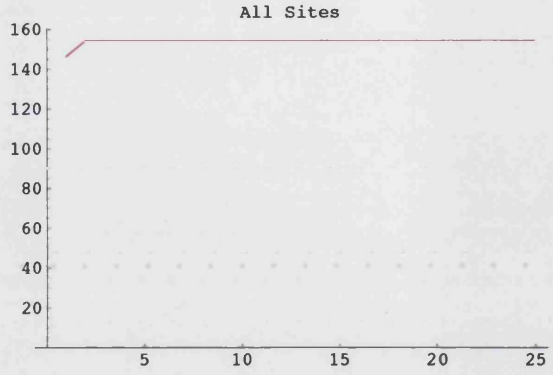


Figure 12.1: Linear homogeneous configuration: $\hat{k} = 100$, $\chi_{i,j} = 0.001, 0.005, 0.01, 0.05, 0.1, 0.5$.

## 12.2 Varying the connectivity value with the disease.

The values of the connectivity, $\chi_{i,j} = 0.001, 0.005, 0.01, 0.05, 0.1, 0.5$, were tested with the disease present. An intermediate value of the virulence of the disease, namely $b = 2000$, and constant threshold $\hat{k} = 100$, were chosen to investigate the effect of varying the connectivity on disease invasion. The results are shown in figures 12.2-12.5. It can be observed that the system is not remarkably sensitive to a change in connectivity, but it should be noticed that varying the connectivity changes on which site the disease is mostly effective, for example for $\chi_{i,j} = 0.001$ the disease has a bigger impact on site 3 (figure 12.2), for $\chi_{i,j} = 0.005$ and for $\chi_{i,j} = 0.01$ (figures 12.3) site 4 is mostly affected while site 5 is least affected; for $\chi_{i,j} = 0.05$ (figures 12.4) and for $\chi_{i,j} = 0.1$ site 5 has its population size lowered more comparing to the others. The case in which $\chi_{i,j} = 0.5$ (figure 12.5) has a more uniform outcome for all the sites: the spatial configuration and the connectivity have a small influence on the model outcome, i.e the sites behave each similarly to an unconnected single site. As a consequence to these observation only one value for the connectivity, namely $\chi_{i,j} = 0.01$, was chosen when testing a system with a constant connectivity between the sites. This value was chosen since it is the value, in the considered range, for which the system seems most sensitive (figure 12.3).

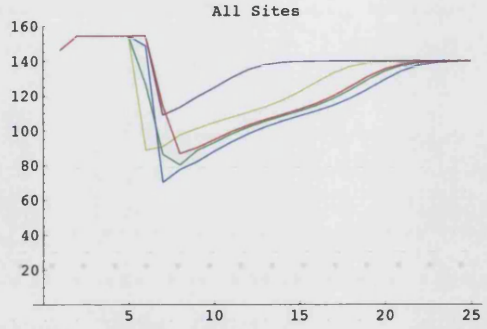


Figure 12.2: Linear homogeneous configuration (figure 11.3): $\chi_{i,j} = 0.001$, $b = 2000$. Site 4 (magenta) is the least affected and site 3 (blue) is the most affected.

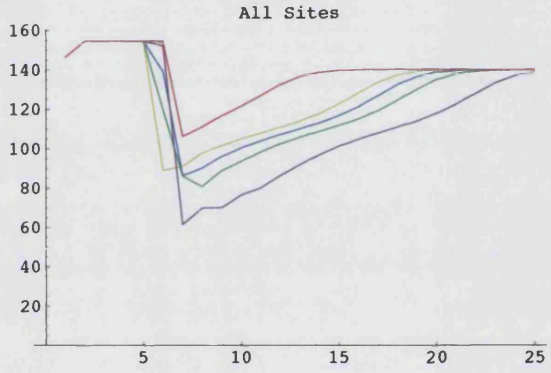


Figure 12.3: Linear homogeneous configuration (figure 11.3): $\chi_{i,j} = 0.01$, $b = 2000$. Site 4 (magenta) is the most affected and site 5 (red) is the least affected.

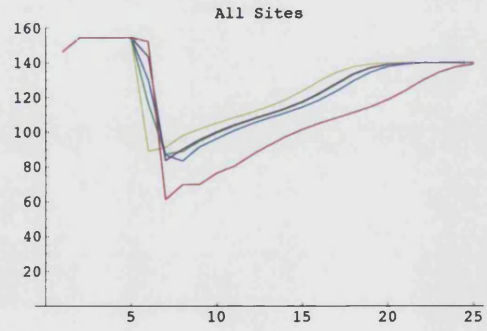


Figure 12.4: Linear homogeneous configuration (figure 11.3): $\chi_{i,j} = 0.05$, $b = 2000$. Site 5 (red) is the most affected.

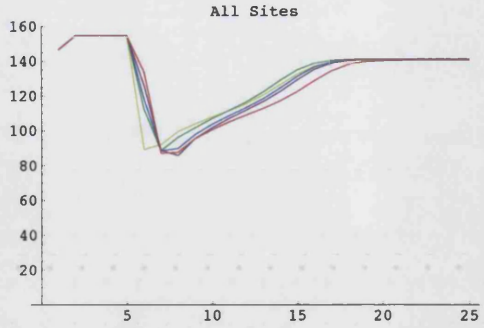


Figure 12.5: Linear homogeneous configuration (figure 11.3): $\chi_{i,j} = 0.5$, $b = 2000$. Similar effect on all the sites.

## 12.3 Non-stochastic constant connectivity with the disease.

Figures 12.6-12.8 illustrate the model results using constant connectivity (spatial configuration in figure 11.3), $\chi_{i,j} = 0.01$, constant threshold capacity, $\hat{k}$, and three different values of the disease parameter $b$, namely $b = 4000, 2000, 1000$: the single site model results indicate that these values of $b$ make the disease more effective and so are more interesting cases to investigate (see figures 7.15-7.17 and 8.11-8.12, where the non-stochastic case is the heavy-dotted line). It is possible to see that for $b = 4000$ (figure 12.6) the population of each site goes into a two year cycle, not in phase for some of the sites, especially for the first 7 years after the appearance of the disease. This happened for $b = 5000$ in the single site model. $b = 2000$ (figure 12.7) is very much like the single site case (see figures 7.15 and 8.12); while it is interesting how in the $b = 1000$ case (figure 12.8), the disease has a very strong effect on site 1, very different from the trends observed in the single site model results. The recovery time for the population on site 1 is much longer compared to the other sites.

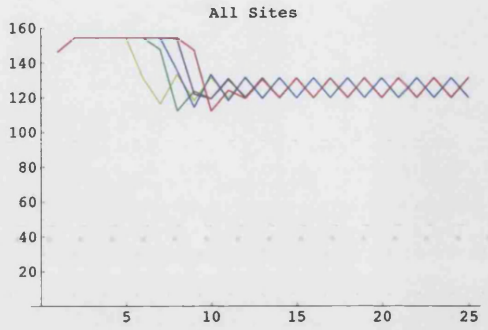


Figure 12.6: Linear homogeneous configuration: $\chi_{i,j} = 0.01$, $b = 4000$ .

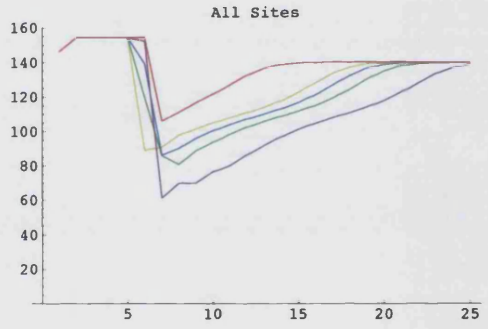


Figure 12.7: Linear homogeneous configuration: $\chi_{i,j} = 0.01$, $b = 2000$ .

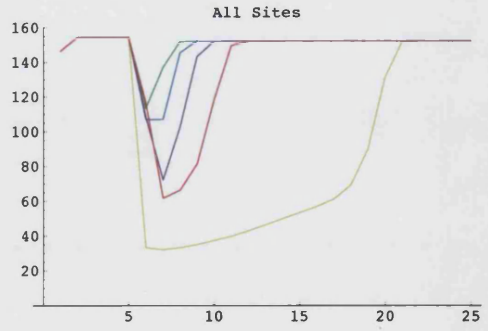


Figure 12.8: Linear homogeneous configuration: $\chi_{i,j} = 0.01$, $b = 1000$ .

## 12.4 Varying the connectivity (non-stochastic case).

Subsequently the connectivity between the sites was increased from site 1 going to site 5 (figure 11.4), i.e. sites 1 and 2 are more weakly connected than sites 4 and 5, namely $\chi_{1,2} = 0.005$, $\chi_{2,3} = 0.01$, $\chi_{3,4} = 0.05$, $\chi_{4,5} = 0.1$. The model results for such a non-homogeneous linear space configuration yielded results identical to the constant connectivity case. This seems to reinforce the fact that the system is not very sensitive to the connectivity value.

In the case of a decreasing connectivity between the sites (figure 11.5), the results show again a low sensitivity to the connectivity. A very similar outcome to the constant connectivity case was observed; for the $b = 2000$ case the site dynamics comes the closest to the single site model. The connectivity values chosen were the following: $\chi_{1,2} = 0.1$, $\chi_{2,3} = 0.05$, $\chi_{3,4} = 0.01$, $\chi_{4,5} = 0.05$

## 12.5 Non-stochastic increasing $\hat{k}$.

The figures in this and the next sections will show the model results obtained by varying the threshold capacity (and hence the carrying capacity) of the sites while keeping a constant connectivity between them, namely $\chi_{i,j} = 0.01$, for all $i, j$. It will be seen that varying the threshold capacity $\hat{k}$, makes a bigger difference from the single site model than varying the connectivity.

The linear configuration is shown in figure 11.3, but the threshold capacity is not the same for all the sites. The first case of $\hat{k}$ variation consists in an increase in $\hat{k}$ from the first site, where the disease is inserted, to the last one; namely, $\hat{k}_1 = 10$, $\hat{k}_2 = 50$, $\hat{k}_3 = 100$, $\hat{k}_4 = 100$ and $\hat{k}_5 = 500$, where $\hat{k}_s$ with $s = 1, 2, 3, 4, 5$ is the threshold capacity of site $s$. The results are illustrated in figures 12.9-12.11. It can be observed that for the non-disease case (figure 12.9), each site still behaves as a single site, as if unconnected; site 3 is hidden under site 4 in the graph as both sites have the same threshold capacity. When the disease is inserted, the $b = 4000$ case (figure 12.10) proves to be the most effective for site 5, which has the highest threshold capacity, but the population recovers completely $5 - 6$ years after disease appearance. Sites 3 and 4, whose populations go through 2-yearly cycles, never reach pre-disease size for the whole run. Sites 1 and 2 are not noticibly affected by the disease. For the cases $b = 2000$ (figure 12.11) and $b = 1000$ (not shown), the disease is less effective on sites 3, 4 and 5, whose population eventually recovers, compared to the $b = 4000$ case, and still not effective at all on sites 1 and 2 which seem not to have a big enough population to

sustain the disease, and just transmit it to more populated sites. It is interesting to notice that in any disease case site 1 is not affected at all by the disease, even though that is where the disease is inserted. It confirms that a high population density is needed for the disease to be effective.

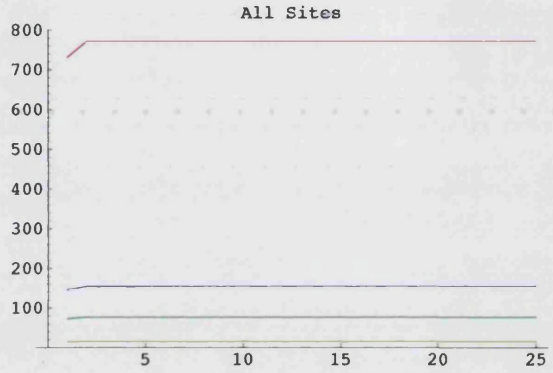


Figure 12.9: Linear configuration (increasing $\hat{k}$): $\chi_{i,j} = 0.01$, no disease .

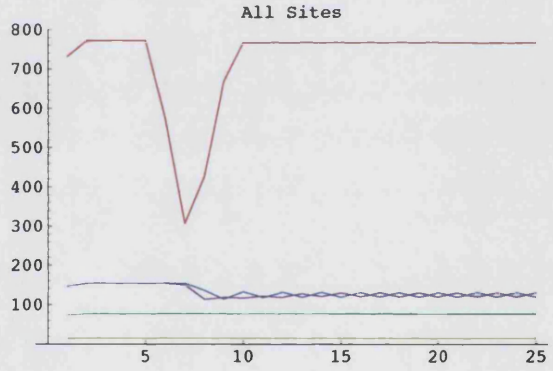


Figure 12.10: Linear configuration (increasing $\hat{k}$): $\chi_{i,j} = 0.01$, $b = 4000$ .

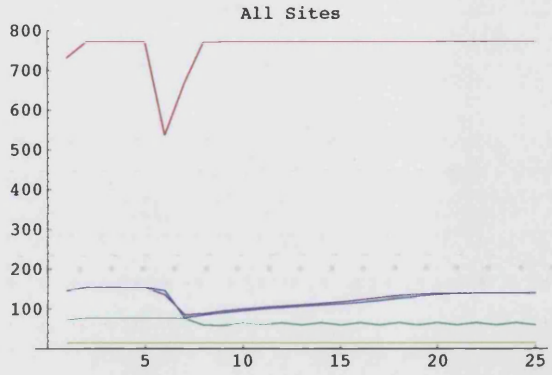


Figure 12.11: Linear configuration (increasing $\hat{k}$): $\chi_{i,j} = 0.01$, $b = 2000$.

## 12.6 Non-stochastic decreasing $\hat{k}$.

A very interesting result came from decreasing the threshold capacity between the sites, starting with site 1 being very favourable and decreasing $\hat{k}$ from site 1 to site 5, namely, $\hat{k}_1 = 500$, $\hat{k}_2 = 100$, $\hat{k}_3 = 100$, $\hat{k}_4 = 50$ and $\hat{k}_5 = 10$. The non-disease case (figure 12.12) is the same as for the single site model and no type of spatial configuration seems to make a difference compared to the non-spatial case. When the disease is inserted, site 1, having the highest threshold capacity, is very strongly affected by the disease, especially in the $b = 4000$ case (figure 12.13), while the other sites with lower threshold capacities have a more similar behavior to what we have observed in the various connectivity cases and the single site. A similar scenario is observed for $b = 2000$ (figure 12.14), but in this case site 4 is affected as well and site 2 and 3 do not have yearly cycles in disease outburst as observed for $b = 4000$ (figure 12.13). When $b = 1000$ (not shown) the disease is less successful in keeping the population size down compared to $b = 4000$ and $b = 2000$; in the single site model results we observed this case to be more effective, especially when compared to the $b = 4000$ case. Varying $\hat{k}$ enhances the power of the disease for the highest carrying capacities site ($\hat{k} = 500$ for site 1) especially for the highest $b$ considered ($b = 4000$).

Overall, inserting the disease at site 1, a decreasing $\hat{k}$ from site 1 to site 5 is more favourable for the disease success than an increasing $\hat{k}$, as described in section 12.5 because of high persistence in the very favourable site 1.

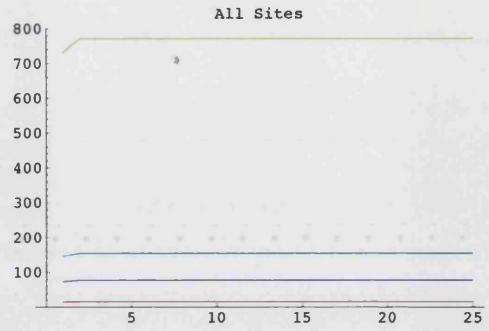


Figure 12.12: Linear configuration (decreasing $\hat{k}$): $\chi_{i,j} = 0.01$, no disease .

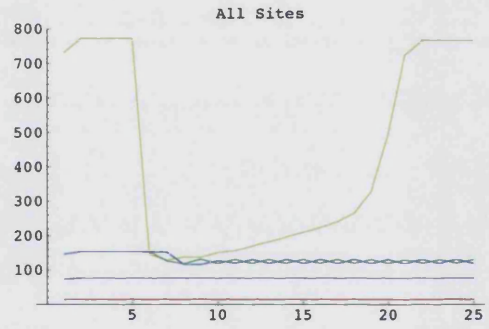


Figure 12.13: Linear configuration (decreasing $\hat{k}$): $\chi_{i,j} = 0.01$, $b = 4000$ .

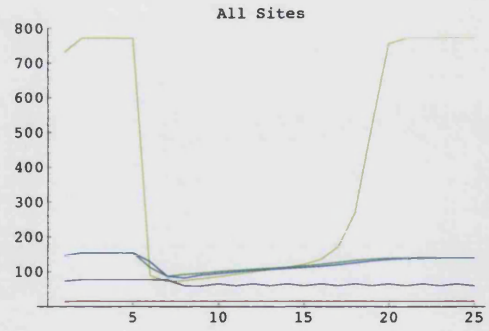


Figure 12.14: Linear configuration (decreasing $\hat{k}$): $\chi_{i,j} = 0.01$, $b = 2000$ .

## 12.7 Non-stochastic favourable borders.

Figures 12.15 and 12.16 illustrate the model result using the linear configuration with the border sites with higher threshold capacity with respect to the middle sites (see figure 11.8), namely $\hat{k}_1 = 500$, $\hat{k}_2 = 100$, $\hat{k}_3 = 10$, $\hat{k}_4 = 100$ and $\hat{k}_5 = 500$. It can be observed that the result is a superimposition of the results obtained from running the model with increasing and decreasing $\hat{k}$ (sections 12.5 and 12.6). The border sites, with $\hat{k} = 500$ are more affected than the middle sites, especially site 1 where the disease has been inserted. $b = 4000$ (figure 12.16) is the most effective disease strain (see figures 12.10 and 12.13 for comparison); while the non-disease case (figure 12.15) makes no difference from the single site model run with no disease. For $b = 2000$ and $b = 1000$ (both not shown), site 1 is till very affected but in site 5 the population starts to recover faster.

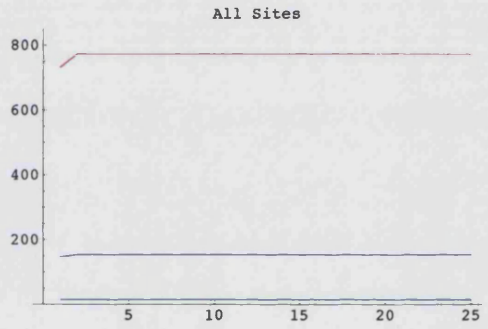


Figure 12.15: Linear configuration (favourable borders): $\chi_{i,j} = 0.01$, no disease .

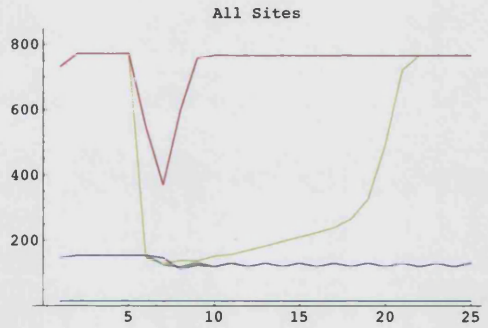


Figure 12.16: Linear configuration (favourable borders): $\chi_{i,j} = 0.01$, $b = 4000$ .

## 12.8 Non-stochastic non-favourable borders.

A linear configuration with non-favourable borders is one for which the middle site has the highest threshold capacity while the border ones can only sustain a very small population size (see figure 11.9), i.e. $\hat{k}_1 = 10$, $\hat{k}_2 = 100$, $\hat{k}_3 = 500$, $\hat{k}_4 = 100$ and $\hat{k}_5 = 10$. In this situation the middle site is more affected by the disease compared to the border ones. In fact the border sites are not noticibly affected by the disease for any $b$, even though the disease is inserted in site 1 which is a border site. Site 2 and site 4 are perfectly in phase (magenta line in the graph), even when the disease appears with 2-yearly cycles, as in the $b = 4000$ case. The disease is not as effective as in the favourable borders case (section 12.7). $b = 1000$ (figure 12.18) seems to be the disease parameter value that characterizes the most effective strain in affecting the population size (especially site 3).

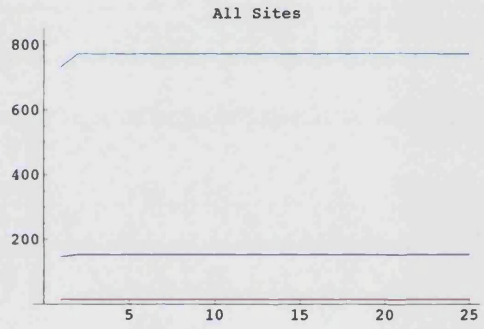


Figure 12.17: Linear configuration (non-favourable borders): $\chi_{i,j} = 0.01$, no disease .

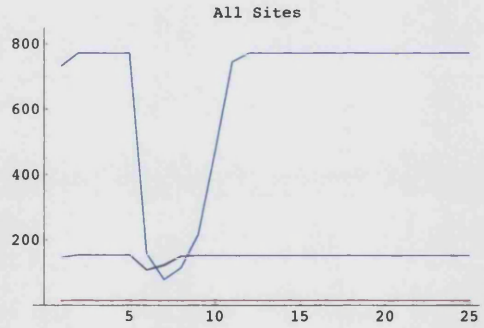


Figure 12.18: Linear configuration: $\chi_{i,j} = 0.01$, $b = 1000$ .

## 12.9 Stochastic Constant connectivity.

For the stochastic cases which follow, only one frequency for the stochastic change was selected for the model runs, namely $f = \frac{2}{365}$. A climatic change taking place twice a year seemed the most realistic for Australia's geographical position. Two variances for the Lognormal distribution were selected, namely $var = 1$ and $var = 10$ since $var = 0.1$ seemed to be not so interesting enough when the single site model was run. All the data points in the graphs represent annual averages, averaged in turn over three independent runs.

Figures 12.19-12.24 show the results from running the linear spatial model (figure 11.3) with stochastic variation, constant connectivity and constant threshold capacity. If we compare figure 12.19 with figure 6.7(b) for the stochastic single site model without the disease, taking into consideration the population dynamics for $var = 1$ (green-dotted line in figure 6.7(b)), we notice that the results, with running the single site model and the spatial model without the disease and with stochastic variation, are very similar. The spatial homogeneous model results behave very much like a single site, both with and without stochastic variation. More interesting is that the annual averages of the population size are totally in phase for all the sites, that is why only one colour appears, red, which is the dominant colour (the last colour plotted). When the variance was changed ($var = 10$) the result did not make much difference in the non-disease case. The first slight change appears for $b = 4000$, $var = 1$ (figure 12.20) where the sites behave perfectly in phase until about 16 years after the disease has been inserted. Site 1 population declines a bit with respect to the other sites, but towards the end of the run it goes back in phase with the rest of the sites. This phenomenon is not explained with the presence of the disease since for the $b = 4000$, $var = 10$ case (figure 12.21) all the sites behave exactly in phase again. In fact if we compare figures 12.20-12.21 with figure 12.19, we notice that the disease has hardly any effect and it is more the stochastic variation that controls the population. This also happened in the single site case (section 8.3). When $b = 2000$ (figures 12.22-12.23), for both $var = 1$ and $var = 10$, the disease has little effect but it seems more to cause the dynamics of the sites to go out of phase. After the disease is inserted the population in site 1 becomes lower. The population in site 5 remains the highest and is in phase with the rest after about 7 years from disease appearance. If we compare the $b = 1000$, $var = 10$ case (figure 12.24) with figure 12.21, we see that a more virulent disease is not more successful in controlling the population size.

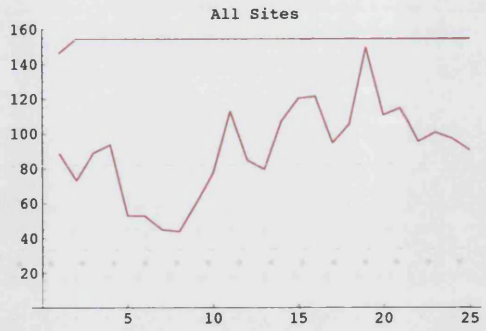


Figure 12.19: Linear homogeneous configuration: no disease, $var = 1$, $freq = \frac{2}{365}$, $\chi_{i,j} = 0.01$ and $\hat{k} = 100$. Straight line refers to the non-stochastic non-disease case.

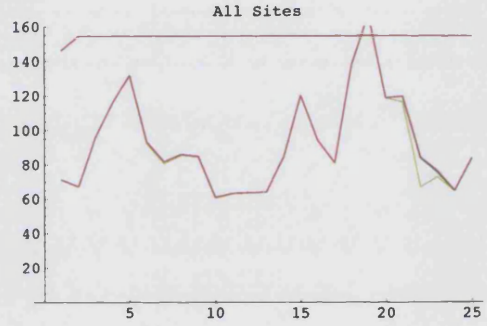


Figure 12.20: Linear homogeneous configuration: $b = 4000$, $var = 1$, $freq = \frac{2}{365}$, $\chi_{i,j} = 0.01$ and $\hat{k} = 100$. Straight line refers to the non-stochastic non-disease case.

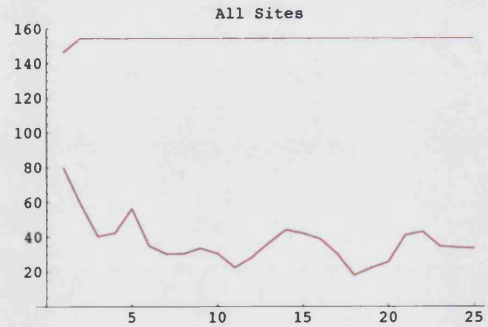


Figure 12.21: Linear homogeneous configuration: $b = 4000$, $var = 10$, $freq = \frac{2}{365}$, $\chi_{i,j} = 0.01$ and $\hat{k} = 100$. Straight line refers to the non-stochastic non-disease case.

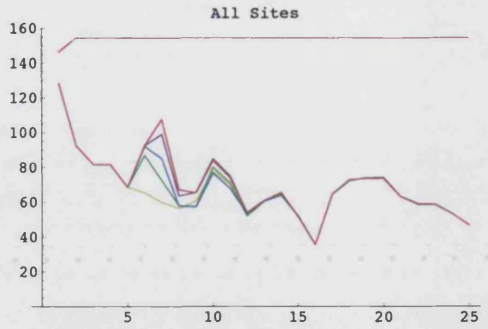


Figure 12.22: Linear homogeneous configuration: $b = 2000$, $var = 1$,$freq = \frac{2}{365}$, $\chi_{i,j} = 0.01$ and $\hat{k} = 100$. Straight line refers to the non-stochastic non-disease case.

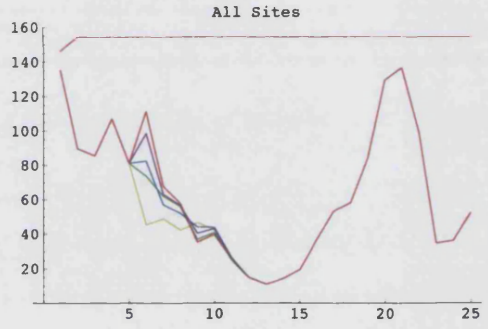


Figure 12.23: Linear homogeneous configuration: $b = 2000$, $var = 10$, $freq = \frac{2}{365}$, $\chi_{i,j} = 0.01$ and $\hat{k} = 100$. Straight line refers to the non-stochastic non-disease case.

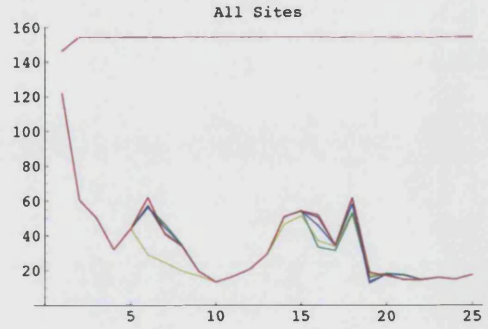


Figure 12.24: Linear homogeneous configuration: $b = 1000$, $var = 10$, $freq = \frac{2}{365}$, $\chi_{i,j} = 0.01$ and $\hat{k} = 100$. Straight line refers to the non-stochastic non-disease case.

## 12.10 Varying the connectivity (stochastic case).

When the connectivity is varied little difference from the constant connectivity case is detected in the stochastic case (as in the non-stochastic case), especially when the connectivity between the sites increases from site 1 to site 5 (figure 11.4). When the connectivity decreases from site 1 to site 5, there are some slight differences. For example in the $b = 4000$, $var = 10$ case (figure 12.25) the population dynamics for all the sites is not in phase, while it is in both the constant (figure 12.21) and increasing connectivity case. Moreover, a decreasing connectivity between the sites, a $b = 4000$ (figure 12.25) and $b = 1000$ (figure 12.26) virulence and $var = 10$ are the cases for which the population size is the lowest because of the interplay between disease and climatic changes.

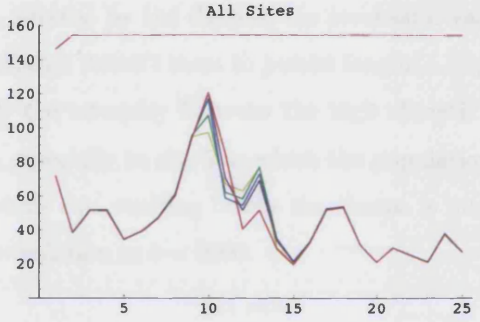


Figure 12.25: Linear homogeneous configuration(decreasing connectivity): $b = 4000$, $var = 10$, $freq = \frac{2}{365}$ and $\hat{k} = 100$. Straight line refers to the non-stochastic non-disease case.

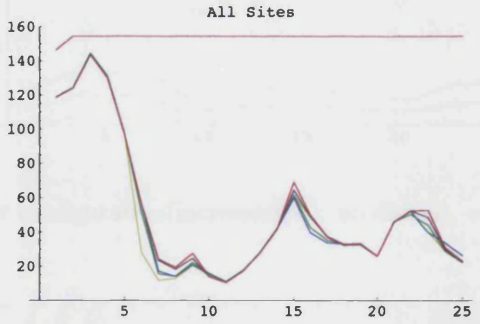


Figure 12.26: Linear homogeneous configuration(decreasing connectivity): $b = 1000$, $var = 10$, $freq = \frac{2}{365}$ and $\hat{k} = 100$. Straight line refers to the non-stochastic non-disease case.

## 12.11 Stochastic increasing $\hat{k}$.

It was observed in the non-stochastic case that varying the threshold capacity of the sites in the spatial model made more of a difference from the single site model than varying the connectivity. Figure 12.27-12.30 show the model results for running the linear model with increasing threshold capacity $\hat{k}$ from site 1 to site 5, namely $\hat{k}_1 = 10$, $\hat{k}_2 = 50$, $\hat{k}_3 = 100$, $\hat{k}_4 = 100$ and $\hat{k}_5 = 500$, where $\hat{k}_s$ with $s = 1, 2, 3, 4, 5$ is the threshold capacity of site $s$. If we compare figure 12.27, showing the non-disease case for $var = 1$, with figure 12.28, it is possible to detect that the disease affects mostly site 5 (highest threshold capacity), while site 1 where the disease has been introduced is not affected at all. For $b = 2000$ and $var = 1$ (figure 12.29) site 5 is now not affected much, in fact it is probably the least affected by the disease; the stochastic variation seems to control the population. High virulence disease doesn't seem to persist long in a large population. For $b = 2000$ and $var = 10$ (figure 12.30) the interplay between the high climatic variability and the disease controls the population well especially in site 5 in which the population remains less than half the threshold capacity for the whole run, starting before the disease is inserted. A $b = 1000$ virulence has the same effect on the population as $b = 2000$.

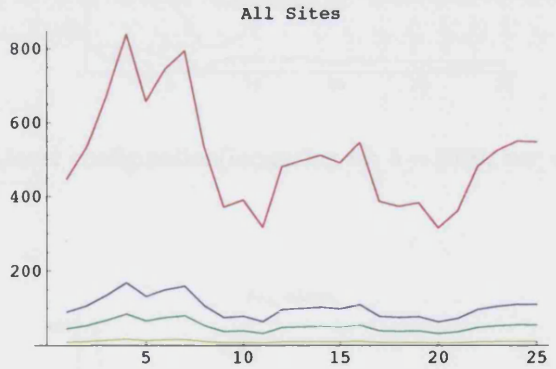


Figure 12.27: Linear configuration(increasing $\hat{k}$): no disease, $var = 1$, $freq = \frac{2}{365}$.

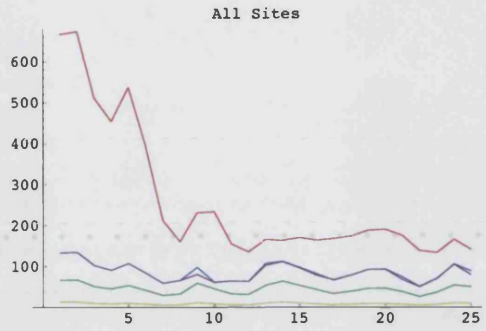


Figure 12.28: Linear configuration(increasing $\hat{k}$): $b = 4000$, $var = 1$,$freq = \frac{2}{365}$.

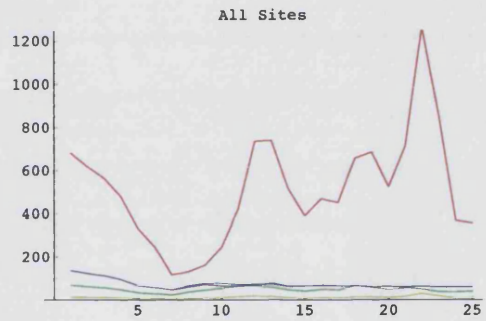


Figure 12.29: Linear configuration(increasing $\hat{k}$): $b = 2000$, $var = 1$,$freq = \frac{2}{365}$.

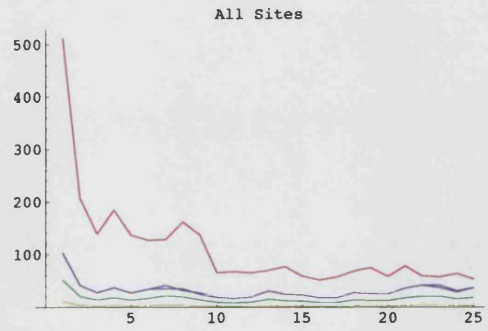


Figure 12.30: Linear configuration(increasing $\hat{k}$): $b = 2000$, $var = 10$, $freq = \frac{2}{365}$.

## 12.12 Stochastic decreasing $\hat{k}$.

Figures 12.31-12.34 show the model results for a linear configuration with decreasing threshold capacity from site 1 to site 5, namely, $\hat{k}_1 = 500$, $\hat{k}_2 = 100$, $\hat{k}_3 = 100$, $\hat{k}_4 = 50$ and $\hat{k}_5 = 10$. Figure 12.31 shows the results for the non-disease case. As in the increasing $\hat{k}$ case, the disease ($b = 4000$) has a strong effect on the high threshold capacity site, which in this case is site 1 (figure 12.32) where the disease is inserted. For $b = 4000$, $var = 1$ (figure 12.32) the disease already controls the population in site 1 while the other sites are little affected until $b = 1000$ (figure 12.33). It is interesting how for $b = 1000$ the disease is very effective at time of introduction for both the variances ($var = 1$ in figure 12.33 and $var = 10$ in figure 12.34), but for $var = 1$ the population recovers to pre-disease size at the end of the run. For $var = 10$ the population is controlled by the interplay of high climatic variability with the disease for the rest of the run, and maintained at an average density of about 50.

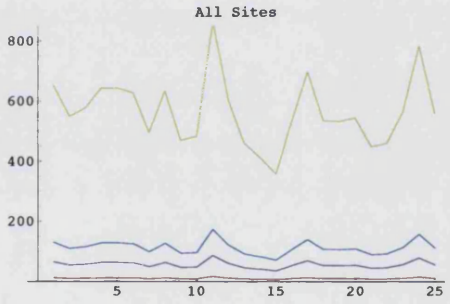


Figure 12.31: Linear configuration(decreasing $\hat{k}$): no disease, $var = 1$, $freq = \frac{2}{365}$.

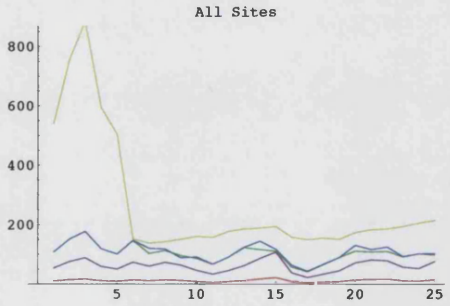


Figure 12.32: Linear configuration(decreasing $\hat{k}$): $b = 4000$, $var = 1$, $freq = \frac{2}{365}$.

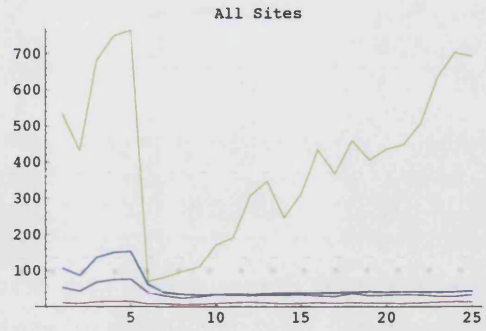


Figure 12.33: Linear configuration(decreasing $\hat{k}$): $b = 1000$, $var = 1$, $freq = \frac{2}{365}$.

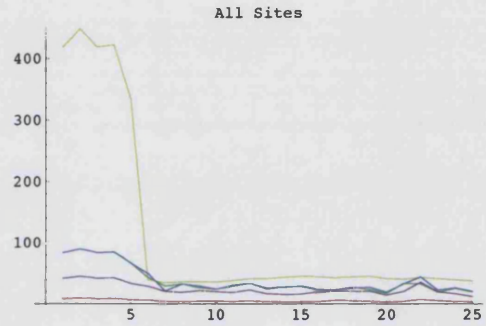


Figure 12.34: Linear configuration(decreasing $\hat{k}$): $b = 1000$, $var = 10$, $freq = \frac{2}{365}$.

## 12.13 Stochastic non-favourable borders.

The linear configuration of figure 11.9 is one for which the middle site has the highest threshold capacity while the border sites can only sustain a very small population size (see figure 11.9), i.e. $\hat{k}_1 = 10$, $\hat{k}_2 = 100$, $\hat{k}_3 = 500$, $\hat{k}_4 = 100$ and $\hat{k}_5 = 10$. The model results for this configuration are not very interesting, all the sites behave like a single site and are perfectly in phase for any value of the virulence and for any variance of the lognormal distribution. The disease has a small impact on the population for $b = 4000$ and controls the population for $b = 2000, 1000$ ($var = 10$). It seems that the climatic variation plays a big role in helping the disease control the population, in fact in the non-stochastic case the population always recovered after maximum 7 years in the most affected site (site 3) and for the highest virulence ($b = 1000$) (see section 12.8).

## 12.14 Stochastic favourable borders.

Figures 12.35-12.38 show the model results for the linear configuration outlined in figure 11.8. This configuration has border sites with higher threshold capacity with respect to the middle sites, namely $\hat{k}_1 = 500$, $\hat{k}_2 = 100$, $\hat{k}_3 = 10$, $\hat{k}_4 = 100$ and $\hat{k}_5 = 500$. Figure 12.35 shows the results without the disease. The sites behave like single sites and their population dynamics is perfectly in phase. When the disease is inserted, the population at site 1 is the most affected, this is because it has a higher population density and it is the site where the disease is inserted. As in the non-stochastic case, we can observe a "superimposition" of the results obtained for the increasing and decreasing $\hat{k}$ (see sections 12.11 and 12.12). Especially for $b = 2000$, $var = 1$ (figure 12.36) the population in site 1 becomes lower than 100 after the disease and recovers to site 5 levels only at the very end of the run. The other sites are hardly affected, and maybe hinder the transmission of the disease to site 5, whose population remains at high densities (though lower than without the disease). This phenomenon is enhanced when $b = 1000$, $var = 1$ (figure 12.37). The middle sites start to be more affected by the disease and transmit the disease to the population in site 5 which (in figure 12.38) shows to be controlled well probably by the interplay between both disease and high climatic variation ($var = 10$).

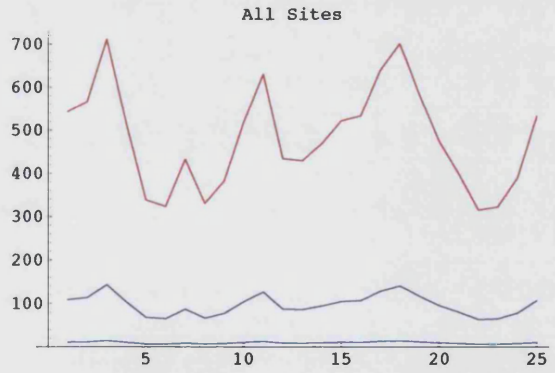


Figure 12.35: Linear configuration(favourable borders): no disease, $var = 1$, $freq = \frac{2}{365}$.

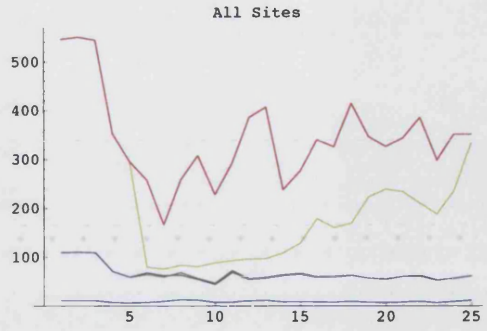


Figure 12.36: Linear configuration(favourable borders): $b = 2000$, $var = 1$, $freq = \frac{2}{365}$.

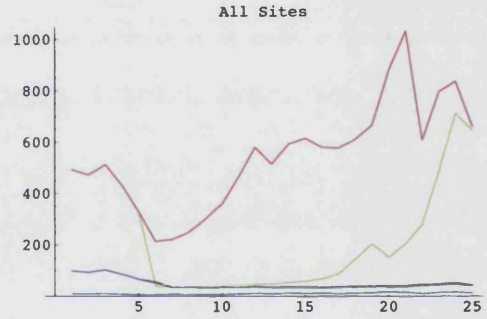


Figure 12.37: Linear configuration(favourable borders): $b = 1000$, $var = 1$, $freq = \frac{2}{365}$.

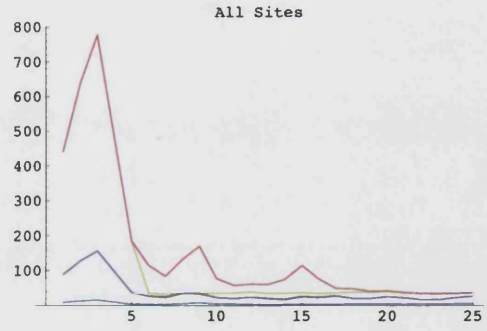


Figure 12.38: Linear configuration(favourable borders): $b = 1000$, $var = 10$, $freq = \frac{2}{365}$.

# Chapter 13

# Results: 2-Dimensional Spatial Model (the Strong Hypothesis).

The following sections illustrate the results obtained from running the model with the symmetric 2-dimensional configuration shown in figure 11.6, and the asymmetric 2-dimensional configuration shown in figure 11.7. The connectivity was kept constant since in the linear case a change in connectivity proved to make little difference in model results: $\chi_{i,j} = 0.01$ for all $i, j$, was used throughout the model runs. The disease is inserted into site 1 after 5 years of model run, just as in the linear case. The colour coding in the different sites follows them in figures 11.6 and 11.7.

## 13.1 Non-stochastic constant $\hat{k}$.

The first case to be investigated was one in which all the sites have the same threshold capacity, $\hat{k}$ (see figure 11.6). If we compare figures 13.1-13.3 with figures 12.6-12.8, illustrating the results for the linear model with constant $\hat{k}$, it is possible to notice a very similar behaviour in model results between the 1-dimensional and the 2-dimensional case. The fact that site 5 is totally connected in the 2-D case does not seem to create a remarkable difference in the model results. For example the 2-year cycles in the appearance of the disease for $b = 4000$ (figure 13.1) is exactly the same as in the linear case, just sites 3 and 4 are more in phase with respect to the linear case. In the 2-D case, the sites are slightly less affected by the disease, apart from site 1 where the disease is inserted. This is observed in particular for $b = 1000$ (figure 13.3).

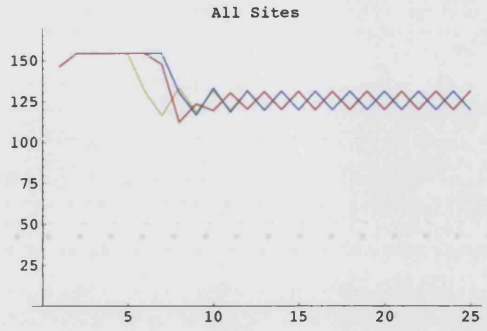


Figure 13.1: 2-D symmetric configuration: $\chi_{i,j} = 0.01$, $b = 4000$ .

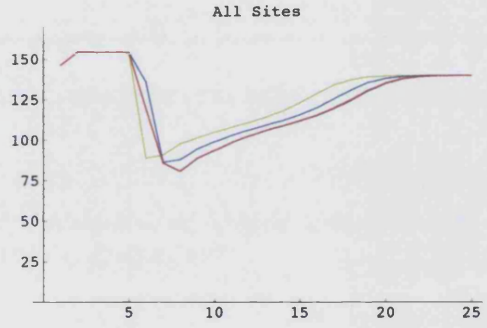


Figure 13.2: 2-D symmetric configuration: $\chi_{i,j} = 0.01$, $b = 2000$ .

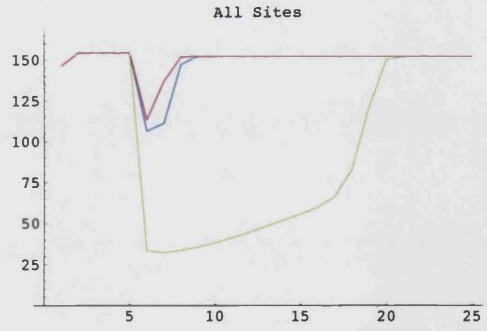


Figure 13.3: 2-D symmetric configuration: $\chi_{i,j} = 0.01$, $b = 1000$ .

## 13.2 Non-stochastic favourable borders.

Figures 13.4-13.7 show the model results for the 2-D symmetric configuration outlined in figure 11.11. The threshold capacity is made to vary in such a way that there is a non-favourable patch ($\hat{k}_5 = 50$) surrounded by a more suitable environment for rabbits ($\hat{k}_{1,2,3,4} = 100$). The non-disease case (figure 13.4) gives the same results as for the single site model. When the disease is inserted, we observe that the border sites behave exactly as in the linear case (see section 12.3) while there is a "$b$-lag" before the central site 5 is affected by the disease, i.e. for $b = 4000$ (figure 13.5) the disease does not invade site 5 (in red), while the populations in the other sites go through 2-yearly cycles. The reverse behaviour is observed for the population in site 5 only for $b = 2000$ (figure 13.6), while the border sites take that behaviour which has been observed for both the linear and single site models (see section 12.3). It is interesting to notice how for $b = 2000$ (figure 13.5), site 5 population does not recover but goes through a self-sustaining cycle, while in the other sites, the disease is more effective for about 18 years after disease introduction, but then largely recovers to almost pre-disease size. When $b = 1000$ (figure 13.7), site 5 behaves more like the rest of the sites and the cycle disappears; site 1 is the most affected site and its population density reaches values lower than site 5.

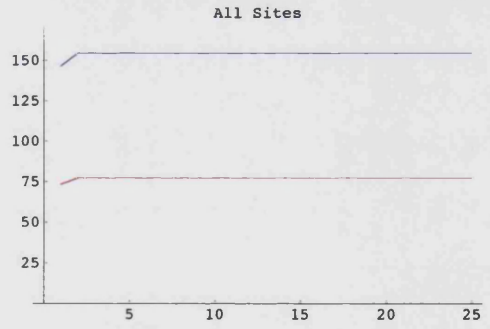


Figure 13.4: 2-D symmetric configuration: $\chi_{i,j} = 0.01$, no disease . Red is population density at site 5.

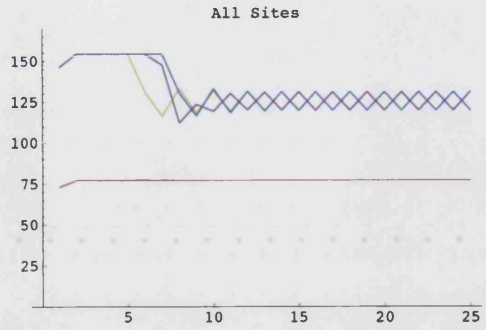


Figure 13.5: 2-D symmetric configuration: $\chi_{i,j} = 0.01$, $b = 4000$ .

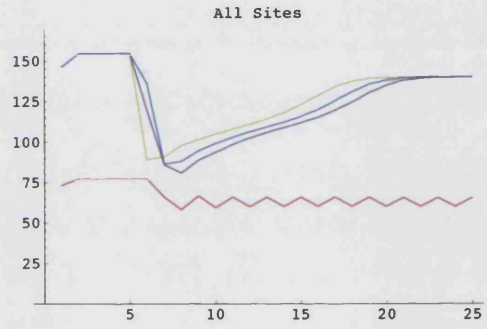


Figure 13.6: 2-D symmetric configuration: $\chi_{i,j} = 0.01$, $b = 2000$ .

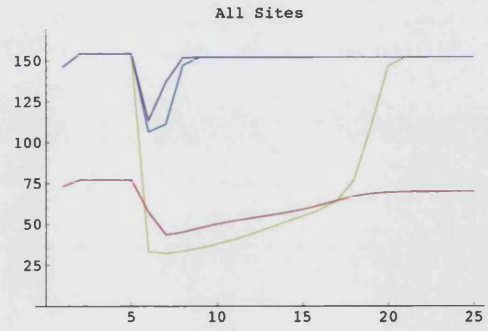


Figure 13.7: 2-D symmetric configuration: $\chi_{i,j} = 0.01$, $b = 1000$ .

## 13.3 Non-stochastic non-favourable borders.

When site 5 is made a suitable environment for rabbits ($\hat{k} = 100$) surrounded by less favourable sites ($\hat{k}_{1,2,3,4} = 50$) (see figure 11.10), we observe that the border sites are now lagging behind site 5 as $b$ is varied, thus for $b = 4000$ (figure 13.8) only site 5 is affected by the disease and the other sites behave as in the non-disease case, even though the disease is inserted at site 1. Site 5 population size varies through 2-yearly cycles and never recovers to pre-disease size. The other sites exhibit this behaviour for $b = 2000$ (figure 13.9); this seems to suggest that the spatial configuration is mostly affected by a change in threshold capacity, $\hat{k}$, within the sites more than the actual position of the sites with respect to one another.

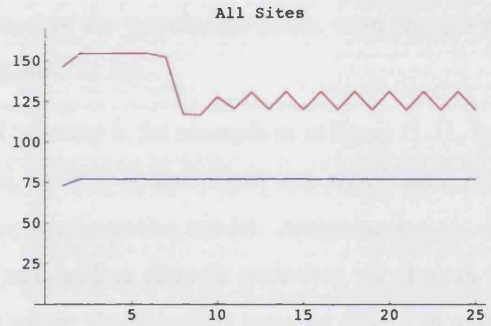


Figure 13.8: 2-D symmetric configuration: $\chi_{i,j} = 0.01$, $b = 4000$ .

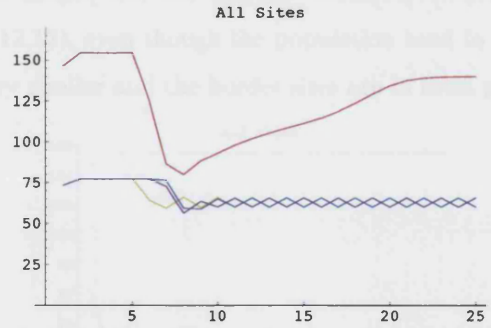


Figure 13.9: 2-D symmetric configuration: $\chi_{i,j} = 0.01$, $b = 2000$ .

## 13.4 Stochastic results for the symmetric 2-Dimensional configuration.

When climatic variation is included in the model run for the 2-D symmetric configuration outlined in figure 11.6, we do not observe remarkable changes from both the single site and linear configuration model results. The sites behave much as a single site and mostly in phase with each other. The interplay between the disease and the climatic variation has a bigger role in controlling the population than the spatial configuration effects. When the threshold capacity is the same for all the sites ($\hat{k}_{1,2,3,4,5} = 100$), a high climatic variation controls the population even without the disease (see figure 13.10). While when the disease is inserted $b = 4000$, $var = 10$ (see figure 13.11) is the most successful strain in keeping the population down, even though there is not much difference from the non-disease case (figure 13.10).

When we vary the threshold capacity $\hat{k}$, for example as in figure 11.11, by allowing a higher threshold capacity for the border sites, we still do not detect any significance change from what observed in the single site and the linear configuration model. Assigning $\hat{k}_{1,2,3,4} = 100$ to the border site and $\hat{k}_5 = 50$ to the middle site, and adding climatic variation, we observe that higher density sites are more affected: particularly where the disease is inserted (site 1 in yellow) (see figure 13.12) while site 5 (in red) is hardly affected by the disease. Similar results are obtained when the model is run using the spatial configuration outlined in figure 11.10, with $\hat{k}_{1,2,3,4} = 50$ (border sites) and $\hat{k}_5 = 100$. In this case the disease and the climatic variation control the population mostly for $b = 2000$, $var = 10$ (figure 13.13), even though the population tend to recover in the long run; the dynamics of each site is very similar and the border sites are in total phase.

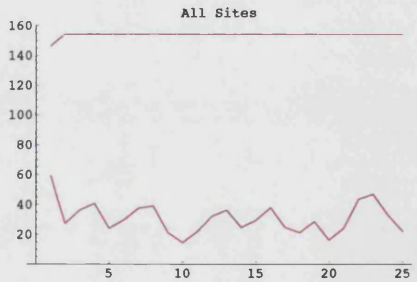


Figure 13.10: 2-D symmetric homogeneous configuration ($\hat{k}_{1,2,3,4,5} = 100$): no disease, $var = 10$, $freq = \frac{2}{365}$. Straight line is non-stochastic, non-disease case.

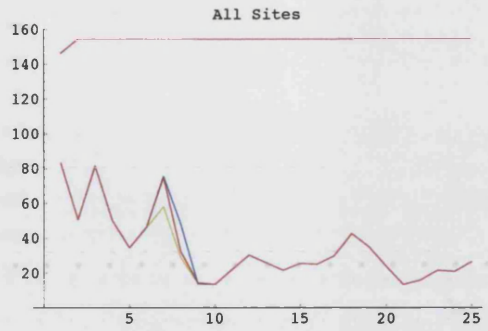


Figure 13.11: 2-D symmetric homogeneous configuration ($\hat{k}_{1,2,3,4,5} = 100$): $b = 4000$, $var = 10$, $freq = \frac{2}{365}$. Straight line is non-stochastic, non-disease case.

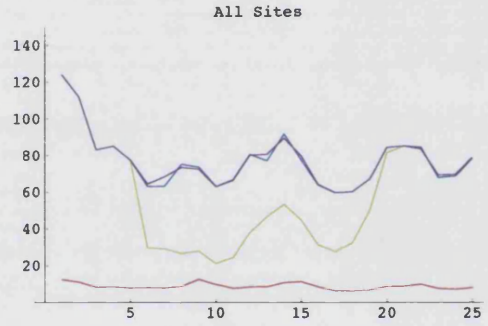


Figure 13.12: 2-D symmetric configuration (favourable borders: $\hat{k}_{1,2,3,4} = 100$, $\hat{k}_5 = 50$): $b = 1000$, $var = 10$, $freq = \frac{2}{365}$.

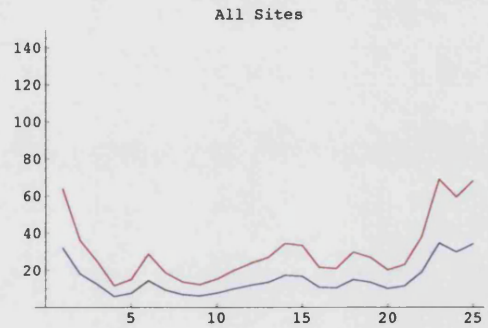


Figure 13.13: 2-D symmetric configuration(non-favourable borders: $\hat{k}_{1,2,3,4} = 50$, $\hat{k}_5 = 100$): $b = 2000$, $var = 10$, $freq = \frac{2}{365}$.

2-Dimensional Asymmetric configuration

The colour coding for the 2-dimensional asymmetric configuration corresponds to the one in figure 11.7, where site 1 is represented by yellow, site 2 is represented by green, site 3 is represented by aqua, site 4 is represented by blue, site 5 is represented by purple, site 6 is represented by magenta and site 7 is represented by red. The disease is always inserted in site 1 after 5 years of model run. As the possible combinations of varying the connectivity and varying the threshold capacity $\hat{k}$ are many, we ran the model choosing four different possible combination of spatial variation:

- constant connectivity, constant $\hat{k}$,
- random connectivity, constant $\hat{k}$,
- constant connectivity, random $\hat{k}$,
- random connectivity, random $\hat{k}$.

The value chosen for the constant connectivity runs is $\chi_{i,j} = 0.01$ for all $i, j$, and the value for the constant threshold capacity runs is $\hat{k} = 100$. When the connectivity values were chosen randomly, they were in the range $\chi_{i,j} = 0.001, 0.005, 0.01, 0.05, 0.1, 0.5$. The threshold capacity values were chosen randomly in the range $\hat{k} = 10, 50, 100, 500$.

## 13.5 Non-stochastic asymmetric configuration: constant and random connectivity, constant $\hat{k}$

Figures 13.14-13.16 confirm that the spatial configuration does not alter the population dynamics of the sites. For $b = 4000$ (figure 13.14) we still observe the 2-yearly cycles for all the sites (compare to figures 12.6 and 13.1). For $b = 2000$ (figure 13.15) the disease lowers the population but then it recovers to almost pre-disease size at the end of the run; site 4 and 6 are the most affected (compare to figure 12.7 and 13.2). Even the $b = 1000$ case (figure 13.16) presents a pattern seen in the linear and symmetric configuration (see figures 12.8 and 13.3): site 1, where the disease, is inserted is the most affected by the disease, but after 15 years from disease appearance, the population goes back to pre-disease levels like the other sites.

When the connectivity was varied randomly, the same results were obtained as for the constant connectivity case. The same phenomenon was observed in the linear and symmetric case.

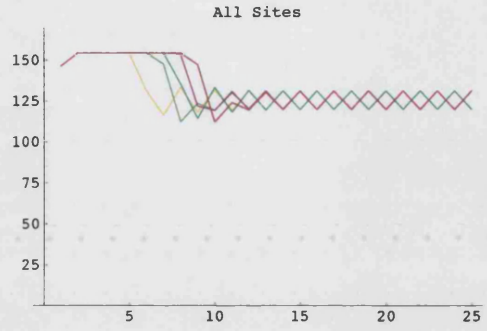


Figure 13.14: Asymmetric homogeneous spatial configuration: $\chi_{i,j} = 0.01$, $\hat{k} = 100$, $b = 4000$ .

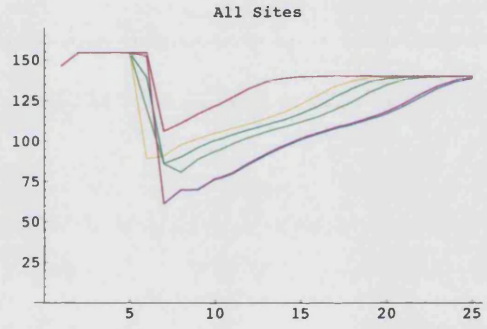


Figure 13.15: Asymmetric homogeneous spatial configuration: $\chi_{i,j} = 0.01$, $\hat{k} = 100$, $b = 2000$ .

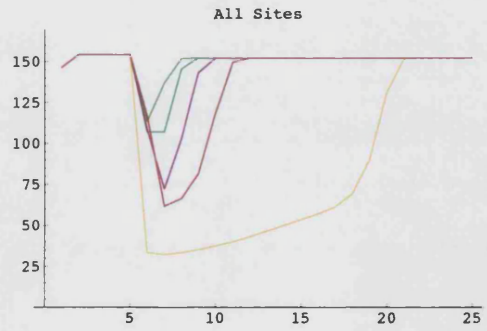


Figure 13.16: Asymmetric homogeneous spatial configuration: $\chi_{i,j} = 0.01$, $\hat{k} = 100$, $b = 1000$ .

## 13.6 Non-stochastic asymmetric configuration: constant and random connectivity, random $\hat{k}$

When the threshold capacity $\hat{k}$ is varied, it is possible to observe the same patterns typical of the linear and symmetric spatial configuration. For example figure 13.17 shows the asymmetric configuration dynamics for $b = 4000$, for a constant connectivity between the sites, namely $\chi_{i,j} = 0.01$: site 1 is mostly affected by the disease because the disease is inserted in this site and mostly because it has the highest population density. The population recovers to pre-disease size after about 18 years. Sites 3, 4, 5, 6 and 7 go through 2-yearly cycles and never recover to pre-disease size; while site 2 with the lowest threshold capacity is not affected by the disease for any value of $b$, even though it is placed between site 1, the most affected, and the rest of the system. The disease is transmitted through the site without affecting the small population. When the connectivity is varied randomly the pattern remains similar to the one observed. Figure 13.18 shows the model results for the asymmetric configurations, for different random values of $\hat{k}_{1,2,3,4,5,6,7}$ and random connectivity $\chi_{i,j}$. The connectivity value makes no difference; the sites with higher threshold capacity are more affected by the disease but eventually recover to pre-disease level, site 1 is affected because the disease appears there and because the population density is quite high. Site 2 and 3 separating site 1 from the rest of the system are not or less affected by the disease but transmit it to more highly populated sites.

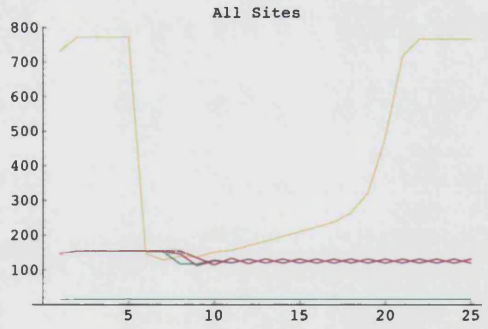


Figure 13.17: Asymmetric spatial configuration: $\chi_{i,j} = 0.01$, $b = 4000$, $\hat{k}_1 = 500$, $\hat{k}_2 = 10$, $\hat{k}_3 = 100$, $\hat{k}_4 = 100$, $\hat{k}_5 = 100$, $\hat{k}_6 = 100$, $\hat{k}_7 = 100$.

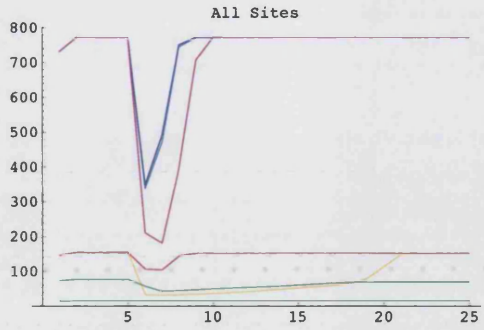


Figure 13.18: Irregular spatial configuration: random connectivity, $b = 1000$, $\hat{k}_1 = 100$, $\hat{k}_2 = 10$, $\hat{k}_3 = 50$, $\hat{k}_4 = 500$, $\hat{k}_5 = 500$, $\hat{k}_6 = 500$, $\hat{k}_7 = 100$ .

## 13.7 Stochastic asymmetric configuration: constant and random connectivity, constant $\hat{k}$

When climatic variation is added to the system, we observe that in absence of the disease all the 7 sites behave perfectly in phase and as a single site even for a high climatic variation (figure 13.19). Considering that the configuration is asymmetric and has a larger number of sites with respect to the linear and symmetric 2-D configuration, we gather that the difference in spatial configuration has no effect on the population dynamics of the sites. The high climatic variation controls the population very well even without the disease (figure 13.19). When the disease is inserted, the sites' dynamics start to be out of phase as in figure 13.20, and site 1 where the disease is inserted is affected the most. Unexpectedly this effect is less evident for a higher climatic variation (figure 13.21). Figures 13.20 and 13.21 refer to a disease with virulence $b = 1000$, but the same outcome is observed for $b = 4000$ and $b = 2000$: a high variance kills most of the spatial effects. Moreover the non-disease case in figure 13.19 seems to control the population as well as the most effective virulence case, $b = 1000$ (figure 13.21). When the connectivity between the sites is varied taking randomly one of the values of the considered range (see page 221), the outcome is the same as for the constant connectivity case. Climatic changes bring more variation to the pattern than the spatial configuration.

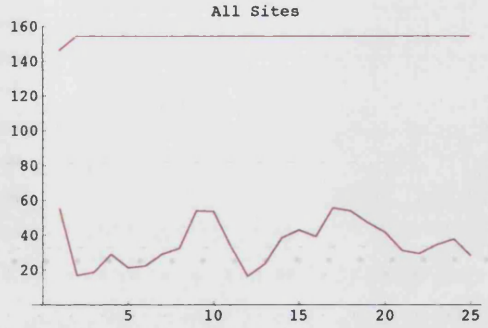


Figure 13.19: Asymmetric spatial configuration: no disease, $var = 10$, $freq = \frac{2}{365}$, $\chi_{i,j} = 0.01$, $\hat{k} = 100$. Red straight line is the non-stochastic non-disease case.

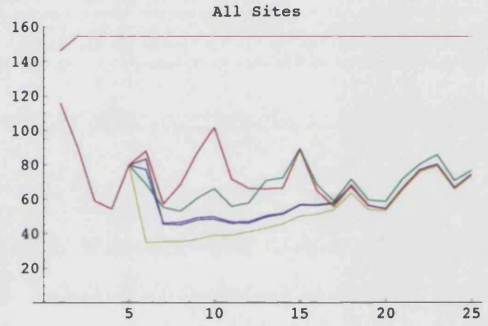


Figure 13.20: Asymmetric spatial configuration: $b = 1000$, $var = 1$, $freq = \frac{2}{365}$, $\chi_{i,j} = 0.01$, $\hat{k} = 100$. Red straight line is the non-stochastic non-disease case.

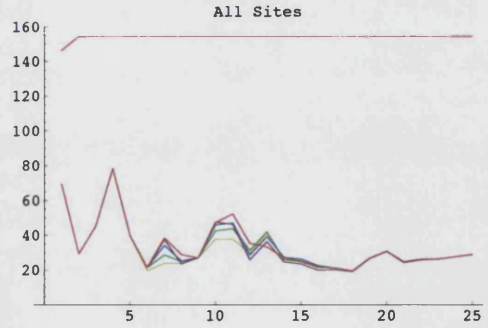


Figure 13.21: Asymmetric spatial configuration: $b = 1000$, $var = 10$, $freq = \frac{2}{365}$, $\chi_{i,j} = 0.01$, $\hat{k} = 100$. Red straight line is the non-stochastic non-disease case.

## 13.8 Stochastic non-regular configuration: constant and random connectivity, random $\hat{k}$.

When a different value of $\hat{k}$ is assigned randomly at each site, we observe a strong variance effect for all the disease strains and for the non-disease case. We show here the case $b = 2000$ (figures 13.22 and 13.23): site 1 where the disease is inserted is remarkably more affected then the other sites for a low climatic variation (figure 13.22). A high climatic variation helps the disease to control the other highly populated sites (site 3 and 6), so that their population reaches the same value as site 1 after about 8 years. Using a value of the connectivity randomly chosen for connecting each site does not give any different result: site 1 is always the most affected because the disease appears there for the first time and because it has a high threshold capacity. The climatic variation plays a main role in controlling the population.

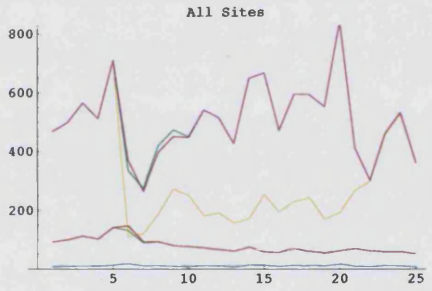


Figure 13.22: Asymmetric spatial configuration: $b = 2000$, $var = 1$, $freq = \frac{2}{365}$, $\chi_{i,j} = 0.01$, $\hat{k}_1 = 500$, $\hat{k}_2 = 100$, $\hat{k}_3 = 500$, $\hat{k}_4 = 10$, $\hat{k}_5 = 100$, $\hat{k}_6 = 500$, $\hat{k}_7 = 100$.

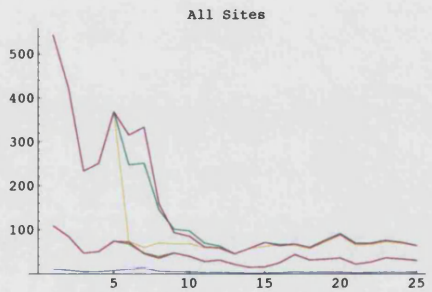


Figure 13.23: Asymmetric spatial configuration: $b = 2000$, $var = 10$, $freq = \frac{2}{365}$, $\chi_{i,j} = 0.01$, $\hat{k}_1 = 500$, $\hat{k}_2 = 100$, $\hat{k}_3 = 500$, $\hat{k}_4 = 10$, $\hat{k}_5 = 100$, $\hat{k}_6 = 500$, $\hat{k}_7 = 100$.

# Chapter 14

# Results: 1-Dimensional Spatial Model (the Weak Hypothesis)

The colour coding of the figures in this chapter will remain the same, where site 1 is represented by yellow, site 2 by green, site 3 by blue, site 4 by magenta and site 5 by red. If more than one site has the same population dynamics, the graph might have only one colour to represent more than one site (the dominant colour, like red, for example). See figures 11.3, 11.4, 11.5, 11.8 and 11.9 for the associated spatial configurations. The disease is always introduced into site 1 after 5 years. All the figures report the average annual population size versus time (in years).

## 14.1 Non-stochastic constant connectivity.

When the way RCD affects a susceptible rabbit population in the spatial model follows the Weak hypothesis (see section 1.5.2) we observe a more chaotic behaviour of the total population dynamics of the system, especially for the non-stochastic case. The non-disease case was not investigated since it is the same as the one reported in the chapters 12 and 13. Figures 14.1-14.3 show the population dynamics for the linear system in figure 11.3, where the connectivity between the sites is constant, namely $\chi_{i,j} = 0.01$ for all $i, j$, and the threshold capacity of the sites is the same, namely $\hat{k} = 100$. Site 1 where the disease is inserted is the first to be affected and the other sites follow with a time delay longer than in the Strong hypothesis case. For example, for $b = 2000$ (figure 14.1), there is an interval of about 7 years before the disease appears effectively in the last

site, i.e. site 5. The sites practically never behave in phase and the disease does not control the populations very effectively which oscillate between the pre-disease size and a lower population size. For $b = 1000$ (figure 14.2) the disease is more effective and the population density of most sites reaches 20; it spreads faster reaching site 5, the last site, in less than 2 years. The population size of the sites still oscillate but does not reach pre-disease size for the entire run. For $b = 100$ (figure 14.3) all the sites are affected instantaneously and the disease controls the population keeping it at very low values. In the Strong hypothesis case the disease lowered the population size of each site for a variable time interval, after which the population mainly recovered or oscillated in 2-yearly cycles (compare figures 14.1-14.3 with figures 12.6-12.8). In the single site model, when using the Weak hypothesis (section 9.3), we observed a more chaotic behaviour when compared to the Strong hypothesis case: this is enhanced in the spatial model.

When the connectivity between the sites was varied as in figures 11.4 and 11.5, no substantial change was observed, just as in the Strong hypothesis case: as the virulence is increased the disease spreads faster and it controls the population more effectively. Even the chaotic pattern is repeated for both increasing and decreasing connectivity. Hence the connectivity will be kept constant for all the other cases investigated.

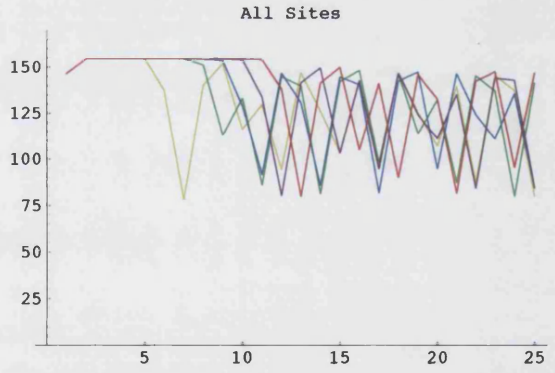


Figure 14.1: Linear homogeneous configuration: $\chi_{i,j} = 0.01$, $\hat{k} = 100$ and $b = 2000$ .

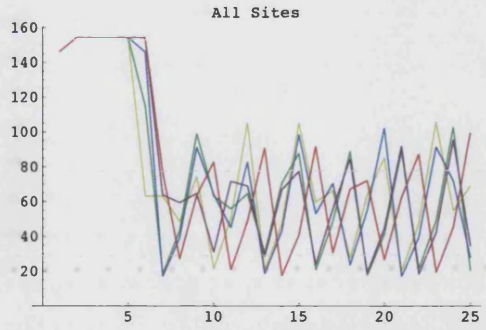


Figure 14.2: Linear homogeneous configuration: $\chi_{i,j} = 0.01$, $\hat{k} = 100$ and $b = 1000$ .

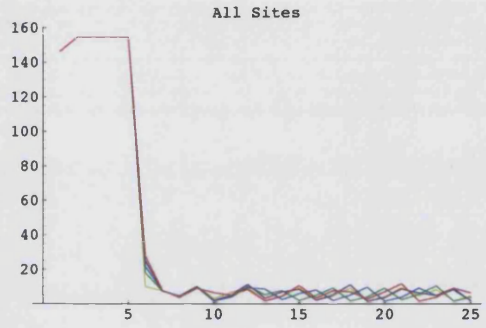


Figure 14.3: Linear homogeneous configuration: $\chi_{i,j} = 0.01$, $\hat{k} = 100$ and $b = 100$ .

## 14.2 Non-stochastic varying $\hat{k}$.

At first the threshold capacity, $\hat{k}$, was varied by progressively increasing and decreasing $\hat{k}$ from site 1 to site 5. We observe that the disease does not affect small population sites apart from when it has a very high virulence ($b = 100$), for which the population crashes for any density in all sites. In the increasing $\hat{k}$ case (figure 14.4), even though the disease is inserted in site 1, the population remains unaffected because of the very low density, and transmits the disease to site 2 which is not affected by the disease for $b = 2000$ but it is for $b = 1000$ and $b = 100$. The same pattern is observed for decreasing $\hat{k}$ (figure 14.5): the most highly populated sites are affected for low and high virulence, while in sites 4 and 5, with lower population densities, the disease appears for $b = 1000$ (in site 4) and $b = 100$ (in site 5).

Subsequently the threshold capacity $\hat{k}$ was varied as shown in figure 11.8. Such configuration has the border sites with higher threshold capacity with respect to the middle sites, namely $\hat{k}_1 = 500$, $\hat{k}_2 = 100$, $\hat{k}_3 = 10$, $\hat{k}_4 = 100$ and $\hat{k}_5 = 500$. Figure 14.6 shows the model results for $b = 2000$. We notice that the dynamics doesn't change with respect to the increasing and decreasing $\hat{k}$, and that the disease success depends mainly on the threshold capacity of the site and not by the spatial configuration, as observed in the Strong hypothesis case.

When the model was run for the non-favourable borders linear configuration (figure 11.9) we still got similar results. The linear configuration with non-favourable borders is one for which the middle site has the highest threshold capacity while the border ones can only sustain a very small population size, i.e. $\hat{k}_1 = 10$, $\hat{k}_2 = 100$, $\hat{k}_3 = 500$, $\hat{k}_4 = 100$ and $\hat{k}_5 = 10$. The population density plays the main role in disease success even though, for the non-favourable borders case, the dynamics of the sites was more in phase for equal threshold capacity sites (see figure 14.7). The same was observed for the Strong hypothesis.

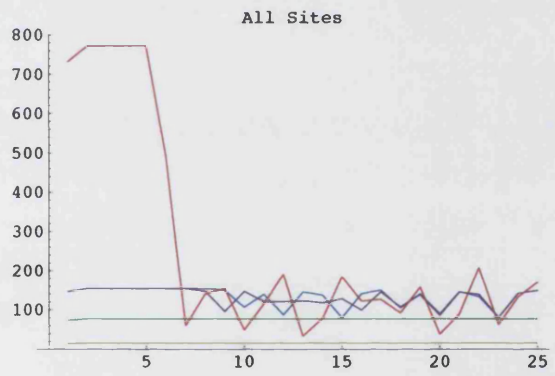


Figure 14.4: Linear configuration (increasing $\hat{k}$): $\chi_{i,j} = 0.01$, $\hat{k}_1 = 10$, $\hat{k}_2 = 50$, $\hat{k}_3 = 100$, $\hat{k}_4 = 100$, $\hat{k}_5 = 500$ and $b = 2000$ .

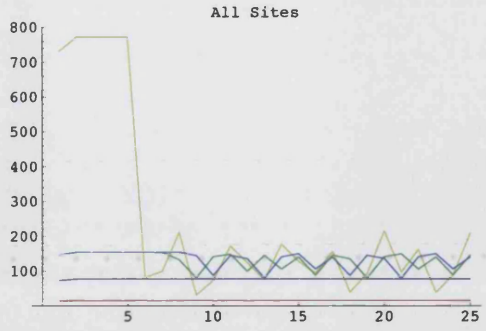


Figure 14.5: Linear configuration (decreasing $\hat{k}$): $\chi_{i,j} = 0.01$, $\hat{k}_1 = 500$, $\hat{k}_2 = 100$, $\hat{k}_3 = 100$, $\hat{k}_4 = 50$, $\hat{k}_5 = 10$ and $b = 2000$ .

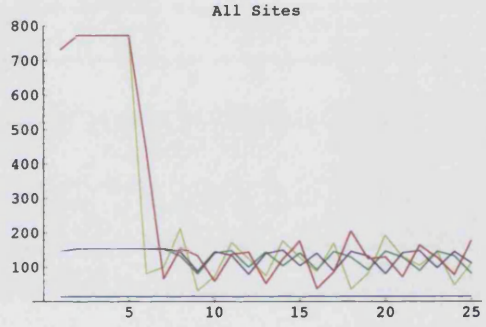


Figure 14.6: Linear configuration (favourable borders): $\chi_{i,j} = 0.01$, $\hat{k}_1 = 500$, $\hat{k}_2 = 100$, $\hat{k}_3 = 10$, $\hat{k}_4 = 100$, $\hat{k}_5 = 500$ and $b = 2000$ .

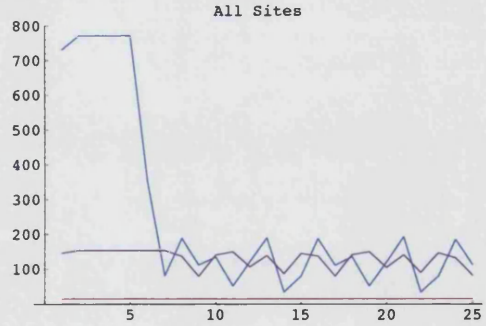


Figure 14.7: Linear configuration (non-favourable borders): $\chi_{i,j} = 0.01$, $\hat{k}_1 = 10$, $\hat{k}_2 = 100$, $\hat{k}_3 = 500$, $\hat{k}_4 = 100$, $\hat{k}_5 = 10$ and $b = 2000$ .

## 14.3 Stochastic Constant $\hat{k}$

Climatic variation was introduced as in the single site model. In general not much difference was observed in the results from the Strong hypothesis. Though it is interesting to notice that a high climatic variation instead of bringing more "disorder" to the system dynamics, it actually makes the system more "orderly" as is shown in figure 14.9. The sites behave perfectly in phase, and the interplay between disease and climatic changes controls the population well. While figure 14.8 shows smaller climatic variation, where the chaotic behaviour is still exhibited, and the population size is less effectively lowered. Both the figures refer to a virulence $b = 2000$ of the disease. A similar kind of behaviour is observed for $b = 1000$. $b = 100$ is still the most successful strain of the disease, crashing the population as soon as the disease appears; climatic variation is not so successful in "synchronizing" the sites' population dynamics.

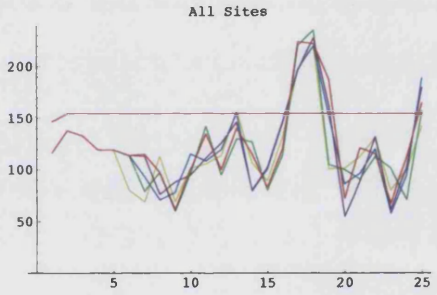


Figure 14.8: Linear homogeneous configuration: $\chi_{i,j} = 0.01$, $\hat{k} = 100$, $b = 2000$, $var = 1$, $f = \frac{2}{365}$. Red straight line is the non-stochastic, non-disease case.

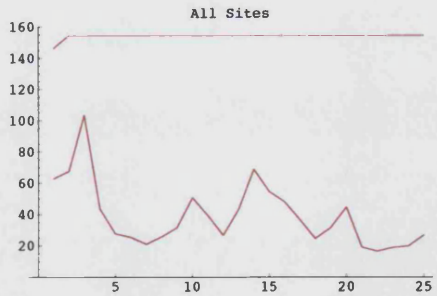


Figure 14.9: Linear homogeneous configuration:$\chi_{i,j} = 0.01$, $\hat{k} = 100$, $b = 2000$, $var = 10$, $f = \frac{2}{365}$. Red straight line is the non-stochastic, non-disease case.

## 14.4 Stochastic Varying $\hat{k}$

Figures 14.10-14.17 show the model results for all the possible threshold capacity variations considered in this research for the single site model; these configurations are outlined in figures 11.3, 11.8 and 11.9. These results refer only to the $b = 2000$ virulence ($b = 1000$ gives similar results and for $b = 100$ the population crashes very fast) so that we can make a direct comparison of the influence of the spatial configuration and the climatic changes on the system and compare it to the non-stochastic case. If we compare figures 14.10-14.17 with figures 14.4-14.7, we notice that the stochastic effects give less "chaotic" results. While in the non-stochastic case the disease plays a main role in lowering the population size, especially in the high density population sites, in the stochastic case the climatic changes have a bigger effect in controlling the population. For example in figures 14.10, 14.11, 14.15 and 14.17 it is clear that before the disease is introduced, i.e. before the $5^{th}$ year, the population is very well controlled by the climatic changes alone; in fact, in figure 14.15 the population size tends to rise after the disease is introduced. The model outcome for the various configurations does not vary much. The disease is still mostly successful in high density sites especially if it is introduced in one of these. Hence the decreasing $\hat{k}$ configuration (figures 14.12 and 14.13) is slightly more successful, especially in site 1 where the disease is introduced, compared to the increasing $\hat{k}$ configuration (figures 14.10 and 14.11). This was observed in the Strong hypothesis case too. For the favourable and non-favorable borders case we notice that the non-favourable borders (figures 14.14 and 14.15) are less chaotic and the sites with equal $\hat{k}$ behave exactly the same.

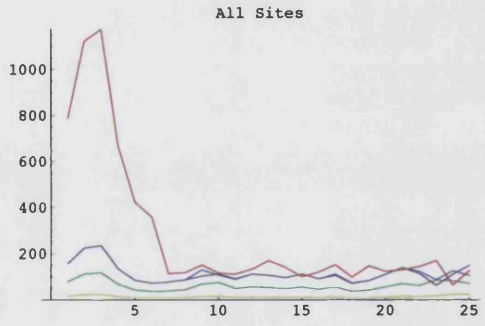


Figure 14.10: Linear configuration (increasing $\hat{k}$): $\chi_{i,j} = 0.01$, $\hat{k}_1 = 10$, $\hat{k}_2 = 50$, $\hat{k}_3 = 100$, $\hat{k}_4 = 100$, $\hat{k}_5 = 500$, $b = 2000$, $var = 1$, $f = \frac{2}{365}$.

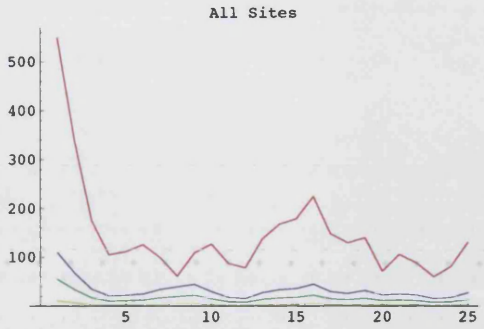


Figure 14.11: Linear configuration (increasing $\hat{k}$): $\chi_{i,j} = 0.01$, $\hat{k}_1 = 10$, $\hat{k}_2 = 50$, $\hat{k}_3 = 100$, $\hat{k}_4 = 100$, $\hat{k}_5 = 500$, $b = 2000$, $var = 10$, $f = \frac{2}{365}$.

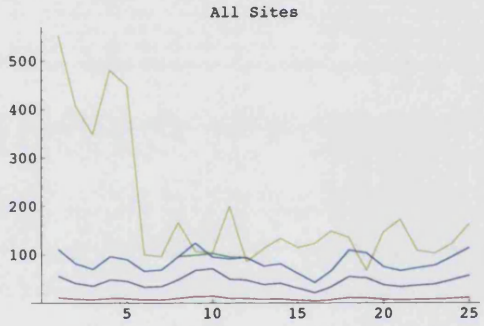


Figure 14.12: Linear configuration (decreasing $\hat{k}$): $\chi_{i,j} = 0.01$, $\hat{k}_1 = 500$, $\hat{k}_2 = 100$, $\hat{k}_3 = 100$, $\hat{k}_4 = 50$, $\hat{k}_5 = 10$, $b = 2000$, $var = 1$, $f = \frac{2}{365}$.

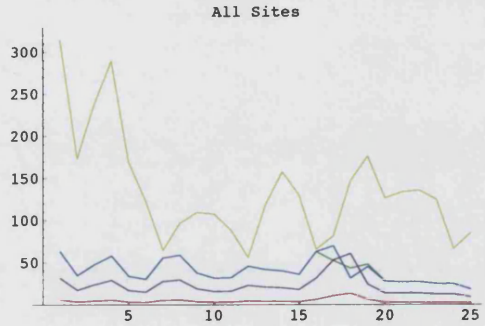


Figure 14.13: Linear configuration (decreasing $\hat{k}$): $\chi_{i,j} = 0.01$, $\hat{k}_1 = 500$, $\hat{k}_2 = 100$, $\hat{k}_3 = 100$, $\hat{k}_4 = 50$, $\hat{k}_5 = 10$, $b = 2000$, $var = 10$, $f = \frac{2}{365}$.

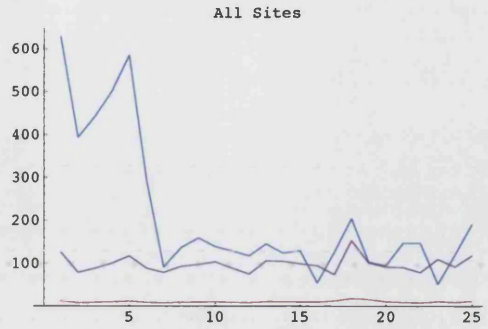


Figure 14.14: Linear configuration (non-favourable borders $\hat{k}$): $\chi_{i,j} = 0.01$, $\hat{k}_1 = 10$, $\hat{k}_2 = 100$, $\hat{k}_3 = 500$, $\hat{k}_4 = 100$, $\hat{k}_5 = 10$, $b = 2000$, $var = 1$, $f = \frac{2}{365}$.

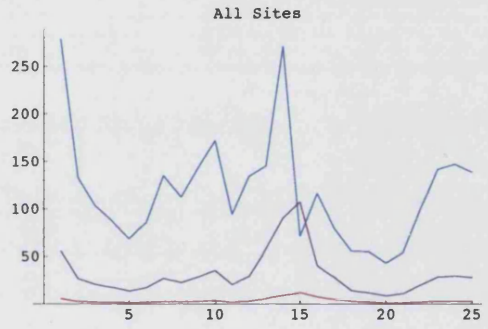


Figure 14.15: Linear configuration (non-favourable borders $\hat{k}$): $\chi_{i,j} = 0.01$, $\hat{k}_1 = 10$, $\hat{k}_2 = 100$, $\hat{k}_3 = 500$, $\hat{k}_4 = 100$, $\hat{k}_5 = 10$, $b = 2000$, $var = 10$, $f = \frac{2}{365}$.

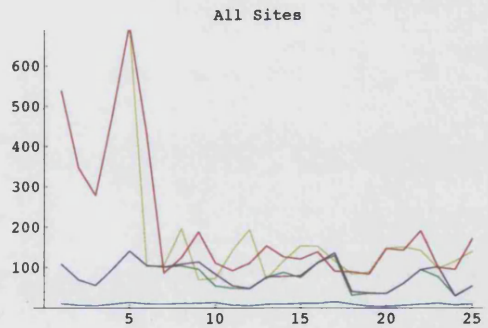


Figure 14.16: Linear configuration (favourable borders $\hat{k}$): $\chi_{i,j} = 0.01$, $\hat{k}_1 = 500$, $\hat{k}_2 = 100$, $\hat{k}_3 = 10$, $\hat{k}_4 = 100$, $\hat{k}_5 = 500$, $b = 2000$, $var = 1$, $f = \frac{2}{365}$.

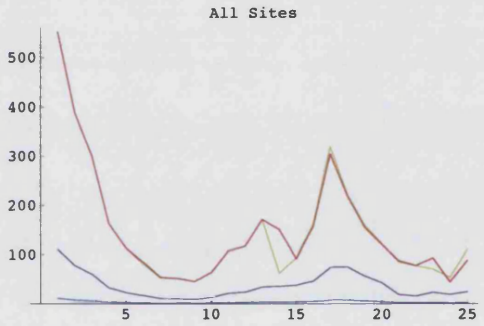


Figure 14.17: Linear configuration (favourable borders $\hat{k}$): $\chi_{i,j} = 0.01$, $\hat{k}_1 = 500$, $\hat{k}_2 = 100$, $\hat{k}_3 = 10$, $\hat{k}_4 = 100$, $\hat{k}_5 = 500$, $b = 2000$, $var = 10$, $f = \frac{2}{365}$.

# Chapter 15

# Results: 2-Dimensional Spatial Model (the Weak Hypothesis)

The following sections illustrate the results obtained running the model with the symmetric 2-dimensional configuration outlined in figure 11.6, and the asymmetric 2-dimensional configuration outlined in figure 11.7, using the Weak hypothesis for the transmission of the disease (see section 1.5.2). The connectivity was not made to vary since in the linear case a change in connectivity proved to make no remarkable difference in model results: $\chi_{i,j} = 0.01$ for all $i, j$, was used throughout the model runs. The disease is inserted after 5 years of model run in site 1, just as in the linear case. All the figures report the average annual population size versus time (in years).

## 15.1 Non-stochastic favourable and non-favourable borders.

For the 2-dimensional spatial configuration outlined in figure 11.6 the model results gave a pattern very similar to the linear case outlined in sections 14.1, except that the disease seems to spread faster for the 2-dimensional configuration then for the linear one. The disease is present in all the sites after 4 years from its appearance for $b = 2000$, and after less then 2 years for $b = 1000$ (as in the linear case). For $b = 100$ the disease transmission to all the sites is instantaneous and the population density crashes to 15. When the threshold capacity is varied such that the border sites have higher (favourable borders, figure 11.11) or lower (non-favourable borders, figure 11.10) threshold capacities we notice that the pattern is less "chaotic" and more similar to what was

observed in some of the Strong hypothesis cases, especially in figures 15.2 and 15.3. The non-favourable borders case still exhibit a chaotic pattern for $b = 1000$ (figure 15.4). In the favourable borders case, the middle site has a threshold capacity of 10: this site is not affected by the disease because the population density is too low (red line in figures 15.1 and 15.2). Thus in the non-favourable borders case we assigned a slightly higher threshold capacity to the borders (namely $\hat{k}_{1,2,3,4} = 50$); still the borders are not affected for $b = 2000$ (figure 15.3).

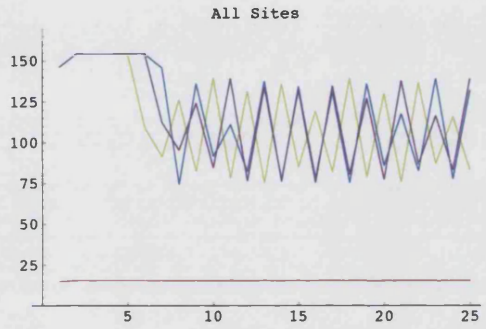


Figure 15.1: 2-Dimensional spatial configuration (favourable borders): $b = 2000$, $\chi_{i,j} = 0.01$, $\hat{k}_{1,2,3,4} = 100$, $\hat{k}_5 = 10$.

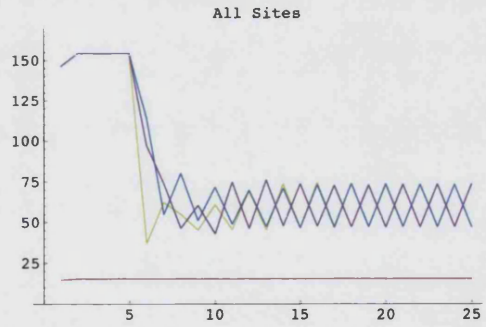


Figure 15.2: 2-Dimensional spatial configuration (favourable borders): $b = 1000$, $\chi_{i,j} = 0.01$, $\hat{k}_{1,2,3,4} = 100$, $\hat{k}_5 = 10$ .

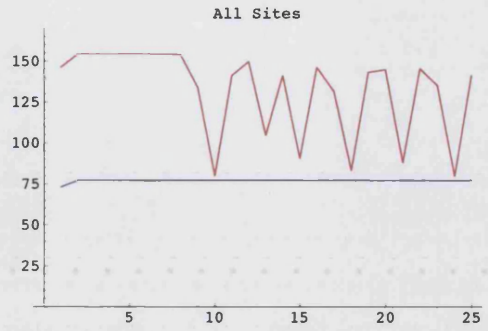


Figure 15.3: 2-Dimensional spatial configuration (non-favourable borders): $b = 2000$, $\chi_{i,j} = 0.01$, $\hat{k}_{1,2,3,4} = 50$, $\hat{k}_5 = 100$ .

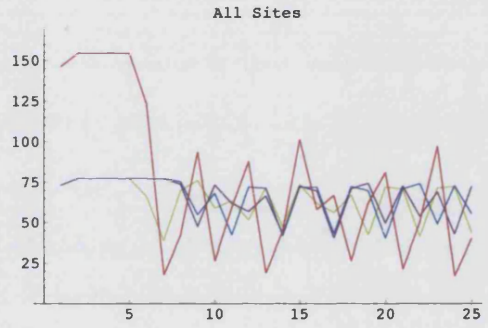


Figure 15.4: 2-Dimensional spatial configuration (non-favourable borders): $b = 1000$, $\chi_{i,j} = 0.01$, $\hat{k}_{1,2,3,4} = 50$, $\hat{k}_5 = 100$ .

## 15.2 Stochastic Varying $\hat{k}$

The climatic variation in the 2-dimensional model contributes in the same way as in the linear model, i.e. it stabilizes the system to certain extent: the pattern is more similar to the single site model. In particular this is observed for the non-favourable borders case outlined in figure 11.10 (figures 15.5 and 15.6), where the sites behave perfectly in phase for both the variances considered ($var = 1$ and $var = 10$) for $b = 2000$. For $b = 100$, the system tends to behave chaotically again, but the higher the variance the more the system behaves as a single site. This is enhanced in the favourable borders case of figure 11.11 (figures 15.7 and 15.8). In the 2-dimensional configuration,

like in the linear one, we notice that for all the stochastic cases the climatic variation plays a bigger role in controlling the population as, even before the disease appears in the system, the population tends to be controlled.

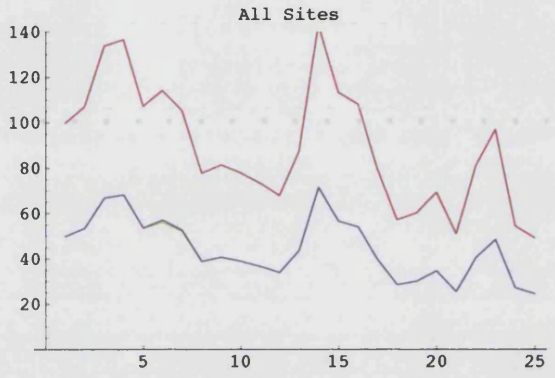


Figure 15.5: 2-D configuration (non-favourable borders): $\chi_{i,j} = 0.01$, $\hat{k}_{1,2,3,4} = 50$, $\hat{k}_5 = 100$, $b = 2000$, $var = 1$, $f = \frac{2}{365}$.

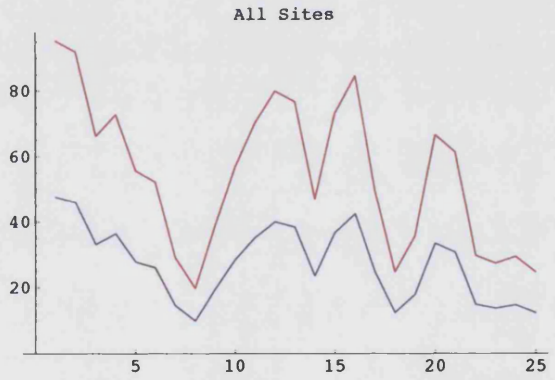


Figure 15.6: 2-D configuration (non-favourable borders $\hat{k}$): $\chi_{i,j} = 0.01$, $\hat{k}_{1,2,3,4} = 50$, $\hat{k}_5 = 100$, $b = 2000$, $var = 10$, $f = \frac{2}{365}$.

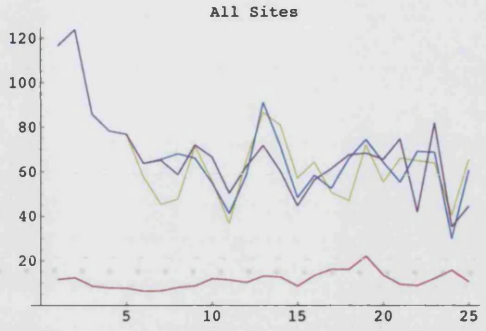


Figure 15.7: 2-D configuration (favourable borders $\hat{k}$): $\chi_{i,j} = 0.01$, $\hat{k}_{1,2,3,4} = 100$, $\hat{k}_5 = 50$, $b = 1000$, $var = 1$, $f = \frac{2}{365}$.

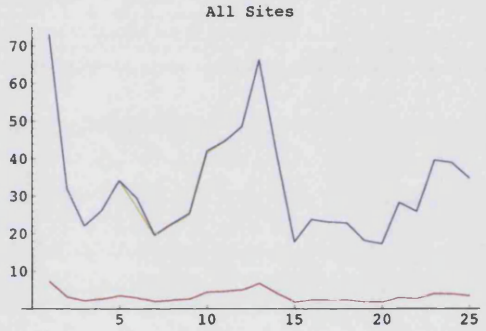


Figure 15.8: 2-D configuration (favourable borders $\hat{k}$): $\chi_{i,j} = 0.01$, $\hat{k}_{1,2,3,4} = 100$, $\hat{k}_5 = 50$, $b = 1000$, $var = 10$, $f = \frac{2}{365}$.

## 15.3 Non-stochastic asymmetric configuration: constant and random connectivity, constant $\hat{k}$

The colour coding for the 2-dimensional asymmetric configuration corresponds to that in figure 11.7, where site 1 is represented by yellow, site 2 by green, site 3 aqua, site 4 by blue, site 5 by purple, site 6 by magenta and site 7 by red. The disease is always inserted in site 1 after 5 years of model run. When the model was run for the asymmetric configuration of figure 11.7 we obtained results similar to the linear and 2-D symmetric case, except that the disease is slower in being transmitted to all the sites compared to the 2-D symmetric case. It takes 7 years (just like in the

linear case) for the disease to have an effect in all the sites for $b = 2000$ (figure 15.9) and less than 2 years for $b = 1000$ (figure 15.10). For $b = 100$ the disease crashes the population in all the sites at the same time. When the connectivity between the sites is varied, the results are the same: the disease takes the same time to be transmitted across the system.

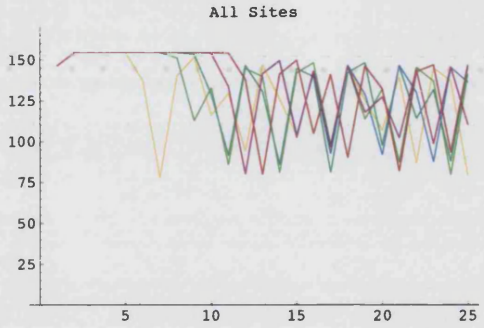


Figure 15.9: Asymmetric spatial configuration: $\chi_{i,j} = 0.01$, $\hat{k} = 100$, $b = 2000$ .

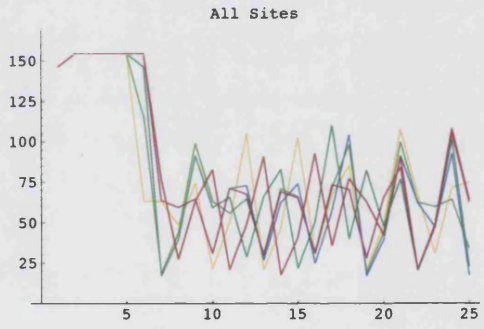


Figure 15.10: Asymmetric spatial configuration: $\chi_{i,j} = 0.01$, $\hat{k} = 100$, $b = 1000$ .

## 15.4 Non-stochastic non-regular configuration: constant and random connectivity, random $\hat{k}$

When the threshold capacity $\hat{k}$ was varied choosing randomly from the values $\hat{k} = 10, 50, 100$ or 500 we did not detect a big variation from what was observed for the linear and 2-D symmetric configuration. The sites with the highest population densities are most affected, especially in the $b = 2000$ case (figure 15.11) in which the sites with lower $\hat{k}$ are not affected by the disease at all. Only in sites 3 and 6 is the disease very successful, even though these are the middle sites in the system. The other sites just transmit the disease to the more populated sites. When the disease becomes more virulent, as in $b = 1000$ (figure 15.12), it affects all the sites, which exhibit the usual pattern previously observed in the linear and 2-D symmetric configurations. For $b = 100$ the population crashes 3 years after the appearance of the disease. When the connectivity was varied choosing randomly between the values of the considered range (see page 221), the model yielded similar results, as the connectivity between the sites does not seem to affect the disease success in the spatial model.

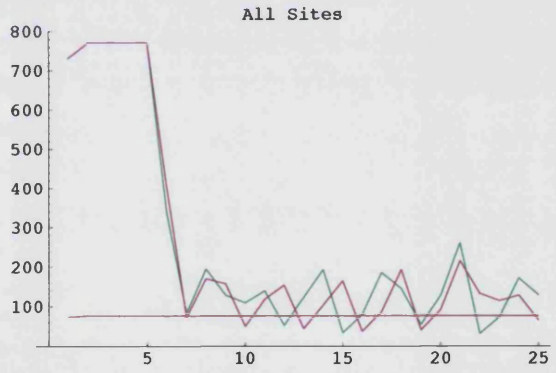


Figure 15.11: Asymmetric spatial configuration: $\chi_{i,j} = 0.01$, $\hat{k}_1 = 50$, $\hat{k}_2 = 50$, $\hat{k}_3 = 500$, $\hat{k}_4 = 50$, $\hat{k}_5 = 50$, $\hat{k}_6 = 500$, $\hat{k}_7 = 50$, $b = 2000$ .

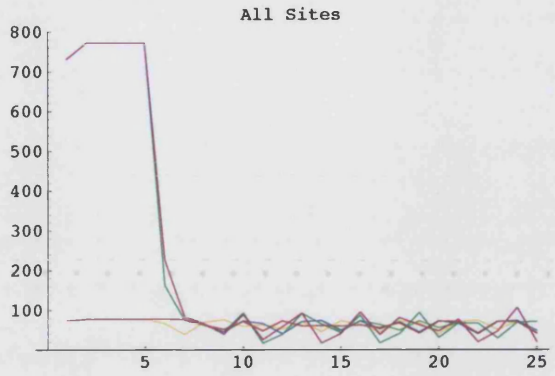


Figure 15.12: Asymmetric spatial configuration: $\chi_{i,j} = 0.01$, $\hat{k}_1 = 50$, $\hat{k}_2 = 50$, $\hat{k}_3 = 500$, $\hat{k}_4 = 50$, $\hat{k}_5 = 50$, $\hat{k}_6 = 500$, $\hat{k}_7 = 50$, $b = 1000$ .

## 15.5 Stochastic asymmetric configuration: constant and random connectivity, constant $\hat{k}$

The model was run for the asymmetric 2-D configuration adding climatic variability to the system. The main feature of the results is that a higher variance of the probability of climatic changes made the sites dynamics more in phase with each other as shown in figures 15.13 and 15.14. The two figures show the results for the $b = 1000$ virulence, and they are the most relevant example of the major role played by the climatic variation in the model simulation. For $b = 2000$ we observe the same pattern, with less random behaviour for lower variance of the climatic change; for $b = 100$ the population crashes and the sites are mostly out of phase since the disease is very virulent and wins over the climatic effects. In figure 15.13 the disease has the effect on the population dynamics of breaking the phase between the sites. When the variance is increased (from $var = 1$ to $var = 10$), the stochastic effects override the disease and, 10 years after the disease is introduced, reestablish the phase between the sites (figure 15.14). The population is still controlled down to an average of half the threshold capacity for the whole run. When the connectivity between the sites is varied we still get the same kind of behaviour.

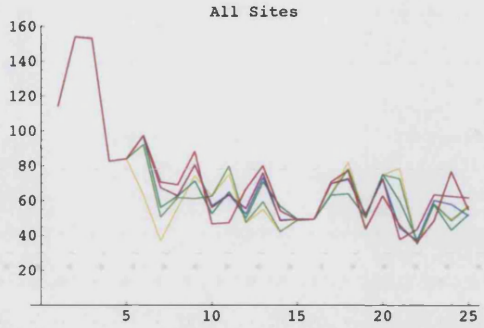


Figure 15.13: Asymmetric homogeneous configuration: $\chi_{i,j} = 0.01$, $\hat{k} = 100$, $b = 1000$, $var = 1$, $f = \frac{2}{365}$.

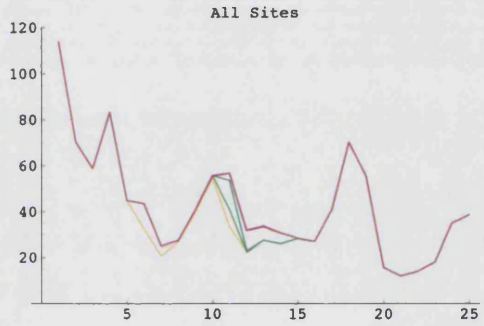


Figure 15.14: Asymmetric homogeneous configuration: $\chi_{i,j} = 0.01$, $\hat{k} = 100$, $b = 1000$, $var = 10$, $f = \frac{2}{365}$.

## 15.6 Stochastic asymmetric configuration: constant and random connectivity, random $\hat{k}$

When the threshold capacity of the sites was varied and climatic changes introduced in the model simulations, we observed similar results to the constant $\hat{k}$ case. The disease is most successful in higher population density sites, like sites 3 and 6 (figures 15.15 and 15.16). In the other sites climatic variation probably takes over in controlling the population size since the sites are perfectly in phase, while for site 3 and 6 dynamics there is a difference in pattern (figure 15.15). Even when the sites' threshold capacity is different we notice that climatic variation reduces the irregularity

in the patterns of the population dynamics of the system. This is highlighted in figure 15.16 where for $var = 10$ sites 3 and 6, the patterns are coming closer in behaviour. We obtained a similar type of behaviour for other values of $b$ and for different values of the connectivity between the sites.

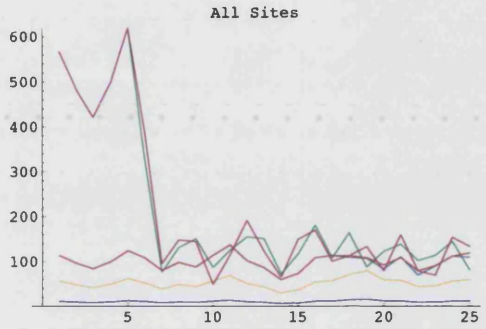


Figure 15.15: Asymmetric configuration: $\chi_{i,j} = 0.01$, $\hat{k}_1 = 50$, $\hat{k}_2 = 100$, $\hat{k}_3 = 500$, $\hat{k}_4 = 100$, $\hat{k}_5 = 10$, $\hat{k}_6 = 500$, $\hat{k}_7 = 100$, $b = 2000$, $var = 1$, $f = \frac{2}{365}$.

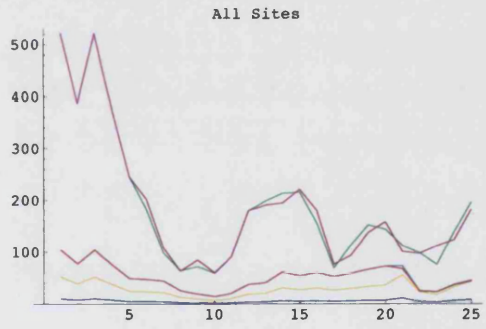


Figure 15.16: Asymmetric configuration: $\chi_{i,j} = 0.01$, $\hat{k}_1 = 50$, $\hat{k}_2 = 100$, $\hat{k}_3 = 500$, $\hat{k}_4 = 100$, $\hat{k}_5 = 10$, $\hat{k}_6 = 500$, $\hat{k}_7 = 100$, $b = 2000$, $var = 10$, $f = \frac{2}{365}$.

# Chapter 16

# Evolution.

In the last part of this research, we consider a model that allows the investigation of the evolution of the disease virus. In fact there will be variation caused by mutation on which selection acts. This variation is reflected in the fact that a virus has normally more than one strain present in the environment, which differ in fitness. Natural selection will privilege that strain that is most effective at survival and reproduction (i.e. has the highest fitness). In general transmission success (=fitness) [4] is maximised for strains of intermediate virulence [6], where by "virulence" we mean the virus growth rate within a host. For example a very virulent strain might kill its host too fast for it to infect other hosts. On the other hand a weak strain might allow the host to recover before it spreads the virus to another individual. Often the natural evolution of a disease sustains an intermediate strain of the virus, as in the case of myxomatosis where the evolution of the virus favoured strains of intermediate virulence in Australia and England [37]. Being a relatively new disease, not much is known on the predominant strain of RCD. The literature mentions low virulence and chronic forms of the disease, but there is not much information. The subacute form is most often described in the later stages of an epidemic, and the chronic form is considered to be extremely uncommon [68]. Not much information is available about the strains associated with other forms of the disease [126]. It has been realised that there is the possibility of change in the virus, and in particular its virulence for rabbits, subsequent to any use of the virus as a biological control agent [139]. New variants of the virus have appeared in Europe between 1997 and 1998 [21], [54], [82] and [107]: they still retain virulence and there is no evidence that the virus will evolve towards a less virulent strain [141]. Various authors reported the presence of an endemic non-pathogenic strain, or a strain cross reactive with RCV, [23], [82], [118], [128] but this was present in rabbit sera collected in Europe

(Czech Republic) before RHD was discovered for the first time in China [100], [101].

We use the single site model to predict which strain of the disease might be selected over time. In the version of the model we consider here, $b[\ell]$ represents the virulence of strain $\ell$ of the virus, while $m_V[\ell]$ is the corresponding decay rate of the virus in the environment. Then $\bar{T}_V[\ell] = \frac{1}{m_V[\ell]}$ is the life expectancy of that virus strain. Fifteen different strains of the virus were represented, namely $b[1] = 100$, $b[2] = 200$, $b[3] = 300$, $b[4] = 400$, $b[5] = 500$, $b[6] = 600$, $b[7] = 700$, $b[8] = 800$, $b[9] = 900$, $b[10] = 1000$, $b[11] = 2000$, $b[12] = 3000$, $b[13] = 4000$, $b[14] = 5000$, $b[15] = 10000$. These values come from experimenting with changes in $b$ in the single site model for both the Strong hypothesis and the Weak hypothesis (see chapter 3). It includes very virulent strains, such as the one characterised by $b = 100$, to very weak strains, such as the one characterised by $b = 10000$.

In section 3.1.4, we defined $b$ as $\frac{c}{w}$, where $c$ is a measure of the virulence of the virus strain and $w$ the rate of virus release (per day) by an infected host. Thus, in the present context we define $w[\ell] = \frac{c}{b[\ell]}$, where the "infectivity", $c = 800$, is kept fixed for any virus strain $\ell$. $c$ is a measure of the infectivity of the virus. That is, for a given environmental viral load $V$, the probability of a rabbit becoming infected increases as $c$ decreases (see section 3.1.4). The virus is "virulent" if it reproduces rapidly within the host: i.e. if $w$ is large. In this chapter, we investigate the evolution of virulence, keeping the infectivity fixed. Varying $c$ at the same time might be very complicated. This value of the infectivity, $c = 800$, is chosen so that for the median value of $b$ in the chosen range, $b = 800$, the rate of virus release is 1. ¿From this we obtain the values $w[\ell]$ for each $b[\ell]$, namely $w[1] = 8$, $w[2] = 4$, $w[3] = 2.66667$, $w[4] = 2$, $w[5] = 1.6$, $w[6] = 1.3333$, $w[7] = 1.14286$, $w[8] = 1$, $w[9] = 0.888889$, $w[10] = 0.8$, $w[11] = 0.4$, $w[12] = 0.266667$, $w[13] = 0.2$, $w[14] = 0.16$, $w[15] = 0.08$. There are three parameters, or traits that play a key role in determining the disease characteristics, namely $w$, $m_V$ and $CM$, and they can be dependent or independent from each other. When they are independent we say that there is *no trade − off* between them. Conversely a trade-off exists between them when they are linked by some functional dependence.

*"In fact the basic hypothesis underlying most analyses of the evolution of life history traits is that variation is constrained in large measure by trade-offs between traits. These trade-offs can be defined and the evolution of the traits can be predicted either by a genetic model or by one which assumes that selection maximizes some measurable metric that defines fitness."*

—Roff [102].

Not much is known on RCD so it is difficult to determine what is fitness for this particular virus. In our evolution model we assume that there are different genetic strains of the virus and we let them compete in the context of the dynamics of the host population. The virus then evolves towards the distribution of strains that "wins"; i.e. persists in the environment. But as Roff [102] says:

*"selection does not produce perfect genotypes, but it favors the best which the numerous constraints upon it allow... Within these constraints there are further trade-offs that dictate the set of possible life history traits."*

—Roff [102].

We then assume that there are constraints in the evolution of the virus, and we express such constraints in the form of trade-offs. We consider only pairwise trade-offs between $w$, $m_V$ and $CM$ and we now discuss the nature of these trade-offs.

Given the complexity of our basic disease model with fixed virulence, we can expect a model which allows evolution of virulence to be even more complex. In fact the non-spatial disease model will be used to investigate the virus evolution, but the presence of more than one strain will enhance the model complexity. In particular the main difficulty is in determining an expression for the virus basic reproductive ratio $\mathcal{R}_0$, i.e. the expected number of new cases resulting from a single newly-infected animal introduced into a susceptible population [10]. In order to investigate $\mathcal{R}_0$ and find the possible forms of the trade-offs, we build first a simpler model which will allow us to determine the shape of the trade-off functions. These trade-offs will then be used in the single site stochastic disease model with multiple strains to determine whether the results predicted by the simple model are sustained in the context of the more complex model. The results between the Strong hypothesis and Weak hypothesis models will then be compared.

## 16.1 The $\mathcal{SIRV}$ Model

In this section we construct a simplified disease model which can be analysed completely. Consider a general simplified version of model (3.2), with no age structure and where the parameters are as follows (note that the term 'rate' refers to 'probability per unit of time', which is one day in our case):

- $\lambda$ is the birth rate (it is assumed that infecteds do not give birth),
- $m$ is the natural death rate,
- $CM$ is the disease case mortality,
- $\nu$ is the recovery rate,
- $\kappa$ is the rate of loss of immunity by recovered individuals,
- $m_V$ is the decay rate of virus in the environment,
- $w$ is the rate of virus release by an infected individual,
- $c_V$ is the rate at which susceptibles become infected.

We assume that $c_V$ has the Michaelis-Menten form $c_V$ (see section 3.1.4)

$$c_V = \frac{V}{c+V},$$

with $c > 0$ the environmental load at which the probability of a susceptible becoming infected in a given unit is one half.

The model we consider is given by the discrete-time dynamical system

$$\left.\begin{aligned} S[t+1] &= \lambda(S[t]+R[t]) + (1-m)\{(1-c_V)S[t] + \kappa R[t]\}, \\ I[t+1] &= (1-m)\{(1-CM-\nu)I[t] + c_V S[t]\}, \\ R[t+1] &= (1-m)\{(1-\kappa)R[t] + \nu I[t]\}, \\ V[t+1] &= (1-m_V)V[t] + wI[t]\}. \end{aligned}\right\} \tag{16.1}$$

The total population size is $N[t] = S[t] + I[t] + R[t]$. We allow for the possibility that one or both of the natural birth and death rates are density dependent. Thus, we assume:

$$\begin{aligned} \lambda &= \lambda(N) \quad \text{with } \lambda'(N) \leq 0 \\ m &= m(N) \quad \text{with } m'(N) \geq 0 \end{aligned} \tag{16.2}$$

[See figure 16.1]. If at least one of the above inequalities are strict, then density-dependence is present.

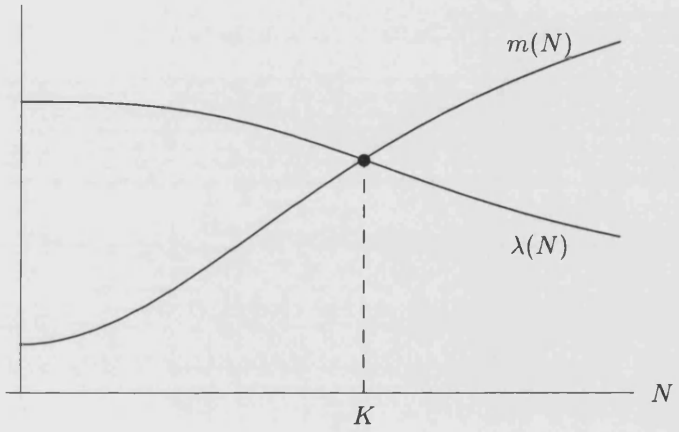


Figure 16.1: The unique disease-free equilibrium $N = K$ when $\lambda$ and $m$ are density dependent.

### 16.1.1 The Disease-free Equilibrium

The disease-free ($\mathcal{DF}$) equilibrium occurs when $I = R = V = 0$, and the population size is $N = S = K$. It follows that $c_V = 0$ (see section 3.1.4). The model (16.1) reduces to

$$N[t+1] = (\lambda + 1 - m)N[t]$$

At equilibrium, $N[t+1] = N[t] = K > 0$, and hence, $\lambda = m$.

If there is density dependence, as in (16.2), then $K$ is uniquely determined (See figure 16.1), i.e. there is only one point for which $\lambda(N) = m(N)$. If there is no density dependence, then $K > 0$ exists only if $\lambda = m$, and is then arbitrary.

To determine the stability of the $\mathcal{DF}$ equilibrium, consider $\Phi(N) = (\lambda + 1 - m)N$. The disease-free dynamics is then $N[t+1] = \Phi(N[t])$. The standard theory of discrete-time dynamical systems says that the $\mathcal{DF}$ equilibrium is locally asymptotically stable provided $\mid \Phi'(K) \mid < 1$, and is unstable if $\mid \Phi'(K) \mid > 1$. Now,

$$\Phi'(N) = (\lambda + 1 - m) + \{\lambda'(N) - m'(N)\}N,$$

and at equilibrium this gives

$$\Phi'(K) = 1 - (m' - \lambda')K,$$

where $\lambda' = \lambda'(K) \leq 0$ and $m' = m'(K) \geq 0$ by (16.2). Thus, $(m' - \lambda') \geq 0$, with equality only if there is no density dependence. It follows that the $\mathcal{DF}$ is locally asymptotically stable provided

$$-1 < 1 - (m' - \lambda')K < 1.$$

The right hand inequality always holds if there is density dependence, and left hand inequality holds if and only if

$$m' - \lambda' < 2.$$

Thus, the difference in slopes at equilibrium between the two curves in figure 16.1 must not be too large. We shall assume this is the case. If it is not, then there may be more complex dynamics (such as cycles) even in the disease-free situation.

### 16.1.2 Disease take-off

For the disease to invade a disease-free equilibrium population, we require that the $\mathcal{DF}$ equilibrium be unstable with respect to the full disease dynamics (16.1). This depends on the *basic reproductive ratio*, defined to be

$$\mathcal{R}_0 = \frac{(\frac{w}{cm_V})K}{\frac{m}{1-m} + \nu + CM}. \tag{16.3}$$

This is the number of new infections generated on average by one infected host in a population of susceptible individuals of size $K$ and it is a ratio of transmission to survival, where we define the *transmission rate* to be

$$\tau = \frac{w}{c m_V} = \frac{1}{b m_V}. \tag{16.4}$$

It is shown in Appendix 1 that the $\mathcal{DF}$ equilibrium is invadable by the disease if $\mathcal{R}_0 > 1$, and is uninvadable if $\mathcal{R}_0 < 1$.

In general, the reproductive success of a specific genetic strain of the virus will tend to depend on the number of hosts infected by the transmission stages produced by the host within the primary infection. This quantity, which effectively measures the Darwinian 'fitness' of the parasite [1], is simply the basic reproductive ratio $\mathcal{R}_0$ defined in (16.3).

Since selection in the parasite population will favour a high $\mathcal{R}_0$ [6], we assume in what follows that the virus evolves so as to maximise $\mathcal{R}_0$, subject to whatever trade-offs between virus characteristics apply.

### 16.1.3 Trade-offs

A more virulent strain will reproduce faster in the body of the host, and hence will produce more virus particles to be discharged into the environment. We therefore assume that the viral discharge rate $w$ is a measure of virulence, with high $w$ representing high virulence, and $w = 0$ representing the absence of virus.

In what follows we shall assume for simplicity that there is no trade-off between virulence and recovery, so that $\nu$ = constant throughout. In fact, under this assumption, there is no loss of generality in taking $\nu = 0$, so there is no recovery. If $\nu > 0$, simply replace $CM$ by $cm = \frac{CM}{1-\nu}$, $c$ by $(1-\nu)c$ and $M = \frac{m}{1-m}$ by $M = \frac{m}{1-m} + \frac{\nu}{1-\nu}$, in the discussion below.

Since case mortality should increase with virulence, we assume that $CM$ is an increasing function of $w$, with $CM = 0$ when $w = 0$ and $CM \to 1$ as $w \to \infty$.

On the other hand, a more virulent virus is characterised by a fast reproduction within the host. If it is assumed that there is a trade-off between this and the ability of survival in the environment (i.e. between hosts), then the viral environment-decay rate should also increase as $w$ increases. That

is, it is assumed that $m_V$ is an increasing function of $w$ with $m_V = 0$ when $w = 0$ (a non-existent virus survives for ever), and $m_V \to 1$ as $w \to \infty$ (a perfectly virulent virus does not survive at all).

A simple and convenient functional form for these trade-offs is given by

$$CM(w) = \frac{w^\alpha}{c_0 + w^\alpha}, \qquad m_V(w) = \frac{w^\beta}{m_0 + w^\beta}, \tag{16.5}$$

where $c_0, m_0 > 0$, and $\alpha, \beta \geq 0$. Note that $\alpha = 0$ is the case in which there is no trade-off between $CM$ and $w$. Similarly, $\beta = 0$ is the case in which there is no trade-off between $m_V$ and $w$. The functions (16.5) are illustrated in Figure 16.2.

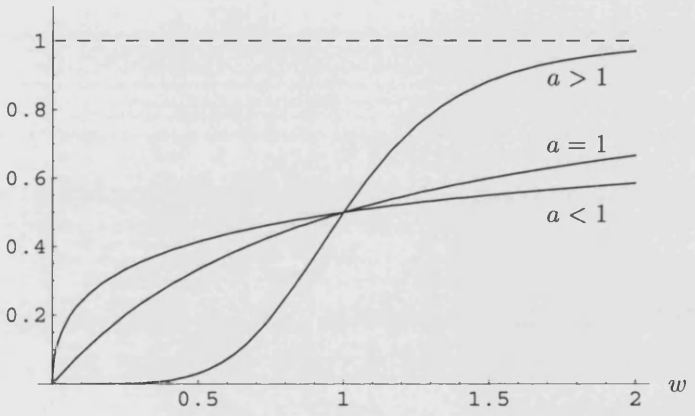


Figure 16.2: The trade-off functions $\frac{w^a}{h+w^a}$ for various $a$ ($a = \alpha$ or $\beta$). In these examples $h = 1$ ($h = c_0$ or $m_0$).

We assume that $w$ is normalised so that $w = 1$, $b = 800$ represents a mid-range virulence. ¿From (16.5) it follows that

$$c_0 = \frac{1}{CM(1)} - 1, \qquad m_0 = \frac{1}{m_V(1)} - 1. \tag{16.6}$$

No trade-offs

This is the case $\alpha = \beta = 0$, and hence $CM$ and $m_V$ are constant as the virulence $w$ changes. ¿From (16.3), $\mathcal{R}_0$ is a linear function of $w$ with positive slope, since all the other parameters are constant. Hence, $\mathcal{R}_0$ increases with $w$; and we expect the virus to evolve to its maximum virulence.

No trade-off between $CM$ and $w$; trade-off between $m_V$ and $w$

In this case $\alpha = 0$ and $\beta > 0$ in (16.5). Then $\mathcal{R}_0$ is proportional to

$$f(w) = \frac{w}{m_V(w)} = w^{1-\beta}(m_0 + w^\beta) = w + m_0 w^{1-\beta},$$

since every other parameter is constant. Thus,

$$f'(w) = 1 + m_0(1-\beta)w^{-\beta}.$$

Clearly this is positive if $\beta \leq 1$, and hence $\mathcal{R}_0$ is monotonically increasing in $w$. We therefore expect the virus to evolve to its maximum virulence.

On the other hand, if $\beta > 1$, then $f'(w) > 0$ for $w > w^*$ and $f'(w) < 0$ for $w < w^*$, where $w^* = [m_0(\beta - 1)]^{\frac{1}{\beta}}$. That is, $f(w)$ has a global minimum at $w^*$, and hence, so does $\mathcal{R}_0$.

It follows that $\mathcal{R}_0$ increases as $w$ decreases for $w < w^*$, and as $w$ increases for $w > w^*$. Thus, there are two possible evolutionarily stable states, namely virus strains of minimum and of maximum virulence. Which of these outcomes is likely to be realised in a given population will depend ultimately on which has the higher $\mathcal{R}_0$. Since $f(w) \sim w$ as $w \to \infty$, and $f(w) \sim \frac{m_0}{w^{\beta-1}}$ as $w \to 0$, it follows that $\mathcal{R}_0$ increases faster as $w \to \infty$ than it does as $w \to 0$ if $\beta - 1 < 1$, and vice versa if $\beta - 1 > 1$. That is, we expect the virus to evolve to maximum virulence if $1 < \beta < 2$, and to minimum virulence if $\beta > 2$.

If $\beta = 2$, then $\frac{w}{m_0 w^{\beta-1}} = \frac{1}{m_0}$, and the limit $w \to \infty$ has the higher $\mathcal{R}_0$ if this is greater than 1, and the limit $w \to 0$ has the higher $\mathcal{R}_0$ if this is less than 1.

Trade-off between $CM$ and $w$; possible trade-off between $m_V$ and $w$

In this case $\alpha > 0$ and $\beta \geq 0$ in (16.5). The case $\beta = 0$ is no trade-off between $m_V$ and $w$. If $\beta > 0$ there is such a tradeoff. We deal with these two cases together.

Since $\alpha > 0$, we may invert the first relation in (16.5) to obtain,

$$w = \left[\frac{c_0 CM}{1 - CM}\right]^{\frac{1}{\alpha}}.$$

Substituting in the second relation gives $m_V$ as a function of $CM$,

$$m_V(CM) = \frac{(c_0 CM)^{\frac{\beta}{\alpha}}}{m_0(1 - CM)^{\frac{\beta}{\alpha}} + (c_0 CM)^{\frac{\beta}{\alpha}}} \tag{16.7}$$

Of course, this gives $m_V = \frac{1}{m_0+1}$ constant when $\beta = 0$.

Substituting in (16.3) and (16.5) we obtain,

$$\mathcal{R}_0 = \frac{\tau(CM)K}{M + CM}, \tag{16.8}$$

where $M = \frac{m}{1-m}$ is a constant, and

$$\tau(CM) = \frac{1}{c}\Big\{\Big(\frac{c_0 CM}{1-CM}\Big)^{\frac{1}{\alpha}} + m_0\Big(\frac{c_0 CM}{1-CM}\Big)^{\frac{1-\beta}{\alpha}}\Big\}. \tag{16.9}$$

It is easily seen that $\tau(CM)$ is monotonically increasing for $\beta \leq 1$, and that $\tau(CM)$ has a unique minimum at $CM = \frac{B}{(c_0+B)}$, where $B = [m_0(\beta - 1)]^{\frac{\alpha}{\beta}}$, for $\beta > 1$. The possible shapes of the transmission curves $\tau(CM)$ for various $\alpha$ and $\beta$ are shown in Fig 16.3.

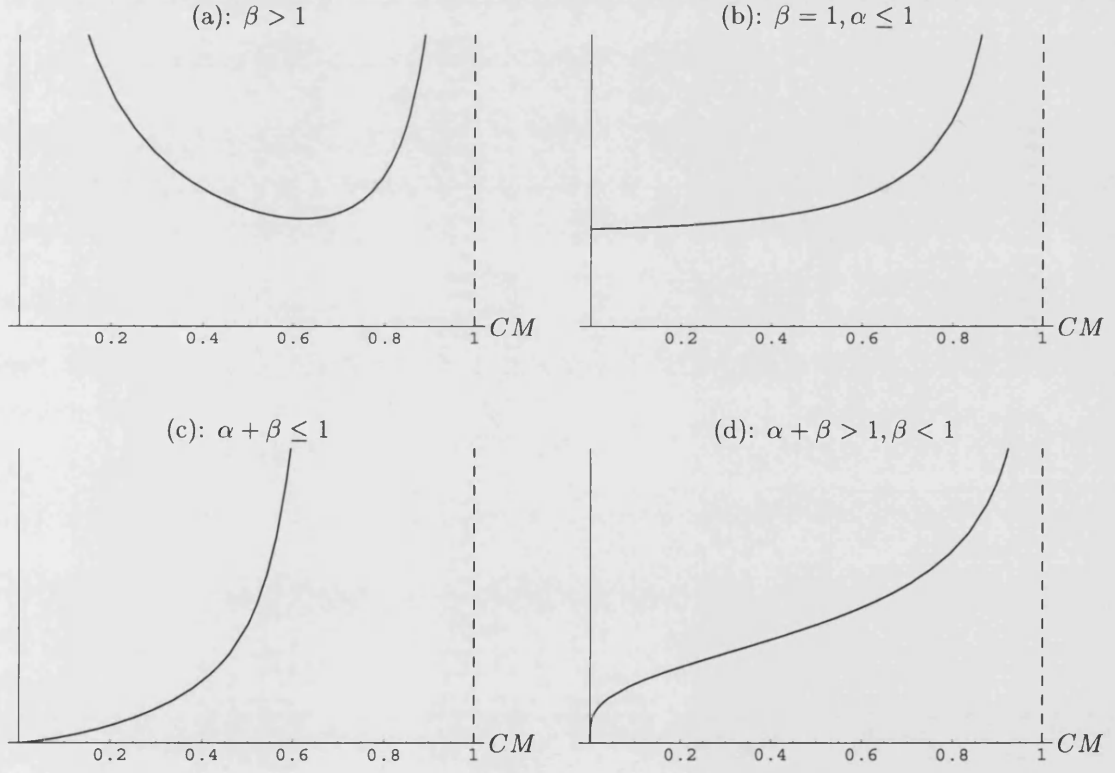


Figure 16.3: The possible forms of the transmission function $\tau(CM)$ given by (16.9) for various $\alpha$ and $\beta$. The case $\alpha > 1$, $\beta = 1$ looks like case (d) except that the curve is raised vertically by an amount $\frac{m_0}{c}$.

It follows from (16.8) that

$$\frac{d\mathcal{R}_0}{dCM} = \frac{\{(M+CM)\tau'(CM) - \tau(CM)\}K}{(M+CM)^2},$$

which is positive if

$$\tau'(CM) > \frac{\tau(CM)}{M+CM}, \tag{16.10}$$

and negative if this inequality is reversed. If $\tau'(CM) = \frac{\tau(CM)}{M+CM}$, then $\mathcal{R}_0$ has a turning point (since $\frac{d\mathcal{R}_0}{dCM} = 0$) . If $CM^*$ is such a turning point, then it is a maximum of $\mathcal{R}_0$ if (16.10) holds for $CM < CM^*$ and the reverse inequality holds for $CM > CM^*$. In this case, we expect virulence to evolve to the value $w^* = w(CM^*)$, i.e. to the maximum value of $\mathcal{R}_0$.

On the other hand, if (16.10) holds for $CM > CM^*$ and the reverse inequality holds for $CM < CM^*$, then $\mathcal{R}_0$ is minimised at $CM^*$. We therefore expect $w$ to evolve to lower values if $w < w^*$, and to higher values if $w > w^*$. Which of these outcomes occurs will depend on which direction, ultimately, gives the largest $\mathcal{R}_0$.

There are four distinct cases to consider, as illustrated in Fig 16.4.

*Case (a):* There is a single turning point at $CM^*$ which is a minimum of $\mathcal{R}_0$. The virus either evolves to its minimum virulence or to its maximum virulence.

*Case (b):* Similar to case (a), except that there should be stronger selection pressure driving evolution to maximum virulence.

*Case (c):* No turning point for $\mathcal{R}_0$ exists and (16.10) holds for all $CM$. The virus therefore evolves to its maximum virulence.

*Case (d):* There are two turning points, $0 < CM_0^* < CM_1^*$, with $CM_0^*$ a local maximum of $\mathcal{R}_0$ and $CM_1^*$ a local minimum. Thus, any initial virulence $w < w_1^*$ should evolve to the intermediate (though not very virulent) stable state $w_0^*$, and any initial virulence $w > w_1^*$ should evolve to the maximum possible virulence.

If we assume that mutations allow $w$ to explore the entire virulence range $w > 0$ (equivalently, the case-mortality range $0 \leq CM < 1$), then it is clear from (16.8) and (16.9) that $\mathcal{R}_0 \to \infty$ as $w \to \infty$ (equivalently, $CM \to 1$). In cases (b) and (d), the low-virulence evolutionarily stable states have finite $\mathcal{R}_0$, and it follows that we should expect the virus to evolve to maximum virulence.

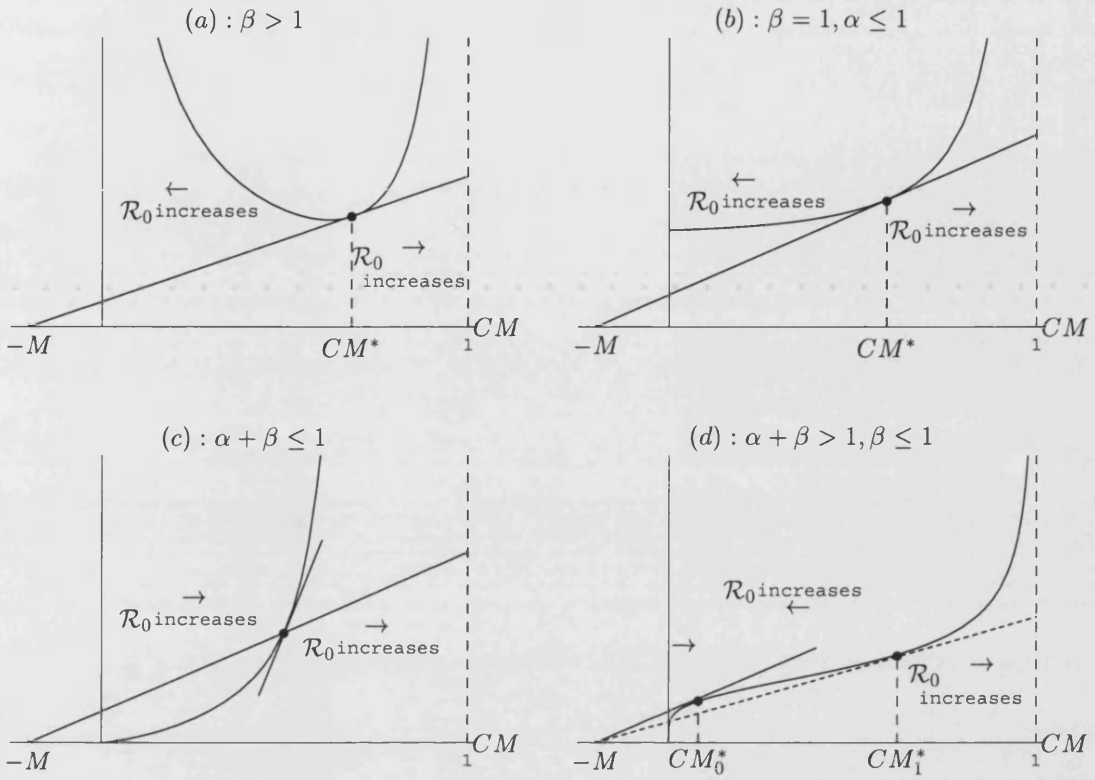


Figure 16.4: The directions of evolution of the virus under the assumption that $\mathcal{R}_0$ increases in the various trade-off scenarios considered in figure 16.3. The case $\alpha > 1$, $\beta = 1$ looks like case (d) except that the curve is raised vertically by an amount $\frac{m_0}{c}$.

In case (a), the situation is more delicate, since $\mathcal{R}_0 \to \infty$ both as $CM \to 1$ and as $CM \to 0$. For $\beta > 1$,

$$\mathcal{R}_0(CM) \sim \frac{K}{c} \cdot \frac{1}{M+1} \cdot \left(\frac{c_0 CM}{1-CM}\right)^{\frac{1}{\alpha}} \qquad \text{as } CM \to 1,$$

$$\mathcal{R}_0(CM) \sim \frac{K}{c} \cdot \frac{m_0}{M} \cdot \left(\frac{1-CM}{c_0 CM}\right)^{\frac{\beta-1}{\alpha}} \qquad \text{as } CM \to 0.$$

Thus, $\mathcal{R}_0 \to \infty$ as $CM \to 1$ faster than it does as $CM \to 0$ if $\beta - 1 < 1$, and vice versa if $\beta - 1 > 1$. That is, we expect the virus to evolve to maximum virulence if $1 < \beta < 2$, and to minimum virulence if $\beta > 2$.

If $\beta = 2$, the limit $CM \to 0$ has the higher $\mathcal{R}_0$ if the ratio $\frac{m_0(M+1)}{M}$ is greater than 1. This is always true if $m_0 \geq 1$. We conclude that the virus evolves to its minimum virulence in this case.

Since these conclusions also holds in the case $\alpha = 0$ (no tradeoff between $CM$ and $w$), we may summarise our findings as follows.

SUMMARY. Assume tradeoff relations of the form (16.5) with $\alpha, \beta \geq 0$. Assume also that unrestricted mutations allow the virus to explore its entire virulence range $w > 0$, and that the virus evolves to maximise the basic reproductive ratio, $\mathcal{R}_0$, given by (16.8). Then if $m_0 > 1$ and $\beta < 2$, the virus will evolve towards a state of maximum virulence ($w \to \infty$). If $\beta \geq 2$, the virus will evolve towards the state of minimum virulence ($w \to 0$).

### 16.1.4 Restricted Virulence

The above analysis assumes that the virus can evolve to arbitrarily high levels of virulence ($w \to \infty$). However, this may not be realistic. In particular, there may be physical limitations on the rate of reproduction within a host (and subsequent discharge into the environment of virus particles) of any virus strain in a given family. In this case, there can be no virus strain with $w > \hat{w}$ for some finite maximum virulence $\hat{w}$.

In this situation, the alternative, low virulence equilibria associated with cases (a), (b) and (d) of Fig 16.4 may be preferred by evolution if they have higher $\mathcal{R}_0$ than the finite value $\hat{\mathcal{R}}_0$ associated with $\hat{w}$. This will certainly be the case if $\hat{w} < w^* = w(CM^*)$ in case (b), or $w_0^* < \hat{w} < w_1^*$ in case (d). In case (a), $\mathcal{R}_0 \to \infty$ as $w \to 0$, and so evolution towards minimum virulence is inevitable for any $\beta > 1$.

### 16.1.5 Results from the $\mathcal{SIRV}$ Model

The evolutionary $\mathcal{SIRV}$ model is outlined in Appendix 2, equation (16.12); the results obtained by running the model are illustrated in figures 16.5-16.8.

The virus has fifteen different strains as explained at the beginning of this chapter. It is assumed that a virus strain can mutate into a neighbouring strain with probability $\mu$. Each strain can switch to the next weaker or stronger strain with probability $\frac{1}{2}\mu$; only the absolute weakest ($\ell = 15$) and strongest ($\ell = 1$) strains can mutate into a stronger and weaker strain respectively with probability $\mu$. In the model runs the value $\mu = 10^{-2}$ was chosen arbitrarily as a suitable value for the mutation rate. This means, on average, one mutation event every 100 days. This value was chosen so high in order to reduce the computer run times.

We assumed density-dependence to be present by allowing $m = m(N)$ (see equation 16.2), where $N$ is the total population size and $\lambda$ to be constant. The model was run for $10,000$ days (i.e. $= 27.49$ years) and the disease was inserted after 5 years on the first day of the year with an intermediate strain of the virus, namely $w[\ell] = 1$ with $\ell = 8$.

Figure 16.5 is obtained by running the model with a transmission shown in figure 16.3(a) which gives a direction of the evolution of the virus as in figure 16.4(a). As predicted in the theory we find that the selected viral strain is of low virulence $[w \to w[15]]$ by the end of the run, i.e. $\mathcal{R}_0$ is maximised for low virulence strains for any shape of the trade-offs for which $\beta > 1$.

Figure 16.6 is obtained by running the model with a transmission shown in figure 16.3(b) which gives a direction of the evolution of the virus as in figure 16.4(b). In this case we get a less expected result, in fact we found that $\mathcal{R}_0$ is maximised for low or high virulence strains depending on the shape of the trade-offs. In fact for $\beta = 1$, $\mathcal{R}_0$ is maximised at high virulence strains $[w \to w[1]]$ when $\alpha \leq 0.2$; on the other hand $\mathcal{R}_0$ is maximised for low virulence strains $[w \to w[15]]$ when $\alpha > 0.2$. Thus depending on the shape of the trade-offs, i.e. on the values of $\alpha$ and $\beta$, the direction of evolution might be maximised towards lower or higher virulence. This might be due to the fact that $\beta = 1$ is a transitional case between $\beta < 1$ and $\beta > 1$ (Cases (a) and (d)).

Figure 16.7 is obtained by running the model with a transmission shown in figure 16.3(c) which gives a direction of the evolution of the virus as in figure 16.4(c). As predicted in the theory we find that the selected viral strain is of high virulence $[w \to w[1]]$ by the end of the run, i.e. $\mathcal{R}_0$ is maximised for high virulence strains for any shape of the trade-offs for which $\alpha + \beta \leq 1$.

Figure 16.8 is obtained by running the model with a transmission shown in figure 16.3(d) which gives a direction of the evolution of the virus as in figure 16.4(d). From the theory we expect to find two possible directions of evolution of the virus which depend on the trade-off shape and the values of $CM_0^*$ and $CM_1^*$. In fact the direction of evolution could be towards the local maximum of $\mathcal{R}_0$ at $CM_0^*$ (intermediate/low virulence), or towards maximum virulence. Figure 16.8 shows that for a fixed $\alpha = 1.5$, we get that $\mathcal{R}_0$ is maximised for high virulence $[w \to w[1]]$ if $\beta \leq 0.3$; on the other hand $\mathcal{R}_0$ is maximised for intermediate/low virulence $[w \to w[13]]$ if $\beta > 0.3$.

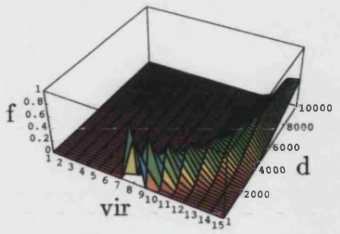


Figure 16.5: Case (a): $\beta > 1$. $\alpha = 0.5$ and $\beta = 1.5$.

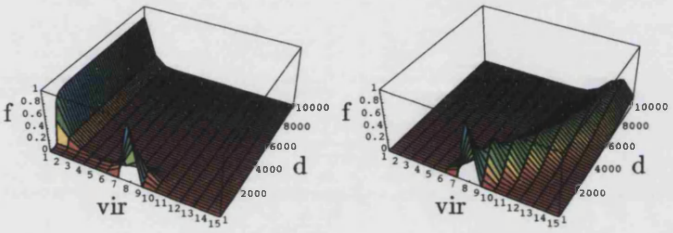


Figure 16.6: Case (b): $\beta = 1$. $\alpha = 0.2$, $\beta = 1$ on the left. $\alpha = 0.3$, $\beta = 1$ on the right.

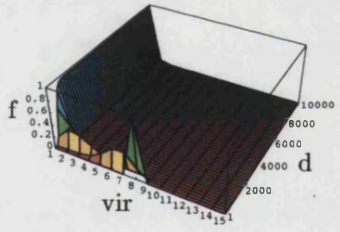


Figure 16.7: Case (c): $\alpha + \beta \leq 1$. $\alpha = 0.5$ and $\beta = 0.2$.

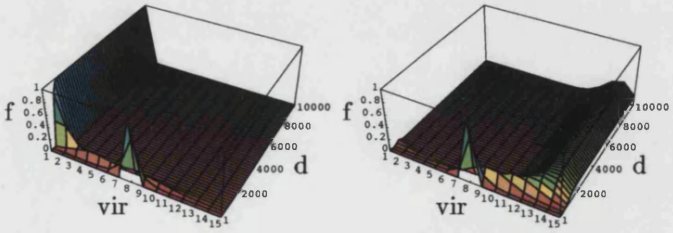


Figure 16.8: Case (d): $\alpha = 1.5$ and $\beta = 0.3$ on the left and $\alpha = 1.5$ and $\beta = 0.4$ on the right.

## 16.2 The Stochastic Single-Site Evolution Models

We will now use the same trade-offs illustrated in section 16.1.3 in a stochastic single-site model which allows for the competition of different strains of the virus. The detailed models, following the Strong and Weak hypothesis , that were used to investigate the evolution of the virus are given in Appendix 2 (equations (16.13) and (16.14)) to this chapter.

It can be observed that the models are very similar to the single site model (equation (3.2)), but in the evolution models the disease parameters are not always constant, but vary as a function of the strain index $\ell$. Each value of $b[\ell]$ represents a different virus strain. We assume $c = 800$ to remain constant.

There are also different population variables for rabbits infected by different strains and a new parameter, namely $\mu$, which represents the mutation probability of the virus. Thus, it is assumed that a virus strain can mutate into a neighbouring strain with probability $\mu$. Each strain can switch to the next weaker or stronger strain with probability $\frac{1}{2}\mu$; only the absolute weakest ($\ell = 15$) and strongest ($\ell = 1$) strains can mutate into a stronger and weaker strain respectively with probability $\mu$. In the model runs the value $\mu = 10^{-2}$ was chosen arbitrarily as a suitable value for the mutation rate. This means, on average, one mutation event every 100 days. This value was chosen so high in order to reduce the computer run times. The other disease parameters vary for each virus strain according to the trade-offs described earlier (equation 16.5).

Since we assume that $w$ is normalised so that $w = 1$, $b = 800$ and $c = 800$ represent a mid-range virulence, from (16.5) and (16.6) it follows that taking $CM(1) = 0.475$ and $m_V(1) = 0.066$ to be the standard empirical values for the median virulence, we obtain

$$c_0 = 1.105, \qquad m_0 = 15.667.$$

Then the life expectancy of the virus, $\bar{T}_V = \frac{1}{m_V(1)} = 15.15$ days is also constant for the median virulence strain.

The probability of infection for a particular strain now takes the form:

$$c_V[\ell] = \frac{V[\ell]}{c + V_{tot}} \tag{16.11}$$

where $V_{tot} = \sum_{\ell=1}^{\ell=15} V[\ell]$; while the probability of being infected by *some* strain is:

$$c_{V_{tot}} = \sum_{\ell} c_V[\ell] = \frac{V_{tot}}{c + V_{tot}}.$$

Moreover, in the evolution models, the case mortality becomes $CM[\ell]$ as it may vary according to the virus strain. The possible values are listed in tables 2, 3, 4 and 5. Note that we have assumed that evolution of the virus does not take place in Juveniles, since their reaction to the virus is not determined as simply as for Adults and Subadults. In particular, in the Weak hypothesis model $CM\_$, the case mortality for Juveniles born to susceptible pregnant females and older than one month, is taken to be independent of the virus strain.

The variables (infected rabbits) are now characterised by three indices: time $t$, age $k$ and virus strain $\ell$, with $1 \leq \ell \leq L = 15$. Thus, $I_a[t, k, \ell]$ is the density of infected rabbits of age class $a$ who have been in the age class for $k$ days on day $t$ and who are infected with virus strain $\ell$.

The models were run for two of the regions for which we have seasonal data. We chose Subalpine and Riverina as they each represent environmental extremes: marginal in Subalpine and favourable in Riverina. Thus, we included seasonality of the birth rate, stochastic variation only for the variance of the lognormal distribution $var = 1$, and on average one climatic change event per year ($f = 1/365$). The threshold level of the population for density dependent effect on Juvenile mortality to be activated was $\hat{k} = 100$. The model was run for 25 years and the disease was introduced in the environment after 5 years on the first day of the year with an intermediate strain of the virus, namely $b[8] = 800$.

The results are given in sections 16.2.1. For each trade-off the results for the Strong hypothesis and the Weak hypothesis are shown together for both regions for an easier comparison.

### 16.2.1 Results obtained from the Stochastic Evolution Models

The values of $b[\ell]$ and $w[\ell]$ for each virus strain $\ell$ are given in table 1. These values are used in running models (16.13) and (16.14) (see Appendix 2):

| $\ell$ | $b[\ell]$ | $w[\ell]$ |
|---|---|---|
| 1 | 100 | 8 |
| 2 | 200 | 4 |
| 3 | 300 | 2.66667 |
| 4 | 400 | 2 |
| 5 | 500 | 1.6 |
| 6 | 600 | 1.33333 |
| 7 | 700 | 1.14286 |
| 8 | 800 | 1 |
| 9 | 900 | 0.888889 |
| 10 | 1000 | 0.8 |
| 11 | 2000 | 0.4 |
| 12 | 3000 | 0.266667 |
| 13 | 4000 | 0.2 |
| 14 | 5000 | 0.16 |
| 15 | 10000 | 0.08 |

Table 1. Values of $b[\ell]$ and $w[\ell]$ for each virus strain.

*Case (a): $\beta > 1$.*

We show here as a representative case the values $\alpha = 0.5$ and $\beta = 1.5$ in the trade-off equations (16.5). A plot of the functions $m_V(w)$, $m_V(b)$, $CM(w)$ and $CM(b)$ is shown in figure 16.9. Thus it is possible to calculate the virus decay rate $m_V[\ell]$, the virus life expectancy $\bar{T}_V[\ell] = \frac{1}{m_V[\ell]}$, the case mortality $CM[\ell]$ and the host life expectancy after catching the disease $\bar{T} = \frac{1}{CM[\ell]+\nu_a}$ for each $b$ and $w$, where the recovery rate $\nu_a = 0.025$ $(a = Y, A)$ is kept constant. The results are given in table 2. Figure 16.10 shows the transmission $\tau$ (see equation 16.9) as a function of the case mortality $CM$, which can be compared to figure 16.3(a). Since the range of $w$ is restricted as explained in section 16.1.4, i.e. $0.08 \leq w \leq 8$, the curve is cut at $CM(w = 8)$.

According to the theory for the $\mathcal{SIRV}$ model in section 16.1.3, we would expect the virus to evolve to a less virulent strain. The stochastic evolution models (16.13) and (16.14) are not likely to have a simple form of $\mathcal{R}_0$ as in the $\mathcal{SIRV}$ model (see equation (16.3)); but we may still expect the same qualitative phenomena for the main types of trade-offs. In order to check that we get similar

results with both models (16.13) and (16.14), we run these models for 25 years using the trade-offs described above, breeding data from the Subalpine and Riverina environments and stochastic climatic changes as described in chapter 4. The results are shown in figure 16.11. We can observe that for both regions and both hypothesis, the virus evolves to a less virulent strain in agreement with the theory. We get similar results for other values of $\alpha$ and $\beta$ for which $\beta > 1$. Note also that there is not much difference in the results obtained from running the model with the Strong or Weak hypothesis, nor between the two different environment Subalpine or Riverina, apart from the Subalpine-Weak hypothesis for which the virus is virtually extinct for about 3-4 years 2 years after the disease appearance (see figure 16.11).

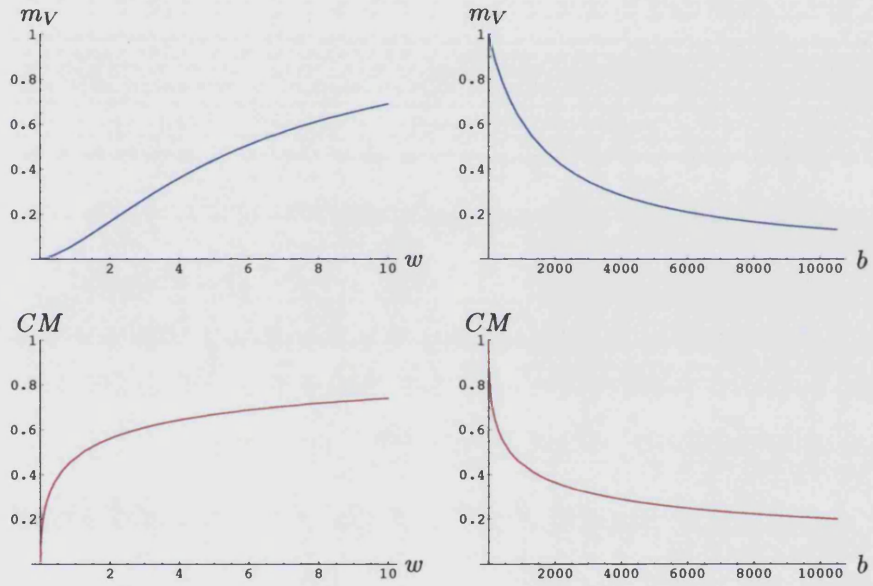


Figure 16.9: *Case*$(a)$: $\beta > 1$. Trade-off functions for $\alpha = 0.5$ and $\beta = 1.5$.

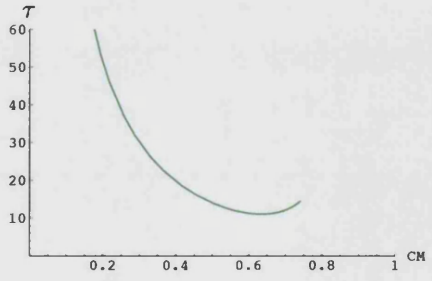


Figure 16.10: *Case*$(a)$: $\beta > 1$. Transmission $\tau$ as a function of $CM$.

| $\ell$ | $b$ | $w$ | $m_V$ | $\bar{T}_V$ | $CM$ | $\bar{T}$ |
|---|---|---|---|---|---|---|
| 1 | 100 | 8 | 0.615 | 1.625 | 0.719 | 1.344 |
| 2 | 200 | 4 | 0.361 | 2.769 | 0.644 | 1.495 |
| 3 | 300 | 2.667 | 0.235 | 4.25 | 0.596 | 1.609 |
| 4 | 400 | 2 | 0.167 | 6 | 0.561 | 1.706 |
| 5 | 500 | 1.6 | 0.125 | 7.992 | 0.534 | 1.790 |
| 6 | 600 | 1.333 | 0.098 | 10.191 | 0.511 | 1.866 |
| 7 | 700 | 1.143 | 0.079 | 12.583 | 0.492 | 1.935 |
| 8 | 800 | 1 | 0.066 | 15.152 | 0.475 | 2 |
| 9 | 900 | 0.889 | 0.056 | 17.886 | 0.460 | 2.06 |
| 10 | 1000 | 0.8 | 0.048 | 20.777 | 0.447 | 2.117 |
| 11 | 2000 | 0.4 | 0.018 | 56.939 | 0.364 | 2.571 |
| 12 | 3000 | 0.267 | 0.01 | 103.766 | 0.318 | 2.912 |
| 13 | 4000 | 0.2 | 0.006 | 159.219 | 0.288 | 3.19 |
| 14 | 5000 | 0.16 | 0.005 | 222.117 | 0.266 | 3.44 |
| 15 | 10000 | 0.08 | 0.002 | 626.415 | 0.204 | 4.371 |

Table 2. Values of $b[\ell]$, $w[\ell]$, $m_V[\ell]$, $\bar{T}_V$, $CM[\ell]$ and $\bar{T}$ when $\alpha = 0.5$ and $\beta = 1.5$.

*Case (b): $\beta = 1$, $\alpha \leq 1$.*

We show here the case for which $\beta = 1$ and $\alpha = 0.5$. A plot of the functions $m_V(w)$, $m_V(b)$, $CM(w)$ and $CM(b)$ for these values of $\alpha$ and $\beta$ is shown in figure 16.12 and the values for the virus decay rate $m_V[\ell]$, the virus life expectancy $\bar{T}_V[\ell] = \frac{1}{m_V[\ell]}$, the case mortality $CM[\ell]$ and the host life expectancy after catching the disease $\bar{T} = \frac{1}{CM[\ell]+\nu_a}$ for each $b$ and $w$ are in table 3. Figure 16.13 shows the transmission $\tau$ as a function of the case mortality $CM$ for this particular trade-off; this figure should be compared with figure 16.3(b) in the theory. Due to restricted virulence (see section 16.1.4), the curve is cut at $CM(w = 8)$. This is probably the reason why we get the unexpected result shown in figure 16.14 from running the stochastic models (16.13) and (16.14) with the above values of $\alpha$ and $\beta$. We observe either an oscillation between high and low virulence (figure 16.14, (a) and (b)) or a more definite prevalence of a low virulence strain (figure 16.14 (c) and (d)). The theory predicts maximisation of $\mathcal{R}_0$ for high virulence but we have observed by running the $\mathcal{SIRV}$ model that depending on the values of $\alpha$ and $\beta$ we can get high or low virulence or an

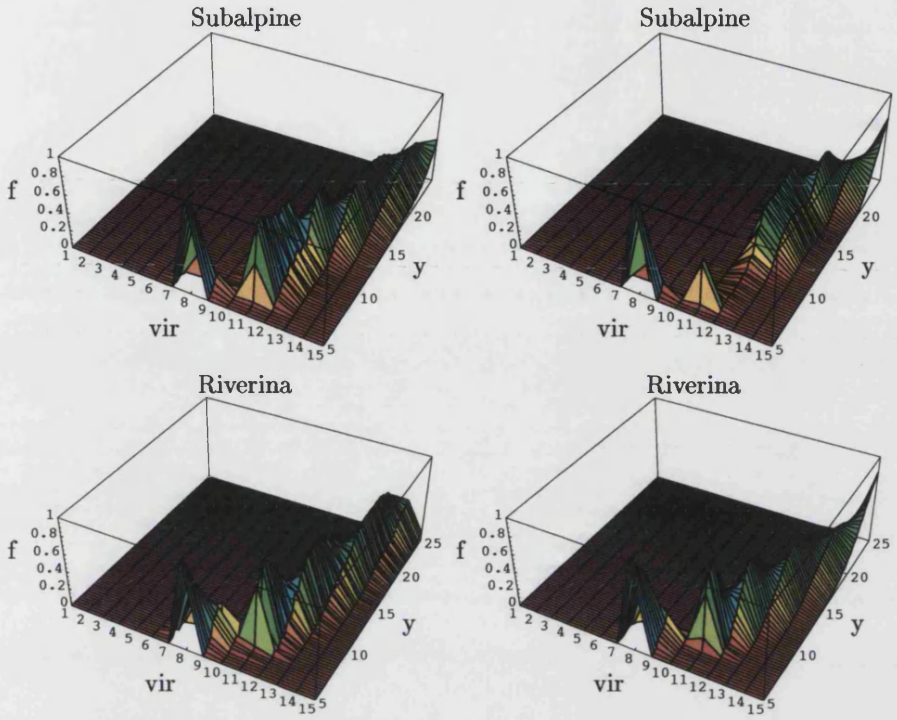


Figure 16.11: Case (a): $\beta > 1$. $\alpha = 0.5$, $\beta = 1.5$. f= frequency of virus strain in the environment, vir= virulence, y= years. (a) Subalpine- Strong Hypothesis (top left). (b) Subalpine- Weak Hypothesis (top right). (c) Riverina- Strong Hypothesis (bottom left). (d) Riverina- Weak Hypothesis (bottom right).

oscillation between the two (see section 16.1.5, figure 16.6). For $\beta = 1$, $\alpha \geq 0.5$ we get oscillations or intermediate (Strong hypothesis)/low (Weak hypothesis) virulence strains are selected; for $\beta = 1$, $\alpha < 0.5$ we observe that high virulence strains are predominant (not shown). Note that in the Riverina case there is a more prominent difference between the strains that are selected depending on the Juvenile immunity hypothesis considered. In fact in the Strong hypothesis (figure 16.14 (c)), after an oscillation of about 5 years, intermediate/low strains are selected. In the Weak hypothesis (figure 16.14 (d)) very low virulence strains are selected without any oscillation. In Subalpine the virus remains at a very low level for 3-4 years in the Strong hypothesis case (figure 16.14 (a)) and for about 13 years in the Weak hypothesis case (figure 16.14 (b)). The virus does not become extinct as figure 16.14 might indicate, as the vertical scale is not small enough to show that the virus in fact remains present, but at extremely low levels. In fact after investigating on the single site and spatial model we found that Subalpine being a marginal environment for rabbits, it cannot sustain a population density large enough for the virus to outbreak.

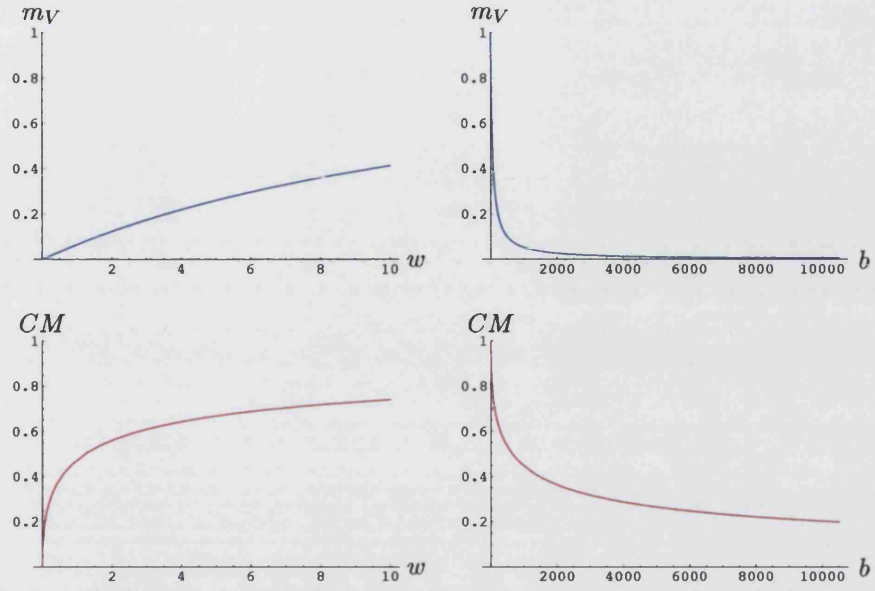


Figure 16.12: *Case*$(b)$: $\beta = 1$, $\alpha \leq 1$. Trade-off functions for $\alpha = 0.5$ and $\beta = 1.5$.

| $\ell$ | $b$ | $w$ | $m_V$ | $\bar{T}_V$ | $CM$ | $\bar{T}$ |
|---|---|---|---|---|---|---|
| 1 | 100 | 8 | 0.361 | 2.769 | 0.719 | 1.344 |
| 2 | 200 | 4 | 0.220 | 4.538 | 0.644 | 1.495 |
| 3 | 300 | 2.667 | 0.159 | 6.307 | 0.596 | 1.609 |
| 4 | 400 | 2 | 0.124 | 8.076 | 0.561 | 1.706 |
| 5 | 500 | 1.6 | 0.102 | 9.845 | 0.534 | 1.790 |
| 6 | 600 | 1.333 | 0.086 | 11.614 | 0.511 | 1.866 |
| 7 | 700 | 1.143 | 0.075 | 13.383 | 0.492 | 1.935 |
| 8 | 800 | 1 | 0.066 | 15.152 | 0.475 | 2 |
| 9 | 900 | 0.889 | 0.059 | 16.921 | 0.460 | 2.06 |
| 10 | 1000 | 0.8 | 0.054 | 18.689 | 0.447 | 2.117 |
| 11 | 2000 | 0.4 | 0.027 | 36.379 | 0.364 | 2.571 |
| 12 | 3000 | 0.267 | 0.018 | 54.068 | 0.318 | 2.912 |
| 13 | 4000 | 0.2 | 0.014 | 71.758 | 0.288 | 3.19 |
| 14 | 5000 | 0.16 | 0.011 | 89.447 | 0.266 | 3.44 |
| 15 | 10000 | 0.08 | 0.006 | 177.894 | 0.204 | 4.371 |

Table 3. Values of $b[\ell]$, $w[\ell]$, $m_V[\ell]$, $\bar{T}_V$, $CM[\ell]$ and $\bar{T}$ when $\alpha = 0.5$ and $\beta = 1$.

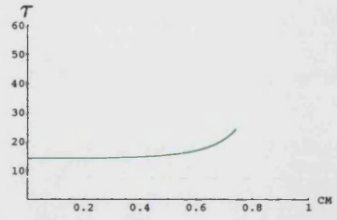


Figure 16.13: *Case*$(b)$: $\beta = 1$, $\alpha \leq 1$. Transmission $\tau$ as a function of $CM$.

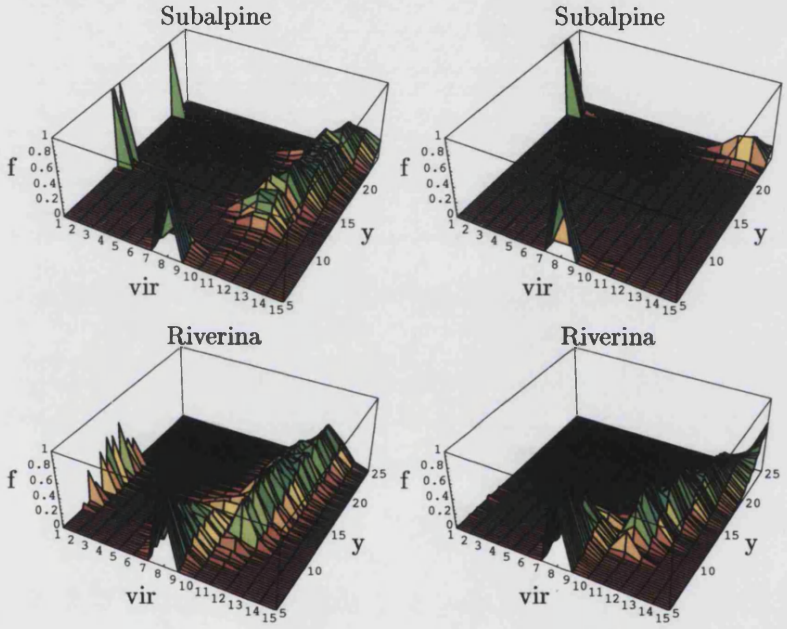


Figure 16.14: Case (b): $\beta = 1$, $\alpha \leq 1$. $\alpha = 0.5$, $\beta = 1$. f= frequency of virus strain in the environment, vir= virulence, y= years. (a) Subalpine- Strong Hypothesis (top left). (b) Subalpine- Weak Hypothesis (top right). (c) Riverina- Strong Hypothesis (bottom left). (d) Riverina- Weak Hypothesis (bottom right).

*Case (c): $\alpha + \beta \leq 1$.*

Figure 16.15 shows the shape of the trade-off functions $m_V(b)$, $m_V(w)$, $CM(b)$ and $CM(w)$ when $\alpha = 0.5$ and $\beta = 0.2$. We take these values for $\alpha$ and $\beta$ as an example of case (c) of figures 16.3 and 16.4. From the trade-off functions we can calculate the value of the virus decay rate $m_V[\ell]$, the virus life expectancy $\bar{T}_V[\ell] = \frac{1}{m_V[\ell]}$, the case mortality $CM[\ell]$ and the host life expectancy after catching the disease $\bar{T} = \frac{1}{CM[\ell]+\nu_a}$ for each $b$ and $w$. These values are tabulated in table 4. A plot of the transmission $\tau$ as a function of the case mortality $CM$ is shown in figure 16.16. In this case we can anticipate that the result will be as we expect from the $\mathcal{SIRV}$ theory (section 16.1.5), i.e. evolution will be towards a maximum virulence strain. In fact restricted virulence is less important in this case and we can observe that even though $w$ cannot go to infinity but has an upper bound, still the transmission is unequivocally maximised for high values of $w$ as shown in figure 16.16. Figure 16.17 shows the result of running the Strong Hypothesis model (16.13) for the Subalpine stochastic data. Similar results were observed for the Weak hypothesis and for the Riverina environment, even though, for Riverina, the virus doesn't become extinct but persists with a high virulent strain (not shown). Moreover we obtained similar results for different values of $\alpha$ and $\beta$ for which $\alpha + \beta \leq 1$.

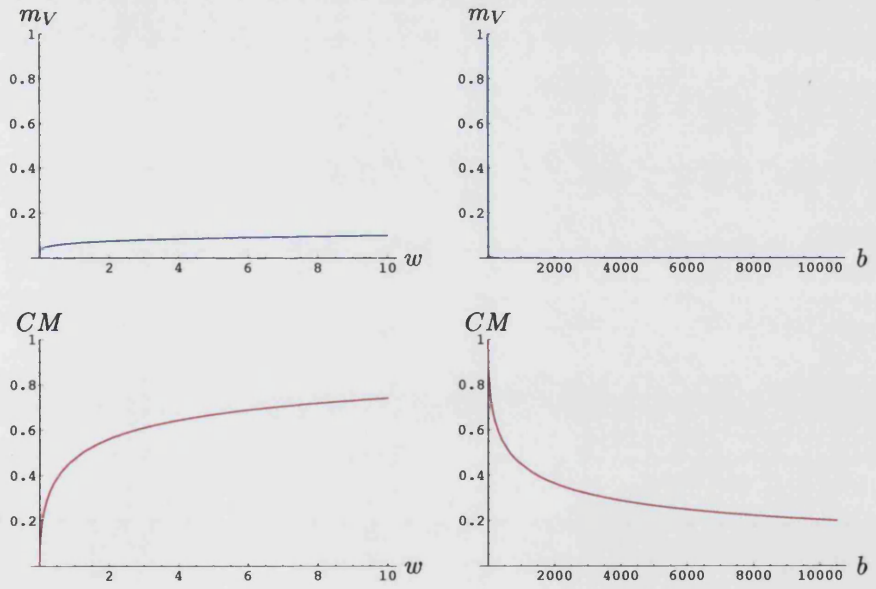


Figure 16.15: *Case(c)*: $\alpha + \beta \leq 1$. Trade-off functions for $\alpha = 0.5$ and $\beta = 0.2$.

| $\ell$ | $b$ | $w$ | $m_V$ | $\bar{T}_V$ | $CM$ | $\bar{T}$ |
|---|---|---|---|---|---|---|
| 1 | 100 | 8 | 0.097 | 10.337 | 0.719 | 1.344 |
| 2 | 200 | 4 | 0.085 | 11.725 | 0.644 | 1.495 |
| 3 | 300 | 2.667 | 0.079 | 12.631 | 0.596 | 1.609 |
| 4 | 400 | 2 | 0.075 | 13.320 | 0.561 | 1.706 |
| 5 | 500 | 1.6 | 0.072 | 13.882 | 0.534 | 1.790 |
| 6 | 600 | 1.333 | 0.070 | 14.360 | 0.511 | 1.866 |
| 7 | 700 | 1.143 | 0.068 | 14.779 | 0.492 | 1.935 |
| 8 | 800 | 1 | 0.066 | 15.152 | 0.475 | 2 |
| 9 | 900 | 0.889 | 0.065 | 15.489 | 0.460 | 2.06 |
| 10 | 1000 | 0.8 | 0.063 | 15.797 | 0.447 | 2.117 |
| 11 | 2000 | 0.4 | 0.056 | 17.998 | 0.364 | 2.571 |
| 12 | 3000 | 0.267 | 0.051 | 19.434 | 0.318 | 2.912 |
| 13 | 4000 | 0.2 | 0.049 | 20.525 | 0.288 | 3.19 |
| 14 | 5000 | 0.16 | 0.047 | 21.416 | 0.266 | 3.44 |
| 15 | 10000 | 0.08 | 0.041 | 24.452 | 0.204 | 4.371 |

Table 4. Values of $b[\ell]$, $w[\ell]$, $m_V[\ell]$, $\bar{T}_V$, $CM[\ell]$ and $\bar{T}$ when $\alpha = 0.5$ and $\beta = 0.2$.

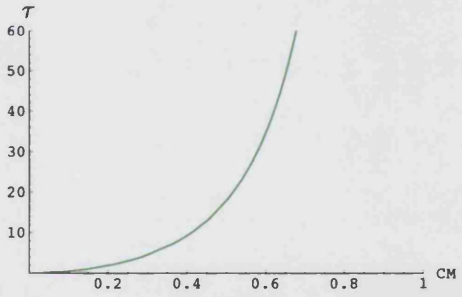


Figure 16.16: *Case(c)*: $\alpha + \beta \leq 1$. $\alpha = 0.5$, $\beta = 0.2$. Transmission $\tau$ as a function of $CM$.

*Case (d):* $\alpha + \beta > 1$, $\beta < 1$.

In section 16.1.3 we explained that for $\alpha + \beta > 1$, $\beta < 1$ we expect two turning points in the curve of the direction of evolution of the virus. One of the points is a local maximum of $\mathcal{R}_0$ and the other is a local minimum (figure 16.4(d)). Thus, any initial virulence should evolve to either an intermediate

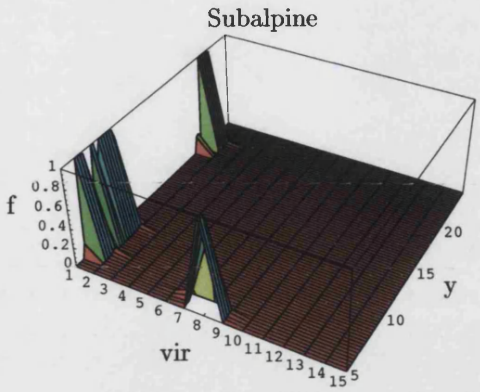


Figure 16.17: *Case*$(c)$: $\alpha+\beta \leq 1$. $\alpha = 0.5, \beta = 0.2$. f= frequency of virus strain in the environment, vir= virulence, y= years. Subalpine, Strong Hypothesis.

(though not very virulent) strain or to the maximum possible virulence. We ran models (16.13) and (16.14) to see if we could find these two turning points. We tried to find the two turning points for both regions and both hypotheses by running the model for a trade-off between $m_V$ and $w$ and $CM$ and $w$ choosing a fixed value of $\alpha$, say $\alpha = 1.5$ and changing value of $\beta$ in the range $\beta < 1$. In the Weak hypothesis case we found the turning points for $\alpha = 1.5$ and $\beta = 0.5$ for both Subalpine and Riverina. But this result doesn't hold for the Strong hypothesis case: for these range of values we get that a high virulence strain is selected (not shown). The trade-off functions $m_V(b)$, $m_V(w)$, $CM(b)$ and $CM(w)$ for these values are shown in figure 16.18. From these trade-off functions we calculated the values of the virus decay rate $m_V[\ell]$, the virus life expectancy $\bar{T}_V[\ell] = \frac{1}{m_V[\ell]}$, the case mortality $CM[\ell]$ and the host life expectancy after catching the disease $\bar{T} = \frac{1}{CM[\ell]+\nu_a}$ for each $b$ and $w$. These values are given in table 5. The transmission function $\tau$ is shown in figure 16.19. For comparison we also include the transmission functions for $\alpha = 1.5$, $\beta = 0.4$ and $\beta = 0.6$. The results from running model (16.14) (Weak hypothesis) with the Subalpine and Riverina stochastic data for trade-off functions with these values of $\alpha$ and $\beta$ are shown in figure 16.20. In the Riverina case the virus is continuously present and doesn't go through intervals of very low levels as it does for Subalpine. We observe that for $\beta \leq 0.4$ the virus evolves to a high virulence strain. When $\beta = 0.5$ we get oscillation between prevalence of high virulence and low virulence strains: these are the two equilibrium points discussed in section 16.1.3 (figure 16.4(d)). When $\beta \geq 0.6$, the virus evolves more to low virulence strains and in Subalpine it tends to be more continuously present in the environment.

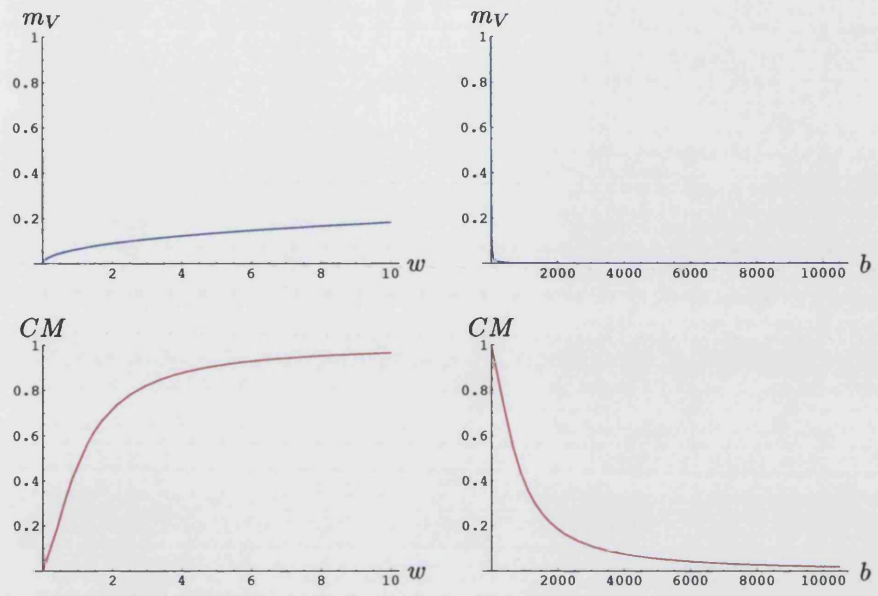


Figure 16.18: *Case(d)*: $\alpha + \beta > 1$, $\beta < 1$. Trade-off functions for $\alpha = 1.5$ and $\beta = 0.5$.

| $\ell$ | $b$ | $w$ | $m_V$ | $\bar{T}_V$ | $CM$ | $\bar{T}$ |
|---|---|---|---|---|---|---|
| 1 | 100 | 8 | 0.167 | 6.003 | 0.953 | 1.022 |
| 2 | 200 | 4 | 0.124 | 8.076 | 0.879 | 1.107 |
| 3 | 300 | 2.667 | 0.103 | 9.666 | 0.798 | 1.216 |
| 4 | 400 | 2 | 0.091 | 11.007 | 0.719 | 1.344 |
| 5 | 500 | 1.6 | 0.082 | 12.189 | 0.647 | 1.489 |
| 6 | 600 | 1.333 | 0.075 | 13.256 | 0.582 | 1.647 |
| 7 | 700 | 1.143 | 0.070 | 14.238 | 0.525 | 1.818 |
| 8 | 800 | 1 | 0.066 | 15.152 | 0.475 | 2 |
| 9 | 900 | 0.889 | 0.062 | 16.010 | 0.431 | 2.192 |
| 10 | 1000 | 0.8 | 0.059 | 16.822 | 0.393 | 2.392 |
| 11 | 2000 | 0.4 | 0.043 | 23.376 | 0.186 | 4.734 |
| 12 | 3000 | 0.267 | 0.035 | 28.404 | 0.112 | 7.364 |
| 13 | 4000 | 0.2 | 0.031 | 32.644 | 0.075 | 10.013 |
| 14 | 5000 | 0.16 | 0.027 | 36.379 | 0.055 | 12.542 |
| 15 | 10000 | 0.08 | 0.020 | 51.033 | 0.020 | 22.192 |

Table 5. Values of $b[\ell]$, $w[\ell]$, $m_V[\ell]$, $\bar{T}_V$, $CM[\ell]$ and $\bar{T}$ when $\alpha = 1.5$ and $\beta = 0.5$.

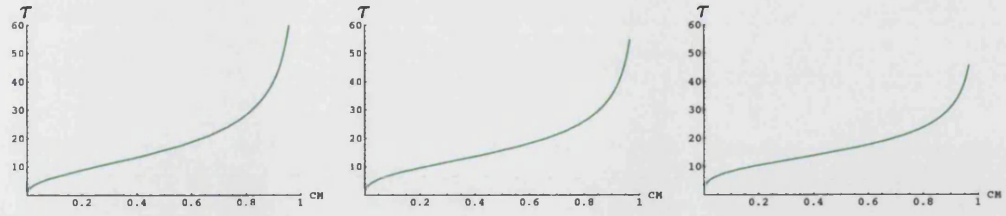


Figure 16.19: *Case(d)*: $\alpha + \beta > 1$, $\beta < 1$. Transmission $\tau$ as a function of $CM$. $\alpha = 1.5$, $\beta = 0.4$ (left), $\beta = 0.5$ (centre) and $\beta = 0.6$ (right).

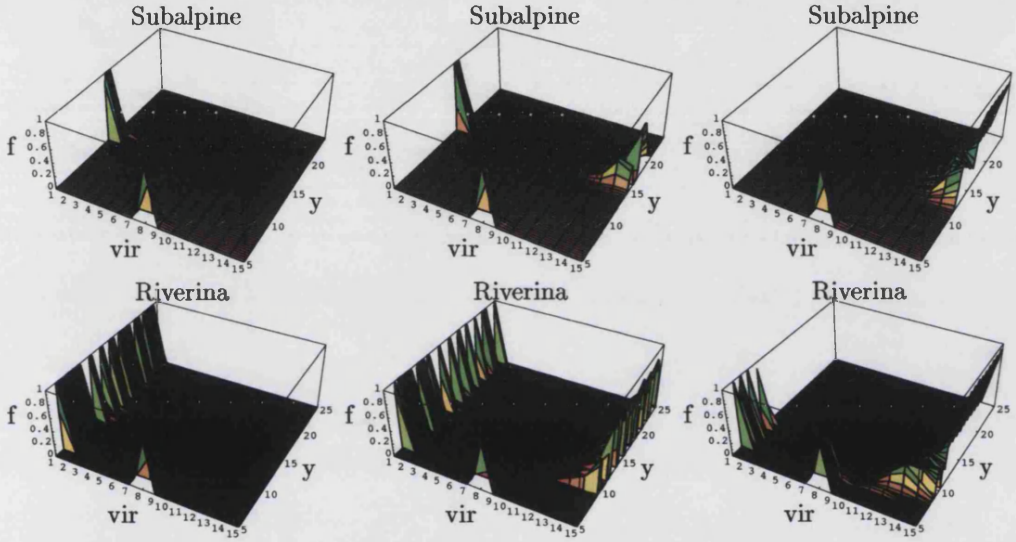


Figure 16.20: Case (d): $\alpha + \beta > 1$, $\beta < 1$. Subalpine and Riverina Weak Hypothesis. f= frequency of virus strain in the environment, vir= virulence, y= years. $\alpha = 1.5$, $\beta = 0.4$ (left). $\alpha = 1.5$, $\beta = 0.5$ (centre). $\alpha = 1.5$, $\beta = 0.6$ (right).

### 16.2.2 Summary of results.

Section 16.2.1 shows results that are in line with the results obtained by running the $\mathcal{SIRV}$ model (section 16.1.5). That is, by running the evolutionary stochastic single site model we get results qualitatively similar to what the theory predicted for the various trade-off scenarios. Generally the main features of the result seem to be independent of the environment in which rabbits live, and independent of the Juvenile immunity hypothesis considered. The two environments and the two hypotheses considered only differ in the persistence of the virus: for Subalpine the virus is sometimes present at very low levels with periodic outbreaks, whereas for Riverina the virus is

present in the environment at more uniform levels.

## 16.3 Appendix 1: Basic Reproductive Ratio and Disease Take-Off.

We derive the $\mathcal{R}_0$ condition for disease take-off for the $\mathcal{SIRV}$ model.

For the disease to invade a disease-free equilibrium population, we require that the $\mathcal{DF}$ equilibrium be unstable with respect to the full disease dynamics (16.1). To determine this , we must compute the Jacobian matrix at the $\mathcal{DF}$ equilibrium ($I = R = V = 0$).

$$\begin{aligned}
\frac{\partial S[t+1]}{\partial S[t]} &= \{\lambda + (1-m)(1-c_V)\} + \lambda'(S[t]+R[t]) - m'\{(1-c_V)S[t] + \kappa R[t]\} \\
&\to 1 - (m'-\lambda')K \qquad \text{at the } \mathcal{DF} \text{ equilibrium.}
\end{aligned}$$

$$\begin{aligned}
\frac{\partial S[t+1]}{\partial I[t]} &= \lambda'(S[t]+R[t]) - m'\{(1-c_V)S[t] + \kappa R[t]\} \\
&\to -(m'-\lambda')K \qquad \text{at the } \mathcal{DF} \text{ equilibrium.}
\end{aligned}$$

$$\begin{aligned}
\frac{\partial S[t+1]}{\partial R[t]} &= \lambda + (1-m)\kappa + \lambda'(S[t]+R[t]) - m'\{(1-c_V)S[t] + \kappa R[t]\} \\
&\to \kappa + (1-\kappa)m - (m'-\lambda')K \qquad \text{at the } \mathcal{DF} \text{ equilibrium.}
\end{aligned}$$

$$\begin{aligned}
\frac{\partial S[t+1]}{\partial V[t]} &= -{c_V}'(1-m)S[t] = -\tfrac{c(1-m)}{(c+V)^2}S[t] \\
&\to -\tfrac{1}{c}(1-m)K \qquad \text{at the } \mathcal{DF} \text{ equilibrium.}
\end{aligned}$$

$$\begin{aligned}
\frac{\partial I[t+1]}{\partial S[t]} &= (1-m)c_V - m'\{(1-CM-\nu)I[t] + c_V S[t]\} \\
&\to 0 \qquad \text{at the } \mathcal{DF} \text{ equilibrium.}
\end{aligned}$$

$$\begin{aligned}
\frac{\partial I[t+1]}{\partial I[t]} &= (1-m)(1-CM-\nu) - m'\{(1-CM-\nu)I[t] + c_V S[t]\} \\
&\to (1-m)(1-CM-\nu) \qquad \text{at the } \mathcal{DF} \text{ equilibrium.}
\end{aligned}$$

$$\begin{aligned}
\frac{\partial I[t+1]}{\partial R[t]} &= -m'\{(1-CM-\nu)I[t] + c_V S[t]\} \\
&\to 0 \qquad \text{at the } \mathcal{DF} \text{ equilibrium.}
\end{aligned}$$

$$\begin{aligned}
\frac{\partial I[t+1]}{\partial V[t]} &= {c_V}'(1-m)S[t] = \tfrac{c(1-m)}{(c+V)^2}S[t] \\
&\to \tfrac{1}{c}(1-m)K \qquad \text{at the } \mathcal{DF} \text{ equilibrium.}
\end{aligned}$$

$$\begin{aligned}
\frac{\partial R[t+1]}{\partial S[t]} &= -m'\{(1-\kappa)R[t]+\nu I[t]\} \\
&\to 0 \qquad \text{at the } \mathcal{DF} \text{ equilibrium.}
\end{aligned}$$

$$\begin{aligned}
\frac{\partial R[t+1]}{\partial I[t]} &= (1-m)\nu - m'\{(1-\kappa)R[t]+\nu I[t]\} \\
&\to (1-m)\nu \qquad \text{at the } \mathcal{DF} \text{ equilibrium.}
\end{aligned}$$

$$\begin{aligned}
\frac{\partial R[t+1]}{\partial R[t]} &= (1-m)(1-\kappa) - m'\{(1-\kappa)R[t]+\nu I[t]\} \\
&\to (1-m)(1-\kappa) \qquad \text{at the } \mathcal{DF} \text{ equilibrium.}
\end{aligned}$$

$$\frac{\partial R[t+1]}{\partial V[t]} = 0.$$

$$\frac{\partial V[t+1]}{\partial S[t]} = 0.$$

$$\frac{\partial V[t+1]}{\partial I[t]} = w.$$

$$\frac{\partial V[t+1]}{\partial R[t]} = 0.$$

$$\frac{\partial V[t+1]}{\partial V[t]} = (1-m_V).$$

It now follows that the Jacobian matrix at the disease-free equilibrium is

$$J = \begin{pmatrix}
1-AK & -(m'-\lambda') & \kappa+(1-\kappa)m-AK & -\frac{1}{c}(1-m)K \\
0 & (1-m)(1-CM-\nu) & 0 & \frac{1}{c}(1-m)K \\
0 & (1-m)\nu & (1-m)(1-\kappa) & 0 \\
0 & w & 0 & (1-m_V)
\end{pmatrix},$$

where we have written $A = (m'-\lambda') \geq 0$.

Clearly, $\mu_0 = 1-AK$ is an eigenvalue of $J$ and, as discussed earlier, our basic assumption is that $\mid \mu_0 \mid < 1$ (which requires density dependence). The remaining eigenvalues of $J$ are the eigenvalues of the matrix

$$J_0 = \begin{pmatrix} (1-m)(1-CM-\nu) & 0 & \frac{1}{c}(1-m)K \\ (1-m)\nu & (1-m)(1-\kappa) & 0 \\ w & 0 & (1-m_V) \end{pmatrix}.$$

Again, $J_0$ clearly has an eigenvalue $\mu_1 = (1-m)(1-\kappa)$, and $\mu_1$ satisfies $0 < \mu_1 < 1$ (since $0 < m < 1$ and $0 < \kappa < 1$). The remaining eigenvalues of $J$ are therefore the eigenvalues of the matrix

$$J_1 = \begin{pmatrix} (1-m)(1-CM-\nu) & \frac{1}{c}(1-m)K \\ w & (1-m_V) \end{pmatrix}.$$

Let $\mu_2$, $\mu_3$ be the eigenvalues of $J_1$. Then,

$$\mu_2, \mu_3 = \frac{1}{2}\Big\{TrJ_1 \pm \sqrt{(TrJ_1)^2 - 4DetJ_1}\Big\},$$

where

$$TrJ_1 = (1-m)(1-CM-\nu) + (1-m_V),$$
$$DetJ_1 = (1-m)\{(1-CM-\nu)(1-m_V) - \frac{wK}{c}\}.$$

Clearly, $TrJ_1 > 0$, and

$$(TrJ_1)^2 - 4DetJ_1 = \{(1-m)(1-CM-\nu) - (1-m_V)\}^2 + 4(1-m)\frac{wK}{c} > 0.$$

It follows that $\mu_2$, $\mu_3$ are both real, and $\mid \mu_3 \mid < \mid \mu_2 \mid$, with $\mid \mu_2 \mid > 0$ ($\mu_2$ is the eigenvalue with the plus sign). It now follows that the disease-free equilibrium is unstable only if $\mid \mu_2 \mid > 1$.

Now, $\mid \mu_2 \mid > 1$ if and only if

$$\sqrt{(TrJ_1)^2 - 4DetJ_1} > 2 - TrJ_1 = (1+m_V) - (1-m)(1-CM-\nu).$$

That is, if and only if,

$$\{(1-m)(1-CM-\nu) - (1-m_V)\}^2 + 4(1-m)\tfrac{wK}{c} =$$
$$(1-m)^2(1-CM-\nu)^2 - 2(1-m)(1-CM-\nu)(1-m_V) + (1-m_V)^2$$
$$+4(1-m)\tfrac{wK}{c}$$
$$> (2-TrJ_1)^2$$
$$= (1+m_V)^2 - 2(1-m)(1-CM-\nu)(1+m_V) + (1-m)^2(1-CM-\nu)^2,$$

which gives

$$4m_V(1-m)(1-CM-\nu)+4(1-m)\frac{wK}{c} > 4m_V.$$

That is, dividing both sides by $4m_V$,

$$(1-m)\frac{wK}{cm_V} > 1-(1-m)(1-CM-\nu) = m+(1-m)(CM+\nu),$$

and hence,

$$\frac{wK}{cm_V} > \frac{m}{1-m}+\nu+CM.$$

That is, the $\mathcal{DF}$ equilibrium is invadable by the disease if

$$\mathcal{R}_0 = \frac{\frac{w}{cm_V}K}{\frac{m}{1-m}+\nu+CM} > 1.$$

Clearly, if $\mathcal{R}_0 < 1$, all the eigenvalues of $J$ have moduli strictly less than 1, and hence the $\mathcal{DF}$ equilibrium is locally stable, and thus uninvadable by the disease.

## 16.4 Appendix 2: The Evolution Models.

### 16.4.1 The $\mathcal{SIRV}$ Evolution Model.

The $\mathcal{SIRV}$ evolution model is outlined below. The evolution model is in structure very similar to the $\mathcal{SIRV}$ model of equation (16.1), but the variable representing the infected population is now characterised by the particular virus strain with which the rabbits have become infected. Thus, $I[t,\ell]$ is the density of infected rabbits whom are infected with virus strain $\ell$ with $1 \leq \ell \leq L = 15$. Some of the disease parameters are also dependent on the strain of the virus. Thus, $c_V[\ell]$ is the probability of infection for a particular strain, $c_{V_{tot}}$ is the probability of being infected by *some* strain (see section 16.2) and $\mu$ is the mutation rate between different strains. The case mortality $CM[\ell]$ also varies according to the virus strain.

$$\left.\begin{aligned}
S[t+1] &= \lambda(S[t]+R[t]) + (1-m(N))\{(1-c_{V_{tot}})S[t] + \kappa R[t]\}; \\
I[t+1,1] &= (1-m(N))\{(1-\mu)(1-CM[1]-\nu)I[t,1] + \tfrac{1}{2}\mu(1-CM[2]-\nu)I[t,2] + \\
&\quad c_V[1]S[t]\}; \\
I[t+1,\ell] &= (1-m(N))\{(1-\mu)(1-CM[\ell]-\nu)I[t,\ell] + \tfrac{1}{2}\mu(1-CM[\ell-1]-\nu)I[t,\ell-1] + \\
&\quad \tfrac{1}{2}\mu(1-CM[\ell+1]-\nu)I[t,\ell+1] + c_V[\ell]S[t]\}; \qquad (2 \leq \ell \leq L-1) \\
I[t+1,L] &= (1-m(N))\{(1-\mu)(1-CM[L]-\nu)I[t,L] + \tfrac{1}{2}\mu(1-CM[L-1]-\nu)I[t,L-1] + \\
&\quad c_V[L]S[t]\}; \\
R[t+1] &= (1-m(N))\{(1-\kappa)R[t] + \nu\textstyle\sum_{\ell=1}^{L} I[t,\ell]\}; \\
V[t+1,\ell] &= (1-m_V[\ell])V[t,\ell] + w[\ell]I[t,\ell]\}.
\end{aligned}\right\} \tag{16.12}$$

### 16.4.2 The Stochastic Evolution Model.

The evolution model is in structure very similar to the single-site model, but the variable representing the infected population is now characterised by the particular virus strain with which the rabbits have become infected, besides their age class. Thus, $I_a[t,k,\ell]$ is the density of infected rabbits of age class $a$ who have been in the age class for $k$ days on day $t$ and who are infected with virus strain $\ell$ with $1 \leq \ell \leq L = 15$. Some of the disease parameters are also dependent on the strain of the virus. Thus, $c_V[\ell]$ is the probability of infection for a particular strain, $c_{V_{tot}}$ is the probability of being infected by *some* strain and $\mu$ is the mutation rate between different strains. The case mortality $CM[\ell]$ also varies according to the virus strain. The recovery rate $\nu[\ell]$ was constant in our runs of the model, but it can be made dependent on the virus strain.

The evolution models according to the two hypotheses on Juvenile immunity are outlined below.

The evolution model according to the Strong hypothesis:

$$
\begin{aligned}
S_J[t+1,0] &= \lambda(1-m_A)(S_P[t,n_P]+R_P[t,n_P]);\\
S_J[t+1,k] &= (1-m_J)(1-c_{V_{tot}})S_J[t,k-1];\\
I_J[t+1,k,1] &= (1-m_J)(c_V[1]S_J[t,k-1]+(1-\tfrac{1}{2}\mu)(1-\nu_J[1])I_J[t,k-1,1]+\\
&\quad \tfrac{1}{2}\mu(1-\nu_J[1])I_J[t,k-1,2]);\\
I_J[t+1,k,\ell] &= (1-m_J)(c_V[\ell]S_J[t,k-1]+(1-\mu)(1-\nu_J[\ell])I_J[t,k-1,\ell]+\tfrac{1}{2}\mu(1-\nu_J[\ell])\\
&\quad (I_J[t,k-1,\ell-1]+I_J[t,k-1,\ell+1])); \qquad (2 \leq \ell \leq L-1)\\
I_J[t+1,k,L] &= (1-m_J)(c_V[L]S_J[t,k-1]+(1-\tfrac{1}{2}\mu)(1-\nu_J[L])I_J[t,k-1,L]+\\
&\quad \tfrac{1}{2}\mu(1-\nu_J[L])I_J[t,k-1,L-1]);\\
R_J[t+1,k] &= (1-m_J)(\textstyle\sum_{\ell=1}^{L}\nu_J[\ell]I_J[t,k-1,\ell]+R_J[t,k-1]); \qquad (2 \leq k \leq n_J)\\
S_Y[t+1,1] &= (1-c_{V_{tot}})(1-m_J)S_J[t,n_J];\\
S_Y[t+1,k] &= (1-c_{V_{tot}})(1-m_Y)S_Y[t,k-1];\\
I_Y[t+1,0,1] &= (1-m_J)(c_V[1]S_J[t,n_J]+(1-\tfrac{1}{2}\mu)(1-\nu_J[\ell])I_J[t,n_J,1]\\
&\quad +\tfrac{1}{2}\mu(1-\nu_J[\ell])I_J[t,n_J,2]);\\
I_Y[t+1,0,\ell] &= (1-m_J)(c_V[\ell]S_J[t,n_J]+(1-\mu)(1-\nu_J[\ell])I_J[t,n_J,\ell]+\\
&\quad \tfrac{1}{2}\mu(1-\nu_J[\ell])I_J[t,n_J,\ell-1])+\tfrac{1}{2}\mu(1-\nu_J[\ell])I_J[t,n_J,\ell+1]); \qquad (2 \leq \ell \leq L-1)\\
I_Y[t+1,0,L] &= (1-m_J)(c_V[L]S_J[t,n_J]+(1-\tfrac{1}{2}\mu)(1-\nu_J)I_J[t,n_J,L]\\
&\quad +\tfrac{1}{2}\mu(1-\nu_J[\ell])I_J[t,n_J,L-1]);
\end{aligned}
\tag{16.13}
$$

$$
\begin{aligned}
I_Y[t+1,k,1] &= (1-m_Y)(c_V[1]S_Y[t,k-1] + (1-\tfrac{1}{2}\mu)(1-CM[1]-\nu[1])I_Y[t,k-1,1]+ \\
&\quad \tfrac{1}{2}\mu(1-CM[1]-\nu[1])I_Y[t,k-1,2]); \\
I_Y[t+1,k,\ell] &= (1-m_Y)(c_V[\ell]S_Y[t,k-1] + (1-\mu)(1-CM[\ell]-\nu[\ell])I_Y[t,k-1,\ell]+ \\
&\quad \tfrac{1}{2}\mu(1-CM[\ell]-\nu[\ell])(I_Y[t,k-1,\ell-1] + I_Y[t,k-1,\ell+1])); \\
&\qquad\qquad (2 \le \ell \le L-1) \\
I_Y[t+1,k,L] &= (1-m_Y)(c_V[L]S_Y[t,k-1] + (1-\tfrac{1}{2}\mu)(1-CM[L]-\nu[L])I_Y[t,k-1,L]+ \\
&\quad \tfrac{1}{2}\mu(1-CM[L]-\nu[L])I_Y[t,k-1,L-1]); \\
R_Y[t+1,0] &= (1-m_J)(R_J[t,n_J] + \textstyle\sum_{\ell=1}^{L}\nu_J[\ell]I_J[t,n_J,\ell]); \\
R_Y[t+1,k] &= (1-m_Y)(R_Y[t,k-1] + \textstyle\sum_{\ell=1}^{L}\nu_Y[\ell]I_Y[t,k-1,\ell]); \qquad\qquad (2 \le k \le n_Y) \\
\\
S_{A_M}[t+1] &= (1-c_{V_{tot}})((1-m_A)S_{A_M}[t] + \tfrac{1}{2}(1-m_Y)S_Y[t,n_Y]); \\
I_{A_M}[t+1,1] &= \tfrac{1}{2}(1-m_Y)(c_V[1]S_Y[t,n_Y] + (1-\tfrac{1}{2}\mu)(1-CM[1]-\nu_Y[1])I_Y[t,n_Y,1])+ \\
&\quad \tfrac{1}{2}\mu(1-CM[1]-\nu_Y[1])I_Y[t,n_Y,2]) + (1-m_A)((1-\tfrac{1}{2}\mu)(1-CM[1]-\nu_A[1]) \\
&\quad I_{A_M}[t,1] + c_V[1]S_{A_M}[t]\tfrac{1}{2}\mu(1-CM[1]-\nu_A[1])I_{A_M}[t,2]); \\
I_{A_M}[t+1,\ell] &= \tfrac{1}{2}(1-m_Y)(c_V[\ell]S_Y[t,n_Y] + (1-\mu)(1-CM[\ell]-\nu_Y[\ell])I_Y[t,n_Y,\ell])+ \\
&\quad \tfrac{1}{2}\mu(1-CM[\ell]-\nu_Y[\ell])I_Y[t,n_Y,\ell-1]) + \tfrac{1}{2}\mu(1-CM[\ell]-\nu_Y[\ell])I_Y[t,n_Y,\ell+1])+ \\
&\quad (1-m_A)((1-\mu)(1-CM[\ell]-\nu_A[\ell])I_{A_M}[t,\ell] + c_V[\ell]S_{A_M}[t]+ \\
&\quad \tfrac{1}{2}\mu(1-CM[\ell]-\nu_A[\ell])I_{A_M}[t,\ell-1] + \tfrac{1}{2}\mu(1-CM[\ell]-\nu_A[\ell])I_{A_M}[t,\ell+1]); \\
&\qquad\qquad (2 \le \ell \le L-1) \\
I_{A_M}[t+1,L] &= \tfrac{1}{2}(1-m_Y)(c_V[L]S_Y[t,n_Y] + (1-\tfrac{1}{2}\mu)(1-CM[L]-\nu_Y[L])I_Y[t,n_Y,L])+ \\
&\quad \tfrac{1}{2}\mu(1-CM[L]-\nu_Y[L])I_Y[t,n_Y,L-1]) + (1-m_A) \\
&\quad ((1-\tfrac{1}{2}\mu)(1-CM[L]-\nu_A[L])I_{A_M}[t,L]+ \\
&\quad c_V[L]S_{A_M}[t]\tfrac{1}{2}\mu(1-CM[L]-\nu_A[L])I_{A_M}[t,L-1]); \\
R_{A_M}[t+1] &= (1-m_A)(R_{A_M}[t] + \textstyle\sum_{\ell=1}^{L}\nu_A[\ell]I_{A_M}[t,\ell]) + \tfrac{1}{2}(1-m_Y)(R_Y[t,n_Y]+ \\
&\quad \textstyle\sum_{\ell=1}^{L}\nu_Y[\ell]I_Y[t,n_Y,\ell]);
\end{aligned}
$$

(16.13)

$$
\begin{aligned}
S_{A_F}[t+1] &= (1-c_{V_{tot}})(1-m_A)((1-\pi)S_{A_F}[t]+S_P[t,n_P])+\tfrac{1}{2}(1-m_Y)(1-c_{V_{tot}})S_Y[t,n_Y];\\
I_{A_F}[t+1,1] &= \tfrac{1}{2}(1-m_Y)(c_V[1]S_Y[t,n_Y]+(1-\tfrac{1}{2}\mu)(1-CM[1]-\nu_Y[1])I_Y[t,n_Y,1]+\\
&\quad \tfrac{1}{2}\mu(1-CM[1]-\nu_Y[1])I_Y[t,n_Y,2])+(1-m_A)\\
&\quad ((1-CM[1]-\nu_A[1])(1-\tfrac{1}{2}\mu)I_{A_F}[t,1]+\tfrac{1}{2}\mu(1-CM[1]-\nu_A[1])I_{A_F}[t,2]+\\
&\quad c_V[1](1-\pi)S_{A_F}[t]+c_V[1]\textstyle\sum_{k=1}^{n_P}S_P[t,k]);\\
I_{A_F}[t+1,\ell] &= \tfrac{1}{2}(1-m_Y)(c_V[\ell]S_Y[t,n_Y]+(1-\mu)(1-CM[\ell]-\nu_Y[\ell])I_Y[t,n_Y,\ell]+\\
&\quad \tfrac{1}{2}\mu(1-CM[\ell]-\nu_Y[\ell])I_Y[t,n_Y,\ell-1]+\tfrac{1}{2}\mu(1-CM[\ell]-\nu_Y[\ell])I_Y[t,n_Y,\ell+1])+\\
&\quad (1-m_A)((1-CM[1]-\nu_A[1])(1-\mu)I_{A_F}[t,\ell]+\\
&\quad \tfrac{1}{2}\mu(1-CM[\ell]-\nu_A[\ell])I_{A_F}[t,\ell-1]+\tfrac{1}{2}\mu(1-CM[\ell]-\nu_A[\ell])I_{A_F}[t,\ell+1]+\\
&\quad c_V[\ell](1-\pi)S_{A_F}[t]+c_V[\ell]\textstyle\sum_{k=1}^{n_P}S_P[t,k]); \qquad (2\le\ell\le L-1)\\
I_{A_F}[t+1,L] &= \tfrac{1}{2}(1-m_Y)(c_V[L]S_Y[t,n_Y]+(1-\tfrac{1}{2}\mu)(1-CM[L]-\nu_Y[L])I_Y[t,n_Y,L]+\\
&\quad \tfrac{1}{2}\mu(1-CM[L]-\nu_Y[L])I_Y[t,n_Y,L-1])+(1-m_A)((1-CM[L]-\nu_A[L])(1-\tfrac{1}{2}\mu)\\
&\quad I_{A_F}[t,L]+\tfrac{1}{2}\mu(1-CM[L]-\nu_A[L])I_{A_F}[t,L-1]+c_V[L](1-\pi)S_{A_F}[t]+\\
&\quad c_V[L]\textstyle\sum_{k=1}^{n_P}S_P[t,k]);\\
R_{A_F}[t+1] &= (1-m_A)(R_P[t,n_P]+(1-\pi)R_{A_F}[t]+\textstyle\sum_{\ell=1}^{L}\nu_A[\ell]I_{A_F}[t,\ell])+\\
&\quad \tfrac{1}{2}(1-m_Y)(R_Y[t,n_Y]+\textstyle\sum_{\ell=1}^{L}\nu_Y[\ell]I_Y[t,n_Y,\ell]);
\end{aligned}
$$

$$
\begin{aligned}
S_P[t+1,0] &= (1-c_{V_{tot}})(1-m_A)\pi S_{A_F}[t];\\
S_P[t+1,k] &= (1-c_{V_{tot}})(1-m_A)S_P[t,k-1];\\
R_P[t+1,0] &= \pi(1-m_A)R_{A_F}[t];\\
R_P[t+1,k] &= (1-m_A)R_P[t,k-1]; \qquad (2\le k\le n_P)
\end{aligned}
$$

$$
\begin{aligned}
V[t+1,\ell] &= (1-m_V[\ell])V[t,\ell]+w[\ell](\textstyle\sum_{k=1}^{n_J}I_J[t,k,\ell]+\sum_{k=1}^{n_Y}I_Y[t,k,\ell]+I_{A_M}[t,\ell]+I_{A_F}[t,\ell]);\\
&\quad (1\le\ell\le L)
\end{aligned}
\tag{16.13}
$$

The evolution model according to the Weak hypothesis:

$$
\begin{aligned}
S_J[t+1,0] &= \lambda(1-m_A)S_P[t,n_P];\\
S_J[t+1,k] &= (1-m_J)S_J[t,k-1]; \qquad (1\le k\le 28)\\
\\
S_{J-}[t+1,1] &= (1-m_J)(1-c_{V_{tot}})S_J[t,28];\\
S_{J-}[t+1,k] &= (1-m_J)(1-c_{V_{tot}})S_{J-}[t,k-1]; \qquad (2\le k\le 28)\\
S_{J+}[t+1,0] &= \lambda(1-m_A)R_P[t,n_P];\\
S_{J+}[t+1,k] &= (1-m_J)S_{J+}[t,k-1]; \qquad (1\le k\le 56)\\
\\
I_J[t+1,0,\ell] &= (1-m_J)c_V[\ell]S_J[t,0]; \qquad (1\le \ell\le L)\\
I_J[t+1,k,1] &= (1-m_J)(c_V[1]S_{J-}[t,k-1]+(1-\tfrac{1}{2}\mu)(1-CM_-[1]-\nu_J[1])I_J[t,k-1,1]+\\
&\quad \tfrac{1}{2}\mu(1-CM_-[1]-\nu_J[1])I_J[t,k-1,2]);\\
I_J[t+1,k,\ell] &= (1-m_J)(c_V[\ell]S_{J-}[t,k-1]+(1-\mu)(1-CM_-[\ell]-\nu_J[\ell])I_J[t,k-1,\ell]+\\
&\quad \tfrac{1}{2}\mu(1-CM_-[\ell]-\nu_J[\ell])(I_J[t,k-1,\ell-1]+I_J[t,k-1,\ell+1]));\\
&\qquad (2\le \ell\le L-1)\\
I_J[t+1,k,L] &= (1-m_J)(c_V[L]S_{J-}[t,k-1]+(1-\tfrac{1}{2}\mu)(1-CM_-[L]-\nu_J[L])I_J[t,k-1,L]+\\
&\quad \tfrac{1}{2}\mu(1-CM_-[L]-\nu_J[L])I_J[t,k-1,L-1]);\\
R_J[t+1,k] &= (1-m_J)(\textstyle\sum_{\ell=1}^{L}\nu_J[\ell]I_J[t,k-1,\ell]+R_J[t,k-1]);\\
&\qquad\qquad (2\le k\le n_J)\\
\\
S_Y[t+1,0] &= (1-m_J)((1-c_{V_{tot}})S_{J-}[t,n_J]+S_{J+}[t,n_J]);\\
S_Y[t+1,k] &= (1-c_{V_{tot}})(1-m_Y)S_Y[t,k-1];\\
I_Y[t+1,0,1] &= (1-m_J)(c_V[1]S_{J-}[t,n_J]+(1-\tfrac{1}{2}\mu)(1-CM_-[\ell]-\nu_J[\ell])I_J[t,n_J,1]+\\
&\quad \tfrac{1}{2}\mu(1-CM_-[\ell]-\nu_J[\ell])I_J[t,n_J,2]);\\
I_Y[t+1,0,\ell] &= (1-m_J)(c_V[\ell]S_{J-}[t,n_J]+(1-\mu)(1-CM_-[\ell]-\nu_J[\ell])I_J[t,n_J,\ell]\\
&\quad +\tfrac{1}{2}\mu(1-CM_-[\ell]-\nu_J[\ell])I_J[t,n_J,\ell-1])+\tfrac{1}{2}\mu(1-CM_-[\ell]-\nu_J[\ell])I_J[t,n_J,\ell+1]);\\
&\qquad (2\le \ell\le L-1)\\
I_Y[t+1,0,L] &= (1-m_J)(c_V[L]S_{J-}[t,n_J]+(1-\tfrac{1}{2}\mu)(1-CM_-[\ell]-\nu_J[\ell])I_J[t,n_J,L]\\
&\quad +\tfrac{1}{2}\mu(1-CM_-[\ell]-\nu_J[\ell])I_J[t,n_J,L-1]);
\end{aligned}
\tag{16.14}
$$

$$
\begin{aligned}
I_Y[t+1,k,1] &= (1-m_Y)(c_V[1]S_Y[t,k-1] + (1-\tfrac{1}{2}\mu)(1-CM[1]-\nu[1])I_Y[t,k-1,1]+ \\
&\quad \tfrac{1}{2}\mu(1-CM[1]-\nu[1])I_Y[t,k-1,2]); \\
I_Y[t+1,k,\ell] &= (1-m_Y)(c_V[\ell]S_Y[t,k-1] + (1-\mu)(1-CM[\ell]-\nu[\ell])I_Y[t,k-1,\ell]+ \\
&\quad \tfrac{1}{2}\mu(1-CM[\ell]-\nu[\ell])(I_Y[t,k-1,\ell-1] + I_Y[t,k-1,\ell+1])); \\
&\qquad\qquad (2 \le \ell \le L-1) \\
I_Y[t+1,k,L] &= (1-m_Y)(c_V[L]S_Y[t,k-1] + (1-\tfrac{1}{2}\mu)(1-CM[L]-\nu[L])I_Y[t,k-1,L]+ \\
&\quad \tfrac{1}{2}\mu(1-CM[L]-\nu[L])I_Y[t,k-1,L-1]); \\
R_Y[t+1,0] &= (1-m_J)(R_J[t,n_J] + \textstyle\sum_{\ell=1}^{L}\nu_J[\ell]I_J[t,n_J,\ell]); \\
R_Y[t+1,k] &= (1-m_Y)(R_Y[t,k-1] + \textstyle\sum_{\ell=1}^{L}\nu_Y[\ell]I_Y[t,k-1,\ell]); \\
&\qquad\qquad\qquad\qquad (2 \le k \le n_Y)
\end{aligned}
$$

$$
\begin{aligned}
S_{A_M}[t+1] &= (1-c_{V_{tot}})((1-m_A)S_{A_M}[t] + \tfrac{1}{2}(1-m_Y)S_Y[t,n_Y]); \\
I_{A_M}[t+1,1] &= \tfrac{1}{2}(1-m_Y)(c_V[1]S_Y[t,n_Y] + (1-\tfrac{1}{2}\mu)(1-CM[1]-\nu_Y[1])I_Y[t,n_Y,1])+ \\
&\quad \tfrac{1}{2}\mu(1-CM[1]-\nu_Y[1])I_Y[t,n_Y,2]) + (1-m_A)((1-\tfrac{1}{2}\mu)(1-CM[1]-\nu_A[1]) \\
&\quad I_{A_M}[t,1] + c_V[1]S_{A_M}[t]\tfrac{1}{2}\mu(1-CM[1]-\nu_A[1])I_{A_M}[t,2]); \\
I_{A_M}[t+1,\ell] &= \tfrac{1}{2}(1-m_Y)(c_V[\ell]S_Y[t,n_Y] + (1-\mu)(1-CM[\ell]-\nu_Y[\ell])I_Y[t,n_Y,\ell])+ \\
&\quad \tfrac{1}{2}\mu(1-CM[\ell]-\nu_Y[\ell])I_Y[t,n_Y,\ell-1]) + \tfrac{1}{2}\mu(1-CM[\ell]-\nu_Y[\ell])I_Y[t,n_Y,\ell+1])+ \\
&\quad (1-m_A)((1-\mu)(1-CM[\ell]-\nu_A[\ell])I_{A_M}[t,\ell] + c_V[\ell]S_{A_M}[t]+ \\
&\quad \tfrac{1}{2}\mu(1-CM[\ell]-\nu_A[\ell])I_{A_M}[t,\ell-1] + \tfrac{1}{2}\mu(1-CM[\ell]-\nu_A[\ell])I_{A_M}[t,\ell+1]); \\
&\qquad\qquad (2 \le \ell \le L-1) \\
I_{A_M}[t+1,L] &= \tfrac{1}{2}(1-m_Y)(c_V[L]S_Y[t,n_Y] + (1-\tfrac{1}{2}\mu)(1-CM[L]-\nu_Y[L])I_Y[t,n_Y,L]) + \tfrac{1}{2}\mu \\
&\quad (1-CM[L]-\nu_Y[L])I_Y[t,n_Y,L-1]) + (1-m_A)((1-\tfrac{1}{2}\mu)(1-CM[L]-\nu_A[L]) \\
&\quad I_{A_M}[t,L] + c_V[L]S_{A_M}[t]\tfrac{1}{2}\mu(1-CM[L]-\nu_A[L])I_{A_M}[t,L-1]); \\
R_{A_M}[t+1] &= (1-m_A)(R_{A_M}[t] + \textstyle\sum_{\ell=1}^{L}\nu_A[\ell]I_{A_M}[t,\ell]) + \tfrac{1}{2}(1-m_Y)(R_Y[t,n_Y]+ \\
&\quad \textstyle\sum_{\ell=1}^{L}\nu_Y[\ell]I_Y[t,n_Y,\ell]);
\end{aligned}
\tag{16.14}
$$

$$
\begin{aligned}
S_{A_F}[t+1] &= (1-c_{V_{tot}})(1-m_A)((1-\pi)S_{A_F}[t]+S_P[t,n_P])+\tfrac{1}{2}(1-m_Y)(1-c_{V_{tot}})S_Y[t,n_Y];\\
I_{A_F}[t+1,1] &= \tfrac{1}{2}(1-m_Y)(c_V[1]S_Y[t,n_Y]+(1-\tfrac{1}{2}\mu)(1-CM[1]-\nu_Y[1])I_Y[t,n_Y,1]+\\
&\quad \tfrac{1}{2}\mu(1-CM[1]-\nu_Y[1])I_Y[t,n_Y,2])+(1-m_A)((1-CM[1]-\nu_A[1])(1-\tfrac{1}{2}\mu)\\
&\quad I_{A_F}[t,1]+\tfrac{1}{2}\mu(1-CM[1]-\nu_A[1])I_{A_F}[t,2]+c_V[1](1-\pi)S_{A_F}[t]+\\
&\quad c_V[1]\textstyle\sum_{k=1}^{n_P}S_P[t,k]);\\
I_{A_F}[t+1,\ell] &= \tfrac{1}{2}(1-m_Y)(c_V[\ell]S_Y[t,n_Y]+(1-\mu)(1-CM[\ell]-\nu_Y[\ell])I_Y[t,n_Y,\ell]+\\
&\quad \tfrac{1}{2}\mu(1-CM[\ell]-\nu_Y[\ell])I_Y[t,n_Y,\ell-1]+\tfrac{1}{2}\mu(1-CM[\ell]-\nu_Y[\ell])I_Y[t,n_Y,\ell+1])+\\
&\quad (1-m_A)((1-CM[1]-\nu_A[1])(1-\mu)I_{A_F}[t,\ell]+\tfrac{1}{2}\mu(1-CM[\ell]-\nu_A[\ell])\\
&\quad I_{A_F}[t,\ell-1]+\tfrac{1}{2}\mu(1-CM[\ell]-\nu_A[\ell])I_{A_F}[t,\ell+1]+c_V[\ell](1-\pi)S_{A_F}[t]+\\
&\quad c_V[\ell]\textstyle\sum_{k=1}^{n_P}S_P[t,k]); \qquad (2\le\ell\le L-1)\\
I_{A_F}[t+1,L] &= \tfrac{1}{2}(1-m_Y)(c_V[L]S_Y[t,n_Y]+(1-\tfrac{1}{2}\mu)(1-CM[L]-\nu_Y[L])I_Y[t,n_Y,L]+\\
&\quad \tfrac{1}{2}\mu(1-CM[L]-\nu_Y[L])I_Y[t,n_Y,L-1])+(1-m_A)((1-CM[L]-\nu_A[L])\\
&\quad (1-\tfrac{1}{2}\mu)I_{A_F}[t,L]+\tfrac{1}{2}\mu(1-CM[L]-\nu_A[L])I_{A_F}[t,L-1]+\\
&\quad c_V[L](1-\pi)S_{A_F}[t]+c_V[L]\textstyle\sum_{k=1}^{n_P}S_P[t,k]);\\
R_{A_F}[t+1] &= (1-m_A)(R_P[t,n_P]+(1-\pi)R_{A_F}[t]+\textstyle\sum_{\ell=1}^{L}\nu_A[\ell]I_{A_F}[t,\ell])+\\
&\quad \tfrac{1}{2}(1-m_Y)(R_Y[t,n_Y]+\textstyle\sum_{\ell=1}^{L}\nu_Y[\ell]I_Y[t,n_Y,\ell]);
\end{aligned}
$$

$$
\begin{aligned}
S_P[t+1,0] &= (1-c_{V_{tot}})(1-m_A)\pi S_{A_F}[t];\\
S_P[t+1,k] &= (1-c_{V_{tot}})(1-m_A)S_P[t,k-1];\\
R_P[t+1,0] &= \pi(1-m_A)R_{A_F}[t];\\
R_P[t+1,k] &= (1-m_A)R_P[t,k-1];\\
&\qquad\qquad (2\le k\le n_P)
\end{aligned}
$$

$$
\begin{aligned}
V[t+1,\ell] &= (1-m_V[\ell])V[t,\ell]+w[\ell](\textstyle\sum_{k=1}^{n_J}I_J[t,k,\ell]+\sum_{k=1}^{n_Y}I_Y[t,k,\ell]+I_{A_M}[t,\ell]+I_{A_F}[t,\ell]);\\
&\qquad (1\le\ell\le L)
\end{aligned}
\tag{16.14}
$$

# Chapter 17

# Discussion

*No model is constructed to capture all the intricacies of the real world, for if it did so it would be as difficult to understand as the real world itself and little would be gained...*

—Roff [102]

In the light of these sentiments we proceed to highlight the main achievements and possible future improvements of this research.

The first step in constructing a model to investigate the impact of Rabbit Calicivirus Disease (RCD) on the European rabbit (*Oryctolagus cuniculus*) in Australia was to construct a model to represent the natural dynamics of rabbit populations without the disease. For this purpose we constructed a single-site time-dependent model that allowed for a seasonal birth rate, age structure, density dependent regulation of the population size, climatic variability, constant and density dependent natural death rate. Emigration and immigration were later introduced in a spatial (multiple-site) model constructed by connecting several single-site models.

We used the available data on pregnancy rates in relation to conception date for four different areas in Australia, namely Subalpine, Western NSW, Riverina and South-Western WA, to build a mathematical representation of the seasonal probability of rabbit breeding. We established an age structure in the model relevant to the disease. In fact, the likelihood of being affected by RCD depends on the age of the rabbit. We divided the rabbit population into four classes: Juveniles (0-56 days of age), Subadults (or Youngsters) (56-83 days of age), Adult Males and Adult Females (83 days- onwards). Adults (Male and Female) are sexually mature and fully susceptible to become

infected with RCD, while we split the pre-sexually mature age interval into two because Juveniles are immune to the disease (totally or partially) and Subadults are susceptible to the disease but are not yet sexually mature. Also, life-history data [31], [131] was used to parameterize the model (see section 3.1.2).

Running the model with a seasonal birth rate and constant death rate gave results showing that the population explodes at different rates for three of the considered areas in Australia: namely Western NSW, Riverina and South-Western WA. For the Subalpine environment, it was necessary to increase the birth rate to make the population viable. In Western NSW the breeding season is short compared to Riverina and South-Western WA, and the number of Juveniles present during the year is more similar to Subalpine (see figure 4.2). Thus, we consider Subalpine and Western NSW more marginal environments, while Riverina and South-Western WA are more favourable areas for rabbits. Thus, in addition to a seasonal birth rate, density dependent regulation of the population size was found to be necessary to make the model a more realistic representation of the rabbit population dynamics. This is reasonable because a finite environment cannot sustain infinite population growth. The literature [31], [47], [86], [111], and [131] (see section 1.3.3) suggests that the most sensitive age class in cases of high population density are younger rabbits, especially because of food scarcity. This led us to incorporate density dependent regulation in the model by increasing Juvenile mortality whenever the population density rises above a certain threshold density determining (or determined by) the carrying capacity of the site. It might be oversimplifying to attribute density dependence to one single factor, but we were encouraged by the literature to choose Juvenile mortality as the key variable controlling population size.

The threshold level at which density dependence affects Juvenile mortality was varied stochastically. Stochastic variation is interpreted in terms of climatic variability. In fact, climatic variability is assumed to affect available food abundance and quality and hence determine the operational carrying capacity of a site. Since the carrying capacity is essentially determined by the threshold for density-dependent Juvenile mortality, we modelled climatic variation by introducing stochastic variation in this threshold. Thus, we assumed a "good" period for rabbits is one for which an environment can sustain a larger number of rabbits compared to the same environment in a "bad" period. This means that density dependence of Juvenile mortality is activated at different threshold levels depending on the time in which we introduce the climatic change. We experimented with different frequencies of climatic variation: once a year, once every 6 months, once every season

(3 months) and once a month. Changes in threshold density were introduced randomly via a Poisson process, with the specific frequency. The magnitude of the threshold density was varied using a lognormal distribution. Three different variances of the lognormal distribution were tested, namely low, medium and high variability in threshold density. No variability is represented by the deterministic model with no stochastic effects.

Density dependence prevented the population from exploding and together with the seasonality of the birth rate gave seasonal fluctuations in rabbit densities. Climatic variation alone did not control the population exponential growth, but especially for a high variance in the threshold level, it contributed noticibly to density dependence in keeping the population size to much lower values that in the non-stochastic case. The same kind of phenomenon was observed for all the Australian region considered, even though the effects are more intensive in the marginal environments of Subalpine and Western NSW where the breeding season is shorter. In fact in Riverina and South-Western WA, in some favourable years, explosions in rabbit populations are possible (see figures 6.5 and 6.6).

One of the main features of this research is that it takes into consideration two different hypotheses on the way RCD affects Juvenile rabbits. In section 1.5.2 we describe all the different observations on RCD present in the literature. There are some discrepancies between the observations, but what arises is that RCD affects Juveniles in a different way compared to Subadults and Adults. We decided to group the observations under two main hypotheses which we called: Strong Juvenile hypothesis and Weak Juvenile hypothesis. Most of the reported observation support one of these two hypotheses (refer to section 1.5.2 for the literature). Two different models were tried to investigate the model outcome for both hypotheses. The Strong Juvenile hypothesis states that Juveniles are immune for the first 2 months of their lives, during which, if they contract the disease, they are carriers and can infect other individuals but do not die from the disease, and retain life immunity after recovering. The Weak Juvenile hypothesis states that Juveniles are immune for about two months if they are born to recovered does, and thereby inherit maternal antibodies. After this they become fully susceptible. If they do not have maternal antibodies, they are nevertheless immune for the first month of life. After the first month they can catch the disease, and suffer from an increasing death rate with increasing age, until the adult death rate is reached at about two months (see section 1.5.2).

We assume an indirect transmission mode of the disease since the means of transmission of the

disease in the field have not yet been fully explained. The foecal-oral route has been suggested as a possible mean of transmission [51], [71], [85], or the presence of a vector [136], [139] for the mechanical transmission of the disease. We postulate the existence of a viral load in the environment which depends on the number of infected animals, has a decay rate and an infectivity, i.e. the probability that a rabbit becomes infected with RCD. This latter is the only unknown parameter in the model, apart from the environmental carrying capacity and parameters associated with climatic variability. We expressed the infectivity as a function of the viral load and (what we call) the "virulence" of the virus, $b$ (see section 3.1.4). It might be more appropriate to call $b$ an "inverse virulence" of the virus since the infectivity is actually a decreasing function of $b$. We investigated the disease dynamics by varying the value of $b$, and we found the range of $b$ for which the disease has an effect on the population. We found different results for the two different immunological hypotheses.

In absence of stochastic effects, for the Strong Juvenile hypothesis, we found that the disease is more successful in controlling the population size in the more marginal environments, Subalpine and Western NSW, since in these regions the breading season is shorter compared to Riverina and Western NSW. Fewer Juveniles are present during the year in the marginal environments: thus, fewer Juveniles will become immune adults when they catch the disease. We found that a very infective disease, that is low values of $b$, will tend to persist in the environment but will not control the population since most of the Juveniles will be infected and will subsequently recover and retain lifelong immunity. Thus, the population size often recovers to pre-disease size through the recovered population. This happens with different time scales for the different regions and for different values of the virulence $b$. Especially in Riverina the population recovers after few years for intermediate values of the virulence $b$ because of the large presence of Juveniles for most of the year.

When the model was run using the Weak hypothesis, without stochastic effects, we found that the disease was much more successful in controlling the population size, and the more infective the disease is (low values of $b$) the more successful the disease is in controlling the population. In fact for a not very virulent disease (high $b$) we observe a disease dynamics very similar to the one for the Strong Juvenile hypothesis but for a very virulent disease (low $b$) the disease behaviour is very different. For the Weak hypothesis there is practically no lower bound for the range of $b$ for which the disease successfully controls the population, reducing it to less than 10% of its pre-disease size for very low values of $b$. The population does not recover for the whole simulation run. This

is explained by the fact that in the Weak hypothesis there are more Juveniles around that are protected by maternal antibodies, but these subsequently become susceptible Adults. Thus fewer of the Juveniles catch, recover and subsequently become immune to the disease than for the Strong Juvenile hypothesis. Juvenile immunity is a key issue in disease persistence and success in lowering the population size.

When stochastic effects are included in the disease model, we observe a similar trend for all the geographical regions. For the Strong Juvenile hypothesis, with high values of the virulence parameter $b$ (i.e. a less virulent disease), the climatic effects are more dominant in controlling the population. As $b$ decreases (i.e. the disease becomes more virulent), the disease plays the main role in the interplay with climatic variability. Finally, when the disease strain is very virulent ($b$ at the lower bound of its range), the population recovery rate is slower, probably delayed by the climatic variability, if compared to the non-stochastic case.

For the Weak hypothesis, we found that for high values of $b$ (low virulence) the trend is similar to the Strong hypothesis case, that is the disease is not persistent and does not affect the population size. Stochastic variation does not enhance the disease effect and the population size is lowered mainly by the climatic variability alone especially for high variances of the lognormal distribution. As the disease becomes more virulent (lower values of $b$), it becomes dominant in controlling the population. Even for very low values of $b$ the disease persists and largely affects the population in contrast to what happens in the Strong hypothesis. The system dynamics becomes very similar to the non-stochastic case showing that the disease plays the main role in keeping the population size at very low levels. The same type of behaviour is observed for all the four geographical regions considered.

The next step was to construct a spatial (multiple-site) model using the single site model as building block. Besides the spatial configuration, it was necessary to model emigration and immigration, which we did not account for in the single-site model. Also, the additional hazard rabbits face when in transit between different sites, leaving one site and trying to become established in another. This hazard is mostly due to additional exposure to predation, but also starvation and dehydration. It is quite likely that it could be seasonal, but we have no information on this so we kept it constant in the form of an additional death rate per day.

In section 1.3.5 we report the observations made on rabbit dispersion. Two main hypothesis are brought forward to justify rabbit dispersion: social and seasonal reasons or density dependence.

In particular Parer [88] obtained data on the emigration of rabbits depending on their age and the season of the year for Lake Urana, Riverina. We used this data to construct a probability model that a rabbit would emigrate on any given day given its age (chapter 5). We tested this model against the available data. We tried in a different model a density dependent probability of emigration and tested the results against the data. The seasonal probability model produced a better fit to the real data than the density dependent one. So the emigration probability used in the models was taken to be seasonally dependent, even though it might have been more realistic to include both a seasonal and a density dependent effect on emigration. The spatial model was then only tested for the Riverina region since the only data available on emigration was for this region. The immigration from one site to another was based on a density dependent acceptance probability [88]: acceptance in a new site is regulated by the population density at the entry site. We assume that a rabbit will try to become established in a site where the competition for food is not high. If a rabbit is not accepted, it will continue as an emigrant, seeking another site.

We experimented with several spatial configurations of sites: one-dimensional, two-dimensional, symmetric and asymmetric. The topology of the spatial configuration was regulated by a connectivity probability, specifying the probability per day that a rabbit coming from any one site would arrive at another one. We called this probability the "connectivity" between the sites. Thus two sites are not connected when the connectivity between them is zero, and they are highly connected (there is a high probability that a rabbit leaving the first site will end up in the second one) when the connectivity is "high" (though usually less than $\frac{1}{2}$). We assumed that it is just as likely that an emigrant from site $j$ will arrive at site $i$, as that an emigrant from site $i$ will arrive at site $j$ for a fixed time interval. However, this might not be realistic since, for example, heterogeneity in the geographical configuration of the environment might make one site easier to reach than the other, say if one is uphill and the other downhill, or the natural food abundance at one site compared to the other might encourage only immigration into that site and not emigration. Nevertheless, for simplicity we assumed an equal probability in both directions linking any two sites. We experimented on the range of the connectivity values to which the system was sensitive. We found that high connectivities between the sites imply that the whole system behaves like a co-ordinated single site, while a system with very low connectivities (i.e. zero connectivities) between the sites behaves like a set of independent sites regardless of the spatial configuration: one-dimensional, two-dimensional, symmetric or asymmetric. We chose to investigate the intermediate range between these two scenarios.

For the Strong hypothesis, the system seemed to be very sensitive to a change in the threshold levels for which density dependent effects are activated. We varied the threshold capacities of the sites and tried several configurations (see section 11.3) and we observed that the disease affects and controls the population more in sites with a bigger population size. Moreover in sites with a low population density the disease does not take off, but it seems to be transmitted through such sites to other sites. When we introduced the disease in a site with a low threshold level, even though the site was not noticibly affected, we found that the disease reached other remote sites with a higher population density, which were strongly affected. Thus we do observe a patchiness in disease pattern in the spatial model as suggested by Barlow [10], Gobbet [49] and Saunders et al. [106], which confirms the threshold theorem according to which when few infectious individuals are introduced in a susceptible community, the density or number of susceptibles must be above a critical value for the disease to take off [60]. In fact while there is no data to show that outbreaks of RCD are density dependent [140], there are some indications that the actual effectiveness of RCD may be influenced by rabbit density, and that the transmission of the virus is reduced at low rabbit densities [142].

Surprisingly, when stochastic variation of the threshold level was introduced, the system still behaved mostly as a set of unconnected single sites. The climatic variability often played the main role in lowering the population size compared to the disease, especially when the threshold level of the sites is low or constant for all the sites. Even with climatic variation, we still observed patchiness in the disease dynamics where sites with a low density population transmit across the disease without being affected. The interplay between disease and climatic variability seem to vary depending on the virulence of the disease. Disease persistence is enhanced by climatic variability for a highly virulent disease, but low virulence disease seems to behave independently of the climatic variation.

For the Weak hypothesis, the general pattern of the population dynamics was much more "chaotic", especially in the absence of climatic variability. But overall the system reacted to a change in spatial configuration, connectivity and threshold level of the carrying capacity in the same way as for the Strong hypothesis. That is, it was more sensitive to changes in threshold levels than to changes in the spatial connectivity. We observed that stochastic variability of the threshold level made the system dynamics more regular than when stochastic effects were absent. The sites' dynamic patterns are more in phase than in the non-stochastic case. As in the Strong hypothesis, we noticed that the stochastic effects had a tendency to "win" over the disease especially for a high variance

in the threshold level. This was observed in the single-site model too.

In general the spatial model results seemed to be mainly sensitive to population density and it might be interesting to find the threshold population level needed by the disease to takeoff. It must be said that we only tried few spatial configurations, and with a maximum number of 7 sites. Truly, the number of possibilities is infinite. It would be certainly interesting to experiment with different asymmetric configurations with more sites. We did not try this mainly due to a difficulty in storing data. The reason for this is that the spatial model is a high dimensional dynamical system, and required extended computer times to run over the relatively long period we considered (day-by-day update over 25 years). Even with the small number of configurations we considered, there were data storage problems with the facilities that were available.

Our last step in this research was to construct a model to investigate the possible long term evolution of the disease virus. No information is available about the strains associated to other forms of the disease in Australia [68], but new variants of the virus have appeared in Europe [21], [54], [107], [128]. We assumed that the virus has more than one strain, each strain differing in virulence. One strain is more virulent than another if its rate of reproduction within a host is greater, assuming a constant "infectivity" (probability that a rabbit exposed to a given environmental load will catch the disease). This means, as in the single-site and multiple-site models, that strains of high virulence are represented by low values of the virulence parameter $b$. Thus, each virus strain is characterised by a different value of $b$. We selected fifteen possible strains. Evolution is constrained in large measure by trade-offs between life-history traits [102]. As far as we know, nothing is known about trade-offs in virus evolution but we assumed that viruses are no exception to this rule. Thus, we postulated the existence of some constraints in the evolution of the life-history traits of RCD. We expressed these constraints in the form of trade-offs between the virus characteristics, namely the rate of virus release by an infected individual $\omega$ (where $\omega = \frac{c}{b}$ and $c$ =constant, see chapter 16), the virus decay rate in the environment $m_V$ and the case mortality $CM$ (mortality rate due to the disease). That is we assumed that these virus traits may not be independent from each other but are linked by some functional dependence. Given the complexity of the single-site model, we constructed a simplified disease model (the $\mathcal{SIRV}$ model) to determine an expression for the virus basic reproductive rate and the shape of the trade-off functions. These trade-offs were then used in the single site stochastic space disease model with multiple strains (see chapter 16 for a detailed description of the type of trade-offs we assumed). We allowed for a mutation rate (per day) between

successive strains of neighbouring virulence, so that the virus can explore its entire virulence range.

When we ran the $\mathcal{SIRV}$ model we found that, depending on the trade-off functions, high or low virulence strains are almost always selected. The virus evolves to maximise the basic reproductive ratio $\mathcal{R}_0$, i.e. the number of new infections generated on average by one infected host in a population of susceptible individuals. Unexpectedly, we found that intermediate levels of disease virulence are not usually selected. We found in the analysis of the $\mathcal{SIRV}$ model that four possible scenarios occur depending on the parameter values of the trade-off functions. In the first case, the virus can evolve to its minimum virulence or to its maximum virulence; the second case is similar to the first, but with stronger selection pressure driving evolution toward maximum virulence. In the third case the virus definitly evolves to its maximum virulence, and in the final case there is a possibility of the virus evolving to an intermidiate/low virulence strain or to the maximum possible virulence (see section 16.1.2 and figure 16.4).

We obtained the same qualitative results when we used these trade-off functions in the more complicated single site stochastic disease model for which it is not possible to obtain an explicit expression of $\mathcal{R}_0$. We ran the model for two contrasting regions, Subalpine (marginal) and Riverina (favourable), and for the different hypotheses regarding Juvenile immunity (the Strong hypothesis and the Weak hypothesis). We introduced a single strain of intermediate virulence after 5 years in the single-site model with an intermediate carrying capacity. Even though the Strong hypothesis and the Weak hypothesis give different results regarding the disease dynamics and its effects in the single site and spatial models, the evolution of the virus is very similar for both hypotheses and for most trade-offs, at least with the relatively high mutation rate we have assumed in our simulations. The two environments and the two hypotheses considered only differ in the persistence of the virus: for Subalpine the virus is sometimes present at very low levels with periodic outbreaks, whereas for Riverina the virus is present in the environment at more uniform levels (see section 16.2.1).

Compared to other areas in population ecology, relatively little work has been done on the mathematical modelling of RCD. In chapter 2 we reported the previous known work in this subject. The first model we describe is Barlow's direct and indirect transmission model [10]. Barlow did not build a spatial model so his results can only be compared to our time model outlined in chapter 3. Barlow's indirect transmission model is more comparable to our time model than his direct transmission model. But, while our key parameter in the investigation of the disease is the virulence $b$, in Barlow's indirect model the key parameter is the virus decay rate $m$ which determines the per-

sistence of the disease irrespective of whether juvenile immunity is included in the model; Juvenile immunity increases the likelihood of disease persistence. While in our model the persistence of the disease depends on the value of $b$, but mainly on the fact that Juveniles are immune carriers of the disease.

Gobbet's approach to building the model is similar to ours in that it is spatial, but his assumptions and choice of parameter values are quite different from those we have adopted. Gobbet's one-warren model starts with different basic assumptions (see section 2.2.1) which are elaborated in the multiple-warren model (section 2.2.2). In the one-warren model there is no births, natural deaths, immigration or emigration, while in our single site model we include birth, litter size, age structure, natural death through climatic variability for Juveniles and constant death rate for Subadults and Adults. Seasonal emigration is fitted to the available data and is later included in a comprehensive spatial model. The assumptions on the spatial structure of Gobbett's multiple-warren model are more similar to ours (see section 2.2.2), apart from the fact that Gobbet assumes that each warren is at an equal distance from its neighbours, while by varying the connectivity we can "vary the distance" between sites. But we found that the connectivity between sites can be varied over quite a large range without substantially altering the qualitative features of the dynamics. Gobbet allows for only two possible sizes of the warren while in our model we can vary the site capacities continuously, which is important as we observed that the disease success is strongly density dependent.

Just as in our spatial model results, Gobbet found that the impact of a field release may be patchy and varies with the size of the warren: the impact can be more severe on larger warrens than smaller ones. No version of Gobbet's model has demonstrated the persistence of RCD through spatial dynamics. We observed in our model that it is not the space configuration which influences the disease but the density of the population of the sites. Thus we get similar results to Gobbet, but in our model disease persists for certain values of the parameter $b$ (see chapter 12 to 15), while Gobbet, changing the virus half-life detected no dramatic change in the impact and duration of the disease in the environment.

The Climex model [137] suggests the investigation of the possibility of a vector, such as blowflies and bushflies for the transmission of RCD. Many insects become contaminated with RCV and so become potential mechanical vectors [141], [139]. Rabbit fleas (*Spilopsyllus cuniculi*), mosquitoes (*Aedes postspiraculosus*) and especially large flies (blow flies such as *Calliphora albofrontalis* and

*Calliphora varifrons*) can become contaminated with RCV and infective for rabbits that can contract RCD if they ingest fly faeces and regurgita [141], [9]. Unfortunately, due to time constraints and the complexity of the system, we did not add this feature to our spatial model. But it might represent a further improvement to the system investigated here.

The multivariate statistical model [140] suggests that the virus success might be strongly related to the environmental and climatic conditions at release time. However, for simplicity of analysis and comparison we always introduced the disease after 5 years and at the beginning of the year (and in the same site in the spatial model); we did not study the impact of releasing the disease at different times during the year. Given that rabbit abundance (especially Juveniles) varies seasonally, this could be important. However all of this could be done within our model framework.

The difficulties arising in the elaboration of this work have highlighted the direction future research should take to allow robust assumptions and predictions on the impact of RCD on a susceptible rabbit population in Australia. More emphasis should be given to laboratory and field research on the way RCD affects the population in order to verify which hypothesis is more realistic regarding Juvenile immunity. Many issues regarding the availability of data on rabbit biology and immunology concerning Rabbit Calicivirus Disease arose: further laboratory immunological studies could provide useful data. In particular, it would be helpful if more research on the existence of different strains of the virus and possible trade-offs were carried out which could be used in the context of our evolution model and its assumed trade-offs. Monitoring of possible field strains of the virus should be undertaken to look for mutant strains. This is of fundamental importance for constructing a realistic model of the long term impact of RCD on rabbits in Australia.

A further possible future line of investigation could be undertaken on the interaction between myxomatosis and RCD [109], [93], by introducing the dynamics of myxomatosis into the model framework, paying particular attention to the seasonality of the two diseases [142]. This is related to rabbit and vector abundance during the year. Moreover it is important to investigate the immune response of rabbits that become infected with both the diseases. In fact the immune system of a rabbit becomes depressed when it is infected with myxomatosis, while it is uncontrollably activated (blood coagulation cascade [63]) when infected with RCD.

The biological world is fascinating since it is almost impossible to isolate one of its elements and study its characteristics: inevitably we would change its nature. There are so many potentially important variables that it is very challenging to isolate their contribution to the integrated system.

Mathematical modelling selects some of these variables and investigates their relevance in the context of the overall system.

*All models necessarily are simplifications of reality...*

—Roff [102]

# Bibliography


[1] Anderson, R.M. and May, R.M. (1981). The population dynamics of microparasites and their invertebrate hosts. *Philosophical Transaction of the Royal Society of London B* **291**, 451-524.

[2] Anderson, R.M. and May, R.M. (1986). The invasion, persistence and spread of infectious diseases within animal and plant communities. *Proccedings of the Royal Society of London B* **314**, 31-66.

[3] Anderson, R.M. and May, R.M. (1991). *Infectious Diseases of Humans.* Oxford University Press, Oxford.

[4] Anderson, R.M. (1994). The Croonian Lecture, 1994. Populations, infectious disease and immunity: a very nonlinear world. *Philosophical Transaction of the Royal Society of London B* **346**, 457-505.

[5] Anderson, R.M. (1994). Mathematical studies of parasitic infection and immunity. *Science. Washington.* **264**, 1884-1886.

[6] Antia, R., Koella, J.C., Levin, B.R., Garnett, G.P. and Anderson, R.M. (1993). Parasite evolution in response to immunological defenses. Pp. 383-405 in: *Oxford surveys in evolutionary biology* edited by D. Futuyma and J. Antonovics. Oxford University Press, Oxford.

[7] Antonelli, P.L. and Seymour, R.M.(1988). A model on myxomatosis based on hormonal control of rabbit-flea reproduction. *Journal of Mathematics Applied in Medicine and Biology.* **5**, 65-80.

[8] Armstrong, P.(1982). Rabbit (Orictolagus cuniculus) on islands: a case study of successful colonisation. *Journal of Biogeography.* **9**, 353-362.

[9] Asgari, S., Hardy, J.R.E., Sinclair, R.G. and Cooke, B.D.(1998). Field evidence for mechanical transmission of rabbit haemorrhagic disease virus (RHDV) by flies (Diptera: Calliphoridae) among wild rabbits in Australia. *Virus Research.* **54**, 123-132.

[10] Barlow, N.D. & Kean J.M.(1998). Simple models for the impact of rabbit calivirus disease (RCD) on Australian Rabbits. *Ecological Modelling.* **109**, 225-241.

[11] Bell, D.J.(1983). Mate choice in the European rabbit. Pp. 221-223 in: P.P. Bateson, ed, *Mate choice.* Cambridge University Press, Cambridge.

[12] Bickel, P.J. and Doksum, K.A. (1977). *Mathematical Statistics: basic ideas and selected topics.* Holden-Day, Inc; San Francisco, California.

[13] Bowen, Z. and Read, J.(1998). Population and demographic patterns of rabbits (*Oryctolagus cuniculus*) at Roxby Downs in arid South Australia and the influence of rabbit haemorrhagic disease. *Wildlife Research.* **25**, 655-662.

[14] Boyd, I.L., Bray, C.J.(1989). Nutritional ecology of the wild rabbit- an input to the timing of reproduction. *Proceeding of the Nutrition Society.* **48**, 81-91.

[15] Brambell, F.W.R(1942). Intra-uterine mortality of the wild rabbit, *Oryctolagus cuniculus* (L.). *Proceedings of the Royal Society of London B.* **130**, 462-479.

[16] Bratley, P., Fox, B.L. and Schrage, L.E. (1983). *A guide to simulation.* Springer-Verlag, Inc; New York.

[17] Bull, L.B. and Dickinson, C.G.(1937). The specificity of the virus of rabbit myxomatosis. *Journal of the Council for Scientific and Industrial Research* **10(4)**, 291-294.

[18] Burbidge, A.A., Johnson, K.A., Fuller, P.J. and Southgate, R.I.(1988). Aboriginal knowledge of the mammals of the central deserts of Australia. *Australian Wildlife Research.* **15**, 9-39.

[19] Cancellotti, F.M. and Renzi, M.(1991). Epidemiology and current situation of viral haemorrhagic disease of rabbits and the European brown hare syndrome in Italy. *Revue Scientifique et Technique Office International des Epizooties.* **10(2)**, 409-422.

[20] Capucci, L., Fusi, P., Lavazza, A., Pacciarini, M.L. and Rossi, C.(1996). Detection and preliminary characterization of a new rabbit calicivirus related to Rabbit Haemorrhagic Disease Virus but nonpathogenic. *Journal of Virology.* **70(2)**, 8614-8623.

[21] Capucci, L., Fallacara, F., Grazioli, S., Lavazza, A., Pacciarini, M.L. and Brocchi, E.(1998). A further step in the evolution of rabbit haemorrhagic disease virus: the appearance of the first consistent antigenic variant. *Virus Research.* **58**, 115-126.

[22] Catling, P.C.(1988). Similarities and contrasts in the diets of foxes, *Vulpes vulpes*, and cats *Felix catus* relative to fluctuating prey populations and drought. *Australian Wildlife Research.* **15**, 307-317.

[23] Chasey, D., Lucas, M.H., Westcott, D.G., Sharp, G., Kitching, A. and Hughes, S.K.(1995). Development of a diagnostic approach to the identification of rabbit hemorrhagic disease. *Veterinary Record.* **137**, 158-160.

[24] Collins, B. J., White, J. R., Lenghaus, C., Morrisy, C. J. and Westbury, H. A. 1996. Presence of rabbit haemorrhagic disease virus antigen in rabbit tissues as revealed by a monoclonal antibody dependent capture ELISA. *Journal of Virological Methods.* **58**, 145-154.

[25] Cooke, B.D. (1974). *Food and other resources of the wild rabbit Oryctolagus cuniculus.* PhD thesis, University of Adelaide, Australia.

[26] Cooke, B.D. (1996). Modelling the Spread of RCD: a Review of Work in Progress. *A report prepared for the Meat Research Corporation, December 1996, as part of Project RCD.003 "Epidemiology of Rabbit Calicivirus".* CSIRO, Division of Wildlife and Ecology.

[27] Cooke, B.D. (2000). Personal Communications.

[28] Cooke, B.D. (2002)(a). Personal Communications.

[29] Cooke, B.D. (2002)(b). Personal Communications.

[30] Cowan, D.P.(1987). Aspects of the social organisation of the European wild rabbit (*Oryctolagus cuniculus*). *Ethology.* **75**, 197-210.

[31] Cowan, D.P.(1987). Patterns of mortality in a free-living rabbit (Orictolagus cuniculus) population. *Symposia of the Zoological Society, London.* **58**, 59-77.

[32] Cowan, D.P.(1991). The availability of burrows in relation to dispersal in the wild rabbit *Oryctolagus cuniculus. Symposia of the Zoological Society of London.* **63**, 213-230.

[33] Crow, E.L. and Shimizu, K.(1988). *Lognormal distribution: theory and applications/ edited by Edwin L. Crow, Kunio Shimizu.* Marcel Dekker, Inc, New York.

[34] Daly, J.C.(1981). Effects of social organisation and environmental diversity on determining the genetic structure of a population of the wild rabbit, *Oryctolagus cuniculus. Evolution.* **35(4)**, 689-706.

[35] Douglas, G.W.(1958). Myxomatosis in Victoria. *Journal of the Department of Agricolture, Victoria* **56**, 779-790.

[36] Farrow, E.P.(1925). *Plant life on East anglian Heaths.* Cambridge, University Press.

[37] Fenner, F. and Ratcliffe, F.N.(1965). *Myxomatosis.* Cambridge University Press, Great Britain.

[38] Fenner, F. and Ross, J.(1994). Myxomatosis. Pp. 205-239 in: H.V. Thompson and C.M. King, eds, *The Rabbit in Britain, France and Australasia: the ecology of a Successful Coloniser.* Oxford University Press, Oxford.

[39] Fenton, E.W.(1940). The influence of rabbits on the vegetation of certain hill-grazing districts in Scotland. *Journal of Ecology.* **28**, 438-49.

[40] Fowkes, N.D. and Mahony, J.J.(1994). *An Introduction to Mathematical Modelling.* John Wiley and Sons, Chichester.

[41] Fuchs, A. and Weissenbock, H.(1992). Comparative histopathological study of rabbit haemorrhagic disease (RHD) and European brown hare syndrome (EBHS). *Journal of Comparative Pathology* **107**, 103-113.

[42] Funk, S.M., Fiorello, C.V., Cleaveland, S. and Gompper, M.E. (2001). The Role of Disease in Carnivore Ecology and Conservation. In: J.L. Gittleman, S.M. Funk, D.W. MacDonald and R.K. Wayne, eds, *Carnivore Conservation.* Published by Cambridge University Press, Great Britain.

[43] Gascoyne, S.C., King, A.A., Laureson, M.K., Borner, M., Schildger, B. and Barrat, J. (1993). Aspects of rabies infection and control in the conseravtion of the African wild dog (*Lycaon pictus*) in the Serengeti region, Tanzania. *Onderspoort Journal of Veterinary Research.* **60**, 415-420.

[44] Gani, R. and Leach, S. (2001). Transmission potential of smallpox in contemporary populations. *Nature.* **414**, 748-751.

[45] Gehrmann, B., and Kretzschmar, C.(1991). Ein experimenteller beitrag zur epizootiologie der Viralen Hamorrhagischen Septikamie der Kanninchen (Rabbit Haemorrhagic Disease, RHD) - Ubertragung durch Fliegen. *Berl. Munsch. Tierarztl. Wschr.* **104**, 192-194.

[46] Gibb, J.A.(1993). Sociality, time and space in a sparse population of rabbits (*Oryctolagus cuniculus*). *Journal of Zoology, London.* **229**, 581-607.

[47] Gilbert, N., Myers, K., Cooke, B.D., Dunsmone, J.D., Fullagar, P.J., Gibb, J.A., King, D.R., Parer, I., Wheeler, S.H. and Wood, D.H. (1987). Comparative dynamics of Australasian rabbit populations. *Australian Wildlife Research.* **14**, 491-503.

[48] Gillman, M. and Hails, R.(1997). *An Introduction to Ecological Modelling. Putting Practice into Theory.* Blackwell Science, Great Britain.

[49] Gobbet, D. (1995) *Modelling Rabbit Calicivirus Disease.* Honours in Zoology - Major Project, Department of Zoology, University of Adelaide.

[50] Goltsman, M., Kruchenkova, E.P. and MacDonald, D.W.(1996). The Mednyi Arctic Foxes: treating a population imperilled by disease. *Oryx.* **30**, 251-258.

[51] Gregg, D.A., House, C., Meyer, R. and Berninger, M.(1991). Viral haemorrhagic disease of rabbits in Mexico: epidemiology and viral characterization. *Revue Scientifique et Technique Office International des Epizooties.* **10**, 435-451.

[52] Grenfell, B.T., and Harwood, J.(1997). (Meta)population dynamics of infectious diseases. *Trends Ecol. Evol.* **12**, 395-404.

[53] Grenfell, B.T., Bjornstadt, O.N. and Kappey, J.(2001). travelling waves and spatial hierarchies in measles epidemics. *Nature.* **414**, 716-723.

[54] Gould, A.R., Kattenbelt, J.A., Lenghaus, C., Morrissy, C., Chamberlain, T., Collins, B.J. and Westbury, H.A. (1997). The complete nucleotide sequence of rabbit haemorrhagic disease Virus (Czech strain V351): use of the polymerase chain reaction to detect replication in Australian vertebrates and analysis of viral population sequence variation. *Virus Research.* **47**, 7-17.

[55] Hall, E.A.A., Specht, R.L. and Eardley, C.M.(1964). Regeneration of the vegetation on Koonamore Vegetation Reserve, 1926-1962. *Australian Journal of Botany.* **12**, 205-264.

[56] Hanski, I. and Gilpin, M.E. (eds)(1997). *Metapopulation Biology.* Published by Academic Press, England.

[57] Hanski, I. (1998). Metapopulation Dynamics. *Nature.* **396**, 41-49.

[58] Hanski, I.(1999). *Metapopulation Ecology.* Published by Oxford University Press, England.

[59] Henderson, B.A.(1981). The role of food quality and social behaviour in the regulation of the size of the breeding population of the European rabbit. Pp. 664-666 in: K. Myers and C.D. MacInnes, eds, *Proceedings of the World Lagomorph Conference, Guelph Ontario 1979.* IUCN, Canada.

[60] Kermack, W.O. and McKendrick, A.G.(1927). A contribution to the mathematical theory of epidemics. *Proceedings of the Royal Society, London A.* **115**, 700-721.

[61] Kiesecker, J.M., Skelly, D.K., Beard, K.H. and Preisser, E.(1999). Behavioral Reduction of Infection Risk. *Proceedings of the National Academy of Science of the United States of America.* **96**, 9165-9168.

[62] Kovaliski, J.(1998). Monitoring the spread of rabbit haemorrhagic disease virus as a new biological agent for the control of wild European rabbits in Australia. *Journal of Wildlife Diseases.* **34(3)**, 421-428.

[63] Lenghaus, C., Westbury, H., Collins, B., Ratnamoban, N., and Morrissy, C. (1994). Overview of the RHD project in the Australian Animal Health Laboratory . Pp. 104-129 in: R.K. Munro and R.T. Williams, eds, *Rabbit Haemorragic Disease: issues in assessment for biological control.* Published for the Bureau of Resource Sciences by the Australian Government Publishing Service, Canberra.

[64] Levins, R.(1969). Some demographic and genetic consequences of environmental heterogeneity for biological control. *Bulletin of Entomological Society. America.* **15**, 237-240.

[65] Lockley, R.M.(1961). Social structure and stress in the rabbit warren. *Journal of Animal Ecology.* **30**, 385-423.

[66] Lugton, I.W.(1992). Rabies and fox control in semi-arid Australia. Pp. 117-124 in: P. O'Brien and G. Berry, eds, *Wildlife Rabies Contingency Planning in Australia.* Australian Government Publishing Service, Canberra.

[67] Madsen, H.(1939). Does the rabbit chew the cud? *Nature, London.* **143**, 981-982.

[68] Marcato P.S., Benazzi C., Vecchi G., Galeotti M., Della Salda L., Sarli G. and Lucidi P. (1991). Clinical and pathological features of viral haemorrhagic disease of rabbits and the European brown hare syndrome. *Revue Scientifique et Technique Office International des Epizooties.* **10(2)**, 371-392.

[69] Marshall, I.D.(1959). The influence of ambient temperature on the course of myxomatosis in rabbits. *J. Hyg., Camb.* **57**, 484-497.

[70] Matthews, L.H.(1952). *British Mammals.* Collins, London.

[71] Morisse, J.-P., Le Galle, G. and Boilletot, E.(1991). Hepatitis of viral origin in Leporidae: introduction and aetiological hypotheses. *Revue Scientifique et Technique Office International des Epizooties.* **10(2)**, 283-295.

[72] Morot, C.H.(1882). Memoire relatif aux pelotes stomacales des leporides. *Recueil de Medecine Veterinaire, Paris.* **59**, 635-46.

[73] Motha, M.J.X. and Clark, R.G.(1998). Confirmation of rabbit haemorrhagic disease in wild New Zealand rabbits using the ELISA. *New Zealand Veterinary Journal* **46(2)**, 83-4.

[74] Munro, R.K., Williams, R.T.(1994). *Rabbit haemorrhagic disease: issues in assessment for biological control.* Bureau of Resource Sciences, Australia.

[75] Murray, J.D. (1993). *Mathematical Biology.* Springer-Verlag, Berlin.

[76] Mutze, G., Cooke, B. and Alexander, P.(1998). The initial impact of rabbit haemorrhagic disease on European rabbit populations in South Australia. *Journal of Wildlife Diseases.* **34(2)**, 221-227.

[77] Myers, K.(1962). A survey of myxomatosis and rabbit infestation trends in the eastern Riverina, New South Wales, 1951-60. *CSIRO Wildlife Research.* **7(1)**, 1-12.

[78] Myers, K. and Schnider, E.C.(1964). Observations on the reproduction, mortality, and behaviour in a small, free-living population of wild rabbits. *CSIRO Wildlife Research.* **9(2)**, 138-143.

[79] Myers, K. and Parker, B.S.(1965). A study of the biology of the wild rabbit in climatically different regions in Eastern Australia. *CSIRO Wildlife Research.* **10(1)**, 1-32.

[80] Mykytowycz, R. and Gambale, S.(1965). A study of the inter-warren activities and dispersal of wild rabbits, *Orictolagus cuniculus* (L.), Living in a 45-AC Paddock. *CSIRO Wildlife Research.* **10**, 111-23.

[81] Newsome, A.E., Parer, I., Catling, P.C.(1989). Prolonged prey suppression by carnivores - predator- removal experiments. *Oecologia.* **78**, 458-467.

[82] Nowotny, N., Bascunana, C.R., Ballagipordany, A., Garvier-Widen, D., Uhlen, M. and Belak, S.(1997). Phylogenetic analysis of rabbit haemorrhagic disease and European brown hare syndrome viruses by comparison of sequences from the capsid protein gene. *Archives of Virology.* **142(4)**, 657-673.

[83] Ohlinger, V.F., Haas, B., Meyers, G., Weiland, F. and Theil, H-J.(1990). Identification and characterization of the virus causing rabbit haemorrhagic disease. *Journal of Virology.* **64(1)**, 3331-3336.

[84] Ohlinger, V.F. and Theil, H-J.(1991). Identification of the viral haemorrhagic disease virus of rabbits as a calicivirus. *Revue Scientifique et Technique Office International des Epizooties.* **10(2)**, 311-323.

[85] Ohlinger, V.F., Haas, B. and Theil, H-J.(1993). Rabbit Haemorrhagic Disease (RHD): characterization of the causative calicivirus. *Vet. Res.* **24(2)**, 103-116.

[86] Omole, T.A.(1982). The effect of level of dietary protein on growth and reproductive performance in rabbits. *Journal of Applied Rabbit Research* **5**, 83-88.

[87] Parer, I.(1977). The population ecology of the wild rabbit, *Orictolagus cuniculus* (L.), in a Mediterranean-type climate in New South Wales. *Australian Wildlife Research.* **4**, 171-205.

[88] Parer, I.(1982). Dispersal of the wild rabbit, *Orictolagus cuniculus*, at Urana in New South Wales. *Australian Wildlife Research.* **9**, 427-41.

[89] Parer, I., Sobey, W.R., Conolly, D. and Morton,R.(1994). Virulence of strains of myxoma virus and the resistance of wild rabbits, *Orictolagus cuniculus* (L.), from different locations in Australasia. *Australian Journal of Zoology.* **42**, 347-362.

[90] Parker, R.F. and Thompson, R.L.(1942). The effect of external temperature on the course of infectious myxomatosis of rabbits. *Journal of Experimental Medicine* **75**, 567-573.

[91] Parra F. and Prieto, M.(1990). Purification and characterization of a calicivirus as the causative agent of a lethal hemorraghic disease in rabbits. *Journal of Virology* **64(8)**, 4013-4015

[92] Pech, R.P., Sinclair, A.R.E., Newsome, A.E. and Catling, P.C.(1992). Limits to predator regulation of rabbits in Australia: evidence from predator-removal experiments. *Oecologia.* **89**, 102-112.

[93] Pech, R.P., Barlow, N.D., and Hood, G.M.(1994). Models of rabbit haemorrhagic disease in Australian and New Zealand wild rabbits . Pp. 152-154 in: R.K. Munro and R.T. Williams, eds, *Rabbit Haemorragic Disease: issues in assessment for biological control.* Published for the Bureau of Resource Sciences by the Australian Government Publishing Service, Canberra.

[94] Pick, J.H.(1942). *Australia's Dying Heart: Soil Erosion in the Inland.* Melbourne University Press, Melbourne.

[95] Ratcliffe, F.(1947). *Flying fox and drifting sand.* Angus and Robertson LTD, Sydney.

[96] Reid, J. and Fleming, M.(1992). The conservation status of birds in arid Australia. *Australian Rangelands Journal.* **14**, 65-91.

[97] Renshaw, E. (1999). Stochastic effects in population models. Pp. 23-63 in: J. McGlade, ed, *Advanced Ecological Theory. Priciples and Applications.* Published by Blackwell Science Ltd, England.

[98] Robinson, A.J. and Holland, M.K.(1995). Testing the concept of virally vectored immunosterilisation for the control of wild rabbit and fox populations in Australia. *Australian Veterinary Journal.* **72(2)**, 65-68.

[99] Rodak L., Smid, B., Valicek, L., Vesely T., Stepanek, J., Hampl, J. and Jurak, E. (1990). Enzyme-linked immunosorbent assay of antibodies to rabbit haemorrhagic disease virus and determination of its major structural proteins. *Journal of General Virology.* **71(5)**, 1075-1080.

[100] Rodak L., Granatova, M., Smid, B., Valicek, L., Vesely T. and Nevorankova, Z. (1990). Monoclonal antibodies to rabbit hemorrhagic disease of rabbit in the Czech and Slovak Federal Republics. *Journal of General Virology.* **71**, 2593-2598.

[101] Rodak, L., Smid, B. and Valicek, L.(1991). Application of control measures against viral haemorrhagic disease of rabbits in the Czech and Slovak Federal Republic. *Revue Scientifique et Technique Office International des Epizooties.* **10(2)**, 513-524.

[102] Roff, D.A. (1992). *The evolution of life histories; theory and analysis.* Chapman and Hall, New York, London.

[103] Rolls, E.C.(1969). *They All Run Wild.* Angus and Robertson LTD, Sydney.

[104] Ross, J.(1982). Myxomatosis: the natural evolution of the disease. *Symposium of the Zoological society of London.* **50**, 77-95.

[105] Ross, J. and Tittensor, A.M.(1986). Influence of myxomatosis in regulating rabbit numbers. *Mammal Review.* **16(3/4)**, 163-168.

[106] Saunders, G., Choquenot, D., McIlroy, J. and Packwood, R.(1998). Initial effects of rabbit haemorrhagic disease on free-living rabbit (*Oryctolagus cuniculus*) populations in central-western New South Wales. *Wildlife Research.* **26(1)**, 69-74.

[107] Schirrmeier, H., Reimann, I., Kollner, B. and Granzow, H.(1999). Pathogenic, antigenic and molecular properties of rabbit haemorrhagic disease virus (RHDV) isolated from vaccinated rabbits: detection and characterization of antigenic variants. *Archives of Virology.* **144(4)**, 719-735.

[108] Seymour, R.M.(1992). A study of the interaction of virulence, resistance and resource limitation in a model of myxomatosis mediated by the European rabbit flea *Spilopsyllus cuniculi* (Dale). *Ecological Modelling* **60**, 281-308.

[109] Simon, M.C., Ortega, C., Maynar, P., Muzquiz, J.L., De Blas, I., Girones, O., Alonso, J.L. and Sanchez, J.(1998). Studies in wild rabbit (*Oryctolagus cuniculus*) populations in Navarra (Spain). I. Epidemiology of Rabbit Viral haemorrhagic Disease. *Gibier Faune Sauvage* **15**, 47-64.

[110] Smid, B., Rodak, L., Valicek, L., Stepanek, J. and Jurak, E. (1989). Experimental transmission and electron microscopic demonstration of the virus of haemorrhagic disease of rabbits in Czechoslovakia. *Journal of Veterinary Medicine B.* **36**, 237-240.

[111] Stodart, E. and Myers, K.(1966). The effects of different foods on confined populations of wild rabbits, *Oryctolagus cuniculus* (L.). *CSIRO Wildlife Research* **11(2)**, 111-124.

[112] Studdert, M.J.(1994). Rabbit haemorrhagic disease virus: a calicivirus with differences. *Australian Veterinary Journal.* **71**, 264-266.

[113] Surridge, A.K., Ibrahim, K.M., Bell, D.J., Webb, N.J., Rico, C. and Hewitt, G.M.(1999). Fine-scale genetic structuring in a natural population of European wild rabbits (*Oryctolagus cuniculus*). *Molecular Ecology.* **8**, 299-307.

[114] Surridge, A.K., Bell, D.J., Ibrahim, K.M. and Hewitt, G.M.(1999). Population structure and genetic variation of European wild rabbits (*Oryctolagus cuniculus*) in East Anglia. *Heredity.* **82**, 479-487.

[115] Surridge, A.K., Bell, D.J. and Hewitt, G.M.(1999). From population structure to individual behaviour: genetic analysis of social structure in the European wild rabbit (*Oryctolagus cuniculus*). *Biological Journal of the Linnean Society.* **68**, 57-71.

[116] Thompson, H.V. and Worden, A.N. (1956). *The Rabbit.* Collins Press; St.James's Place, London.

[117] Trout, R.C. and Tittensor, A.M.(1989). Can predators regulate wild rabbit *Oryctolagus cuniculus* population density in England and Wales?. *Mammal review.* **19**, 153-173.

[118] Trout, R.C., Chasey, D. and Sharp, G. (1997). Seroepidemiology of rabbit hemorrhagic disease (RHD) in wild rabbits (*Oryctolagus cuniculus*) in the United Kingdom. *Journal of Zoology.* **243**, 846-853.

[119] Twigg, L.E. and Williams, C.K. (1999). Fertility control of overabundant species; can it work for feral rabbits? *Ecology Letters.* **2**, 281-285.

[120] Villafuerte, R., Calvete, C., Gortazar, C. and Moreno, S.(1994). First epizootic of Rabbit Haemorrhagic Disease in free living populations of *Oryctolagus cuniculus* at Donana National Park, Spain. *Journal of Wildlife Diseases.* **30(2)**, 176-179.

[121] Xu Z.J, Chen W.X., Chen J.X. and Yu J.Y. (1985). Studies on control and prevention of a new rabbit disease. *Animal Husbandry and Veterinary Medicine Journal..* **10**, 12-13.

[122] Xu, Z.J, Du, N., and Liu S. (1988). A new virus isolated from Hemorrhagic Disease in rabbits. *Proccedings of 4th World Rabbit congress (Godollo, Hungary).*, 456-462.

[123] Xu, Z.J. and Chen, W.X.(1989). Viral Haemorrhagic disease in rabbits: a review. *Veterinary Research Communications.* **13**, 205-212.

[124] Wallis, A.(1904). The flora of the Cambridge district. Pp.209-237 in: J.E. Marr and A.E. Shipley, eds, *The Handbook to the Natural History of Cambridgeshire.* Cambridge, University Press.

[125] Watson, J.S.(1961). Feral Rabbit Populations on Pacific Islands. *Pacific Science.* **15(4)**, 591-593.

[126] Westbury, H., Lenghaus, C. and Munro, R. (1994). A Review of the Scientific Literature relating to RHD . Pp. 91-103 in: R.K. Munro and R.T. Williams, eds, *Rabbit Haemorragic Disease: issues in assessment for biological control.* Published for the Bureau of Resource Sciences by the Australian Government Publishing Service, Canberra.

[127] Wheeler, S.H. and King, D.R.(1985). The European rabbit in south-western Australia. *Australia Wildlife Research* **12**, 213-225.

[128] White, P.J., Normann, R.A., Trout, R.C., Gould, E.A. and Hudson, P.J.(2001). The emergence of rabbit haemorrhagic disease virus: will a non-pathogenic strain protect the UK?. *Philosophical Transactions of the Royal Society of London. B* **356**, 1087-1095.

[129] Wickwire, K. (1977). Mathematical Models for the Control of Pests and Infectious Disease: a Survey. *Theoretical Population Biology.* **11**, 182-238.

[130] Williams, E.S., Thorne, E.T., Appel, M.J.G. and Belitsky D.W.(1977). Canine distemper in black-footed ferrets (*Mustela nigripes*) in Wyoming . *Journal of Wildlife Diseases.* **25**, 385-398.

[131] Williams, K., Parer, I., Coman, B., Burley, J. and Braysher, M. (1995). *Managing Vertebrate Pests: Rabbits.* Australian Government Publishing Service, Canberra.

[132] Wood, D.H.(1980). The demography of a rabbit population in an arid region of New South Wales Australia. *Journal of Animal Ecology.* **49**, 55-79.

[133] Woodroffe, R.(1999). Managing disease threats to wild mammals. *Animal Conservation.* **2**, 185-193.

[134] Newsome, A., Pech, R., Smyth, R., Banks, P., Dickman, C.(1997). *Potential Impact on Australian Native Fauna of Rabbit Calicivirus Disease.* Report for the Australian Nature Conservation Agency, Canberra.

[135] Bureau of Resource Sciences (1996). *Rabbit calicivirus disease: a report under the Biological Control Act 1984.* Bureau of Resource Sciences, Canberra.

[136] Wardhaugh, K. and Rochster, W. (1996). *Australian & New Zeland Rabbit Calicivirus Disease Program: Wardang Island. A Retrospective Analysis of Weather Conditions in Relation to Insects Activity and Displacement.* A report of research conducted September-October 1995 by Keith Wardhaugh CSIRO Division of Entomology, Camberra, ACT and Wayne Rochester Centre for Tropical Pest Management, Brisbane, Qld. Meat research corporation, Sidney, NSW.

[137] Cooke, B.D. (1996). *Australian & New Zeland Rabbit Calicivirus Disease Program: Analysis of the Spread of Rabbit Calicivirus from Wardang Island through Mainland Australia.* A report of research conducted September 1995-October 1996 by B.D. Cooke, CSIRO Division of Wildlife and Ecology, Camberra, ACT. Meat research corporation, Sidney, NSW.

[138] CSIRO Australian Animal Health laboratory (1996). *Australian & New Zeland Rabbit Calicivirus Disease Program: Testing non-Target Species for Susceptibility to RCV.* A report of research conducted in 1996 by CSIRO Australian Animal Health Laboratory, Geelong, Vic. Meat research corporation, Sidney, NSW.

[139] CSIRO Division of Animal Health and Wildlife and Ecology (1996). *Australian & New Zeland Rabbit Calicivirus Disease Program: Field Evaluation of RCD under Quarantine.* A report of research conducted in 1996 by CSIRO Australian Animal Health and Wildlife and Ecology, Camberra, ACT. Meat research corporation, Sidney, NSW.

[140] Neave, H.M. (1999). *Rabbit Calicivirus Disease Program Report 1: Overview of Effects on Australian Wild Rabbit Population and Implications for Agriculture and Biodiversity.* A report of research conducted by participants of the Rabbit Calicivirus Disease Monitoring and Surveillance Program and Epidemiology Research Program. Prepared for the RCD Management group. Bureau of Rural Sciences, Camberra.

[141] Cooke, B.D. (1999). *Rabbit Calicivirus Disease Program Report 2: Epidemiology, Spread and Release in Wild Rabbit Populations in Australia.* A report of research conducted by participants of

the Rabbit Calicivirus Disease Monitoring and Surveillance Program and Epidemiology Research Program. Prepared for the RCD Management group. Bureau of Rural Sciences, Camberra.

[142] Edwards, G.P. and Dobbie, W. (1999). *Rabbit Calicivirus Disease Program Report 3: Use and Benefits of Integrated Control of Wild Rabbits in Australia.* A report of research conducted by participants of the Rabbit Calicivirus Disease Monitoring and Surveillance Program and Epidemiology Research Program. Prepared for the RCD Management group. Bureau of Rural Sciences, Camberra.

[143] Sandell, P.R. and Start, A.N. (1999). *Rabbit Calicivirus Disease Program Report 4: Implications for Biodiversity in Australia.* A report of research conducted by participants of the Rabbit Calicivirus Disease Monitoring and Surveillance Program and Epidemiology Research Program. Prepared for the RCD Management group. Bureau of Rural Sciences, Camberra.

[144] Saunders, G. and Kay, B. (1999). *Rabbit Calicivirus Disease Program Report 5: Implications for Agricultural Production in Australia.* A report of research conducted by participants of the Rabbit Calicivirus Disease Monitoring and Surveillance Program and Epidemiology Research Program. Prepared for the RCD Management group. Bureau of Rural Sciences, Camberra.